ELECTROPORATION-MEDIATED DELIVERY OF MACROMOLECULES TO INTESTINAL EPITHELIAL MODELS

A Dissertation
Presented to
The Academic Faculty

By

Esi B. Ghartey-Tagoe

In Partial Fulfillment
Of the Requirements for the Degree
Doctor of Philosophy in the
Wallace H. Coulter Department of
Biomedical Engineering

Georgia Institute of Technology
January 2004

ELECTROPORATION-MEDIATED DELIVERY OF MACROMOLECULES TO INTESTINAL EPITHELIAL MODELS

Approved by:

Dr. Mark R. Prausnitz, Advisor

Dr. Andrew S. Neish, Co-Advisor

Dr. Julia Babensee

Dr. Robert Cargill

Dr. Dennis Hess

Dr. Athanassios Sambanis

Date Approved: January 5, 2004

DEDICATION

To my family for their love and support.

ACKNOWLEDGEMENTS

I would like to thank all those who have provided guidance and support while I pursued my degree. First and foremost, I must thank God without whom none of this would have been possible. I would like to thank my co-advisors Mark Prausnitz and Andy Neish for everything they have done for me. Thanks for the helpful discussions, answering my questions, and in general just making yourselves available. I have learned so much from the two of you (too much to list here) and I am a better researcher and scientist for having known you both. Additional thanks go to Andy for making room for me in his lab and for making me feel like a part of the group.

I would like to thank the members of the Prausnitz Drug Delivery Group (past and present) for their help and support. Thanks to my undergraduate assistants Kashif Ahmed and Jeremy Morgan. Kashif for being my first undergrad (and therefore my guinea pig) and Jeremy for making those long days in the lab a little more bearable. As for my colleagues, I definitely have to thank Paul Canatella, my mentor (even if he doesn't realize it), for letting me tag along with him for his experiments and for teaching me all about the experimental work we did. I would also like to acknowledge Hector Guzman for helpful discussions and for being a friend, Devin McAllister for his "encouragement", Joseph Cooke for just being fun to be around, Mangesh Deshpande and Vladimir Zarnitsyn, my gene delivery partners, for helpful discussions and for being great guys to work with, Pavel Kamaev for entertaining me with his "theories" and Dr. Ping Wang, our office mate, for putting up with us as we discussed Pavel's "theories".

Special thanks to the women of the Prausnitz lab, especially Robyn Schlicher, Arlena Coulberson, and Christina Easley, who have been and I hope will continue to be,

good friends. Other members of the lab that I would like to acknowledge include Harold Azencott, Shawn Davis, Harvinder Gill, Daniel Hallow, Jason Jiang, Wijaya Martanto, Jung-Hwan Park, and Sean Sullivan. For help with flow cytometry confocal microscopy training, thanks go to Bob Karaffa, Steve Woodard, and Johnafel Crowe. Finally, I would like to acknowledge Donna Bondy for all of her help with administrative issues and for the yummy treats and Trudy Walker, my other mom, for keeping me in line with her "beat downs".

I would next like to thank the many people at Emory University who have helped me over the years. I am sure to forget someone, but here goes. Thanks to the past and present post-docs and technicians of the Neish lab, Anjali Rao, Vinit Karmali, Dr. Lauren Collier-Hyams, Dr. Andrew Young, Adam Carlson, Amelia Tomlinson, Dr. Hui Zheng, Brigid Batten, Srividya Malkapuram, and Heather Pryor for welcoming me into the lab and for their invaluable help with all aspects of my research. They taught me everything from bacterial transformation to ELISA tests to immunofluorescence and I appreciate their time and patience. I would like to also thank other members of the Epithelial Pathobiology Group at Emory including, Dr. Asma Nusrat, Dr. Charles Parkos, Dr. Andrew Gewirtz, Dr. Didier Merlin, Dr. Sean Walsh, Dr. Ann Hopkins, Dirk Hunt, Brian Babbin, and Dr. Susan Voss.

I would like to acknowledge the friends I made while here Georgia Tech, especially Stacye Thrasher, Judith Thompson, Cindy Pang Cao, Ying Chen, Gul Tokdemir, Michelle Depp, Andre Taylor, Tazrien Kamal, Punit Chiniwalla, and other members of the GLC Crew. We had some great times that I will remember always. Special thanks to Stacye and Judy for their support and encouragement.

Last, but certainly not least, I have to thank my family here and abroad. My father and mother, Dr. Nanabanyin and Mrs. Abenaa Ghartey-Tagoe, my sisters, Adwoa and Amma, and my niece Aba, have given me their love and support, even when I was at my most stressed, and have been my biggest fans. Thanks for everything. I love you guys!

TABLE OF CONTENTS

LIST OF TABLES

LIST OF FIGURES

SUMMARY

This study was conducted to determine if electroporation could deliver membrane-impermeant molecules intracellularly to intact, physiologically competent monolayers that mimic the intestinal epithelium. The long-term effects of electroporation on these monolayers were studied to determine the kinetics with which monolayers recover barrier function. The ability of electroporation to introduce biologically active molecules, e.g., plasmid DNA and siRNA, into these monolayers, to either express a protein of interest or modify cellular function, was also studied.

Results showed that intracellular uptake of calcein, a small tracer molecule, and bovine serum albumin, a globular protein, occurred uniformly throughout the monolayers and increased as a function of voltage, pulse length, and pulse number. There was no significant difference in uptake resulting from single and multiple pulses of the same total exposure time. Barrier function recovery depended on the electroporation conditions applied, with some monolayers recovering normal physiologic function within a day. Electroporation also increased the permeability of the monolayers to calcein and BSA, possibly through a combination of increased paracellular and transmonolayer transport.

When compared to cationic lipid transfection (lipofection), transfection of intestinal epithelial monolayers with reporter plasmids by electroporation was more efficient in situations where high concentrations of DNA, and as a result, higher levels of expression were needed. Although uptake of DNA was high after electroporation and increased with increasing amounts of DNA, overall expreseion efficiency was still low (~3%). Electroporation-mediated transfection of intestinal epithelial monolayers with a

plasmid that expressed inflammation inhibitor protein, IκBα, was not always successful, probably because of low levels of protein expression. Introduction of the much smaller siRNA molecules into the monolayers by electroporation, on the other hand, was very successful at inhibiting the production of the nuclear envelope proteins lamin A and lamin C.

The results of these experiments demonstrated that electroporation can introduce a wide variety of molecules intracellularly into model intestinal epithelia. These results should be useful to identify optimal electroporation conditions for transporting drugs, proteins, and genes into intestinal and, possibly, other epithelia for local drug and gene therapy, as well as for development of improved models of intestinal epithelium.

CHAPTER I

1. INTRODUCTION

Inflammatory intestinal disorders such as cholera and Crohn's disease are of widespread concern because of their prevalence in both developing and developed countries (Blaser et al., 2002; Targan et al., 2003). The study and treatment of these, and other, disorders could be facilitated by the ability to introduce therapeutic drugs, proteins, or genes into intestinal epithelium. The unique features that define intestinal epithelium *in vivo* can be partially modeled *in vitro* by cell lines such as the Caco-2 and T84 lines. When cultured as monolayers on porous membranes, these cells exhibit the same structural polarity and functional characteristics of intestinal epithelial cells found *in vivo* (Madara et al., 1987; Shaw, 1996b). However, both *in vitro* and *in vivo* intestinal epithelium have well developed barrier functions that make it difficult to introduce exogenous agents. The similarity between these cells and *in vivo* epithelium makes them especially useful for our study of the ability of electroporation to deliver compounds intracellularly to polarized epithelial monolayers.

Electroporation involves the application of a short electric pulse that transiently disrupts cellular membranes and thereby transports membrane-impermeant molecules into the cytosol and/or nucleus (Chang et al., 1992). The electric field is typically applied as one or more short (μs to ms) pulses with a rectangular or exponential-decay waveform. The resulting increase in cell permeability is thought to be due to the formation of short-lived aqueous pathways ("pores") in the plasma membrane (Weaver, 1993), which can be reversible or irreversible depending upon the field strength, length, and number of pulses.

Although the exact molecular mechanisms of how electroporation affects the cell membrane are not fully understood, this phenomenon has been widely employed as a research tool to transfect cells with exogenous proteins or genes (Baron et al., 2000) and, more recently, to transport drugs across the skin for local or systemic therapy (Prausnitz, 1999), and to enhance chemotherapeutic delivery into tumors (Heller et al., 1999).

This study was conducted to determine whether electroporation could be used to uniformly and efficiently deliver macromolecules into polarized intestinal epithelial monolayers that mimic *in vivo* epithelium. The dependence of molecular uptake, short-term cell viability, and long-term monolayer recovery kinetics on electroporation parameters was quantified and used to help guide future experiments. Since confluent intestinal epithelial monolayers are refractory to most conventional methods of gene transfection, electroporation was evaluated for its ability to transfect two reporter plasmids into these cells. The results of these transfections were compared to those of lipid-mediated transfection to determine which was more efficient. Finally, monolayers were transfected with two types of nucleic acids in an attempt to inhibit particular cell functions.

CHAPTER II

2. INTESTINAL STRUCTURE, FUNCTION, AND PATHOLOGY

The primary purpose of the gastrointestinal tract is to serve as the route by which nutrients are digested and absorbed from the foods we eat (Yamada et al., 1999). However, another necessary and important function of the tract is to act as a barrier to protect the body from pathogenic organisms and other harmful substances present in the intestinal lumen. When this barrier malfunctions or is compromised, inflammatory responses may arise in the form of various intestinal diseases. Diseases such as cholera and Crohn's disease, both of which predominately affect the epithelial lining of the intestine, are of major public health importance because of their prevalence in both developing and industrialized countries (Blaser et al., 2002; Targan et al., 2003).

2.1 Functional Anatomy of the Intestine

The gastrointestinal tract is a hollow, continuous tube approximately 30 feet in length that winds through the body from mouth to anus (Figure 2.1) (Stalheim-Smith and Fitch, 1993). After food has been ingested by the mouth, it passes down the esophagus into the stomach where it is broken down and digested under highly acidic conditions. The digested food passes from the stomach to the small intestine, where absorption occurs, and then into the large intestine (colon). Undigested material (feces) is eliminated as waste through the anus.

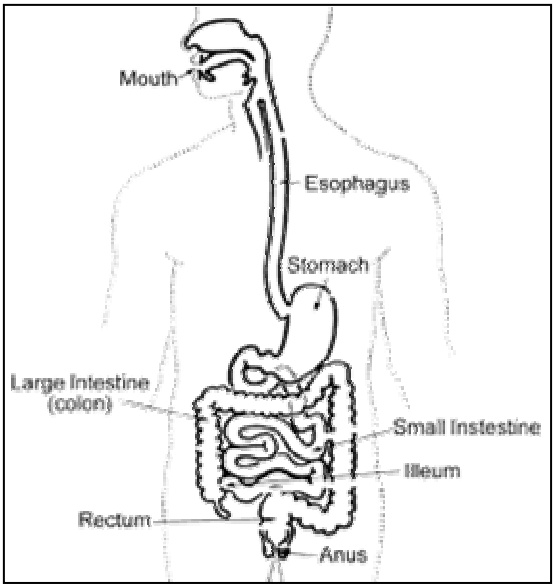

Figure 2.1 Illustration of the entire gastrointestinal tract. The major organs of the tract, including the small and large intestines, have been identified. [Source: National Digestive Diseases Information Clearinghouse, 2003]

The walls of the entire digestive tract are made up of four basic layers. One or more of the layers may be specialized to suit the function of a particular organ. From the outer layer to the inner, these layers are the serosa, the muscularis externa, the submucosa, and the mucosa (Marieb, 2000) (Figure 2.2). The serosa covers the exterior of the intestinal tube and is in contact with the peritoneal cavity. The muscularis externa is primarily composed of smooth muscle tissue and is responsible for the contractions necessary for segmentation (mixing food with digestive secretions) and peristalsis (propulsion of food forward through the tract). The submucosa is a layer of loose connective tissue housing a network of blood lymphatic vessels that extend into the adjacent layers and a network of neurons that help control some digestive functions.

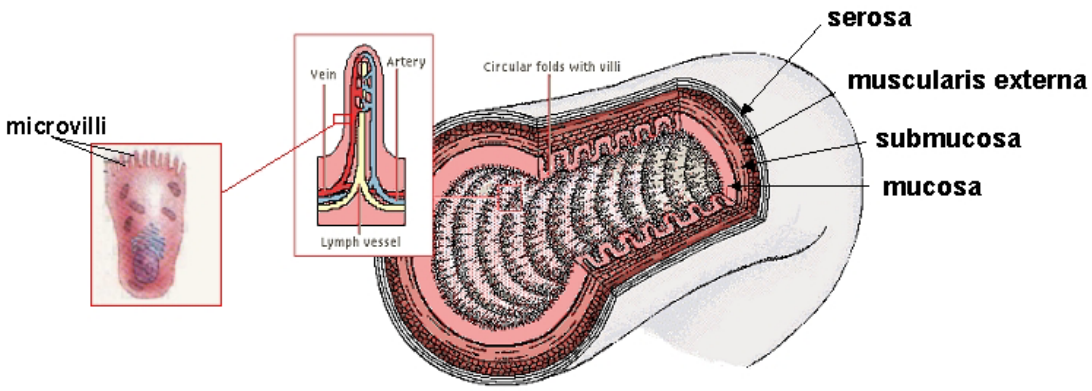

Figure 2.2 Structural anatomy of the small intestine. The four layers of the intestinal wall as well as the structure of an epithelial cell and a villus are depicted. (Source: MSN Encarta, 1999)

The mucosa is the layer that is of interest for this study. It lies next to the lumen of the intestine and, therefore, is exposed to the external environment. Its main functions are to 1) secrete mucus, digestive enzymes, or other products necessary for digestion, 2) absorb the digestive products, and 3) protect the body from the luminal contents and infection (Marieb, 2000). The mucosal layer is lined with epithelium (the type depends on location), under which lies the lamina propria, a layer of connective tissue containing the blood supply for the epithelia, and the muscularis mucosa, a layer of smooth muscle.

In the small and large intestine, the epithelial lining is made up of simple columnar epithelial cells specialized for secretion and absorption. The majority of nutrient absorption occurs in the small intestine because of several modifications that greatly increase the surface area available for absorption. The plicae circulares (~1 cm folds of the submucosal and mucosal layers), villi (~1 mm fingerlike projections of the mucosa that extend from the plicae circulares), and microvilli (~ 1 μm hair-like projections of the

plasma membrane of the absorptive epithelial cells that line the villi) all serve to increase the surface area of the small intestine for maximum absorption (Stalheim-Smith and Fitch, 1993). In fact, these features increase intestinal surface area by ~600 times relative to that of a comparable smooth surfaced tube (Stalheim-Smith and Fitch, 1993) and they allow the small intestine to absorb 90-95% of the nutrients that enter (Stalheim-Smith and Fitch, 1993; Marieb, 2000).

2.1.1 Epithelial Cell Structure and Function

Epithelial cells typically line the surfaces of organs, body cavities, and, in general, all parts of the body exposed to the external environment (e.g., skin, respiratory tract, digestive tract) (Burkitt et al., 1993). In the small intestine, some of the characteristics of intestinal epithelial cells include apical-basal polarity, a basement membrane, specialized intercellular junctions, and a capacity to regenerate (Shaw, 1996a) (Figure 2.3).

The polarity of the epithelial cells refers to the structural and functional distinction between the apical and basolateral (basal and lateral) membranes of the cells (Shaw, 1996b; Marieb, 2000). The apical (upper) membrane is exposed to the lumen and exhibits microvilli for increased absorption. The cell nucleus is typically located towards the basal (lower) end of the cell. The basal surface is also the location of cellular attachment to the basement membrane. The basement membrane is composed of laminin and other glycoproteins secreted by the cells above it and collagen secreted by the fibroblasts in the connective tissue layer below. It is across the basal surface and the basement membrane that the transport of signaling molecules and nutrients to and from the cells takes place.

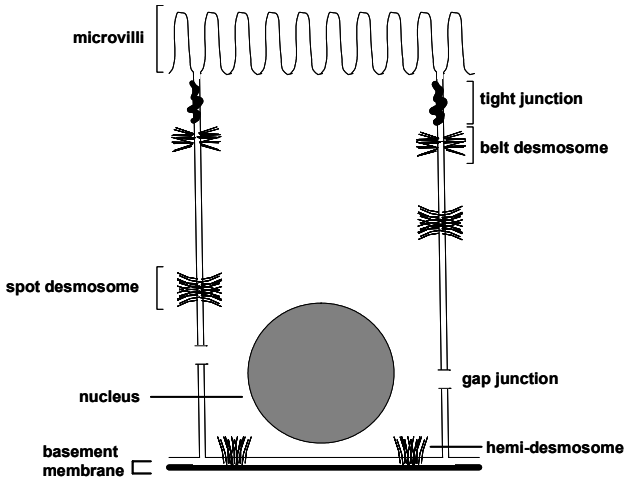

Figure 2.3 Drawing of an absorptive intestinal epithelial cell (enterocyte). Several types of intercellular junctions found on the cell serve to regulate processes such as nutrient absorption and intercellular communication.

There are three categories of intercellular junctions that serve as connections between adjacent cells and between the cells and the basement membrane: 1) tight junctions, 2) adhering junctions, and 3) gap junctions. Tight junctions form a continuous band around the circumference of the cell, delineating the apical aspect from the basolateral aspect (Burkitt et al., 1993). These junctions regulate the flow of material across the epithelial lining, by allowing ions and nutrients to pass through the space between the cells and preventing the passage of luminal contents (e.g., undigested food, microorganisms, and other foreign material), thus giving the epithelium its barrier function (Shaw, 1996b).

Adhering junctions bind adjacent cells of the epithelium together and also serve as anchors for the cells' cytoskeletal networks (Burkitt et al., 1993). The belt desmosome (or *zonula adherens*) encircles the entire cell just below the tight junction, while the spot desmosomes occur as small patches located around the cell on the lateral membrane. The

hemidesmosome is typically found anchoring the cell to the basement membrane (Histology, ; Burkitt et al., 1993; Shaw, 1996b). Gap junctions, or communicating junctions, allow the passage of small molecules (< 2 nm) from the cytoplasm of one cell to that of an adjacent cell (Burkitt et al., 1993). Cells can communicate with and aid each other through these junctions by exchanging nutrients and signaling molecules that regulate growth and development.

The intestinal epithelium undergoes a natural process of self-renewal in which epithelial cells arise from stem cells located in crypts at the base of each villus. The new epithelial cells migrate up the villi and are eventually shed at their tips. In this process, the epithelium is renewed every 3-6 days (Marieb, 2000). Intestinal epithelial cells can also be shed or killed off due to physical, chemical, or microbial injury. In order to maintain function, the epithelium must be able to regenerate quickly to replace lost cells (Madara, 1999). This process of regeneration, in which mature epithelial cells rapidly dedifferentiate and proliferate, will be discussed in more detail in Chapter 7.

Together, all of the characteristics of intestinal epithelium discussed above demonstrate that these cells function as a unit. Thus, the epithelium should be considered not as a collection of independent cells, but as a functional tissue.

2.2 Experimental Models of the Intestinal Epithelium

Epithelia can be cultured under *in vitro* conditions and used to obtain a better understanding of the structure and function of the epithelial lining of the intestine as well as a tool for studying intestinal diseases. Two cell lines commonly used for research are the Caco-2 and T84 lines, both of which are derived from human colon carcinoma. As

illustrated in Figure 2.4, when these cells are cultured as monolayers on microporous membranes, they develop monolayers that exhibit many of the same structural (e.g., polarity, intercellular tight junctions, and presence of microvilli) and functional (e.g., enzyme secretion and transport systems) characteristics of the absorptive intestinal epithelial cells found *in vivo* (Shaw, 1996a).

Caco-2 cells were isolated from human colon adenocarcinoma and initially cultured by Fogh et al. (1977a; 1977b). These cells grow as monolayers and when confluent, differentiate into polarized columnar epithelial cells similar to those present on the villi of the small intestine. They have a well developed brush border (microvilli) and intercellular junctions and are also able to express digestive enzymes and other products. Caco-2 monolayers are the most widely used epithelial models for studying drug absorption in the intestine (Artursson et al., 2001). Experiments with various drugs have shown that Caco-2 monolayers have absorption properties that make them useful for predicting both active and passive transport in intestinal tissues (Artursson and Karlsson, 1991; Bailey et al., 1996; Rubas et al., 1996; Anderle et al., 1998; Karlsson et al., 1999; Palm et al., 1999; Artursson et al., 2001; Krishna et al., 2001).

T84 cells were derived from a lung metastasis of a human colon carcinoma (Dharmsathaphorn et al., 1984). These cells also grow to form tight monolayers of polarized columnar epithelial cells with microvilli on their apical membranes and intercellular junctions; however, in many ways, they are more similar to the colonic epithelium from which they originated (Dharmsathaphorn et al., 1984; Madara et al., 1987). T84 monolayers have been used as models of the intestine in several areas

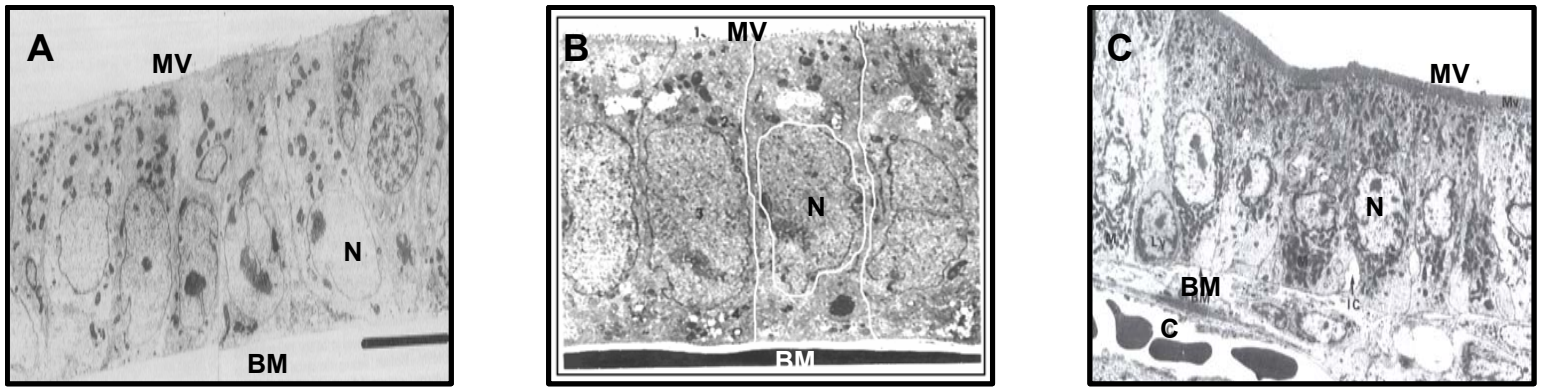

Figure 2.4 Electron micrographs of (A) Caco-2 and (B) T84 monolayers and (C) *in vivo* colonic epithelium. MV = microvilli, N = nucleus, BM = basement membrane, C = capillary. (Madara et al., 1987; Burkitt et al., 1993)

of research including studies about intestinal barrier function (Madara and Dharmsathaphorn, 1985) and wound repair (Nusrat et al., 1992), transepithelial electrolyte transport (Dharmsathaphorn and Madara, 1990), neutrophil migration across intestinal epithelia (Parkos, 1997), and bacterial invasion of intestinal epithelium (McCormick et al., 1993).

Although epithelial models have the advantage of being structurally simple, inexpensive, and relatively easy to work with compared to animal models, there are some limitations to these models. The primary limitation is that cultured epithelia are usually cancerous lines and are not a substitute for the more complex epithelium found *in vivo*. Cultured epithelia are grown on a flat substrate as monolayers, not on villi as they would *in vivo*. In addition, the many cell types that are present in normal epithelium, e.g., lymphocytes, mucus-producing goblet cells, etc., are not present in culture (Shaw, 1996b). Also, the characteristics that are desired in model epithelium (e.g., barrier function and polarity) are the same characteristics that make it difficult to manipulate these models through the introduction of different molecules by conventional means. Despite these disadvantages, epithelial cell monolayers have still been one of the most useful tools for studying different aspects of intestinal structure and function, including the mechanisms of how inflammatory diseases affect intestinal epithelium.

2.3 Inflammatory Intestinal Disorders

Inflammatory intestinal disorders typically arise when the epithelial barrier is not functioning properly or when harmful organisms or substances come into contact with the

epithelium. There are two classes of inflammatory intestinal diseases with which we are primarily concerned: enteric infections and inflammatory bowel disease.

2.3.1 Enteric Infections

Enteric infections are caused by complex interactions of the epithelial lining of the intestinal tract with pathogens such as viruses (e.g., rotavirus), bacteria (e.g., *Salmonella*, *Vibrio cholerae*, and *Escherichia coli*), or parasites (e.g., parasitic worms) (Blaser et al., 2002). Some pathogens, such as *V. cholerae*, secrete soluble toxins that cause disease (Sears and Acheson, 2002), while others, such as salmonella, physically invade the epithelium (Pegues et al., 2002). Many of these pathogens, or their by-products, have been shown to cause an innate immune response in the form of inflammation in intestinal epithelial cells (Eckmann et al., 1993; Schuerer-Maly et al., 1994; Jung et al., 1995; Li et al., 1998; McCormick et al., 1998; Elewaut et al., 1999). The symptoms of infection by proinflammatory organisms include abdominal cramping, nausea, bloody and/or purulent diarrhea, fever, and dehydration (Smith and Lamont, 1989).

Is has been estimated that close to 1 billion people worldwide become ill from these infections (Greenberg et al., 1999); developing countries are especially hard hit because effective sanitary measures for the proper handling and treatment of food, water, and sewage may not be in place (Black and Lanata, 2002). Infections in industrial countries are still a cause for concern. In the United States alone, there are over 200 million cases of gastric inflammation each year (Sobel and Tauxe, 2002). Of this number, 38% of cases are caused by viral, bacterial, or parasitic infections of known origin

leading to almost 200,000 hospitalizations and 3000 deaths per year (Sobel and Tauxe, 2002). People typically become infected when new pathogens arise or when they become lax in taking precautions, as evidenced by reports of the detection of contaminated foodstuffs.

In most cases, treatment consists of allowing the infection to run its course while replacing fluids the patient has lost because of diarrhea. For more severe or prolonged cases sometimes accompanied by nausea or vomiting, antibiotic, antiemetic, and antisecretory drugs may be prescribed (Soltis, 2002). Antidiarrheal medications may also be prescribed in some cases, but are usually avoided because they can slow down elimination of the organisms (Mayo, 1994).

2.3.2 Inflammatory Bowel Disease

Inflammatory bowel disease (IBD) is the term used to collectively describe two disorders: ulcerative colitis and Crohn's disease. Both diseases are characterized by chronic inflammation of the intestinal tract. Currently it is estimated that IBD affects approximately 1 million people in the United States (CCFA, 2003a). Unlike many infectious diseases, IBD is more prevalent in Western countries, e.g., North America, northern Europe, etc., and in people of European descent. Ulcerative colitis and Crohn's disease affect men and women almost equally and it appears that genetic, as well as environmental, factors may play a role in both diseases (Karlinger et al., 2000). The exact cause of IBD is not known, although many theories have been put forth. The most popular theory is that the body's immune system is triggered by the presence of foreign

substance, e.g., bacteria (commensal or foreign) or viruses in the intestine, leading to ongoing, uncontrolled inflammation (CCFA, 2003a, b).

2.3.2.1 Ulcerative Colitis

Ulcerative colitis (UC) is a chronic, relapsing condition that causes inflammation resulting in small ulcers and abscesses in the mucosal epithelial lining of the large intestine (colon) (CCFA, 2003b). Inflammation typically occurs in the rectum and sigmoid colon and can spread into the rest of the colon. In rare cases, UC can be found in the ileum, the lower section of the small intestine. People of any age can develop UC, but the highest incidence of occurrence is found between the ages of 15 and 30 (NDDIC, 2003b; Targan et al., 2003). The primary symptoms of UC are abdominal pain and bloody diarrhea, but other symptoms, such as fever, rectal bleeding, nausea, fatigue, and weight loss, are also common. Complications that can result from severe UC include toxic megacolon (enlargement and paralysis of the colon) and an increased risk of colon cancer.

2.3.2.2 Crohn's Disease

Crohn's disease (CD) is also a chronic condition that leads to inflammation of the intestine. In contrast to ulcerative colitis, CD involves multiple layers of the entire intestinal wall in an inflammatory process that can affect any part of the gastrointestinal tract from mouth to anus (CCFA, 2003a). The majority of cases, however, primarily involve the small intestine and/or the colon. Also unlike UC, which is characterized by contiguous inflammation of the intestinal lining, CD tends to affect the intestine in

patches, so that normal intestine is separated by areas of diseased tissue. CD can also occur at any age, but most often begins between the ages of 14 and 24 (NDDIC, 2003a; Targan et al., 2003). The symptoms of CD are very similar to those of UC including abdominal pain, diarrhea, rectal bleeding, weight loss, and fever. Complications that can result from CD include intestinal obstruction, development of abscesses (pus filled masses) and fistulas (abnormal channels between the intestine and bladder, skin, or other parts of the intestine).

2.3.2.3 Diagnosis and Treatment of IBD

Diagnosis of ulcerative colitis and Crohn's disease can be very difficult because the symptoms and pathologic features are similar to each other and to those of other intestinal disorders, e.g., irritable bowel syndrome and certain infectious diseases. The techniques that are used to aid in diagnosis include blood and urine analysis, stool examination, x-rays, diagnostic ultrasound, and endoscopic procedures. Endoscopy is used to image the intestine and is the most helpful at distinguishing between UC and CD. Biopsies of intestinal tissue may be taken during the procedure for observation on a microscope.

There are no drug-based cures for IBD so treatment is usually aimed at controlling the inflammatory immune response with systemic anti-inflammatory drugs and/or immunosuppressive drugs (Egan and Sandborn, 2003). Mesalamine, sulfasalazine and several other modified forms of the anti-inflammatory drug 5-aminosalicylic acid (5-ASA), have been the standard for treating mild to moderate UC and CD affecting the colon for many years. Corticosteroids, such as prednisone and prednisolone, are another family of anti-inflammatory agents used to treat people with severe IBD and those who

do not respond to the various 5-ASA formulations. Long term therapy with immunosuppressive drugs, such as azathiopine and 6-mercaptopurine, may be necessary for treating IBD patients that do not respond to standard treatment. Although extended use of some of these medications can cause serious side effects, combinations of the medications described above can sometimes cause both UC and CD to go into remission for months or even years. Most patients, however, will have one or more relapses during their lifetime (Targan et al., 2003).

Surgical removal of the colon or other affected parts is performed as a last resort, i.e., if IBD becomes life threatening, if the patient is not responding to the drug therapy, or if there are indications of cancer. Surgery can cure ulcerative colitis, but only reduces the symptoms of Crohn's disease (NDDIC, 2003b, a). Several surgical options are available for treating UC, although a total cure is only achieved by removal of the entire colon and rectum. For some patients, only the colon and the diseased inner layer of the rectum need to be removed. Surgery for CD usually involves correcting intestinal blockages, removing fistulas, and surgical removal of the diseases portions of the intestine followed by reattachment of the remaining segments. Inflammation, however, tends to reoccur in areas next to the removed portion. As a result, the majority of CD surgical patients will need second operations at some point (Baert et al., 2003).

2.4 Cellular Inflammatory Pathway

The search for an effective cure or treatment for inflammatory intestinal diseases can be aided by developing a better understanding of the inflammatory reaction of cells

on a molecular level. Laboratory models such as the ones described in Section 2.2 have been very helpful in elucidating events that occur during inflammation (Jung et al., 1995; Elewaut et al., 1999). Inflammation is a tightly controlled process that arises in response to a physical or chemical injury. It is characterized by 1) an increase in blood flow leading to reddening (hyperemia) of the affected area, 2) leakage of vascular fluids leading to swelling (edema), and 3) an influx of immune inflammatory cells (e.g., neutrophils, leukocytes, macrophages) necessary to destroy or inhibit harmful stimuli and repair any damaged tissue (Stalheim-Smith and Fitch, 1993).

The trigger for the initiation of an inflammatory reaction could be invasion by a virus or bacterium, physical or chemical injury to tissue, the presence of bacterial products, or the secondary release of inflammatory cytokines like tumor necrosis factor (TNF) or interleukin-1 (IL-1), which function in cell-to-cell communication. All of these pro-inflammatory stimuli activate signal transduction pathways in epithelial cells and other cells. One of the better-defined pro-inflammatory pathways, NFκB is illustrated in Figure 2.5 in a simplified diagram. This pathway is known to play a role in bacterial infections (Elewaut et al., 1999), IBD and other chronic inflammatory disorders (Schreiber et al., 1998; Makarov, 2000; Tak and Firestein, 2001), apoptosis (Yamamoto and Gaynor, 2001), and cancer (Schwartz et al., 1999).

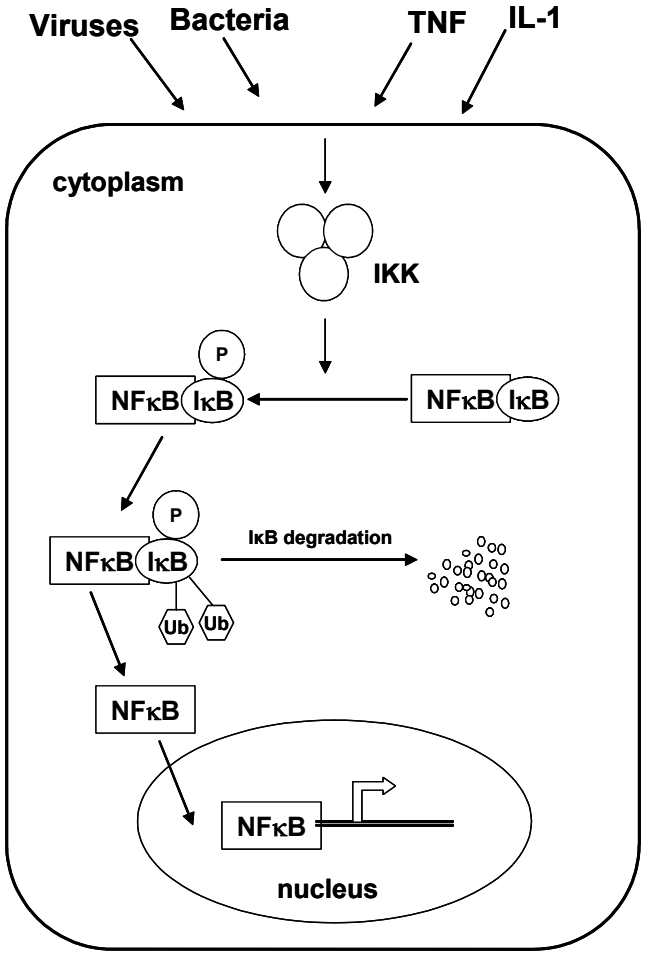

Figure 2.5 Simplified diagram of the NFκB-mediated inflammatory signal transduction pathway in a cell. NFκB activation plays a role in several inflammatory disorders, but also helps to regulate normal cellular functions.

NFκB and IκB each represent a family of proteins, however, these names will be used to collectively describe these proteins to make the explanation more clear. NFκB is a DNA-binding transcription factor that is active in the nucleus. It is sequestered in the cytoplasm because of its binding with IκB, which masks its nuclear localization signal (Baeuerle, 1998). When proinflammatory stimuli (cytokines, UV, bacterial by products) come into contact with epithelial cells, they are recognized by specific receptors on the cell surface which lead to the activation of the IκB kinase (IKK) complex, a 900 kDa multi-unit protein complex located in the cytoplasm (DiDonato et al., 1997). IKK in turn catalyzes the phosphorylation of two serine residues on the 37 kDa inhibitor protein IκB, which is found in a complex with nuclear factor kappaB (NFκB) (Zandi et al., 1998). Upon phosphorylation, IκB is polyubiquitinated by the enzyme ubiquitin ligase E3, which targets IκB for degradation by the 26S proteosome (Baldwin, 1996). When IκB is degraded, NFκB's nuclear localization signal is exposed and the protein is free to translocate to the nucleus (DiDonato et al., 1995).

When the released NFκB migrates into the nucleus, it binds to target genes at the promoter region to induce the expression of a wide variety of inflammatory mediators, such as interleukin-8 (IL-8), that may trigger inflammation in other cells and/or attract cells involved in host immunity to the site of invasion or injury. NFκB also plays a role in the regulation of cellular adhesion, cell growth and proliferation (Baldwin, 1996). To terminate the inflammatory response, NFκB also induces expression of IκB, which binds to and dissociates NFκB from the promoter and transports it back to the cytoplasm in a negative feedback loop (Zabel and Baeuerle, 1990).

Chronic diseases, such as IBD, are considered to be diseases in which the genes that regulate inflammation are inappropriately activated and/or can't be "turned off". In fact, many of the medications used to treat IBD act by inhibiting NFκB activation either directly or indirectly (Yamamoto and Gaynor, 2001). For example, corticosteroids appear to act by two primary mechanisms: direct interaction with NFκB to prevent DNA binding and upregulation of IκB levels to enhance retention of NFκB in the cytoplasm. Sulfasalazine acts by inhibiting phosphorylation of IκB and, as a result, its degradation. Immunosuppressive drugs can act to inhibit the proteasome that degrades IκB after phosphorylation or inhibit the migration of NFκB from the cytoplasm to the nucleus.

Several research studies have focused on finding other ways to inhibit one or more of the steps that play a role in inflammation. Methods such as inhibiting the kinases that phosphorylate IκB (Baeuerle, 1998), inhibiting the enzymes that ubiquitinate and degrade phosphorylated IκB (Beg and Baldwin, 1993; Thanos and Maniatis, 1995; Yaron et al., 1997), and inhibiting NFκB by introducing exogenous IκB into the cell (Read et al., 1994; Elewaut et al., 1999) have been investigated. In the latter case, a variation of which will be explored in this study, the additional IκB could bind the free NFκB and prevent it from entering the nucleus and initiating the expression of inflammatory genes. Techniques such as electroporation could be very valuable for delivering IκB and other relevant molecules into affected cells so that this pathway can be interrupted.

CHAPTER III

3. ELECTROPORATION

3.1 Theory of Electroporation

Electroporation is a technique that has been used extensively for incorporating membrane impermeable molecules, e.g., DNA (Cataldo et al., 1998), proteins (Prausnitz et al., 1994), or drugs (Heller et al., 1999), into cells. It involves the application of an electric field pulse to cause the transient increase in permeability of the lipid bilayer of cellular membranes. The electric field is usually applied for short periods of time (on the order of microseconds to milliseconds), as a single pulse or as multiple pulses, and, typically, has a rectangular or exponential-decay wave form. Although electroporation is a widely used method, the exact molecular mechanism of how it affects the cell membrane is not completely understood. However, electrical measurements have shown that electroporation causes the transmembrane potential of a cell, which is normally around 70 mV, to increase to a threshold of a few hundred millivolts (Chang et al., 1992). Above this threshold, a breakdown of the membrane occurs and an increase in the cell membrane's permeability is observed (Ho and Mittal, 1996; Weaver and Chizmadzhev, 1996).

The enhanced permeability of the cell is thought to be the result of the formation of transient, hydrophilic, aqueous pathways ("pores") in its membrane (Chernomordik, 1992; Weaver, 1993). The hypothesis is that the precursors to these pathways are hydrophobic pores (Figure 3.1A), which expand to a critical radius and then change conformation to more stable hydrophilic pores (Figure 3.1B) that require less energy to

maintain (Weaver, 1993). These aqueous pores may be reversible or irreversible depending upon electrical parameters such as electric field strength, pulse length, and number of pulses. Typically, the pore sizes are greater than or equal to a nanometer and take anywhere from milliseconds to a few minutes to reseal. Transport of macromolecules into cells via these pores can take place by one or more of the following mechanisms: diffusion (Xie et al., 1990), electro-osmosis (Dimitrov and Sowers, 1990), or electrophoresis (Klenchin et al., 1991). One study found that depending upon the electrical conditions and molecule size, transport can take place during the pulse by electrophoresis and/or electro-osmosis and after the pulse by diffusion (Prausnitz et al., 1995).

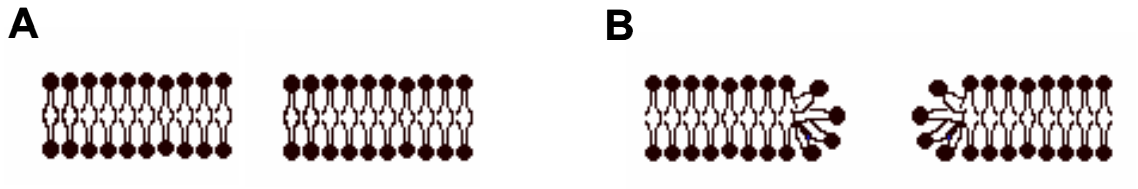

Figure 3.1 Diagram of the (A) hydrophobic and (B) hydrophilic pore structures hypothesized to form during electroporation (Weaver, 1993).

3.2 Electroporation of Monolayers

Several researchers have demonstrated that electroporation can be successfully applied to different types of cells, e.g., mammalian cells (Rols and Teissie, 1990), yeast

(Gift and Weaver, 1995), bacteria (Taketo, 1988), plant cells (Saunders and Bates, 1992), and red blood cells (Dimitrov and Sowers, 1990). In most of these studies, adherent cells were chemically or physically removed from their support and then electroporated in suspension. This type of electroporation is not meaningful for some cells, e.g., epithelial cells, because it poorly mimics *in vivo* cell function and geometry found in tissues.

While there is an extensive amount of research about electroporation of cells in suspension, in comparison, little research has been performed to study electroporation of cells as monolayers, and even less with intestinal epithelial cell monolayers. Studies of electroporation of cells in monolayers (Liang et al., 1988; Kwee et al., 1990; Kwee and Celis, 1991; Zheng and Chang, 1991; Kwee et al., 1992; Ghosh et al., 1993; Raptis et al., 1995a; Raptis et al., 1995b; Yang et al., 1995; Bright et al., 1996; Wegener et al., 2002; Muller et al., 2003), have involved cells that were not epithelial, did not originate from the intestine, or were not of human origin, which limits their ability to model human intestinal tissue function. In related studies, Leonard et al. (2000b; 2000a), used iontophoresis to electrophoretically enhance transport across intestinal epithelium, but did not employ electroporation and, therefore, did not deliver molecules into cells. Thus, the ability to electroporate functional human intestinal epithelium and thereby transport molecules intracellularly has not yet been established.

3.3 Applications of Electroporation

Although the exact molecular mechanisms of how electroporation affects the cell membrane are not fully understood, this phenomenon has been widely employed as a

research tool to transfect cells with exogenous proteins or genes (Baron et al., 2000; Canatella and Prausnitz, 2001), to transform plant cells (Chowrira et al., 1995), to sample cytosolic contents (Neumann et al., 1989), to transport drugs across the skin for local or systemic therapy (Prausnitz, 1999) and to enhance chemotherapeutic delivery into tumors (Heller et al., 1999).

Electroporation has gained most of its popularity as a tool for transfecting cells with nucleic acids such as plasmids. Plasmids are small, double-stranded, circular DNA molecules that replicate in prokaryotic cells. In purified form, a recombinant plasmid with a eukaryotic promoter upstream of a coding sequence can be transfected, or delivered, into a eukaryotic cell to have a particular gene expressed. The gene must undergo transcription (synthesis of messenger RNA from the DNA template) and translation (synthesis of proteins from the RNA template) in order for expression to occur and could have some biologic therapeutic activity. Depending upon where the plasmid DNA localizes, expression can be transient (plasmid does not integrate into cell chromosome) or stable (plasmid integrates into the genomic DNA).

In addition to electroporation, there are several other methods used to introduce exogenous genes into cells and tissues including 1) calcium phosphate coprecipitation (Conn et al., 1998), 2) DEAE dextran (diethylaminoethyl-dextran) (Schwartz and Rosenberg, 1998), 3) microinjection (Yaron et al., 1997), 4) viral vectors (Hicks et al., 1998; Thomas et al., 2003), 5) sonication (Greenleaf et al., 1998), and 6) cationic lipids (Tseng et al., 1997; Bichko, 1998). Table 3.1 lists some of the major advantages and disadvantages of these methods.

Table 3.1 Comparison of the advantages and disadvantages of common gene transfection methods.

Transfection Method	Advantages	Disadvantages
Calcium phosphate	• Commonly used • Relatively inexpensive • Useful for stable and transient transfection	• Cell toxicity • Cell type dependent (does not work in difficult to transfect cell lines) • DNA degradation in endosomes
DEAE-dextran	• Ease of use • High efficiency • Useful for transient transfection	• Cell toxicity • Cell type dependent (does not work in difficult to transfect cell lines) • DNA degradation in endosomes • Not useful for stable transfection
Microinjection	• Ability to inject DNA directly into nucleus	• Special equipment • Labor intensive • Difficult to perform on large numbers of cells
Viral vectors	• High efficiency	• Adverse inflammatory response
Sonication	• Cell type independent	• Special equipment • Low transfection efficiency
Cationic lipids	• Ease of use • High efficiency	• Low transfection efficiency in differentiated or confluent cells

Cationic lipids have rapidly become one of the most common methods of transfection being used today. Lipid-mediated transfection (lipofection) involves the formation of complexes with DNA through the ionic interactions between the positively charged lipid and the negatively charged DNA molecule. The resulting lipophilic complex is then either endocytosed or binds to the cell and the DNA released through an unknown mechanism (Tseng et al., 1997). Although lipofection can be very efficient, some differentiated cell lines, including Caco-2 cells (Uduehi et al., 1999), are resistant to this form of transfection.

Since electroporation generally does not affect long-term cell function and can be performed on almost any cell type, it shows great promise as a tool for targeted drug delivery and gene therapy. We propose to use electroporation as a tool for incorporating several macromolecules into epithelial cell monolayers that model intestinal epithelia. If successful, these models can be manipulated through the use of genetic material or proteins for the purpose of studying cellular processes or mimicking actual diseases. Experimental drugs or gene-based therapies can also be tested on these disease models, thus reducing the need for research animals. New or improved therapeutic techniques (e.g., an endoscopic-like device) could also be developed based on the success of using electroporation to introduce these molecules.

CHAPTER IV

4. EXPERIMENTAL METHODS AND PROCEDURES

4.1 General Experimental Methods

4.1.1 Cell Culture

The Caco-2 and T84 tumor cell lines were chosen to model the intestinal epithelium. Both cell lines were derived from human colon carcinomas (Fogh et al., 1977a; Dharmsathaphorn et al., 1984) and when cultured on microporous membranes, they exhibit many of the same structural and functional characteristics of *in vivo* intestinal epithelium (see Chapter 2). This makes them very useful as models of the intestinal epithelium.

Caco-2 cells (American Type Culture Collection, Manassas, VA) were cultured in tissue culture flasks using standard complete media consisting of Dulbecco's Modified Eagle's Medium (DMEM) supplemented with 10% (v/v) heat-inactivated fetal bovine serum, 100 IU/ml penicillin, 100 μg/ml streptomycin, 2 mM L-glutamine, 10 mM HEPES buffer (Mediatech, Herndon, VA), and 0.1 mM non-essential amino acids. T84 cells were cultured in a 1:1 mixture of DMEM and Ham's F-12 Nutrient Mixture supplemented with 6% (v/v) heat-inactivated newborn calf serum, 15 mM HEPES buffer, 14 mM $NaHCO_3$, and antibiotics (40 μg/ml penicillin, 8 μg/ml ampicillin, and 90 μg/ml streptomycin). Unless otherwise stated, all media ingredients were obtained from Life Technologies, now Invitrogen (Carlsbad, CA). Both cell types were cultured in a 37^{o}C, 5% CO_2 environment and were passaged using standard cell culture techniques (Dharmsathaphorn and Madara, 1990; Madara et al., 1992).

4.1.2 Monolayer Culture

To grow intact, polarized monolayers, harvested cells were seeded onto collagen-coated Transwell microporous cell culture inserts (Corning Costar, Acton, MA) in six-well culture plates using well-established techniques (Madara et al., 1992). Caco-2 cells were seeded at a density of ~4 x 10^4 cells per ml onto polyester membrane inserts with a growth area of 4.7 cm^2 and a pore size of 0.4 μm (Costar #3450). Unless otherwise stated, T84 cells were seeded at a density of ~3 x 10^5 cells per ml onto polycarbonate inserts with a growth area of 4.7 cm^2 and pore size of 3 μm (Costar #3414). Caco-2 cells were cultured on membranes with smaller pores because they are known to grow through pores larger than 1 μm and form a monolayer on the other side of the membrane (Tucker et al., 1992).

Monolayers of both cell lines were incubated in a 5% CO_2, 37°C environment in their respective growth media and allowed to grow to confluence. Caco-2 monolayers were allowed to remain in culture for 14-28 days, while T84 monolayers were cultured for 7-14 days. Spent media was replaced with fresh media approximately every 48 hours.

4.1.3 Transepithelial Resistance Measurements

To ensure monolayer integrity, the transepithelial electrical resistance (TEER) of each monolayer was measured. In initial experiments with these monolayers, TEER was measured by connecting the apical and basal media to calomel and Ag·AgCl electrodes using agar bridges as described previously (Madara et al., 1992). A voltage clamp system (Model 558-C5, Dept. of Bioengineering, University of Iowa, Iowa City) measured the

transepithelial voltage generated in response to a small current (60 μamps for Caco-2's and 25 μamps for T84's). Ohm's law was then used to calculate the resistance of the monolayers. The resistance of empty monolayer culture inserts was subtracted from the total resistance to obtain the resistance of the monolayer alone. A disadvantage of using this method was that the apparatus was not easily transported because of its bulkiness. In addition, this method required monolayers to be exposed to the external environment in order for measurements to be made. As a result, if the monolayers had not achieved maximal resistance at the time of measurement, they could not be placed back in incubation because of the potential for contamination.

An alternative apparatus sold by Millipore called the Millicell ERS (Millipore, Bedford, MA) was found to work quite well for measuring monolayer resistance under aseptic conditions. This apparatus consisted of a much smaller portable ohmmeter (Figure 4.1) and incorporated the use of portable 'chopstick' electrodes, which could be easily sterilized with ethanol. The use of this system allowed us to track the resistance of the monolayers post-seeding, while still maintaining sterility. Because the chopstick electrodes may not provide an accurate resistance for the entire monolayer, but only for the region in which the measurement was made, readings were taken at three points around the monolayer and then averaged.

TEER values of 500-600 ohm·cm^2 for Caco-2 monolayers (Artursson et al., 1996) and 1500-3000 ohm·cm^2 for T84 monolayers (Dharmsathaphorn and Madara, 1990) are considered normal, and were used to indicate the health and confluence of the

Figure 4.1 Millicell ERS apparatus used to measure the transepithelial electrical resistance (TEER) of Caco-2 and T84 monolayers. [Source: Millipore, Inc.]

monolayers. Monolayers with lower than normal resistances were considered unable to maintain proper physiology and either were allowed to continue in culture until the desired resistance was reached, or were discarded.

Prior to electroporation, monolayers were rinsed with warm Hanks' Balanced Salts Solution (HBSS+) with Ca^{2+} and Mg^{2+} (Sigma Chemical, St. Louis, MO) supplemented with 10 mM HEPES and then placed in fresh electroporation medium (serum-free DMEM buffered with 25 mM HEPES). The presence of calcium in the rinse solution is necessary to maintain the integrity of monolayer tight junctions (Gonzalez-Mariscal et al., 1990). Since the rinse step could affect the resistance, the monolayers were returned to a 37^{o}C environment for 15-20 minutes until resistance recovered to within 10% of initial values.

4.2 Electroporation of Intestinal Epithelial Monolayers

4.2.1 Electroporation Apparatus

Electroporation was carried out using a high voltage pulser (BTX ElectroCell Manipulator 600, Genetronics, San Diego, CA) coupled with an adherent-cell cuvette with parallel, 4-mm gap, aluminum electrodes (InSitu™ Electroporation System, Thermo Hybaid, Middlesex, UK) (Figure 4.2). The BTX pulser supplied exponential-decay pulses and was capable of delivering voltages ranging from 10 V to 2500 V. By adjusting the resistance and/or the capacitance of the system, a wide range of pulse lengths could also be delivered. Multiple pulses required an interpulse spacing of at least 15 seconds to allow the pulser to recharge after delivering a pulse. The InSitu System was developed especially for electroporating adherent cells cultured on microporous membrane inserts. The inserts on which the monolayers were cultured fit inside the cuvettes as illustrated in Figure 4.3.

4.2.2 Electroporation Protocol

Exponential decay electric pulses were delivered at room temperature for voltages ranging from 30 to 400 volts, pulse lengths ranging from 1 to 20 ms, and pulse numbers ranging from 1 to 20 pulses. For multiple pulse conditions, the interpulse spacing was ~20 s. An oscilloscope (HP54602B, Hewlett Packard, Colorado Springs, CO) and a 10:1 voltage probe (Hewlett Packard) were used to measure the applied voltages and pulse lengths. For all experiments, the voltages are reported as the voltage applied to the electroporation cuvette. Voltages across the monolayer are expected to be much less (see Section 4.2.3). The pulse length was measured as the time constant,τ, of the exponential

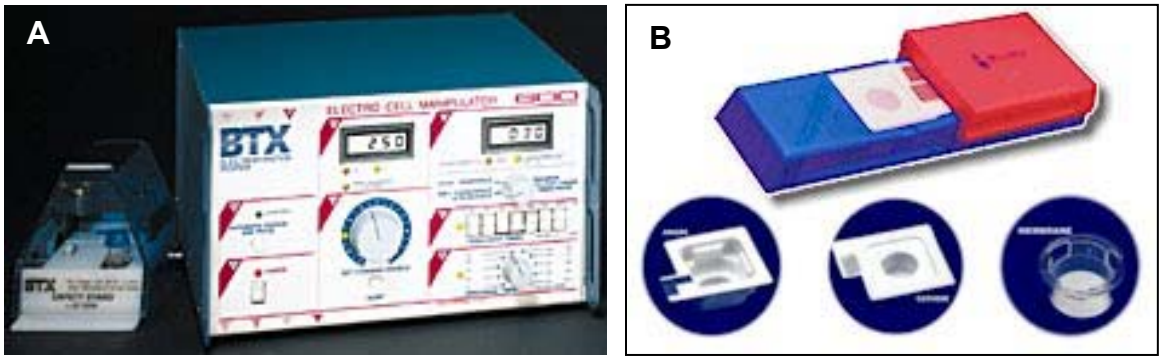

Figure 4.2 Electroporation system used for treating adherent monolayers. The BTX ECM 600 (A) was used to deliver exponentially decaying pulses to monolayers housed in the InSitu™ adherent cell electroporation chamber (B).

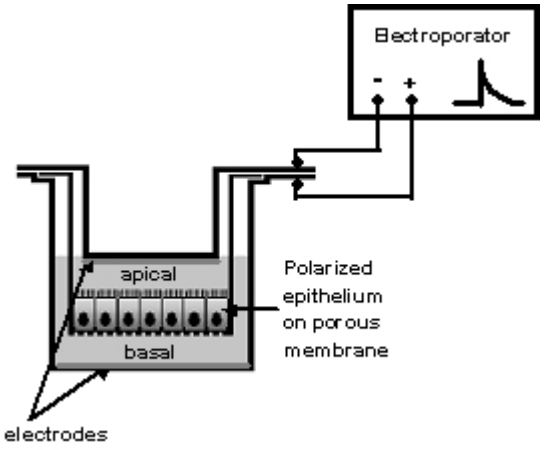

Figure 4.3 Diagram of polarized epithelial monolayer grown on a microporous membrane inside an electroporation cuvette. Electrodes located above and below the monolayer were connected to an electroporation pulse apparatus.

decay pulse, i.e., the time it takes for the voltage to drop from its maximum value to 1/e (~37%) of its maximum value (see Figure 4.4). Control monolayers were treated in the same manner, but were not pulsed.

4.2.3 Estimating Voltage Across the Monolayer

The voltage across the monolayers should be less than the voltage applied by the pulser due to voltage drops across the electrode-medium interface and within the culture medium. The voltage across the monolayers can be estimated by first electroporating a monolayer of cells and measuring the voltage ($V_{APPLIED}$) and current ($I_{APPLIED}$) applied by the pulser using an oscilloscope (Hewlett Packard) and a current monitor (#411, Pearson Electronics, Palo Alto, CA). Figure 4.4 shows representative voltage and current traces that can be used to determine the voltage across the monolayer. The traces were recorded using BenchLink XL software (Agilent Technologies, Palo Alto, CA).

The total resistance of the electroporation cuvette with cells, R_{TOTAL}, was then calculated using Ohm's law. Next, the cells were removed from the cell culture insert by trypsinization (see Section 4.3.2), and the same electrical condition was applied to the cell-free insert. Again voltage and current were measured and used to calculate the resistance of the cuvette with no monolayer, $R_{CUVETTE}$. The difference between R_{TOTAL} and $R_{CUVETTE}$ results in the approximate resistance of the monolayer during the pulse, $R_{MONOLAYER}$. Since the monolayer and the total system are in series with each other, the current through the monolayer is equal to the current through the total system. The voltage across the monolayer, $V_{MONOLAYER}$, can then be calculated as:

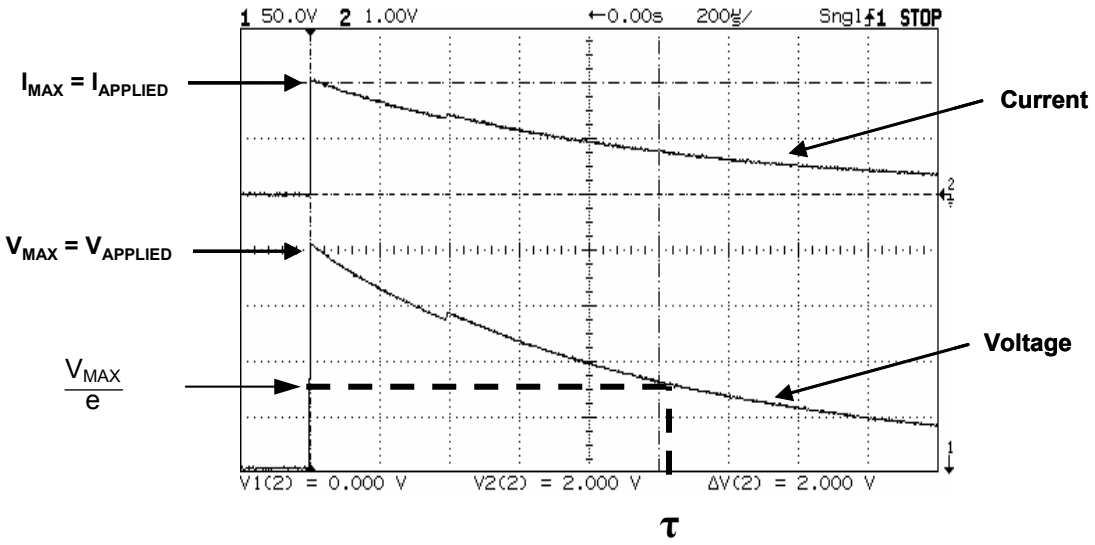

Figure 4.4 Representative current and voltage traces captured by the oscilloscope. Pulse length is determined as the length of time it takes for the voltage to fall from its maximum to 1/e (~2.718) its maximum. The x-axis represents time and the y-axis represents voltage. In this image, the scale for the x-axis is 200 µs/division. The scale for the y-axis is 50 V/division for the lower trace and 1 V/division for the upper trace. The upper trace is read in amps.

$$V_{MONOLAYER} = V_{APPLIED}\left(\frac{R_{MONOLAYER}}{R_{TOTAL}}\right) \quad (4.1)$$

Although the procedure for determining the voltage across the monolayer appears to be straightforward, there was some difficulty obtaining values that made sense. As illustrated in Figure 4.5, in many cases, subtracting the resistance of the cuvette from the resistance of the total system ($R_{MONOLAYER}$) resulted in negative values. The variability seen in these measurements could perhaps be due to differences in monolayer integrity, cuvette geometry, electrical conditions, and other small changes in the experimental conditions that affected the calculation. Because of this uncertainty in determining the voltage across the monolayer, all voltages reported in this study are the voltages applied to the cuvettes.

4.2.4 Fluorescent Uptake Marker Molecules

Two molecules were initially used to measure delivery to cells: calcein (623 Da, 0.6 nm radius) and fluorescein-labeled bovine serum albumin (BSA; 66,000 Da, 3.5 nm radius) (Molecular Probes, Eugene, OR). Both molecules are membrane-impermeant and fluoresce green when excited at 488 nm. A 1.5 ml[1] solution of electroporation medium containing 100 μM calcein or 10 μM BSA was placed on the apical (upper) side of a monolayer to model luminal administration of drugs. The monolayer was incubated for at least 5 minutes with the fluorescent molecules, placed in a cuvette with 3 ml of

[1] Note: The instruction manual for the InSitu System recommended 800 μL of medium on the apical side of the monolayers. This volume was not sufficient to allow the upper electrode to contact the medium and, as a result, had to be increased to 1.5 ml.

With Cells

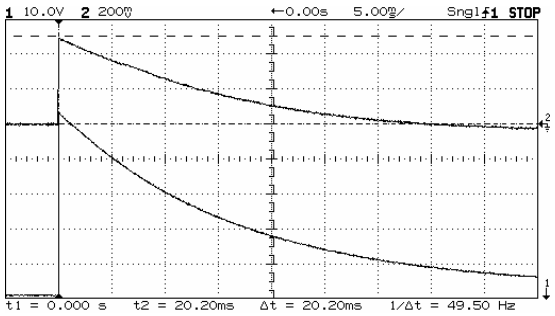

V_{MAX} (V)	I_{MAX} (A)	τ (ms)	R_{TOTAL} (Ω)
52.5	0.481	18.6	109.1

Without Cells

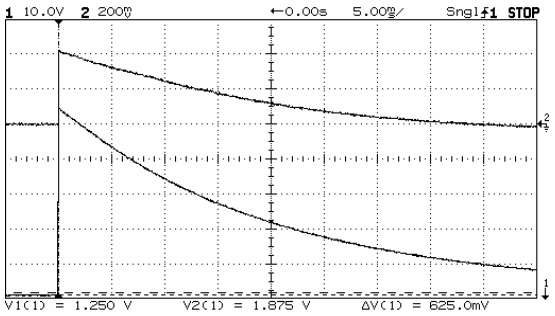

V_{MAX} (V)	I_{MAX} (A)	τ (ms)	$R_{CUVETTE}$ (Ω)
54.1	0.413	22.0	131.0

$$R_{CUVETTE} > R_{TOTAL}$$

Figure 4.5 Current and voltage traces used to determine total resistance of the system with cells (A; R_{TOTAL}) and without cells (B; $R_{CUVETTE}$). A monolayer of cells was electroporated at the reported condition. The cells were then trypsinized from the membrane and the same insert was electroporated again. This is an example of the results obtained when the calculated monolayer resistances were negative.

electroporation medium on the basal (lower) side, and pulsed. Immediately after pulsing, the monolayers were placed in a 37^{o}C dry incubator with warm DMEM on the basolateral side to recover for at least 15 minutes and were then incubated further until experiments with other monolayers were completed (≤ 1 h).

4.3 Fluorescence Analysis of Electroporation

Cell viability and molecular uptake of the fluorescent molecules were visualized and quantified using fluorescence microscopy and flow cytometry, respectively. Fluorescence microscopy (both epifluorescence and confocal) allowed us to verify uptake of marker molecules, as well as the localization of the molecules. Flow cytometry provided quantitative, statistically relevant information about the number of cells and their fluorescence properties.

4.3.1 Epifluorescence and Confocal Microscopy

Table 4.1 shows excitation and emission values for uptake and viability markers, as well as the various other dyes that were used to identify structures within the monolayers. Conventional epifluorescence images were made using an Olympus IX-70 inverted system microscope (Olympus America, Inc., Lake Success, NY) with a fluorescence attachment (IX-FLA inverted fluorescence observation attachment; Olympus). A short-arc, mercury lamp (OSRAM, Munich, Germany) was used to excite red and green fluorophores, which were detected with 515 nm and 610 nm longpass filters, respectively. Images were collected using a Spot RT™ Digital Camera (Diagnostics Instruments, Sterling Heights, MI) controlled by ImagePro Plus (ver.4.5,

Media Cybernetics, Carlsbad, CA) acquisition software. For analysis by conventional fluorescence microscopy, monolayers were imaged from the bottom of their inserts, which were seated in six-well plates. The media was replaced with HBSS+ to avoid background fluorescence from the phenol red present in DMEM.

Table 4.1 Fluorophores used for fluorescence microscopy and/or flow cytometry.

Fluorescent Molecule	**Staining Purpose**	**Laser Line (nm)**	**Peak Excitation (nm)**	**Peak Emission (nm)**	**Emission Color**
Calcein	Uptake	488	494	517	Green
FITC-BSA	Uptake	488	494	518	Green
Green Fluorescent Protein	Protein Expression	488	489	509	Green
Propidium Iodide	Viability	488, 543	536	617	Red
Hoechst 33342	Nucleus	351	347	483	Blue
FM 4-64	Lipid	543	515	640	Red

Unlike conventional fluorescence microscopy, which detects fluorescence throughout the entire sample, Laser Scanning Confocal Microscopy (LSCM) detects fluorescence only within the focal plane, while filtering out out-of-focus light. This allows one to optically section a 3-dimensional sample (e.g., a tissue) and obtain information from successive x-y planes while moving in the z-direction. This series of planes can then be digitally reassembled to provide a 3-D reconstruction of the sample.

For analysis by confocal microscopy after electroporation, monolayers were washed with HBSS+ as described above to remove residual media and marker molecules and then fixed in 3.7% paraformaldehyde solution at room temperature for 20-30 minutes. The fixed monolayers were washed again with HBSS+ and the membranes on which the monolayers were cultured were then excised from the inserts. The membranes were mounted onto microscope slides using a fluorescence antifade reagent as mounting medium (SlowFade, Molecular Probes)[2]. A laser scanning confocal microscope (LSM 510, Carl Zeiss Inc., Thornwood, NY) equipped with argon (351 nm and 488 nm) and helium-neon (HeNe; 543 nm) lasers was used to visualize incorporation and localization of calcein, BSA, and several other fluorophores in the monolayers.

Although fluorescence microscopy is very useful for qualitative analysis of the incorporation of marker molecules within the monolayers, quantitative information about how many molecules are take up is not so easily obtained, which is why flow cytometry is so useful. This technique allows one to observe the physical and fluorescence properties of individual cells and ultimately calculate the amount of uptake in each cell.

4.3.2 Flow Cytometry

Flow cytometry is one of the most widely used methods for measuring the properties of cells and other particles. The technique is based on the flow of particles in single file past a laser source. As the cells pass the laser, information about the light scattering and fluorescence properties of the cells is collected. Light that is scattered in the forward direction (forward scatter, FSC) because of diffraction provides information about the size of the cells. Light scattered at 90^{o} to the beam is referred to as side scatter

[2] Phenylenediamine also works well as an antifade reagent.

(SSC) and is an indicator of the granularity within the cell and the surface characteristics of the cell.

In a flow cytometer, the fluorescence of the cells is detected by a series of mirrors, filters, and splitters, which send the emitted light to a particular channel. Green fluorescence, such as that emitted by calcein, is typically detected in the FL1 channel. Orange-red fluorescence is usually detected in the FL2 channel. Red fluorescence is detected in channel FL3. These capabilities, along with the ability to analyze thousands of cells in a short period of time, make flow cytometry very useful in aiding our efforts to quantify molecular uptake and viability of the cells after electroporation.

4.3.2.1 Dissociation of Monolayers for Flow Cytometry

Since flow cytometry requires cells to be in single-cell suspensions, monolayers were dissociated after electroporation was completed to allow quantification of the fluorescence and scattering properties of each individual cell. Each monolayer was washed in warmed HBSS+ (with calcium and magnesium) to remove media and free calcein and BSA. A 0.5 ml solution containing 0.25% trypsin and 0.1% EDTA (Mediatech) warmed to 37^{o}C was applied apically and basally to dissociate the monolayers into individual cells. The apical volume of trypsin was then neutralized 5 minutes later (after incubation of monolayers in 37^{o}C incubator) by the addition of 3 ml of serum-supplemented DMEM. The cell suspensions were washed by centrifuging and decanting 4 times using cold PBS to remove any residual trypsin, media, calcein, or BSA. The first wash (3.5 ml) was done using a Beckman Coulter GS-6R centrifuge (3200 rpm,

1660 rcf). The remaining washes (0.5 ml) were done using an Eppendorf 5415C microcentrifuge (3000 rpm, 735 rcf).

After the final wash, cell pellets were prepared for flow cytometry analysis by resuspension in 0.5 ml of PBS with propidium iodide (Molecular Probes, Cat. #P-3566) and LinearFlow green fluorescent polystyrene microspheres (Molecular Probes, Cat. #L-14821) added to make a final concentration of 10 μg/ml and 120,000 microspheres/ml, respectively. Propidium iodide, which stains the nuclei of nonviable cells red, and the fluorescent microspheres, which serve as an internal volumetric standard, were used together to determine the fraction of cells remaining intact and viable after electroporation, as described below.

4.3.2.2 Flow Cytometry Analysis

Cell viability and molecular uptake of calcein and BSA were quantified using flow cytometry. Data were collected using a FACSort or FACSCalibur flow cytometer and CellQuest software (Becton Dickinson, Franklin Lake, NJ). In later experiments, the more advanced BD LSR flow cytometer, controlled by FACSDiva software (Becton Dickinson), was used. Each sample was run until data from ~20,000 viable cells were collected by the cytometer. The cytometer was able to distinguish between cells, microspheres, and cellular debris based on size and shape using light scatter measurements (forward scatter and side scatter) as illustrated in Figure 4.6A.

For the FACSort and FACSCalibur cytometers, the samples were excited using a 15-mW, 488-nm argon laser (Cyonics, now part of Uniphase Corp., San Jose, CA) to analyze for propidium iodide (FL3) and calcein/BSA (FL1) fluorescence using a 650 nm

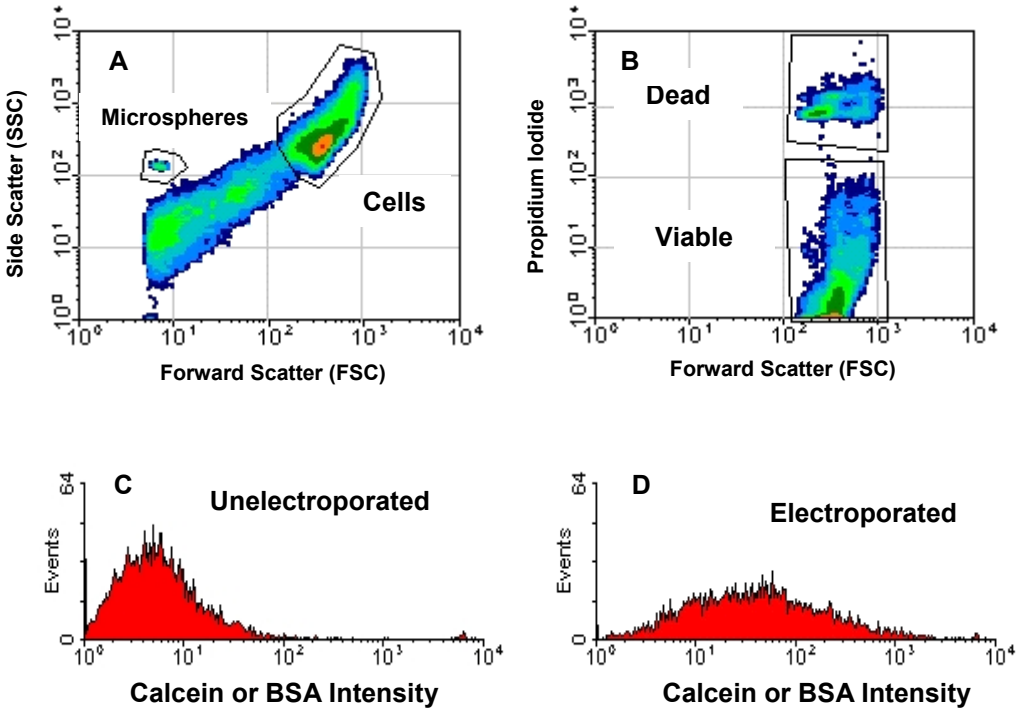

Figure 4.6 Representative density plots and histograms obtained by flow cytometry analysis of electroporated monolayers. (A) Cells and microspheres are identified on FSC vs. SSC plots and then (B) the cell population is further broken down into viable and dead cell populations based on propidium iodide fluorescence. (C,D) Fluorescence intensity histograms for the viable cell populations are then analyzed for an increase in fluorescence compared to controls, which indicates molecular uptake.

longpass filter and 530/30 nm bandpass filter, respectively. On the BD LSR flow cytometer, which was equipped with an argon laser (488 nm) and a HeNe laser (633 nm), FITC-like molecules and propidium iodide were detected using a 530/28 nm bandpass filter and 670 nm long pass filter, respectively. The concentration of viable cells in each sample was determined by multiplying the ratio of viable (propidium iodide negative) cells (Figure 4.6B) to microspheres by the known microsphere concentration. Percent viability could then be calculated by normalizing the viable cell concentration of each electroporated sample to the average concentration of the control samples. Calculating viability in this way takes into account cells that may have been physically destroyed during electroporation, as well as those remaining intact, but nonviable (Prausnitz et al., 1993). It should be mentioned that cells stained with propidium iodide can be either necrotic (death by lysis) or in the late stages of apoptosis (programmed cell death). No distinction was made between the two types of cells in our analysis.

The average calcein or BSA fluorescence intensity (see Figure 4.6C,D) of each sample was converted into the average number of molecules taken up by each viable cell using a set of quantitative, fluorescent calibration beads (Bangs Laboratories, Fishers, IN, Cat. #825) with fluorescence intensities (Figure 4.7A) that correspond to a known number of free fluorescein molecules, as described previously (Prausnitz et al., 1993). Briefly, a solution containing 2-3 drops of each of the four calibration bead suspensions was analyzed at the end of each flow cytometry experiment. Depending on the flow cytometry settings, the four bead populations had certain intensity values that showed a linear relationship with the number of fluorescein molecules associated with each population (see Figure 4.7B). The average fluorescence intensities of the analyzed cell

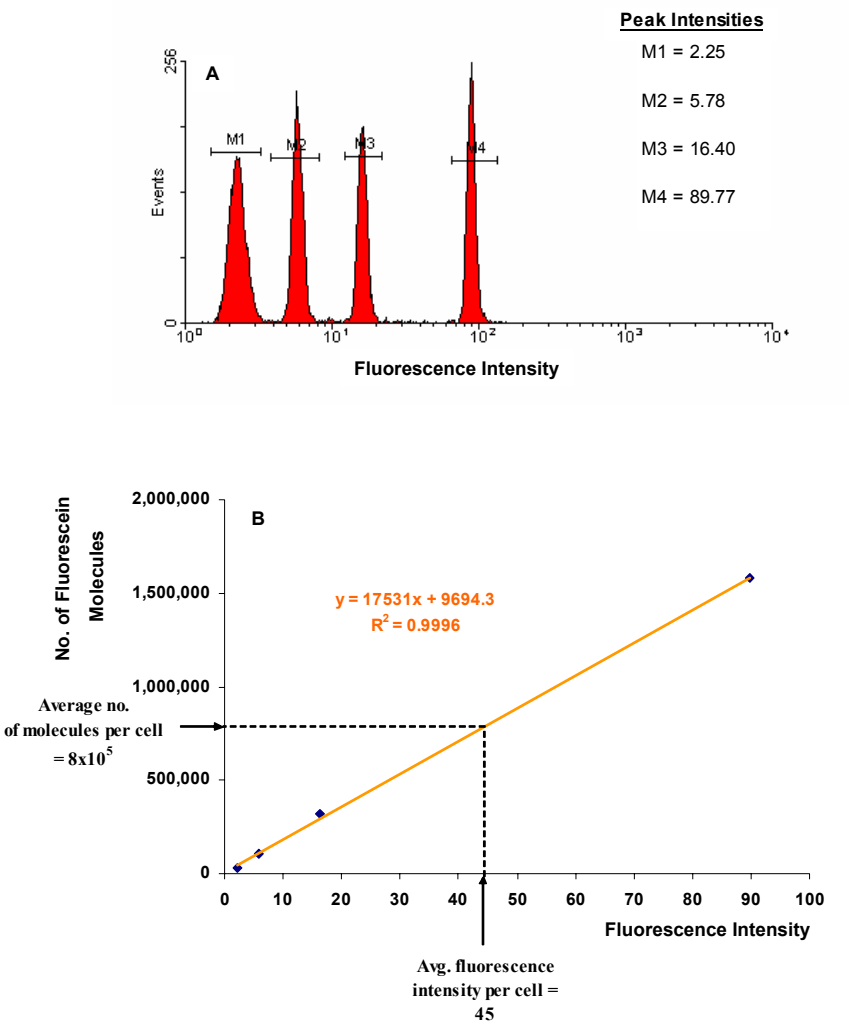

Figure 4.7 Calculation of molecular uptake using MESF calibration beads. (A) MESF beads are run on the flow cytometer after each experiment to obtain four populations of different fluorescence intensities. (B) A calibration curve of the number of fluorescein molecules associated with each bead population vs. the fluorescence of that population is then made. The average fluorescence of each event in a histogram, such as the ones shown in Figure 4.6, is converted to the average number of molecules per cell using this curve. An arbitrary average fluorescence value of 45 was chosen for this example.

samples could then be converted to the average number of fluorescein molecules based on that linear relationship.

Since the intensity of fluorescein is slightly different from that of calcein and BSA, a correction factor was employed to convert from the number of fluorescein molecules to the number of calcein or BSA molecules. The correction factor, which was calculated by fluorimetric analysis (Photon Technology International, South Brunswick, NJ) of equivalent concentrations of fluorescein and calcein or BSA, was determined to be 1.01 ± 0.20 for calcein and 0.93 ± 0.14 for BSA. Flow cytometry results were analyzed using the WinMDI Flow Cytometry Application (Scripps Research Institute Flow Cytometry Core Facility, http://facs.scripps.edu/).

4.4 Recovery of Monolayers After Electroporation

4.4.1 Physical Recovery of Monolayers

The recovery of monolayers after electroporation was measured using transepithelial resistance as an indicator of monolayer integrity. Each monolayer was electroporated under sterile conditions in HEPES-buffered DMEM with electroporation pulse conditions of different strengths: "mild," "moderate," and "strong". Although we believe flow cytometry measurements underestimate the actual cell viability in this study, as explained in Chapter 7, conditions yielding approximately 90%, 70%, and 50% viability according to flow cytometry were used as indicators of mild, moderate, and strong electroporation conditions. For Caco-2 monolayers, the conditions that were used to give these viabilities were 50V – 1 ms, 50 V – 10 ms, and 100 V – 10 ms, respectively.

The conditions used for the T84 monolayers were 50 V – 5 ms, 50 V – 20 ms, and 200 V – 5 ms, respectively (see Chapter 6). Using the Millicell ERS, transepithelial resistance measurements were made immediately (<25 s) and every minute after the electroporation pulse for 5 min. Successive measurements were made at 10, 15, and 30 min, 1, 2, 4, 6, 12, and 24 h, and then each day for up to 14 days. Media was replaced every 48 h.

During the course of the experiment, it was observed that temperature had a significant effect on the resistance of the monolayers. The difference in resistance was especially evident when resistances of monolayers that remained at room temperature during electroporation were compared to subsequent resistances measured immediately after removal from the 37^{o}C incubator. In order to minimize the effect of temperature on the recovery trends, electroporated monolayer resistances were normalized to those for unelectroporated monolayers. These normalized resistances were then normalized again to their initial (pre-electroporation) values. For each experiment, conditions were applied in triplicate and each experiment was repeated three times.

4.4.2 Functional Recovery of Monolayers

While conducting recovery experiments for T84 monolayers, samples of the basolateral medium (200 μl) were collected (an equal volume of fresh medium was added each time) at different time points after electroporation (0, 2, 4, 6, 12, 24 h) and tested for the presence of the inflammatory cytokine, IL-8. A colorimetric enzyme-linked immunosorbent assay (ELISA), which is used to detect a single protein in the presence of other proteins, helped determine the amount of IL-8 secreted after electroporation. IL-8

protein standards were prepared by making serial dilutions of a 20 ng/ml solution of recombinant human IL-8 protein (rhIL-8; R&D Systems, Minneapolis, MN).

In a 96-well plate, the IL-8 present in the standards and samples was detected with an anti-human IL-8 capture antibody (α-hIL-8; 8 μg/ml; R&D Systems, Minneapolis, MN), an anti-human IL-8 detecting antibody purified from rabbit serum (7.6 μg/ml; Endogen, Woburn, MA), and an anti-rabbit, horseradish peroxidase-conjugated antibody (71.5 ng/ml; Kirkegaard & Perry Laboratories, KPL, Gaithersburg, MD). When a peroxidase substrate (SureBlue™ TMP Microwell Peroxidase Substrate, KPL) was added, a blue color developed. The plate was read on an absorbance plate reader (UVMax, Molecular Devices, Sunnyvale, CA) at a wavelength of 650 nm and the standard curve was used to determine the amount of IL-8 in each sample. The linear portion of the standard curve typically ranged from 0.02 ng/ml to 1.25 ng/ml.

4.5 Transport across Monolayers after Electroporation

In addition to determining how many molecules are transported into the cells by electroporation, it was also of interest to determine whether electroporation enhanced the transport of molecules *across* the monolayers. In some cases, treatment of a disease or delivery of a vaccine may require a drug to cross the epithelial barrier to be effective. Transport across the monolayer was evaluated using calcein and fluorescein-labeled BSA as representative small and large molecules.

Monolayers of Caco-2 cells were cultured for 21-28 days as described above. Before starting the experiment, monolayers were washed and incubated in HBSS+

supplemented with 25 mM HEPES at 37°C for 30 minutes to acclimate them to the solution. Several six-well plates with 2 ml of HBSS+ in each well were also placed in the incubator. Calcein or BSA was added to the apical compartment (1.5 ml) to give an extracellular concentration of either 100 μM or 10 μM. For early experiments, monolayers were monitored every 15 min for six hours and unelectroporated monolayers served as controls. In later experiments, the baseline permeability of each monolayer was obtained by transferring the inserts on which the monolayers were grown to new wells containing fresh HBSS+ at 30 minute intervals for 3 hours prior to electroporation.

Electroporation was initially carried out using the mild and moderate electroporation conditions, 50 V - 1 ms and 50 V - 10 ms, respectively, used in the recovery experiments (Section 4.4). However, to determine whether permeability could be increased even further, ten 50 V - 1 ms pulses were also delivered to the monolayers. This condition has an effect that is essentially the same as the 50 V – 10 ms pulse (total exposure time is equivalent; see Section 6.2.3), but allows more time for diffusion of the markers across the cells between pulses. After electroporation, the inserts were transferred to fresh wells of HBSS+ every 30 minutes for three hours. With the exception of the time required to transfer the inserts and perform electroporation, monolayers were maintained at 37°C on an orbital plate shaker (RotoMix Model M50825; Barnstead Thermolyne, Dubuqe, IA) at ~90 rpm for the duration of the experiment. The transepithelial resistance of each monolayer was measured every hour for the three hours before and after electroporation. The permeabilities of calcein and BSA across cell-free filters, collagen-coated cell-free filters, and monolayers fixed with 95% ethanol at -20°C for 20 minutes were also measured for comparison.

To evaluate the passive diffusion of calcein through the paracellular space (between the cells) when tight junctions are opened, the monolayers were incubated in HBSS- (without Ca^{2+} and Mg^{2+}) for up to 40 minutes. Calcium is known to play a role in the maintenance of tight junctions (Gonzalez-Mariscal et al., 1990; Ma et al., 2000). Calcein in HBSS- (10 μM) was added apically and the monolayers were moved to fresh wells of basal HBSS- every 5 minutes. TEER was monitored to track the drop in resistance. After this treatment, the apical volume was replaced with calcein in HBSS+ (10 μM) and the monolayers were moved to fresh wells of basal HBSS+ every 5 minutes until TEER returned to about 90% of initial values.

Samples of the basal solutions in each well were analyzed for calcein or BSA concentration using a fluorescence plate reader (FluoStar Galaxy, BMG Technologies, Germany). Samples of the apical solution, collected at the very beginning of the experiment and at the end of the experiment, were also analyzed. One hundred microliters of each sample were dispensed into opaque, black, 96-well plates (Costar# 3944) along with known concentrations of the markers to make a standard curve. The plate was analyzed using an excitation wavelength of 485 nm and an emission of 520 nm.

The apparent permeabilities of calcein and BSA, P_{app} (cm/s), were calculated according the following equation derived from Fick's Law of Diffusion:

$$P_{app} = \frac{dQ}{dt} \times \frac{1}{AC_o} \tag{4.2}$$

where dQ/dt is the rate at which the molecule of interest appears in the receiver solution (mol/s), C_o is the initial concentration of the donor solution (mol/ml), and A is the growth area of the monolayer (4.7 cm^2). The appearance rate was calculated by plotting the accumulation of the number of moles of calcein or BSA in the samples collected versus

time and determining the slope of the resulting line. The initial concentration was measured from 50 µl samples taken from the apical solution at the start of each 3 hour period, i.e., at the start of measuring for baseline permeability and immediately before electroporation. Apical samples were diluted 1:1000 so that the fluorescence would not saturate the reader.

The concentration of calcein and BSA in the apical samples was on the order of 10^{-5} mol/L, although some concentrations were lower (perhaps due to dilution error). Concentrations of the two markers in the receiver solution were a few orders of magnitude less than the apical concentrations. Monolayers incubated with calcein had receiver sample concentrations on the order of 10^{-9} to 10^{-8} mol/L for unelectroporated monolayers and on the order of $5x10^{-8}$ to 10^{-7} for electroporated monolayers. Concentrations of BSA in the receiver solution samples ranged from 10^{-10} to 10^{-9} mol/l for unelectroporated monolayers and were about 7×10^{-9} mol/l for electroporated monolayers.

4.6 Reporter Plasmid Transfection

4.6.1 Plasmid Amplification and Purification

Two sets of plasmids that expressed either green fluorescent protein (GFP) or luciferase were used to evaluate electroporation as a tool for transfection of intestinal epithelial monolayers. The first set of plasmids, pEGFP-N1 (a GFP expression vector) and pGL3-Control (a luciferase expression vector sold by Promega, Madison, WI), were obtained in small amounts from BD Biosciences Clontech (Palo Alto, CA) and as a gift

from Dr. Harish Radhakrishna's laboratory, respectively. In order to have enough DNA for experiments, the plasmids were transformed into *E. coli* bacteria, amplified, and finally purified using procedures detailed in Appendix B.

Briefly, a small amount of either plasmid was introduced into competent E. coli cells by heat shock transformation. To check the transformation, a small liquid culture of bacteria was used to isolate ~20 µg of plasmid using a Qiaprep Miniprep Spin Kit (Qiagen, Valencia, CA). One or two micrograms of the newly isolated and original plasmids were cut by restriction digest and the resulting linear fragments analyzed by electrophoresis on a 1% w/v agarose gel containing 0.5 µg/ml of the fluorescent dye ethidium bromide. This allowed us to verify that the size and construction of the newly grown plasmid was the same as that of the original plasmid obtained from the manufacturer. Gels were viewed on a UV light box (Transilluminator, VWR Scientific, West Chester, PA) to verify that there was sufficient separation between bands and photographed using the AlphaImager™ 2200 Documentation and Analysis System (Alpha Innotech Corp., San Leandro, CA).

When the newly grown plasmid was confirmed to be the same as the original plasmid, a much larger bacterial culture was grown to isolate enough plasmid to use in experiments. The Qiagen Plasmid Giga Kit, which should yield ~10 mg of plasmid, was used to isolate and purify the plasmid according to the manufacturer's instructions. The purified plasmid was checked again on an agarose gel and its concentration was determined using a UV-capable spectrophotometer (Ultrospec 1100 *pro*, Biochrom Ltd, Cambridge, England) based on the relationship that 50 µg/ml of DNA has an optical density of 1.0.

Although amplifying and purifying the plasmid is very straightforward, the procedures required to do so for large amounts of plasmid were quite labor intensive, sometimes requiring as many as 3-4 days to complete. Many times the yields of the plasmid were relatively low (10-20% of the maximum yield) and variation in expression from different batches of plasmid could be large. For this reason, a switch was made to a new set of plasmids, the gWiz™ High Expression GFP (lot# 7018, 7491) and Luciferase (lot# 6591) vectors**.** These plasmids, which have modified promoters for increased protein expression, were developed by Gene Therapy Systems (San Diego, CA). Milligram quantities of both plasmids were obtained at a very reasonable price from Aldevron, Inc (Fargo, ND). Using these plasmids saved time and money and minimized variation in the results since a single lot of plasmid could be used for an entire series of experiments.

4.6.2 Green Fluorescent Protein Expression

Green fluorescent protein (GFP) was originally isolated from the bioluminescent jellyfish, *Aequorea victoria* (Tsien, 1998). It has rapidly become one of the most widely used reporter genes for studying transfection. The primary advantages of GFP are that its fluorescence is independent of the organism in which it is expressed and no other substrates or reagents are necessary for emission. In addition, the protein is very stable under many different conditions and its fluorescence can be observed in both live and fixed specimens (Schenborn and Groskreutz, 1999).

Wild type, or native, GFP (wtGFP) emits green light (508 nm) when it is excited by ultraviolet (395 nm) or blue (475 nm) light (Tsien, 1998). Recently, however, the use

of enhanced GFP (EGFP) has become popular because of its red-shifted excitation spectrum, which makes its excitation peak at 490 nm. This wavelength is especially well suited for use with most flow cytometers and confocal microscopes, which typically have 488 nm argon laser lines. Another advantage of using EGFP is that it has 4 to 35-fold brighter fluorescence than wtGFP. Although GFP expression can provide quantitative information about the number of cells that were transected, the drawback is that it is not as sensitive an assay as other reporters. As a result, when the protein is expressed at low levels, it can be difficult to detect by both flow cytometry and fluorescence microscopy.

Caco-2 and T84 monolayers were used for all GFP expression studies. Expression was assayed by fluorescence microscopy using the Olympus IX70 inverted microscope and the image acquisition software ImagePro Plus (Media Cybernetics). Monolayers were imaged *in situ* to track expression of the protein after transfection of the plasmid. GFP positive cells were identified and marked using the software program and an estimate of the density of cells showing GFP expression was made by dividing the number of GFP positive cells in a given field of view by the area of the field. The field area was determined by the software based on calibrations made with a micrometer under different powers of magnification.

4.6.3 Luciferase Protein Expression

Firefly luciferase is another commonly used reporter for evaluating gene transfection and expression. The ~61 kDa enzyme produced by a gene isolated from the firefly, *Photinus pyralis*, catalyzes the oxidation of its substrate, luciferin, in the presence of ATP and Mg^{2+} and produces light. The light emitted by this chemiluminescent reaction

occurs as a flash and then rapidly decays in seconds. With the addition of coenzyme A (CoA), light emission lasts for at least one minute. This sustained emission provides more reproducible results and increased sensitivity (Schenborn and Groskreutz, 1999). The light produced is directly related to the catalytic activity of luciferase and can be detected using a luminometer or a scintillation counter. Luminometers can detect as little as 0.001 pg of luciferase, making luciferase one of the most sensitive reporters available. The primary disadvantage of the luciferase reporter assays is that since the cells are lysed to release the protein, it is not possible to obtain quantitative information about the number of cells that were transfected.

T84 monolayers were used for all luciferase transfection experiments with electroporation and lipofection. After the monolayers were treated and allowed to express luciferase, they were washed in PBS and lysed in 200 µL of Cell Culture Lysis Reagent (CCLR; Promega) according the manufacturer's instructions. The cell lysate was assayed for luciferase expression in opaque, white 96-well plate (OptiPlate™-96, Packard Biosciences) using the Luciferase Assay System (Promega) and a plate reading luminometer (LumiCount™, Packard Biosciences, Perkin Elmer, Boston, MA). Since luminescence was constant for only 1 minute, no more than six wells were read at a time. Each well was read in triplicate and read for two seconds each time. The three readings were averaged for each well and are reported as relative light units (RLU).

Luciferase expression in relative light units is usually normalized to the amount of protein present in the cell lysate, which corresponds to the number of cells present. Protein concentration was determined using the modified Bradford assay. The method is based on the addition of an acidic solution of the dye Brilliant Blue G to the protein

solution. The complex formed between the dye and the protein shifts the dye absorption maximum from 465 nm to 595 nm. Either Bradford Reagent (Sigma Aldrich) or 5X Bio-Rad Protein Assay Reagent (Bio-Rad) was mixed with the cell lysates in 96-well plates (Fisher Scientific). Serial dilutions of bovine serum albumin (BSA) were prepared in CCLR to serve as protein standards. Since the detergent present in CCLR interfered with the dye solution, the cell lysates and the BSA protein standards were diluted 1:10 in water. A plate reading spectrophotometer (SpectraMAX, Molecular Devices) was used to read the plate at a wavelength of 595 nm. The approximate protein concentration in each sample was calculated based on the BSA standard curve.

4.6.4 Methods of Transfection

4.6.4.1 Lipid-Mediated Transfection

Two lipid-based transfection systems were used in these experiments. Lipofectin® Reagent (Invitrogen) is a 1:1 (w/w) mixture of two cationic lipids, DOTMA[3] and DOPE[4]. It was used in initial experiments to test the use of lipids for DNA transfection in subconfluent and confluent intestinal monolayers. The LipoTAXI® Mammalian Transfection Kit (Stratagene, La Jolla, CA) is a proprietary lipid formulation and was used in all subsequent DNA transfection experiments on confluent monolayers and for comparison with electroporation.

Initial experiments with Lipofectin were conducted to become familiar with the process of transfecting monolayers with lipids. The protocol provided by the manufacturer was followed with little modification. Subconfluent and confluent Caco-2

[3] DOTMA: N-[1-(2,3-dioleoyloxy)propyl]-N,N,N-trimethylammounium chloride
[4] DOPE: dioleoyl phosphatidylethanolamine

and T84 monolayers were treated with either 30 μg or 60 μg of Lipofectin and either 5 μg or 10 μg of pEGFP-N1 in ~1.5 ml of 25 mM HEPES-buffered DMEM. Control monolayers were treated with DNA and no lipid. The monolayers were incubated at 37^{o}C and checked for GFP expression by fluorescence microscopy at 24, 48, and 96 hours after addition of the lipid.

LipoTAXI, which, according to its manufacturer, is a low toxicity lipid solution, was used to deliver various plasmids to confluent T84 monolayers. For GFP expression experiments, monolayers were treated with either 0.05 mM or 0.08 mM LipoTAXI and 10 μg pEGFP-N1. The gWiz-luciferase expression plasmid was used in the majority of the experimental comparisons with electroporation. Again the protocol supplied by the manufacturer was used with little modification. To identify the "optimum" condition that would be used for comparison with electroporation, the LipoTAXI concentration and amount of DNA was varied from 0 mM to 0.1 mM and 5 μg to 30 μg, respectively. The monolayers remained in culture 24-72 hours after lipid addition depending on the experiment or the reporter being used.

4.6.4.2 Electroporation-Mediated Transfection

Confluent T84 monolayers were used for gene delivery experiments using electroporation. The amount of plasmid DNA was varied from 5 μg to 60 μg, depending on the experiment and the plasmid. In all cases, the appropriate amount of DNA was diluted in 1 ml of 25 mM-buffered DMEM in a microcentrifuge tube. The T84 monolayers were washed once with DMEM and left with 2 ml of DMEM on the basal side. The DNA solution was then added drop-wise to the monolayers along with 0.5 ml

of DMEM (to bring the total volume to 1.5 ml for electroporation) and allowed to incubate with the monolayers at room temperature for ~20 min. It has been shown that a preincubation period with DNA increases transfection efficiency in cells (Xie et al., 1990; Klenchin et al., 1991). The TEER for each monolayer was measured prior to electroporation to ensure monolayer integrity.

Many researchers have employed electroporation for *in vivo* gene delivery experiments (Oshima et al., 1998; Rols et al., 1998; Dujardin et al., 2001). A common theme in some experiments is that increased transfection efficiency results when cells or tissues are first permeabilized with short (μs), high voltage pulses followed by electrophoresis of the DNA into the resulting holes using multiple low voltage, long pulses (ms) (Klenchin et al., 1991; Bureau et al., 2000; Satkauskas et al., 2002). A similar approach was used for the T84 monolayers using 300 V - 300 μs as our high voltage (HV) pulse and 25 V – 20 ms as our low voltage (LV) pulse. The high voltage condition was chosen because ~300 μs was the shortest pulse length the BTX pulser was capable of delivering. A quick TEER recovery test was conducted using this pulse length, to determine whether a 400V pulse would result in an acceptable length of recovery. However, since the monolayer pulsed with 300V recovered more quickly (1 day vs. ~4 days), this voltage was chosen for our high voltage pulse.

The high and low voltage pulses were applied as single pulses, multiple pulses, or in some combination of the two. In addition to varying the electroporation conditions, the amount of plasmid was also varied. Immediately after electroporation, the monolayers were transferred to a six-well plate with 2 ml of warm T84 growth medium in the wells. T84 medium with 24% calf serum (0.5 ml) was added apically to make a total volume of

2 ml with 6% serum. The monolayers were then placed in a 37°C incubator for 24-72 hours (depending on the experiment) to allow expression of the protein of interest.

4.6.5 DNA Uptake Protocol

To evaluate DNA uptake (not expression) in the monolayers after lipofection and electroporation, plasmid DNA (either gWiz™-Luciferase or gWiz™-GFP) was stained with the high affinity nucleic acid stain YOYO®-1 iodide (YOYO-1; Molecular Probes). YOYO-1 can be excited at 488 nm with an argon laser and detected at 509 nm. Plasmid DNA was stained with YOYO-1 at a molar ratio of 100:1 (DNA bp:dye molecule). This ratio corresponded to 150 μg of DNA and 2.3 μl of 1mM dye stock solution. The plasmid and DNA were mixed and incubated at room temperature for 60 minutes in a light sensitive microcentrifuge tube. Stained DNA was stored at ≤ 4°C. Pre-stained DNA was transfected as usual into monolayers by electroporation and lipofection as described in Section 4.6.4.

4.7 IκB-Expression Plasmid Delivery

As stated in the Background section, a potential treatment for chronic intestinal disorders could involve the use of gene therapy. Since electroporation has been used extensively as a gene delivery tool, it is very possible that it could be useful in this situation as well. To evaluate whether electroporation could be used to inhibit the NFκB-mediated inflammatory pathway by gene delivery, a plasmid that expressed the inhibitory protein IκB was introduced into confluent T84 monolayers and monitored for

its effects on inflammation in the cells. The amplification and purification procedures used to grow up this plasmid can be found in the Appendix.

4.7.1 Electroporation with IκB-HA Plasmid

Confluent T84 monolayers were electroporated with 20 μg/ml of the plasmid pIκB-HA using the high voltage pulse plus multiple low voltage pulses protocol (see Section 4.6.4). When the plasmid is introduced into cells it expresses the protein IκB with a hemagluttinin (HA) sequence incorporated into the protein. This tag allowed us to distinguish between endogenous IκB and the IκB expressed by the plasmid because the HA tag makes the expressed protein larger than the endogenous protein (43 kDa vs. 37 kDa). Monolayers electroporated with pEGFP-N1 and gWiz-Luc, as well as unelectroporated monolayers, were used as controls. Monolayers were allowed to recover and express the protein overnight (no more than 24 h) at 37°C. During the recovery period, samples (205 μl) of the basal medium were collected and tested for the presence of IL-8 by ELISA (See Appendix for protocol). This assay would tell us whether the IκB-HA expressed during this time, inhibited the temporary inflammatory response observed after electroporation.

After recovery, monolayers were stimulated basally for 6-8 hours with human tumor necrosis factor (hTNF-α; 10 μg/ml; R&D Systems) at a concentration of 10 ng/ml in complete medium. Samples of the basal medium were collected before and after TNF stimulation and tested for IL-8 secretion by ELISA. Both stimulated and unstimulated monolayers that had not been exposed to electroporation were used as controls.

4.7.2 Analysis of IκB-HA Expression

SDS-PAGE and Western blot analysis were used to determine whether IκB-HA was expressed. SDS-PAGE (sodium dodecyl sulfate polyacrylamide gel electrophoresis) involves the separation of proteins in a sample by electrophoresis through a polyacrylamide gel, which separates the proteins according to their molecular weights (larger proteins migrate more slowly through the gel). Western blotting involves the electrical transfer of the separated proteins to a nitrocellulose membrane and the subsequent detection of the protein of interest using a detecting antibody and a labeled reporting antibody. Please see the appendix for solution recipes and more detailed descriptions of the different procedures.

After TNF stimulation, the monolayers were washed twice with HBSS+ and then lysed on ice in 500 μL of SDS lysis buffer using a rubber policeman. Protein electrophoresis was carried out using the Lamelli discontinuous gel system (Sambrook et al., 1989; Sambrook and Russell, 2001) composed of a 12.5% polyacrylamide lower separating gel and a 4.5% polyacrylamide upper stacking gel, which were used to identify and detect both endogenous and expressed IκB. The gel was placed in a vertical electrophoresis system (Mini-PROTEAN 3 Cell System, Bio-Rad), connected to a DC power supply (PowerPac 300, Bio-Rad), and run at 100 V for approximately ~2 hrs.

After the proteins were separated, they were transferred at 4°C by electrophoresis to a small piece of nitrocellulose membrane (Trans-Blot Transfer Medium; BioRad) at 200 mA for 2 hours. The nitrocellulose membrane was then blocked and probed with the necessary antibodies. To detect the presence of IκB, two primary (1°) antibodies were used: 1) a mouse monoclonal antibody to hemagglutinin (α-HA, 1 mg/ml, Covance,

Berkeley, CA) to detect expressed IκB-HA and 2) a rabbit polyclonal IgG antibody to IκBα (α-IκBα, 0.2 mg/ml, Santa Cruz Biotechnology, Santa Cruz, CA) to detect both endogenous and expressed IκBα. The 1° antibodies were diluted 1:200 for α-HA and 1:1000 for α-IκBα. The 2° antibodies for α-HA and α-IκBα were, respectively, a peroxidase-conjugated goat antibody to mouse immunoglobulins (α-mouse HRP, 1 mg/ml, ICN Pharmaceuticals, Aurora, OH) and a peroxidase-conjugated donkey antibody to rabbit immunoglobulins (α-rabbit HRP; Amersham Bioscience, Piscataway, NJ). Both antibodies were diluted 1:1000.

ECL™ Western Blotting Detection Reagents (Amersham Bioscience), which emit light in a chemiluminescent reaction with horseradish peroxidase, were used to detect the labeled proteins. The blot was then exposed to autoradiograph film (XOMAT; Eastman Kodak, Rochester, NY) for the following exposure times: 5 s, 30 s, 1 min, 2 min, 5 min, and 30 min, in a dark room. The films were developed using a developer (M35 XOMAT Processor, Kodak) and the exposed protein bands observed on a light box. Band intensities were quantified and compared using the publicly available ImageJ software (version 1.3, National Institutes of Health, http://rsb.info.nih.gov/ij/)

4.8 IκB Plasmid Co-transfection Experiments

After a few experiments with electroporating pIκB-HA alone into T84 monolayers, it was observed that IL-8 secretion was not being inhibited by the expressed IκB-HA. We surmised that IκB-HA was probably not being expressed in a high enough number of cells to completely inhibit IL-8 secretion by the monolayers because of low transfection

efficiency. It is possible that the IL-8 secretion by those cells that were not transfected with the plasmid overwhelmed the decrease in secretion by the transfected cells. To see if this problem could be avoided, a different approach was used. Instead of assaying the effect of transfection on the entire monolayer, only the effect on those cells that took up the plasmid would be assayed by co-transfecting pIκB-HA with another plasmid that expressed a reporter protein when the cells are stimulated by TNFα.

4.8.1 pIκB-HA/pIL8-CAT Co-transfections

In the first set of co-transfection experiments, the plasmid that expressed IκB-HA was co-transfected with a plasmid that expressed the enzyme chloramphenicol acetyl-transferase (CAT) upon the binding of NFκB to its IL8 promoter (pIL8-CAT). CAT is yet another reporter protein, similar to GFP and luciferase, which has been used extensively to study gene transfection (Roche Biochemicals). The amplification and purification procedures used to grow up pIL8-CAT can be found in the Appendix.

In these experiments, confluent T84 monolayers were electroporated with pIκB-HA and pIL8-CAT (obtained as a gift from the laboratory of Dr. Andrew Neish), at the same time using the high voltage-low voltage pulse protocol described in Section 4.6.4. The two plasmids were electroporated in equal amounts (1:1 ratio) into the cells. The following controls were also included in the experiment: a monolayer electroporated with no plasmid, an unelectroporated monolayer with pIL8-CAT, a monolayer electroporated with pIL8-CAT, and a monolayer co-transfected with pEGFP-N1 and pIL8-CAT (1:1 ratio).

After electroporation, the monolayers were incubated at 37°C overnight (16-18 hours) for recovery and to allow expression of IκB-HA. They were then washed with warm DMEM and exposed basally to 10 ng/ml TNFα in complete media (2 ml) for 6-8 hours to stimulate IL-8 production. After TNF stimulation, the monolayers were lysed in 500 μL of lysis buffer provided in a commercially available CAT ELISA kit (Roche Molecular Biochemicals, Germany) and analyzed for CAT expression according to the manufacturer's instructions. The released NF-κB should bind to the promoter of the pIL8-CAT plasmid and initiate the expression of CAT. If IκB-HA has been expressed in sufficient quantity to inhibit NFκB, CAT expression should be decreased.

Although pIκB-HA/pIL8-CAT co-transfections were attempted several times, CAT levels were always found to be negative (data not shown). One reason for this could be that the amount of CAT expressed after IL-8 binding was below the detection limit of the assay (50 pg/ml or 10 pg/well). To test that this was the problem, a standard CAT reporter plasmid, pCMV-CAT (obtained from Dr. Lauren Collier, a member of Dr. Neish's lab), which did not require the presence of another molecule for expression, was electroporated into T84 monolayer and assayed for CAT expression after 48 hours. Again, CAT expression assayed by ELISA was negative. Since the amount of CAT being expressed was too low to detect by ELISA, a change was made to use luciferase as the reporter. Luciferase assays are much more sensitive than CAT and other reporter assays. As little as 0.001 pg of luciferase (10,000x that of CAT) can be detected in most cases (Promega).

4.8.2 pIκB-HA/pNFκB-Luc Co-transfections

Co-transfection experiments were repeated using pIκB-HA and a plasmid that expressed luciferase when free NFκB binds to its promoter (pNFκB-Luc; obtained from the laboratory of Dr. Neish). The two plasmids were electroporated into T84 monolayers at a specified ratio using the same pulsing protocol. For most experiments, the amount of pNFκB-Luc was held constant at 15 μg, while the amount of pIκB-HA was varied (see Table 4.2). A standard luciferase reporter plasmid, pCMV-Luc (also obtained from Dr. Neish), was electroporated under the same conditions, and at the same ratios with pIκB-HA, as a control. The plasmids were amplified and purified using standard molecular biology techniques (see Appendix).

Table 4.2 Amounts of plasmids used in pIκB-HA/pNFκB-Luc co-transfection experiments.

pNFκB-Luc/pIκB-HA Ratio	pNFκB-Luc (μg)	pIκB-HA (μg)
pNFκB	15	0
pNFκB/pIκB (1:1)	15	15
pNFκB/pIκB (1:2)	15	30
pNFκB/pIκB (1:4)	15	60

After electroporation the monolayers were incubated at 37°C and allowed to recover overnight. The old media was removed and the apical volume (2 ml) replaced with fresh complete media, while the monolayers were exposed basally to 10 ng/ml TNFα in complete media (2 ml) for 6-8 hours to stimulate IκB degradation and NFκB

release. A companion set of monolayers, which were electroporated with the same amount of the two plasmids, but were not exposed to TNF was also included as a control. The monolayers that were not exposed to TNF should yield very little luciferase expression, since there is no trigger for the release of NFκB. The TNF-stimulated monolayers should show a significant increase in luciferase expression compared to the unstimulated monolayers.

At the end of the stimulation period, the monolayers were washed twice with PBS and then lysed in 200 μL Promega's Cell Culture Lysis Reagent (CCLR) according to the manufacturer's instructions. The cell lysates were stored at -70°C until ready for analysis of luciferase expression, as described in Section 4.6.3, using the Luciferase Assay System (Promega) and a plate reading luminometer (LumiCount™). The protein content in each of the lysates was determined by the modified Bradford assay so that the amount of light produced could be normalized to an approximation of the number of cells present.

4.9 Gene Silencing by siRNA Transfection

4.9.1 Electroporation of siRNA

These experiments were conducted to test whether electroporation could efficiently introduce short, interfering RNA (siRNA) into confluent intestinal epithelial monolayers and knockdown the production of a protein of interest by RNA interference (RNAi). The nuclear envelope proteins, lamin A and lamin C (lamin A/C), have become the standard proteins used to demonstrate the ability of siRNA to mediate gene silencing in mammalian cells (Elbashir et al., 2001a), and were chosen for these experiments as well.

A new electroporation cuvette setup was used for all siRNA transfection experiments. The new cuvettes were designed by Dirk Hunt and Brian Babbin, members of the laboratory of Dr. Asma Nusrat, especially for use with monolayers grown on smaller membrane inserts. These inserts required a much smaller apical electroporation volume (100 μl vs. 1.5 ml for the larger cuvettes used in previous experiments). As a result, more experiments could be carried out with much less reagent.

T84 cells were harvested and seeded as described in Section 4.1 onto collagen-coated Transwell microporous cell culture inserts in 24-well plates. The inserts had a growth area of 0.33 cm^2 and a pore size of 0.4 μm (Costar #3470). The monolayers were incubated in a 5% CO_2, 37^oC environment and maintained in culture for 7-10 days before use. Transepithelial electrical resistance (TEER) was monitored to ensure monolayer integrity.

Lamin A/C siRNA was obtained from Qiagen-Xeragon (Germantown, MD) along with non-silencing, FITC-labeled siRNA to serve as a control. When the monolayers were ready, they were washed twice with DMEM and then an appropriate amount of siRNA suspended in 100 μL of HEPES-buffered DMEM was added apically. The monolayers were electroporated at a condition of 50V – 20 ms. The amount of lamin siRNA and the amount of time allowed for turnover of the protein were varied to identify conditions that yielded the greatest silencing effect. Unelectroporated monolayers and monolayers that were electroporated with no siRNA present also served as controls. Immediately after electroporation, the monolayers were transferred to a 24-well plate with 1 ml of warm T84 growth medium in the wells. T84 medium with 12% calf serum (100 μL) was then added apically to bring to a total volume of 200 μL with 6% serum.

The monolayers were then placed in a 37°C incubator for 24-72 hours (depending on the experiment) to allow silencing of the protein of interest.

4.9.2 Analysis of Gene Silencing

SDS-PAGE and Western blotting were used to confirm whether the siRNA electroporated into the T84 monolayers inhibited the production of lamin A/C (see Appendix for detailed protocols). At the end of each experiment, the monolayers were lysed, on ice, in 50 μL of SDS lysis buffer. In this case, 15 μL of sample were loaded into a 4.5% polyacrylamide stacking gel and separated on a 7.5% polyacrylamide gel. Using a lower percentage gel put lamin A/C, which have molecular weights of ~70 kDa, in the middle of the gel at the end of the run. The proteins were transferred to a nitrocellulose membrane blot, which was then blocked and probed with a mouse monoclonal IgG antibody to lamin A/C (1:500; type 636; Santa Cruz Biotechnology) followed by a peroxidase-conjugated goat antibody to mouse immunoglobulins (1:1000; ICN Pharmaceuticals). The blot was placed in ECL ™ for one minute, dried, and then exposed to autoradiography film for specific periods of time up to 10 minutes.

To ensure that any decrease in the amount of lamin A/C observed in the Western blot was due to silencing and not to a decrease in the number of cells after electroporation, endogenous IκB was used as an internal standard. The membrane blot was stripped to remove the lamin A/C primary and secondary antibodies and re-probed with the antibodies used to detect IκBα (see Section 4.6.2). The presence of bands of similar intensity for all samples should indicate that there is little cell loss after electroporation.

Immunofluorescence staining was used to visualize the lamin proteins (see Immunofluorescence Protocol #2 in Appendix). A counterstain for the tight junction protein JAM was used to help identify the cell boundaries. After the monolayers were electroporated with lamin siRNA and incubated to allow silencing to take effect, they were probed with the 1° antibodies mouse monoclonal anti-lamin A/C (1:200; Santa Cruz Biotechnology) and rabbit polyclonal anti-JAM (1:1000; obtained from the laboratory of Dr. Charles Parkos, Emory University) and he 2° antibodies, a FITC-labeled (green) anti-mouse antibody and a TRITC-labeled (red) anti-rabbit antibody (both from Jackson Immunochemicals). The membranes on which the monolayers were cultured were excised and mounted, cell-side up, in p-phenylenediamine (an anti-fade reagent) on microscope slides and then viewed by confocal microscopy.

4.10 Statistical Analysis

Unless otherwise stated, each data point represents the average (mean) of at least three replicates for all of the graphs presented in this study. Either the standard deviation of the mean (SD) or the standard error of the mean (SEM) was calculated and used to make the error bars. When a comparison between two or more means was required, a one-way analysis of variance with a 95% level of confidence (ANOVA, $\alpha = 0.05$) was used. Two-way ANOVAs were used to determine the dependence of a population on two independent variables. A p-value < 0.05 was considered to indicate statistical significance.

CHAPTER V

5. ELECTROPORATION OF MODEL INTESTINAL EPITHELIUM

5.1 Introduction

Electroporation is used extensively to deliver molecules such as drugs, proteins, and genes to a wide variety of cell types (Chang et al., 1992; Nickoloff, 1995). The majority of these experiments have involved placing cells in suspension and then electroporating them in a cuvette. Unfortunately, trypsin, the most common method used to chemically dissociate adherent cells can affect the cellular membrane (Vogel, 1978). In addition, when adherent cells are dissociated, they lose many characteristics they would normally have possessed when in their correct geometry (Zheng and Chang, 1991). Therefore, the ability to carry out electroporation on adherent cells is necessary to ensure a more accurate representation of *in vivo* conditions.

A wide variety of methods for electroporating adherent cells have been developed over the years. Some techniques involved plating the cells on glass coverslips or plastic tissue culture dishes and electroporating them with electrodes of different geometries, e.g., parallel wire (Zheng and Chang, 1991) or concentric ring (Liang et al., 1988; Bright et al., 1996) electrodes. Other techniques involved actually plating the cells on one of the electrodes, which could be small pieces of gold-film (Ghosh et al., 1993; Wegener et al., 2002) or glass slides coated with an electrically conductive material (Raptis et al., 1995a; Raptis et al., 1995b; Firth et al., 1997). A counter electrode could then be used to deliver the pulses.

A limitation of these studies is that they all required specially designed electrodes and, in some cases, electroporation pulsers. In addition, plating on nonporous glass or

plastic would not be ideal for polarized epithelia since these cells only form the desired columnar structure when cultured on porous membranes (Madara et al., 1987). In one study conducted by Yang et al. (1995), cells were grown on microporous membranes that had been cut into strips. The strips were then electroporated in a standard cuvette used for cell suspensions. The InSitu™ adherent cell electroporation chamber was used in this study, which allowed the monolayers to be cultured on a rigid membrane insert and remain there during electroporation and the subsequent recovery period.

To determine if polarized model intestinal epithelial monolayers could be electroporated, confluent monolayers of Caco-2 and T84 human colon carcinoma cells were subjected to electric pulses while bathed in an apical solution containing either calcein, a small molecule (623 Da), or fluorescein-labeled bovine serum albumin, a globular protein (BSA; 66,000 Da). Laser scanning confocal microscopy was used to image uptake of fluorescent molecules and cell death in monolayers exposed to electric pulses expected to cause electroporation. Confocal microscopy allowed us to also visualize both the extent and distribution of uptake within cells of the monolayer. Histological staining was employed to further determine the effects of electroporation on the monolayers.

5.2 Experimental Results

5.2.1 Intestinal Epithelial Models Take Up Molecules after Electroporation

Figure 5.1 shows representative confocal micrographs of control and electroporated monolayers that were incubated with calcein or BSA. Control monolayers exposed to calcein or BSA in the absence of an electric pulse took up essentially no marker

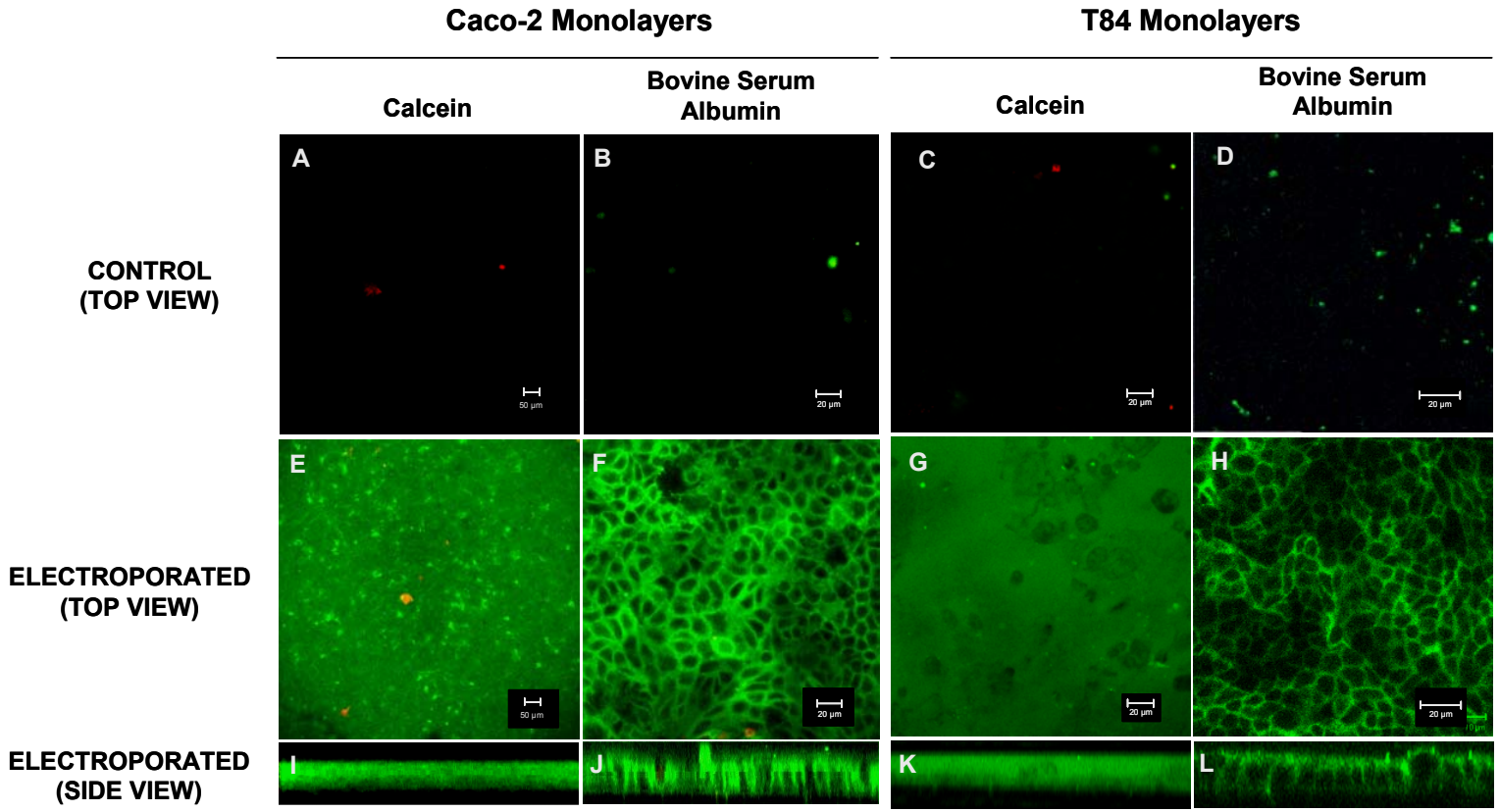

Figure 5.1 Confocal images illustrating uptake of calcein and BSA in electroporated Caco-2 and T84 monolayers. While unelectroporated monolayers show almost no fluorescence (A-D), uptake of calcein (E,G) and BSA (F,H) is seen in x-y sections of the monolayers for both cell types. Cross-sectional (z-section) views further demonstrate intracellular localization of the molecules (I-L). Monolayers electroporated with BSA exhibited nuclear exclusion of the protein because of its large size.

compounds (Figures 5.1A-D), whereas monolayers exposed to a single electroporation pulse contain large amounts of intracellular calcein (Figures 5.1E and 5.1G) and BSA (Figures 5.1F and 5.1H). Calcein delivery appears to occur throughout each cell, whereas BSA is present throughout the cytosol, but excluded from the nucleus.

These observations are further supported by images from cross-sectional views of monolayers, which show calcein throughout the cell interiors (Figures 5.1I and 5.1K) and BSA filling the cytoplasm outlining the nuclei (Figures 5.1J and 5.1L). In addition, when monolayers were observed under low power magnification, the distribution of calcein and BSA uptake appeared to occur uniformly over the entire monolayer, i.e., there were no 'hot spots' of high fluorescence intensity (data not shown).

5.2.2 Cell Death Results after Electroporation

Although a significant amount of uptake can take place after electroporation, cell death can also occur. For some electroporation conditions, cells began lifting off the membrane within 24 hours after treatment, leaving holes in the monolayers (image not shown). Figure 5.2 shows portions of Caco-2 monolayers exposed to electroporation after incubation with calcein (A-B) and BSA (C-D). The monolayers were allowed to recover for 15 minutes and were then stained with propidium iodide, a vital stain used to identify membrane compromised or dead cells. After electroporation, propidium iodide stained cells were observed, either singly or in patches, scattered around the monolayer. The number of dead cells present in the monolayer appeared to depend on the strength of the electroporation conditions applied, i.e., the stronger the condition, the more dead cells there were.

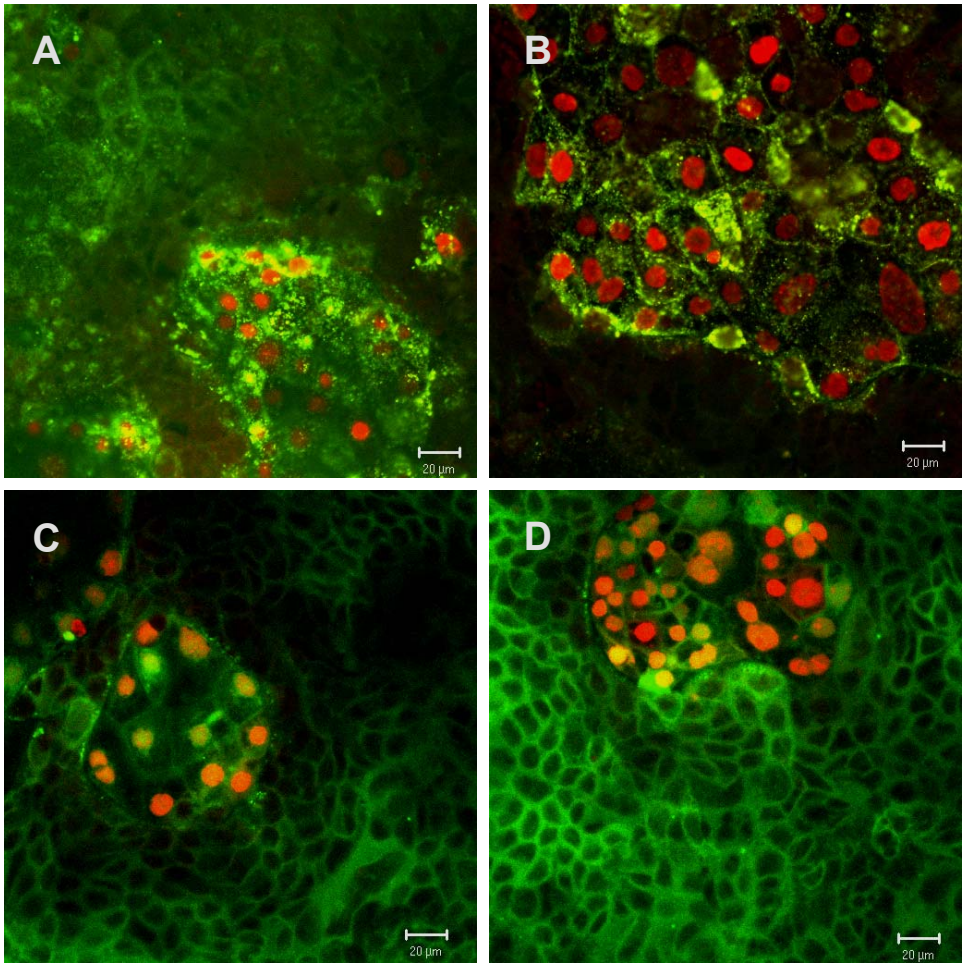

Figure 5.2 Confocal images of cell death in Caco-2 monolayers electroporated at 75V – 10 ms with calcein (A,B) and BSA (C,D). The nuclei of the dead cells were stained red with propidium iodide. Cell death increased as the strength of the electroporation condition increased.

5.2.3 Monolayers Repair Themselves After Electroporation

In a small set of experiments, T84 and Caco-2 monolayers were electroporated and then observed over time as they recovered. Monolayers were fixed and stained using the hematoxylin and eosin (H & E) histological staining technique. Hematoxylin stains nucleic acids blue, while eosin stains cytoplasmic proteins pink. Unelectroporated monolayers typically showed fully confluent cells with large, tightly packed nuclei surrounded by relatively small amounts of cytoplasm, similar to the confocal fluorescence image in Figure 5.3. A day after electroporation, holes in the monolayer, where dead cells have lifted off, were apparent. At the edges of these holes, it appeared that the adjacent cells began to extend their cytoplasm into the empty area. This indicated that these cells may have begun the initial stages of a recovery process that will be discussed in more detail in Chapter 7.

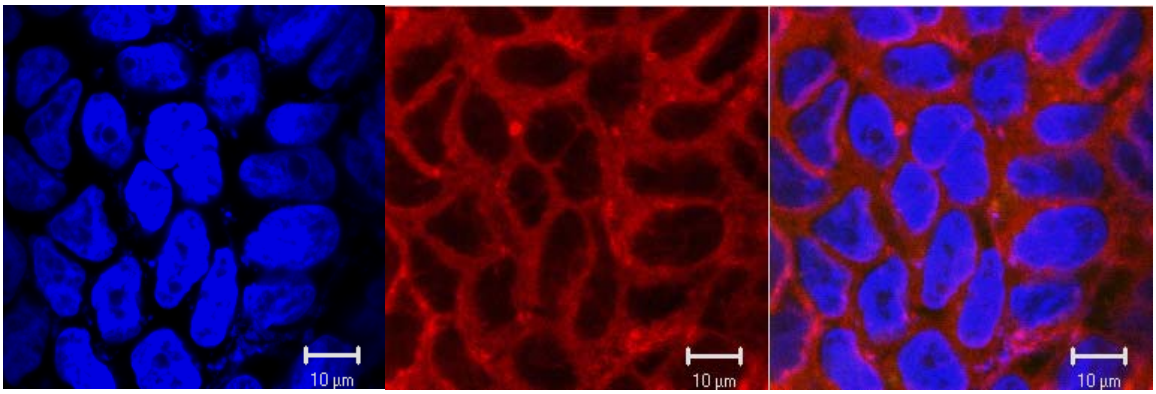

Figure 5.3 Confocal micrographs of a Caco-2 monolayer with nuclei stained on the left by Hoechst 33342 (blue), lipid membranes stained in the middle by FM® 4-64 (red), and a composite image (right) of both dyes.

5.3 Discussion

Caco-2 and T84 intestinal epithelial cells were electroporated as monolayers to determine whether electroporation could be used to uniformly deliver two classes of molecules. Confocal microscopy confirmed that electroporation was successful at intracellular delivery of both a small, inert molecule (calcein) and a large macromolecular protein (BSA). As stated earlier, calcein was found throughout the cell in both the cytoplasm and the nucleus, whereas BSA was primarily found only in the nucleus. This nuclear exclusion of BSA is probably due to its large molecular size (66,000 Da), which would limit its diffusion through nuclear pore complexes (Talcott and Moore, 1999; Bagley et al., 2000).

The nuclear pore complexes (NPC) are 125 MDa structures located on the nucleus that regulate the import and export of all molecules across the nuclear membrane (Bagley et al., 2000; Adam, 2001). The central channel of the NPC has a diameter of approximately 9 nm and is the primary route by which molecules can pass into and out of the nucleus. Proteins less than 30 kDa can easily diffuse through the NPC, while those greater than 50 kDa or 6 nm can take as long as 24 hours to passively diffuse through (Pouton, 1998; Talcott and Moore, 1999; Gasiorowski and Dean, 2003). Large proteins and even some small molecules require the presence of a nuclear localization signal (NLS), a sequence of amino acids recognized by receptors on the nuclear membrane, in order to pass more quickly into the nucleus.

It should also be noted that the lack of fluorescence in the nucleus suggests that there was probably little degradation of BSA by proteolytic enzymes. Small, fluorescein-

labeled protein fragments would have passed easily through the nuclear pore complex, which would have resulted in an image similar to that of calcein.

If the condition applied is strong enough, the pores that are formed become irreversible leading to an influx of extracellular fluid and/or leakage of intracellular contents resulting in cell necrosis. Release of intracellular contents can elicit an inflammatory response in adjacent cells (Chopra and May, 1989). Apoptosis, which is another term for programmed cell death or suicide, typically involves individual injured cells, which do not lyse, but undergo shrinkage, nuclear condensation, and eventual death (Chopra and May, 1989). It is likely that the individual dead cells observed scattered throughout the monolayers after electroporation could be cells in the late stages of apoptosis (images not shown). During this stage, the cells have compromised membranes and, as a result, can be stained by propidium iodide. The end result of both necrosis and apoptosis is that the cells become non-viable and, in the case of adherent cells, are released from the monolayer. Histological staining suggested that the viable cells located near the exposed areas might be able to repair the wound in the monolayer. In Chapter 7, results from experiments in which transepithelial resistance was tracked after electroporation indicate that this is a possibility. Since it appears that cell death is dependent on the strength of the electroporation condition applied, it will be useful to try to minimize death, while maximizing uptake of the molecule of interest. Quantification of molecular uptake and cell viability will be useful for trying to achieve this result.

5.4 Conclusions

Two human colon carcinoma cell lines (Caco-2 and T84) that serve as accepted models of the intestinal epithelium were electroporated. Calcein (a small fluorescent tracer) and fluorescein-labeled bovine serum albumin (a protein) were chosen as marker molecules. Electroporation was able to uniformly deliver both molecules intracellularly, where calcein localized throughout the entire cell interior and BSA localized primarily in the cytoplasm. Cell death occurred after electroporation and was dependent on the condition applied. Although dead cells lifted off from the membrane support, as would be expected, the remaining cells appeared to attempt to repair the hole left in the monolayer. Once it was established that electroporation could deliver molecules to polarized intestinal epithelial monolayers, the next step was to quantify molecular uptake and cell viability, as discussed in Chapter 6.

CHAPTER VI

6. QUANTIFICATION OF MOLECULAR UPTAKE AND CELL VIABILITY

6.1 Introduction

Electroporation and its effect on cells have been a topic of interest for many years (Neumann et al., 1989; Chang et al., 1992). It is believed that electroporation creates transient aqueous pathways in the lipid bilayer of cell membranes, which results in enhanced uptake of membrane-impermeant molecules through the resulting pores. Because electroporation can be universally applied to almost any cell type, it has proven to be a very useful laboratory tool for introducing small molecules, macromolecules, and genetic material into cells (Prausnitz et al., 1993; Prausnitz et al., 1994; Bright et al., 1996; Cataldo et al., 1998; Neumann et al., 1998; Baron et al., 2000; Canatella et al., 2001; Canatella and Prausnitz, 2001) and has been used to clinically treat some forms of cancer (Heller et al., 1999).

The dependence of molecular uptake and cell viability on electroporation parameters such as voltage/field strength, pulse length, and pulse number has been explored in many different studies. Most report uptake as the percentage of cells that demonstrate the presence of a membrane-impermeant molecule intracellularly after electroporation. This does not provide information about the extent of uptake within each cell. A small number of studies have quantified molecular uptake in this fashion using flow cytometry (Bartoletti et al., 1989; Prausnitz et al., 1993; Prausnitz et al., 1994; Gift and Weaver, 1995; Canatella et al., 2001), which is the approach that was used in this study.

In this set of experiments, we sought to develop methods for electroporation of *in vitro* models of intestinal epithelium and determine if large numbers of small molecules and macromolecules could be delivered into epithelial cell monolayers. Polarized Caco-2 and T84 epithelial monolayers were exposed to electrical pulses over a range of different voltages, pulse lengths, and pulse numbers and then quantified levels of cell viability and uptake of two model compounds: calcein, which served as a model for small, membrane-impermeant drugs, and fluorescein-labeled bovine serum albumin, which modeled macromolecular proteins. The cells were dissociated and analyzed in large numbers (20,000 cells) by flow cytometry to determine the molecular uptake (the number of molecules taken up by each cell) and cell viability (the percentage of cells still viable after electroporation). The dependence of these two outcomes on electrical parameters was then evaluated.

6.2 Experimental Results

6.2.1 Effect of Pulse Voltage and Length on Uptake

Having established that cells forming a functional epithelial monolayer can be uniformly electroporated, flow cytometry was used to quantify the average number of calcein and BSA molecules taken up by each cell as a function of pulse voltage and length. Figure 6.1 shows that the average number of calcein and BSA molecules taken up by each Caco-2 and T84 cell generally increased with increasing applied voltage to an apparent plateau or maximum (one-way ANOVA, $p < 0.05$). Uptake also increased with increasing pulse length, which was statistically significant for voltages less than 300 V ($p < 0.05$).

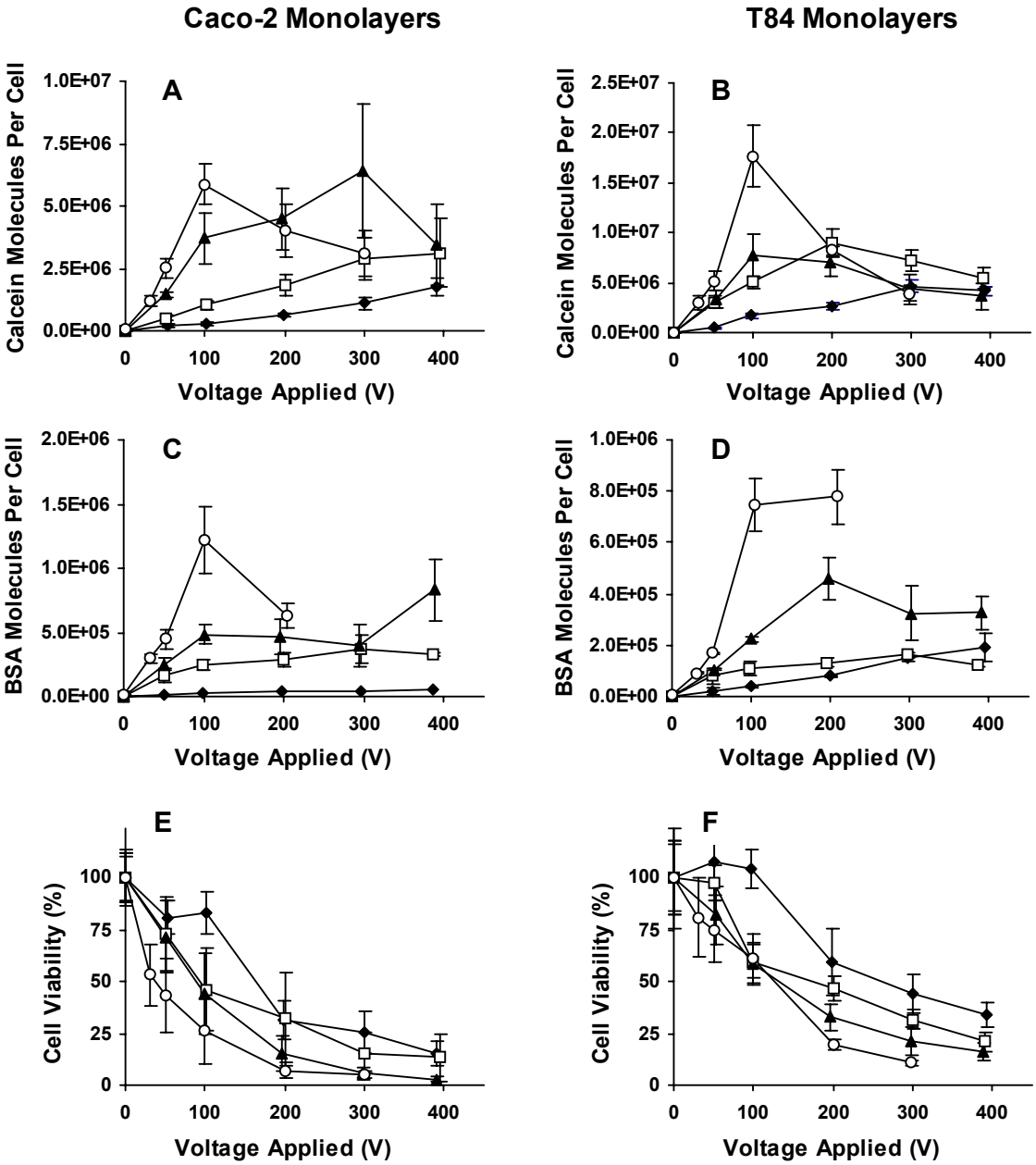

Figure 6.1 Dependence of intracellular uptake and cell viability on electroporation voltage and pulse length. Uptake of calcein and BSA by epithelial monolayers increased as voltage and pulse length were increased (A-D). Cell viability decreased with voltage and pulse length (E,F). Pulse lengths were 1 ms (◆), 5 ms (□), 10 ms (▲), and 20 ms (○). [n=4-7]

This analysis also showed that it is possible to transport more than 10^6 calcein molecules per cell and more than 10^5 BSA molecules per cell into both Caco-2 and T84 monolayers using electroporation (Figures 6.1A-D). Moreover, these average uptake values represent a homogeneous response of the cells in the monolayer, as shown by the approximately Gaussian distribution about the mean uptake level among the 20,000 viable cells per sample analyzed by flow cytometry (Figure 6.2). This uniform response is consistent with previous observations for electroporation of cells in suspension (Prausnitz et al., 1993; Canatella et al., 2001).

6.2.2 Effect of Pulse Voltage and Length on Viability

The above analysis discussed the number of molecules delivered into those cells that remained viable after electroporation. However, electroporation can render cells non-viable. Figures 6.1E and 6.1F show that the viability of electroporated cells generally decreased with voltage ($p<0.05$) and, to a lesser extent, with pulse length. This observation indicates that there is a tradeoff between conditions that yield large levels of uptake (i.e., long pulses and possibly high voltages) and those that maintain high viability (short pulses and low voltages). The significance of this sometimes large viability loss and its possible overestimation by flow cytometry is discussed further in Section 7.3.2.

6.2.3 Effect of Pulse Number on Uptake and Viability

Additional experiments were performed to determine the effect of multiple pulses on calcein uptake and cell viability. Between 1 and 20 pulses were applied over a range of pulse lengths, while the applied pulse voltage was held constant at 50 V. Figures 6.3A

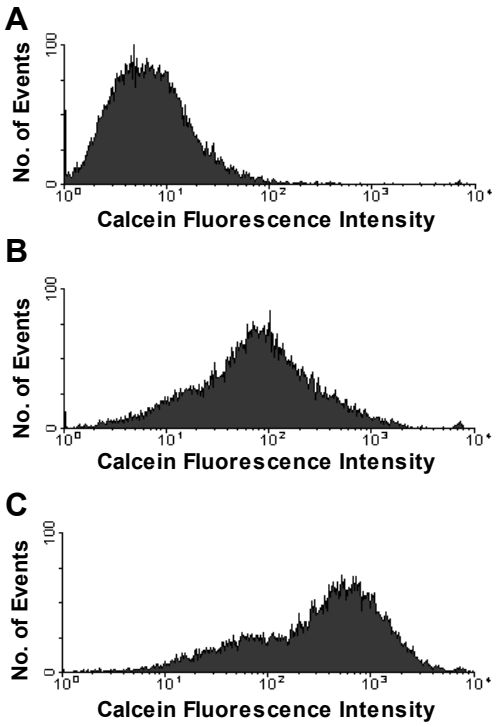

Figure 6.2 Flow cytometry histograms of calcein fluorescence intensity for Caco-2 monolayers exposed to (A) no electroporation, (B) moderate electroporation (50V-10ms), and (C) strong electroporation conditions (200V-10ms). Histograms are similar to those observed for T84 monolayers and for BSA.

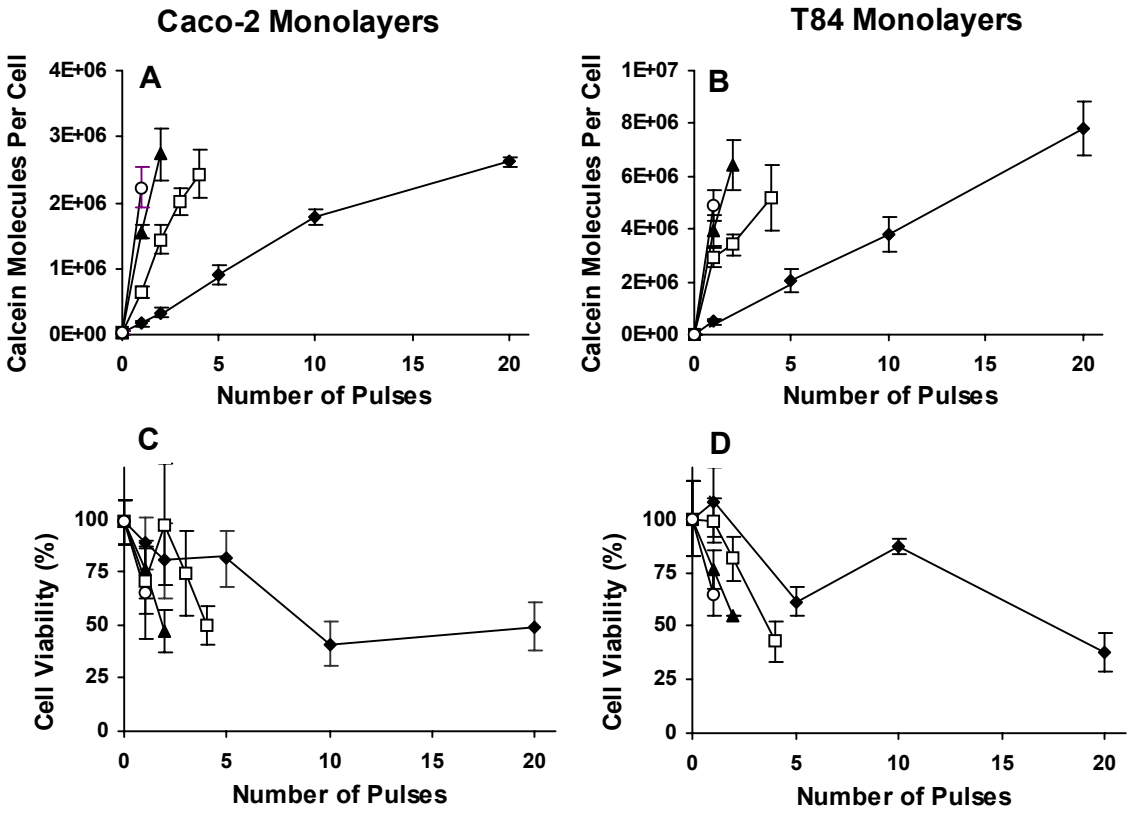

Figure 6.3 Dependence of intracellular uptake and cell viability on electroporation pulse number and pulse length. Calcein uptake increased with increasing pulse number and pulse length (A,B). Cell viability decreased with increasing pulse number and pulse length (C,D). Applied voltage was held constant at 50 V. Pulse lengths were 1 ms (◆), 5 ms (□), 10 ms (▲), and 20 ms (○). [n=2-9]

and 6.3B show that as the number of pulses was increased and as pulse length was increased, the amount of uptake increased in both Caco-2 and T84 monolayers ($p < 0.05$). In Figures 6.3C and 6.3D, the viability of the Caco-2 and T84 cells appears to decrease as the number of pulses and pulse length were increased (although not always with statistical significance; $0 < p < 0.78$), thus illustrating the inverse relation between uptake and viability.

Since increasing the number of pulses and increasing the pulse length have similar effects (i.e., they both increase the duration of exposure to electroporation), we wanted to determine whether single long pulses yielded the same effects as several short pulses having the same total exposure time (TET; defined as the product of pulse length and number of pulses). Using combinations of pulses having TET of 5 ms, 10 ms, and 20 ms, uptake of calcein by both Caco-2 and T84 cells was not found to be statistically different at constant TET (Figures 6.4A and 6.4B; one-way ANOVA, $p > 0.05$ for all TET). Similarly, cell viability in both types of monolayers was statistically indistinguishable at the same TET (Figures 6.4C and 6.4D; one-way ANOVA, $p > 0.05$ for all TET).

6.3 Discussion

6.3.1 Dependence of Uptake on Pulse Voltage, Length, and Number

Caco-2 and T84 epithelial monolayers were electroporated using a range of voltages, pulse lengths, and pulse numbers. Quantification of molecular transport and cell viability showed that for both cell types, uptake of calcein and BSA increased with

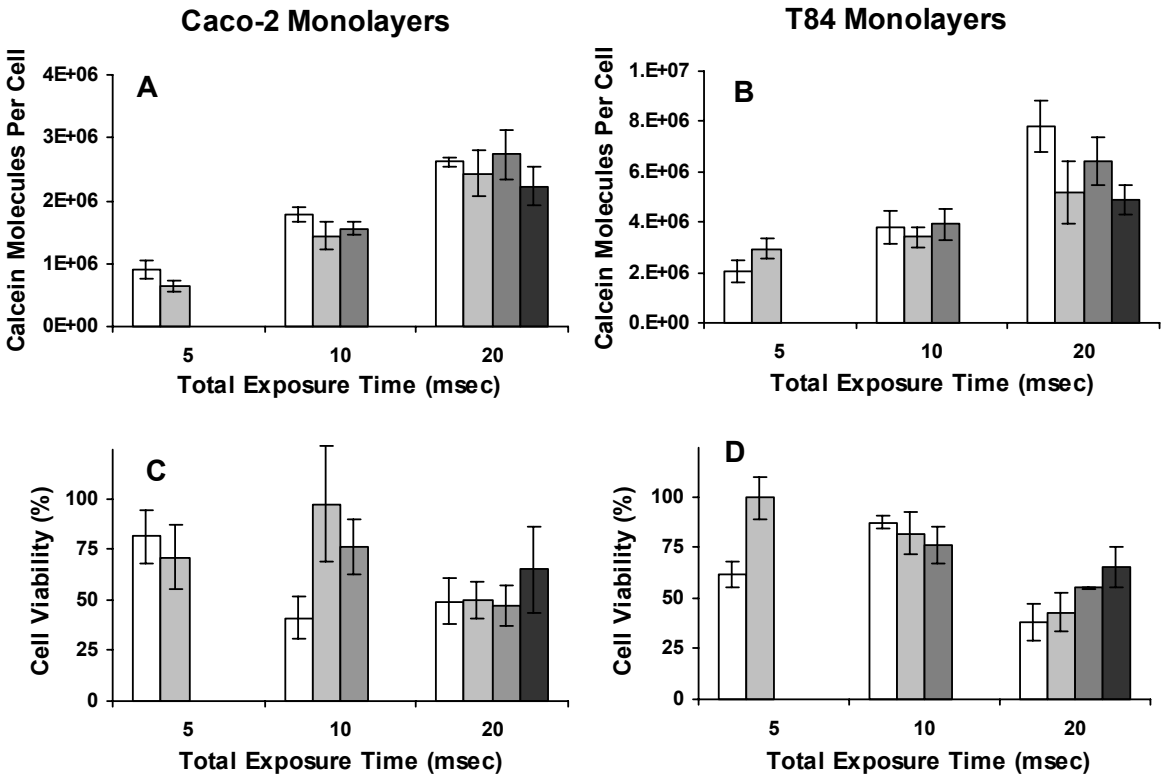

Figure 6.4 Intracellular uptake of calcein (A,B) and cell viability (C,D) were similar for the same total exposure time to electroporation (TET; defined as the product of pulse length and number of pulses). Data are replotted from Figure 5. Pulse lengths were 1 ms (□), 5 ms (▒), 10 ms (▓), and 20 ms (■). [n=2-9]

increasing voltage and pulse length, reaching levels up to 10^7 molecules per cell. It was also observed that uptake tends to decrease at higher voltages (> 100 V) and/or longer pulses (>10 ms). One possible reason for this could be the low number of cells surviving at these conditions (< 20%), which could lower the resulting average uptake in the cells. It is also possible that electroporation, which is size dependent, killed off the larger, more easily electroporated cells, leaving the more difficult to electroporate small cells. Since the smaller cells would not hold as much of the marker molecules, uptake would be decreased.

Multiple pulse experiments indicated that the total 'on time' of a pulse determined levels of uptake and viability, independent of whether that 'on time' was achieved through a single long pulse or multiple shorter pulses (Figure 6.4). In contrast, results from multiple pulse experiments conducted with prostate cancer cells in suspension reported by Canatella et al. (2001) showed more uptake and lower cell viability when single long pulses were applied than when several short pulses were applied. This difference may be due to differences in cell type, suspension versus monolayer configuration, or error bars that may obscure small variations in the measurements.

6.3.2 Sub-equilibrium Uptake of Molecules

The number of molecules delivered per cell should be thermodynamically limited to an intracellular concentration in equilibrium with (i.e., equal to) the extracellular concentration, which was 100 μM for calcein and 10 μM for BSA. Based on measurements of cell dimensions using multiple x-y sections of 10 cells and 10 nuclei chosen randomly from different confocal micrographs, cell volumes were estimated as

2500 ± 400 μm^3 and 1600 ± 200 μm^3 for Caco-2 and T84 cells, respectively, and nuclear volumes as 2000 ± 1000 μm^3 and 760 ± 200 μm^3 for Caco-2 and T84 cells, respectively. According to these measurements, the volume of the nucleus makes up a significant portion of the cell volume. This result is supported by additional observations of these cells in microscopy images collected during the course of these experiments (not shown) and in images published by others (Madara et al., 1987; Lu et al., 1996).

Using these volumes, intracellular concentrations of calcein and BSA were calculated. When the intracellular concentration equals the extracellular concentration, maximum calcein uptake (100 μM) should occur at 1.5 x 10^8 molecules per Caco-2 cell and 9.4 x 10^7 molecules per T84 cell and maximum BSA uptake (10 μM), assuming nuclear exclusion, should occur at 3.3 x 10^6 molecules per Caco-2 cell and 4.9 x 10^6 molecules per T84 cell. Inspection of Figure 6.1 indicates that although large numbers of molecules were delivered, uptake of neither calcein nor BSA reached its maximum value. Uptake was usually 1-2 orders of magnitude below equilibrium, which is consistent with previous quantitative measurements of uptake by cells electroporated in suspension (Canatella et al., 2001).

6.3.3 Choosing an Optimal Electroporation Condition

The choice of an optimal electroporation condition will depend on the application for which it is being used. Most applications will require efficient delivery of a molecule of interest while minimizing cell death. Typically, the goal would be to alter or restore the functional processes of living cells. In such cases, short, low voltage pulses (e.g., 50 V, 1-10 ms) should be most effective. If cell death is not a concern, and more extensive

uptake by the surviving fraction of cells is needed, then much stronger electroporation conditions could be used.

6.4 Conclusions

Electroporation of polarized intestinal epithelial monolayers was demonstrated for the first time, showing that intestinal epithelial monolayers can be electroporated to induce extensive uptake of extracellular, membrane-impermeant molecules, including proteins. In both Caco-2 and T84 cell lines, uptake increased and cell viability decreased with increasing pulse voltage, length, and number. When total exposure time was kept constant, however, neither uptake nor viability changed significantly. The results of these experiments suggest the feasibility of using electroporation to deliver drugs, proteins, and other therapeutic molecules to the intestinal epithelium.

CHAPTER VII

7. PHYSICAL AND FUNCTIONAL RECOVERY OF MONOLAYERS AFTER ELECTROPORATION

7.1 Introduction

Electroporation is very proficient at introducing molecules into cells, but it can also cause significant cell damage and death. When working with polarized intestinal epithelial monolayers, it is important that the monolayers are confluent so that they function like *in vivo* epithelium. To help maintain this barrier, epithelial monolayers are comprised of proliferating cells that can repair small injuries and the possible damage caused by electroporation (Lacy, 1988). Transepithelial electrical resistance (TEER), a measurement of the epithelial resistance to the flow of current, is regularly used as an index of monolayer health and integrity (Shaw, 1996b). In this study, the recovery kinetics of transepithelial resistance after electroporation were monitored to determine which conditions permitted rapid recovery and which caused long-term injury.

7.2 Experimental Results

7.2.1 Physical Recovery of Intestinal Epithelial Monolayers after Electroporation

Figures 7.1A and 7.1C show the long-term recovery of Caco-2 monolayer resistance after electroporation at a "mild," "moderate," or "strong" condition (see Section 4.4.1). There was an initial drop in TEER immediately after each pulse, which then recovered at varying rates depending upon the condition applied (Figure 7.1A).

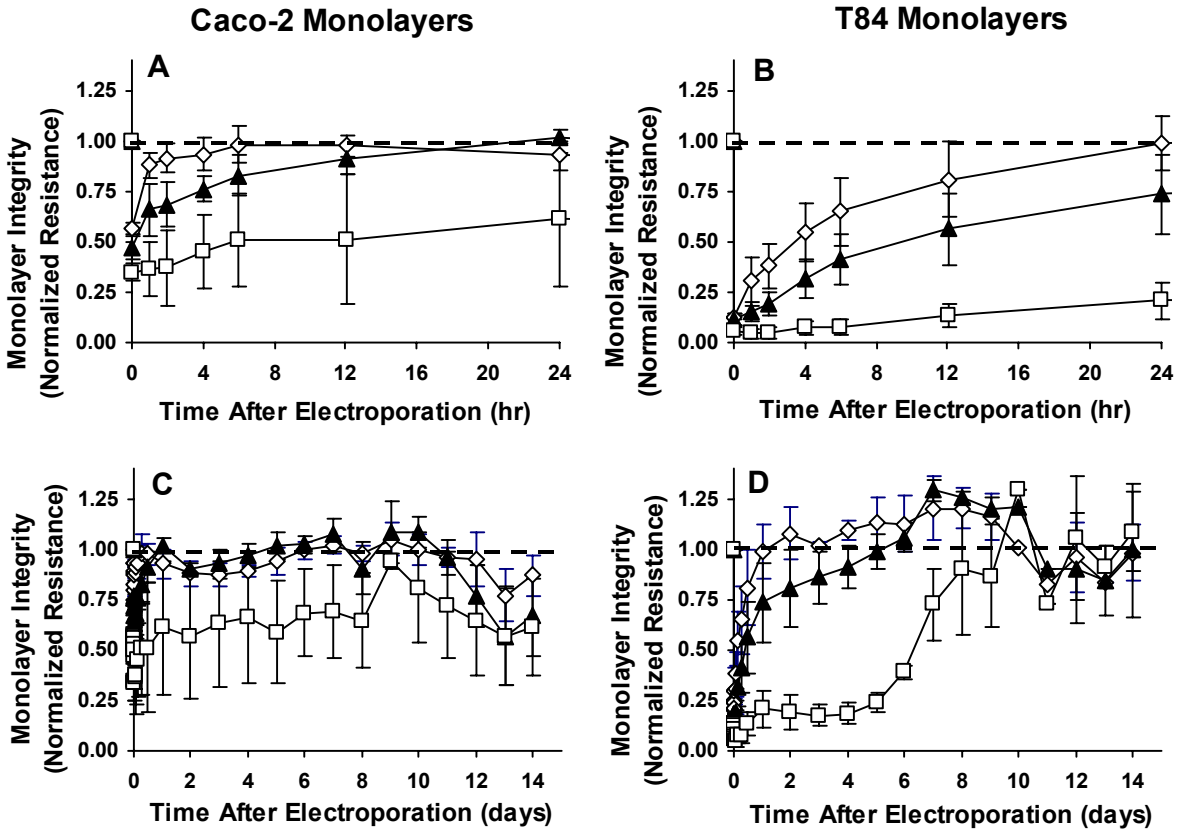

Figure 7.1 Kinetics to restore barrier integrity of monolayers in the first 24 hours (A,B) and 14 days (C,D) after electroporation. Caco-2 (A,C) and T84 (B,D) monolayers were electroporated under mild (◇), moderate (▲), and strong (□) electroporation conditions (see Materials and Methods section). Monolayer integrity was measured using transepithelial electrical resistance (TEER) of the monolayers, which was normalized relative to unelectroporated control monolayers and initial resistance. [n = 9]

Mildly electroporated monolayers (uptake ~ 2 x 10^5 calcein molecules per cell, mpc, viability ~ 81%; see Figure 3) were able to recover their original resistance in less than 6 hours. Moderately electroporated monolayers (uptake ~ 2 x 10^6 mpc, viability ~ 71%) recovered within a day. Finally, strongly electroporated monolayers (uptake ~ 4 x 10^6 mpc, viability ~ 44%) did not recover their initial resistance until more than a week later.

Figures 7.1B and 7.1D show the recovery of electroporated T84 monolayers, which behaved similarly to the Caco-2 monolayers. For mild electroporation (uptake ~ 3 x 10^6 calcein mpc, viability ~ 98%), T84 monolayers recovered their initial resistance in 24 hours. Monolayers that were moderately electroporated (uptake ~ 5 x 10^6 mpc, viability ~ 75%) recovered within a few days, and those that were strongly electroporated (uptake ~ 9 x 10^6 mpc, viability ~ 47%) required more than a week to recover. T84 recovery rates were slower than Caco-2 rates probably because of their longer doubling time, i.e., 60 h for T84 cells versus 30 h for Caco-2 cells (Dharmsathaphorn and Madara, 1990; Gres et al., 1998). Together, these recovery experiments show that on the order of 10^6 molecules per cell can be delivered under mild to moderate electroporation conditions into monolayers that require hours up to one day to fully recover barrier integrity, which is an indicator of good tissue function and health.

7.2.2 Functional Recovery of T84 Monolayers After Electroporation

Interleukin-8 (IL-8), a pro-inflammatory cytokine, is secreted by injured cells as part of the stress response, thus, in a companion study the measurements of the secretion of this cytokine by the T84 monolayers monitored in Section 7.2.1 were made. Caco-2

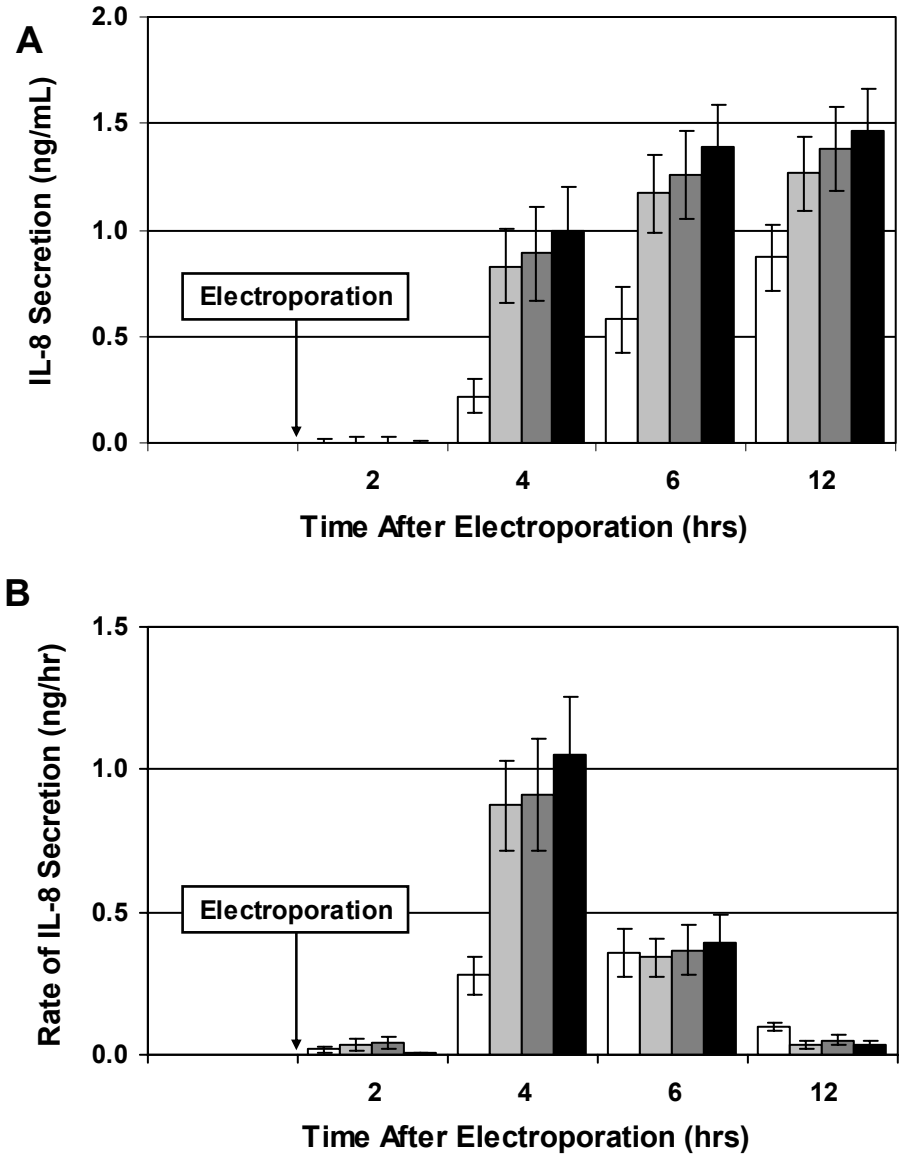

Figure 7.2 Electroporation induces a temporary inflammatory response. T84 monolayers were exposed to no (□), mild (▒), moderate (▓), or strong (■) electroporation. (A) IL-8 secretion by the monolayers increased with time after electroporation. (B) When secretion is plotted as a rate of secretion, the rate increases to maximum at 4 hrs and then returns to basal levels after 12 hours. [n = 9]

monolayers were not included in this study because they secreted IL-8 at levels below the detection limit of the assay. Figure 7.2A depicts the concentration of IL-8 secreted after electroporation of the monolayers used in the resistance recovery experiments shown in Figure 7.1. IL-8 secretion increased after treatment, indicating the presence of necrotic cells in the monolayers, which triggered the induction of an inflammatory response in neighboring cells. However, when the data is replotted as the rate of IL-8 secretion (Figure 7.2B), the rate of IL-8 secretion increased to a peak at 4 hours after electroporation and then decreased over time until the rate reached basal levels 12 hours later. Secretion did not depend on the strength of the electroporation condition applied (ANOVA; $p = 0.78$).

7.3 Discussion

7.3.1 Physical Recovery

When coupled with the molecular uptake studies discussed in Chapter 6, monolayer recovery experiments showed that even under relatively mild electroporation conditions (~50 V), monolayers were able to take up many thousands to millions of molecules per cell and still recover barrier properties within hours. This ability to take up molecules and then recuperate quickly should be useful for laboratory studies of gastrointestinal inflammation or other intestinal conditions. For example, one could electroporate an experimental drug or protein into an epithelial monolayer, wait 1 - 2 days and then carry out tests to evaluate the resulting effects on monolayer function.

There are also potential clinical applications for electroporation of epithelia, e.g., treatment of intestinal disorders by introduction of drugs, proteins, or genes. Although electroporation causes some temporary cell damage, it might still be useful clinically as long as the epithelium is able to recover and regain confluence relatively quickly. When superficial wounds to the epithelial lining of the intestinal wall naturally occur in the body due to physical injury, microorganisms, or other agents, cells adjacent to the wound quickly dedifferentiate and migrate to cover the exposed area as illustrated in Figure 7.3 (Lacy, 1988; Dignass, 2001). This frequent and natural healing process, called restitution, occurs within minutes to hours in both *in vivo* epithelium and cultured epithelium (Moore et al., 1989; Nusrat et al., 1992; Nusrat et al., 1997) and serves to maintain the barrier necessary to protect the body from the external environment. The electroporation conditions from which monolayers recovered in less than 24 hours in this study may similarly permit rapid resealing of epithelia *in vivo*.

7.3.2 Underestimation of Cell Viability by Flow Cytometry

Although measures of cell viability from flow cytometry experiments have been provided (e.g., Figures 6.1, 6.3, 6.4), we believe these may overestimate the loss of cell viability. For example, fluorescence imaging of intact electroporated monolayers show far fewer dead cells (by PI staining) than what is observed by flow cytometry analysis of cells dissociated from similarly treated monolayers (images not shown). Moreover, monolayer resistance measurements made just after electroporation at mild to moderate conditions show drops to at most 50% (Caco-2) or 20% (T84) of pre-electroporation TEER values. These levels of resistance drops have been shown to occur when tight

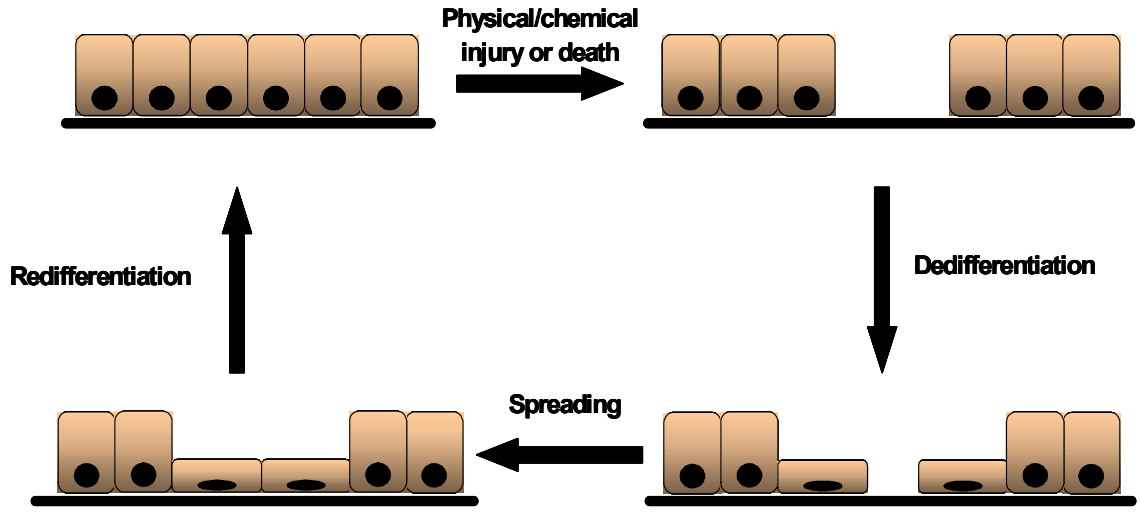

Figure 7.3 Illustration of the process of restitution in an intestinal epithelial monolayer. When cells are lost due to injury or natural death, nearby cells flatten and migrate into the exposed area. They then differentiate back into their original polarized form.

junctions between cells are disrupted (Liu et al., 2000; Ma et al., 2000), and do not require killing of large numbers of cells. If up to 30% of the cells in the monolayer were destroyed, as flow cytometry measurements under the same conditions estimated, then based on cell doubling times (60 h for T84 cells and 30 h for Caco-2 cells (Dharmsathaphorn and Madara, 1990; Gres et al., 1998)), the process of replicating new cells to regain confluence should have required more than the 24 hours observed.

For these reasons, we believe that cell viability losses calculated using flow cytometry are overestimated probably due to monolayer dissociation and artifacts of preparing cells for flow cytometry analysis. Although viabilities were determined by comparing to unelectroporated controls, cells that have been electroporated could be more fragile and, thus, more likely to be adversely affected by the trypsin and physical treatments used to dissociate the monolayers. Since it appears that the cells are better able to recover when left in monolayer form, transepithelial resistance may be a more useful indicator of monolayer viability than flow cytometry measurements.

7.3.3 Functional Recovery

Experiments showed that electroporation induces an inflammatory response in T84 monolayers by causing an increase in IL-8 secretion. This is to be expected since electroporation is a form of injury to the cells. Fortunately, the response is temporary and the cells appear to return to normal, at least in this respect, within 12 hours. It is understood that IL-8 is only one of many markers that could be used to assay functional recovery of the monolayers after electroporation, but it is an especially useful one since it relates to our interest in inflammation. In addition, the information about the effect of

electroporation alone on IL-8 secretion, aided our interpretation of results from later experiments involving the same IL-8 system (Chapter 10).

7.4 Conclusions

Intact intestinal epithelial monolayers electroporated with mild, moderate, and strong conditions experienced a loss of resistance and tissue barrier function that recovered at different rates depending on the cell line and the strength of the condition applied. For some conditions, monolayers were able to recover physically in less than a day. Electroporation was found to induce a temporary inflammatory response (increased secretion of IL-8), but cells were able recover normal function within 12 hours. These experiments will help identify conditions that would be useful for delivering molecules, but still allow rapid recovery of the monolayers.

CHAPTER VIII

8. TRANSPORT OF MOLECULES ACROSS MONOLAYERS AFTER ELECTROPORATION

8.1 Introduction

Oral administration is the most common method of drug delivery used today. Drugs administered in this fashion must be absorbed across the gastrointestinal barrier before entering the systemic circulation and acting on their target (Foye et al., 1995). While many drugs are absorbed fairly easily, others may have poor oral bioavailability because of first pass metabolism in the GI tract or poor absorption across the intestinal epithelial barrier (Brody et al., 1998). This is especially true for larger molecules, such as proteins. To address this problem, many researchers modify the physical characteristics of the drug, e.g., charge, polarity, lipid solubility, pH sensitivity, etc., to aid absorption (Langer, 1998).

As an alternative to modifying the drug to increase absorption, the barrier function of the intestinal epithelium itself could be altered. Experiments conducted to test this possibility were conducted by Leonard et al. (2000a) who used an electrically-based technique similar to electroporation, called iontophoresis (Banga et al., 1999), to increase the paracellular transport of several compounds across intact Caco-2 monolayers. Since the Caco-2 line is the most widely used cell line for drug absorption studies (Palm et al., 1999; Artursson et al., 2001; Krishna et al., 2001) and since transport across these cells has been shown to correlate fairly well with *in vivo* intestinal permeability (Artursson and Karlsson, 1991; Rubas et al., 1995; Rubas et al., 1996; Yee, 1997; Yamashita et al., 2000), it was chosen for our studies.

This study was conducted o determine whether, in addition to being able to introduce molecules into the cells of the monolayer, electroporation could increase transport *across* the cells. To answer this question, intact Caco-2 monolayers were electroporated at various conditions with either the small molecule, calcein, or the macromolecular protein, BSA, and monitored for changes in transepithelial permeability.

8.2 Experimental Results

8.2.1 Increase in Epithelial Permeability after Electroporation

In initial experiments, confluent Caco-2 monolayers were treated with the mild (50 V – 1 ms) and moderate (50 V – 10 ms) electroporation conditions used in the monolayer recovery experiments described in Chapter 7. The rate of appearance of calcein in the basal compartment was monitored. The inset of Figure 8.1 shows the steady increase in calcein accumulation for the first three hours. The main graph in Figure 8.1 shows that electroporation increases the apparent permeability (P_{app}) of confluent Caco-2 monolayers to calcein. Permeability tended to increase with the strength of the electroporation condition applied, although not with statistical significance ($p = 0.37$). When compared to the permeability of the unelectroporated monolayers ($1.9 \pm 0.4 \times 10^{-7}$ cm/s), the monolayers electroporated with the mild pulse ($2.7 \pm 0.7 \times 10^{-7}$ cm/s) and moderate pulse ($3.4 \pm 1.3 \times 10^{-7}$ cm/s) had p-values of 0.10 and 0.07, respectively. Application of the mild and moderate electroporation pulses increased permeability by

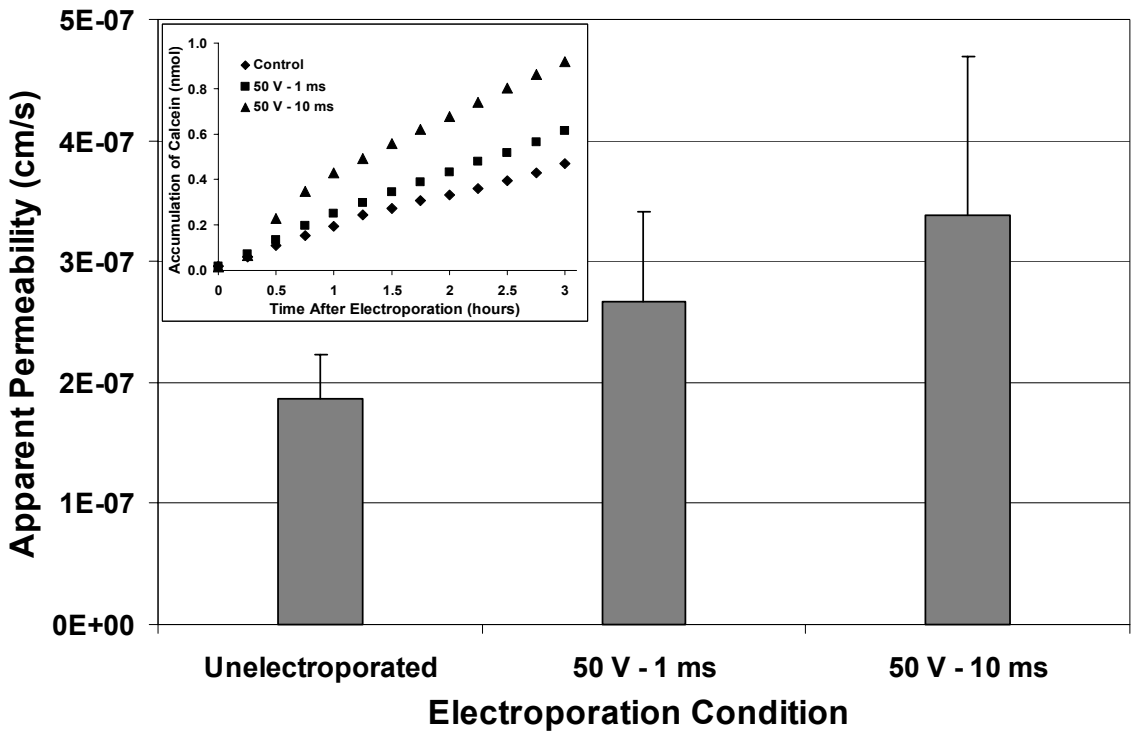

Figure 8.1 Apparent permeability of confluent Caco-2 monolayers to 100 μM calcein after treatment with mild (50 V – 1 ms) and moderate (50 V – 10 ms) electroporation conditions. Although permeability appeared to increase with the strength of the condition applied, the difference between the two conditions was not statistically significant ($p = 0.37$). Monolayers were monitored for 6 hours after electroporation. Unelectroporated monolayers served as controls. Inset: Representative plot of calcein accumulation (nmol) in basal compartment for the first 3 h after electroporation. Accumulation was relatively linear with time. [n = 4]

42% and 81% over the controls, respectively.

Although the results in Figure 8.1 show that electroporation increases transport across the monolayer, this increase was, at most, only twice that of the control. To determine whether a further increase in permeability could be obtained, ten 50 V - 1 ms pulses with an interpulse spacing of 15-20 s were applied to each monolayer. This condition has an effect that is essentially the same as the 50 V – 10 ms pulse (see Section 6.2.3), but allows more time for diffusion of the markers across the cells between pulses. When multiple pulses were applied to a new set of Caco-2 monolayers, the permeability to calcein increased 6-fold over that of the single pulse condition (Figure 8.2; $p = 0.01$). Comparisons to the unelectroporated monolayers showed that the single pulse condition increased permeability almost 2-fold ($p = 0.07$), while the multiple pulse condition increased it 12-fold ($p = 0.03$). These results illustrate that, when the total exposure time is kept constant, multiple pulses are more efficient than single pulses at increasing intestinal epithelial permeability.

8.2.2 Dependence of Epithelial Permeability on Molecular Size

After determining that electroporation could significantly increase the permeability of intestinal epithelial monolayers, the dependence of permeability on the size of the molecule being transported was evaluated. In the next set of experiments, a modification was made in the protocol. Initially, unelectroporated monolayers were monitored for permeability alongside the treated monolayers. This made it difficult to make comparisons between the two sets of monolayers because of the uncertainty about whether the pre-electroporation permeabilities of the treated monolayers were similar to

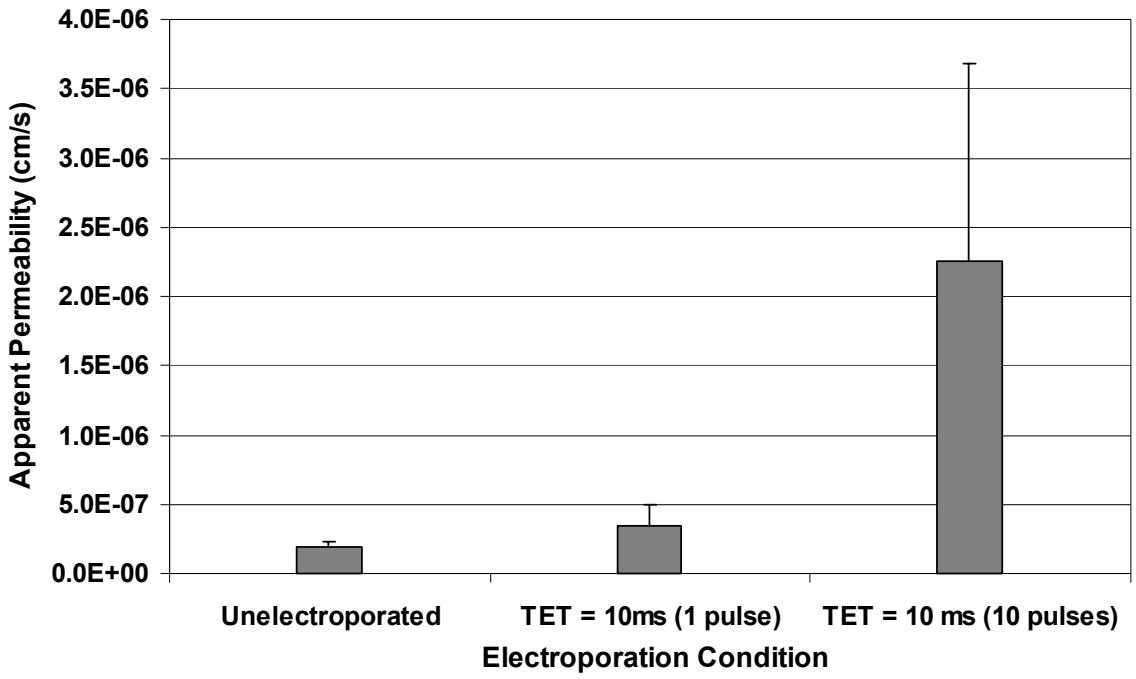

Figure 8.2 Transepithelial transport of calcein is significantly higher after treatment with multiple pulses versus a single pulse, when total exposure time (TET) is held constant. When TET = 10 ms, Caco-2 permeability was 12 times higher than the unelectroporated controls (n = 4) after the multiple pulse condition (n = 4; p = 0.03) and only 2 times higher after the single pulse condition (n = 6; p = 0.07). The multiple pulse condition was 6 times higher than the single pulse condition (p = 0.01). Monolayers were treated with 100 μM calcein and either one 50 V – 10 ms pulse or ten 50 V – 1 ms pulses and then monitored for three hours. [n=4-6]

those of the controls. To address this issue, each monolayer served as its own control. Baseline permeabilities were monitored for three hours prior to electroporation and then the monolayer was treated and monitored for an additional three hours.

Caco-2 monolayers incubated with 10 μM apical solutions of calcein (radius = 0.6 nm) or FITC-labeled BSA (radius = 3.5 nm) were electroporated with ten 50 V – 1 ms pulses and monitored for an increase in permeability. Table 8.1 and Figure 8.3 shows that for both molecules, electroporation induced an increase in permeability over the baseline permeability. For some individual monolayers, permeability increased as much as 20-fold for both molecules, but the average increase for all monolayers was approximately 8-fold for calcein and 7-fold for BSA (Table 8.1). Transport across the monolayers was found to be size dependent since permeability to calcein was 12 - 13 times higher than permeability to BSA for both unelectroporated and electroporated monolayers (Table 8.1).

Table 8.1 Permeabilities of unelectroporated and electroporated confluent Caco-2 monolayers to calcein and BSA.[a]

Marker Molecule[b]	MW (Da)	Radius (nm)	**Permeability, P_{app} (x 10^{-7} cm/s)** Before Electroporation	After Electroporation[c]	Fold Increase	p-value*
Calcein	623	0.6	3.43 ± 2.10	25.6 ± 14.9	7.5	0.000
BSA	66,000	3.5	0.28 ± 0.22	1.92 ± 0.83	6.8	0.001
Calcein:BSA			12.1	13.4		
p-value**			0.002	0.002		

[a] Tabulation of the results from Figure 8.3.
[b] Calcein: n = 12; BSA: n = 6
[d] Monolayers were electroporated with ten, 50 V – 1 ms pulses.
* Comparison between unelectroporated and electroporated monolayers.
** Comparison between calcein and BSA.

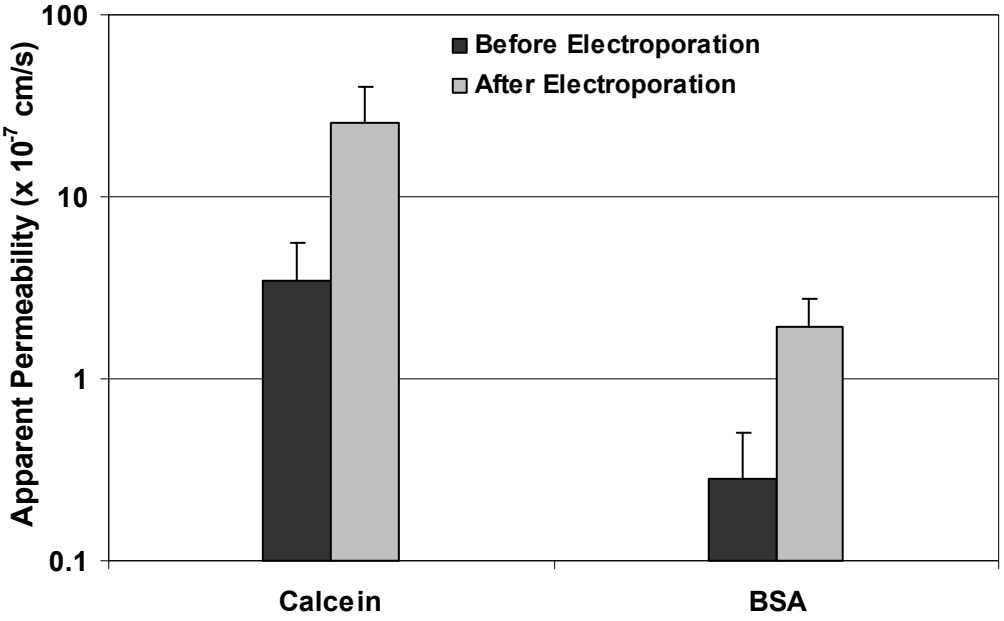

Figure 8.3 Comparison of permeability to calcein and BSA for unelectroporated (■) and electroporated (■) Caco-2 monolayers. For both sets of monolayers, permeability increased ~8-fold after electroporation. Permeability to calcein was more than 10-fold higher than permeability to BSA. Monolayers were treated with ten 50 V – 1 ms pulses and/or 10 μM calcein (radius = 0.6 nm) or 10 μM BSA (radius = 3.5 nm). All experiments were carried out at 37°C. Data plotted on a log scale to make the increase in permeability to BSA more apparent. [n=6-12]

For comparison, the permeabilities of ethanol-fixed monolayers to calcein and BSA were measured to establish the highest permeability that could be achieved while the cells were still present on the filter support. Figure 8.4 shows that after exposure to 95% ethanol, which permeabilizes cells and opens tight junctions (Ma et al., 1999), permeability to calcein was $1.13 \pm 0.06 \times 10^{-5}$ cm/s, an ~30-fold increase over pre-electroporation monolayer permeability ($p < 0.0001$) and a 4-fold increase over post-electroporation monolayer permeability ($p < 0.0001$). Permeability to BSA after ethanol fixation was $1.93 \pm 0.07 \times 10^{-6}$ cm/s, which was about 70-fold higher than pre-electroporation levels ($p < 0.0001$) and 10-fold higher than post-electroporation levels ($p < 0.0001$). The difference between calcein and BSA was about 6-fold ($p < 0.0001$). These results show that although electroporation increases transepithelial permeability, it does not increase permeability to its fullest extent.

In another comparison, the experimentally determined permeabilities of empty filters and collagen-coated filters to calcein and BSA were measured to aid the analysis of the contribution of the different barriers to transport to the permeabilities observed for the monolayers (see next section). The results of these experiments are represented in Figure 8.5 and tabulated in Table 8.2. The permeabilities of unelectroporated, electroporated, and ethanol (EtOH) fixed monolayers to the two solutes (previously discussed) have been included in the figure and the table for comparison. It should be noted that permeability across collagen-coated filters may not be a true representation of permeability across the extracellular matrix, which is synthesized by the cells as they grow in culture and is composed of other material besides collagen (Alberts, 1994). It would have been more

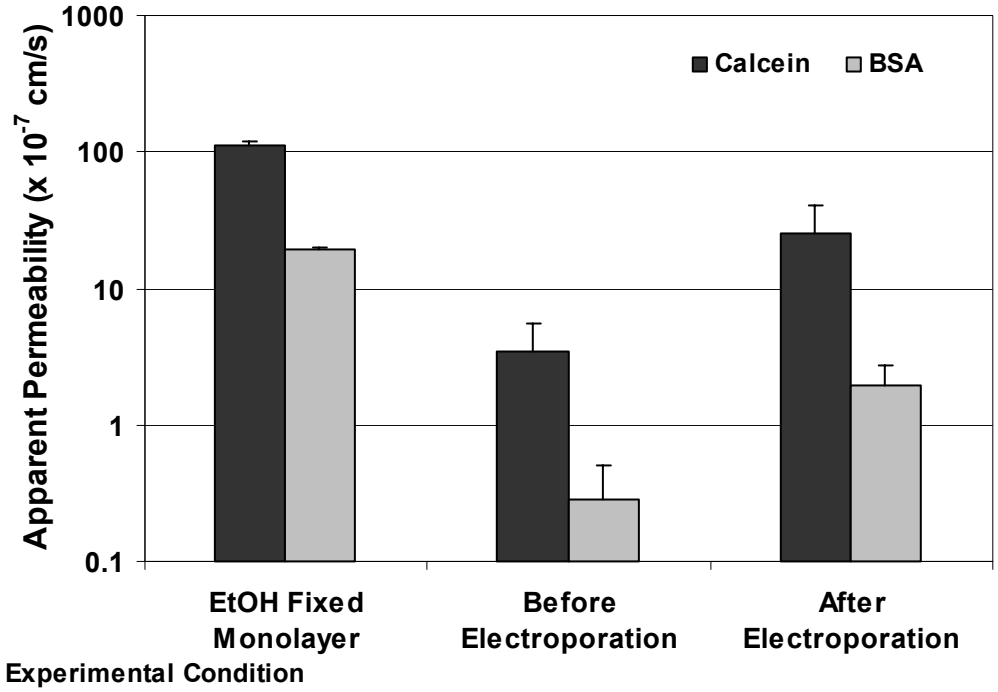

Figure 8.4 Apparent permeability of ethanol-fixed monolayers to calcein and BSA. Results from Figure 8.3 have been replotted for comparison. Caco-2 monolayers were treated with 95% ethanol (EtOH) for 20 minutes at -20°C and then monitored at 37°C for calcein and BSA transport to determine the highest permeability possible with the cells still present on the membrane. The resulting permeabilities of the ethanol-fixed monolayers to calcein and BSA were approximately 4-fold and 10-fold higher than electroporated monolayers, respectively. Data plotted on a log scale to make the permeabilities to BSA more apparent. [n=3 for EtOH fixed monolayers; $p < 0.0001$ for all comparisons]

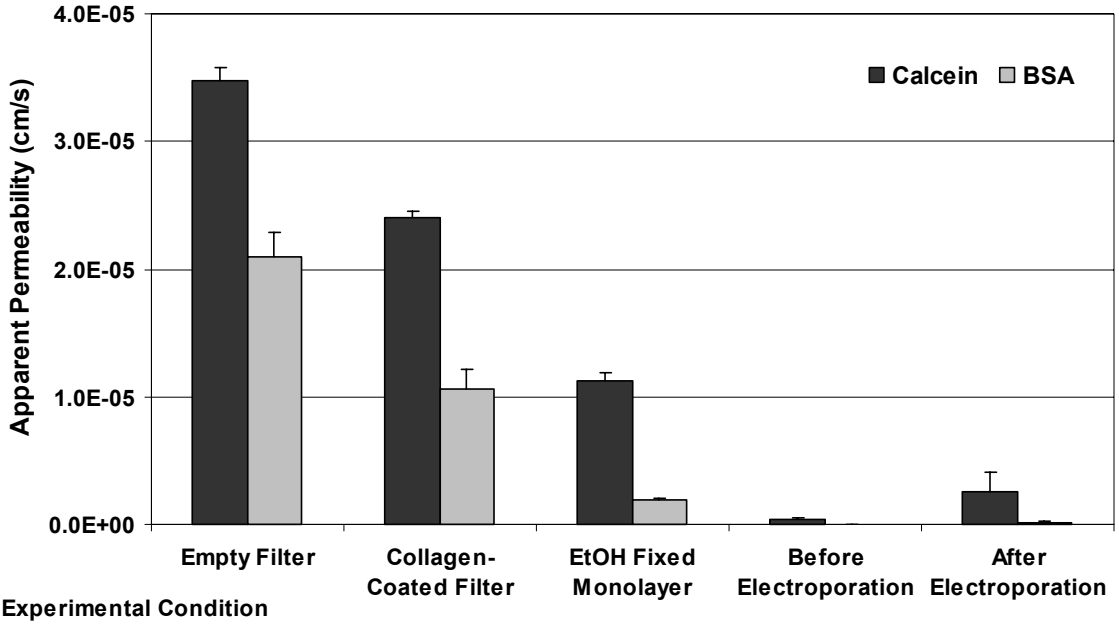

Figure 8.5 Calcein and BSA permeability comparisons for different experimental configurations. Permeability across empty and collagen-coated cell culture filter inserts with 0.4 μm pores was measured for both marker molecules and will be used to determine whether they acted as barriers to transport. Permeability across the collagen-coated filter was significantly lower than the empty filter, probably because of reduced transport of the molecules between the collagen fibers. Permeabilities for the ethanol-fixed, unelectroporated, and electroporated monolayers have been included for comparison. [n=3 for filter permeabilities]

Table 8.2 Solute properties and experimentally measured permeabilities for calcein and BSA under different experimental configurations.

	Solute Properties	
	Calcein	**BSA**
Solute Radius, nm	0.6	3.5
Diffusivity (@ 37°C), cm^2/s	5.4×10^{-6}	9.3×10^{-7}
	Permeability, P_{app} ($\times 10^{-6}$ cm/s)	
Empty filter	34.8 ± 0.92	21.0 ± 1.90
Collagen-coated filter	24.1 ± 4.41	10.7 ± 1.47
EtOH fixed monolayer	11.3 ± 0.62	1.93 ± 0.078
Electroporated monolayer	2.56 ± 1.49	0.19 ± 0.083
Unelectroporated monolayer	0.34 ± 0.21	0.028 ± 0.022

All experiments at 37°C.

accurate to carefully remove the cells, leaving the matrix behind, and then measure permeability, which could be less than that for filter coated with just collagen.

8.2.3 Delineating Barriers to Transport

The permeability values reported here are termed apparent permeabilities (P_{app}) because they are not just the permeabilities of the monolayer, but also include the permeabilities of other barriers to transport. The aqueous boundary layers (ABL), which are regions of low mixing adjacent to the apical surface of the monolayer and the basal surface of the filter, the collagen matrix used to coat the filter, and the filter support itself can all impede transport (Figure 8.6). Thus, it is necessary to determine to what extent these additional barriers to transport contribute to the permeabilities obtained.

If each of the transport barriers are considered to be resistances (R) in series, then

$$R_{total} = R_{ABL} + R_{monolayer} + R_{collagen} + R_{filter} \quad (8.1)$$

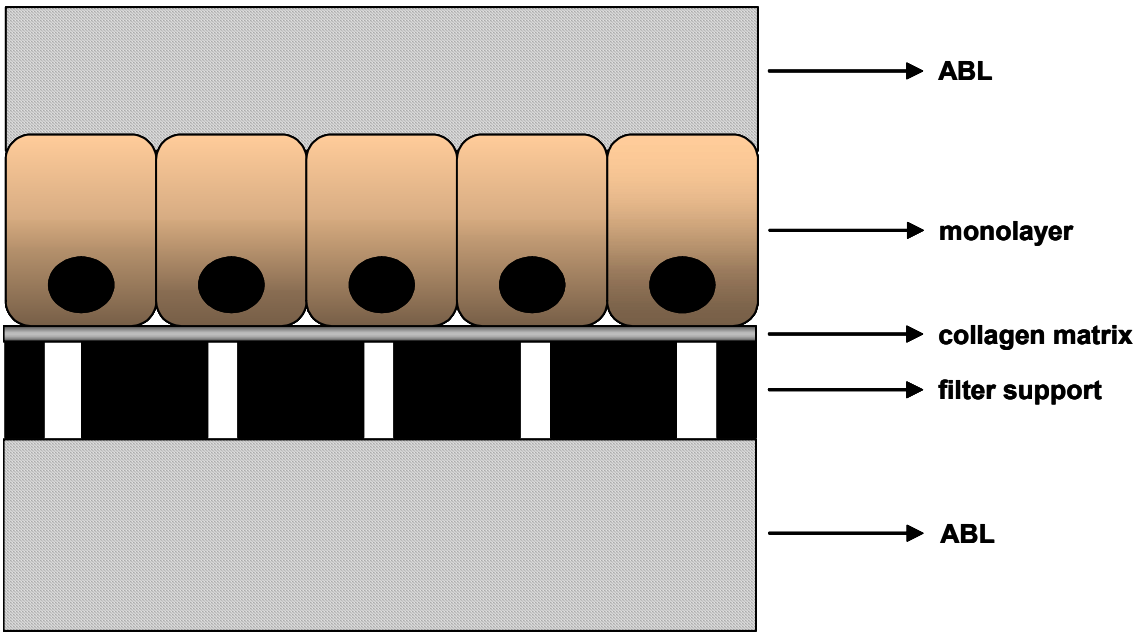

Figure 8.6 Illustration depicting the various barriers to transport that could affect the permeability of calcein and BSA across intestinal epithelial monolayers. The resistances associated with the aqueous boundary layers (ABL), the porous filter of the cell culture insert, the collagen matrix coating the filter, and the monolayer itself can all play a role in inhibiting permeability.

permeability, P, which is defined as the inverse of resistance, can then be calculated as

$$\frac{1}{P_{app}} = \frac{1}{P_{ABL}} + \frac{1}{P_{monolayer}} + \frac{1}{P_{collagen}} + \frac{1}{P_{filter}} \tag{8.2}$$

where P_{app} is the experimentally measured permeability of the monolayer. To find the actual permeability of the monolayer, $P_{monolayer}$, the values of each of the other terms in the equation must be determined.

The permeability of the filter, P_{filter}, can be determined based on the physical properties of the filter obtained from the manufacturer and is typically calculated using the following equation (Ho et al., 2000):

$$P_{filter} = \frac{N\pi R^2 D}{h_f} \times F\left(\frac{r}{R}\right) \tag{8.3}$$

where

N = pore density = 4 x 10^6 pores/cm^2
R = pore radius = 0.2 μm
h_f = filter thickness = 10 μm
r = solute radius
D = diffusivity of the solute (cm^2/s)

F(r/R) is the Renkin function, a molecular sieving function for cylindrical channels defined as

$$F\left(\frac{r}{R}\right) = \left(1 - \frac{r}{R}\right)^2 \left[1 - 2.014\left(\frac{r}{R}\right) + 2.09\left(\frac{r}{R}\right)^3 - 0.95\left(\frac{r}{R}\right)^5\right] \tag{8.4}$$

For r<<R, which is the case for both calcein and BSA, F(r/R) ≈ 1. The diffusivity of the solutes can be approximated using the Stokes-Einstein equation, which states that

$$D = \frac{kT}{6\pi\mu r} \tag{8.5}$$

where at 37°C

k = Boltzmann's constant, 1.38 x 10^{-16} erg/K
T = absolute temperature = 310 K
μ = solvent (water) viscosity = 0.007 poise
r = solute radius [=] cm

Using this equation, the diffusivities of calcein (r = 0.6 nm) and BSA (r = 3.5 nm) were calculated to be 5.4 x 10^{-6} cm^2/s and 9.3 x 10^{-7} cm^2/s, respectively. Inserting these diffusivity values into Eq. 8.3 yielded theoretical permeabilities of 2.72 x 10^{-5} cm/s and 4.67 x 10^{-6} cm/s across empty filters with 0.4 μm pores for calcein and BSA, respectively.

Although the monolayers were kept on an orbital shaker during the course of each experiment to minimize the effect of the ABL, it is possible that there may be small effects on filer permeability that would need to be accounted for. To determine the permeability of the ABL, P_{ABL}, the following equation would be used

$$\frac{1}{P_{filter+ABL}} = \frac{1}{P_{filter}} + \frac{1}{P_{ABL}} \tag{8.6}$$

since, in the case of the empty filter, only the filter and the ABL should contribute to the permeability. $P_{filter+ABL}$, the total apparent permeability of the empty filter, was experimentally measured to be 3.48 ± 0.09 x 10^{-5} cm/s for calcein and 2.10 ± 0.19 x 10^{-5} cm/s for BSA. These values were significantly higher than the filter permeabilities (P_{filter}) calculated using Eq. 8.3, P_{filter} = 2.72 x 10^{-5} cm/s for calcein and 4.67 x 10^{-6} cm/s for

BSA. Consequently, calculation of the permeability of the ABL, P_{ABL}, was made difficult since negative values were obtained. While the shaking may have increased permeability by decreasing the ABL resistance, it is also possible that there was some convective flux of the calcein and BSA solutions through the pores of the filter.

When the filters were coated with collagen, the measured permeability to calcein ($2.41 \pm 0.04 \times 10^{-5}$ cm/s) and BSA ($1.07 \pm 0.15 \times 10^{-5}$ cm/s) dropped by 30% and 50%, respectively, when compared to the empty filter (Figure 8.5; Table 8.2). The decrease is probably due to the collagen fibers, which would impede diffusion of the molecules across the filters. The permeability across the collagen matrix alone, $P_{collagen}$, can be calculated with the following equation, assuming no contribution from the ABL:

$$\frac{1}{P_{collagen}} = \frac{1}{P_{collagen+filter}} - \frac{1}{P_{filter}} \tag{8.7}$$

Instead of using the P_{filter} determined with Eq. 8.3, which resulted in a negative collagen permeability value for BSA, the measured permeabilities of the empty filters for both calcein and BSA were used in Eq. 8.7. Using the appropriate values, the permeability of the collagen alone, $P_{collagen}$, was calculated to be 7.84×10^{-5} cm/s for calcein and 2.17×10^{-5} cm/s for BSA. When the resistance of the collagen ($1/P_{collagen}$,) was divided by the total resistance of the collagen coated filter ($1/P_{collagen+filter}$), the collagen matrix was found to account for 30% of the resistance to calcein transport and 50% of the resistance to BSA transport across the coated filter. This means in cell-free, collagen-coated filters, the filter is the most important barrier to transport of calcein and for BSA, the filter and collagen contribute equally to resistance.

The permeability of unelectroporated and electroporated monolayers to calcein and BSA can now be calculated using the following equation modified from Eq. 8.2

$$\frac{1}{P_{monolayer}} = \frac{1}{P_{app}} - \frac{1}{P_{collagen}} - \frac{1}{P_{filter}} \tag{8.8}$$

where P_{app} is the experimentally measured total permeability of the Caco-2 monolayers to calcein and BSA (see Table 8.2), $P_{collagen}$ is the permeability of the collagen matrix to calcein (7.84×10^{-5} cm/s) and BSA (2.17×10^{-5} cm/s), and P_{filter} is assumed to be the same as the measured permeability across the empty filter ($3.48 \pm 0.09 \times 10^{-5}$ cm/s for calcein and $2.10 \pm 0.19 \times 10^{-5}$ cm/s for BSA). Using Eq. 8.8, the permeabilities of the unelectroporated monolayers, $P_{monolayer,}$ were calculated to be 3.48×10^{-7} cm/s for calcein and 2.84×10^{-8} cm/s for BSA. For the electroporated monolayers, $P_{monolayer}$ was calculated to be 2.87×10^{-6} cm/s for calcein and 1.95×10^{-7} cm/s for BSA.

In each case, the true permeability of the monolayer was slightly higher than the total permeability that was experimentally measured, which indicated that the filter and collagen matrix may have provided some resistance to transport. To determine the extent each barrier contributed to the permeabilities of unelectroporated and electroporated monolayers, the resistance (1/P) of each barrier, e.g., filter, collagen, monolayer, was divided by the total resistance ($1/P_{app}$). Table 8.3 shows the results of these comparisons. For the unelectroporated monolayers, the filter support and collagen provided very little resistance to calcein ($\leq$ 1%) and BSA transport (0.1%), while the monolayer resistance accounted for ~99% of the resistance to transport. When the monolayers were electroporated, the resistance contribution of the filter and collagen coating increased for

both calcein (7% and 3%) and BSA (~1%) but, again, the monolayer was the dominant barrier to transport.

Table 8.3 Delineation of permeabilities across unelectroporated and electroporated Caco-2 monolayers and the contribution of each barrier to transport to overall permeability.

		Calcein		BSA	
		Permeability	**% Resistance[a]**	**Permeability**	**% Resistance[a]**
Unelectroporated	P_{app}*	0.343 (0.21)	—	0.0283 (0.022)	—
	$P_{collagen}$	78.4	0.4	21.7	0.1
	P_{filter}*	34.8 (0.92)	1.0	21.0 (1.90)	0.1
	$P_{monolayer}$	0.348	98.6	0.0284	99.6
Electroporated	P_{app}*	2.56 (1.49)	—	0.192 (0.083)	—
	$P_{collagen}$	78.4	7.4	21.7	0.9
	P_{filter}*	34.8 (0.92)	3.3	21.0 (1.90)	0.9
	$P_{monolayer}$	2.87	89.2	0.195	98.5

All permeability values have units of 10^{-6} cm/s. Where applicable, standard deviations are in parentheses.
[a] % Resistance values may not add up to 100% because of rounding.
* Experimentally measured

8.2.4 Monitoring TEER of Monolayers during Permeability Studies

Since transepithelial permeability is directly related to the integrity of the monolayers, the transepithelial electrical resistances (TEER) of all monolayers were monitored during the course of each permeability experiment. Figure 8.7 shows the TEER of Caco-2 monolayers, which were measured each hour for the three hours prior to and after electroporation. During the 3 hour period when baseline permeability was measured for the unelectroporated monolayers, TEER was initially ~700 Ω-cm^2 and then dropped to a constant level of about 500 Ω-cm^2 over the next three hours. TEER values measured between 1 and 3 hours were not statistically different ($p = 0.83$).

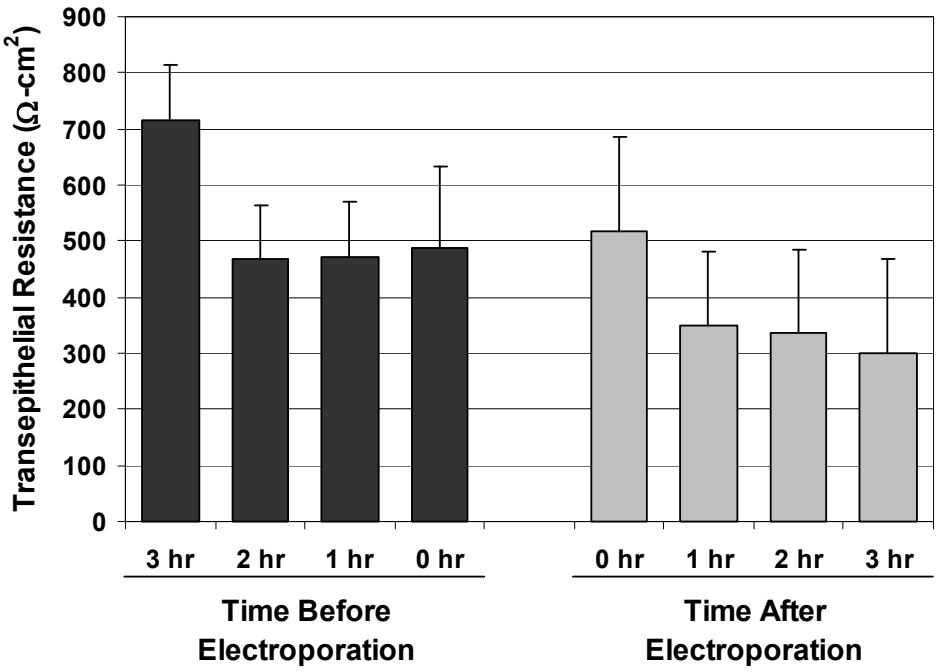

Figure 8.7 Monitoring transepithelial electrical resistance (TEER) of confluent Caco-2 monolayers during permeability studies. Resistance was measured each hour for three hours before and three hours after electroporation Post-electroporation resistance was approximately 60% lower than pre-electroporation resistance and remained relatively constant ($p > 0.05$). Resistance measurements at $t = 0$ hr, which were made immediately before and after electroporation, are elevated because of the dependence on temperature (see text). If measurements had been taken for a longer period time after electroporation, TEER would likely have returned to initial values. [n=18]

The resistance was initially high because of its dependence on temperature. Although monolayers were incubated at 37°C prior to starting the experiment, the pre-electroporation measurements made at t = 0 hr were usually made after the fluorescent marker solution had been added, by which time the monolayers had cooled to room temperature. This resulted in elevated resistance values. Subsequent measurements made after the monolayers were returned to the incubator are more indicative of the true resistances of the monolayers.

Just after electroporation, the resistance was initially a little over 500 Ω-cm^2 and then dropped and maintained levels ranging from about 300 to 350 Ω cm^2 in the three hours after electroporation. Again, the initial post-electroporation resistances were higher than subsequent measurements because the monolayers cooled to room temperature during the electroporation procedure. For the measurements taken 1 – 3 hours after electroporation, the resistances were not statistically different from each other ($p = 0.62$).

When the post-electroporation resistances were compared to the pre-electroporation resistances, the former were found to be about 60% - 75% of the latter ($p < 0.0001$). This indicated that the monolayers did not completely recover their initial TEER values, which would explain why permeability did not ultimately decrease with time. Based on our previous experience with monolayer recovery after electroporation (Chapter 7), it is likely that an increase in resistance, coupled with a decrease in permeability, would have been observed if measurements had been taken for longer than three hours.

8.2.5 Modulating Paracellular Permeability of Caco-2 Monolayers

For most hydrophilic molecules, transport across the intestinal epithelium occurs in the paracellular space between the cells and is regulated by the tight junctions. Since increased paracellular transport may contribute to the increase in permeability observed after electroporation, experiments were conducted to determine how much transport occurs when the tight junctions are opened. The role of extracellular calcium in the formation and maintenance of tight junctions has been well-documented (Gonzalez-Mariscal et al., 1990; Ma et al., 2000). Incubation of epithelial monolayers in a calcium free solution has been found to cause a decrease in epithelial resistance and an increase in permeability. The increase in permeability was due to contraction of the cytoskeletal network and subsequent opening of the tight junctions (Gonzalez-Mariscal et al., 1990; Ma et al., 2000).

In this set of experiments, Caco-2 monolayers were incubated in HBSS without Ca^{2+} and Mg^{2+} (HBSS-) for the period of time required for the transepithelial resistance to drop to approximately half of initial values. At this point, the monolayers were switched to calcium supplemented HBSS (HBSS+) and allowed to recover for at least 30 minutes. During both time periods, the permeability of calcein across the monolayers was monitored. Control monolayers were incubated in HBSS+ for the duration of the experiment.

Figure 8.8 shows the results from two independent experiments conducted to monitor the paracellular permeability of calcein across monolayers with opened tight junctions. In Experiment #1 (Figure 8.8A), the permeabilities of monolayers in HBSS-

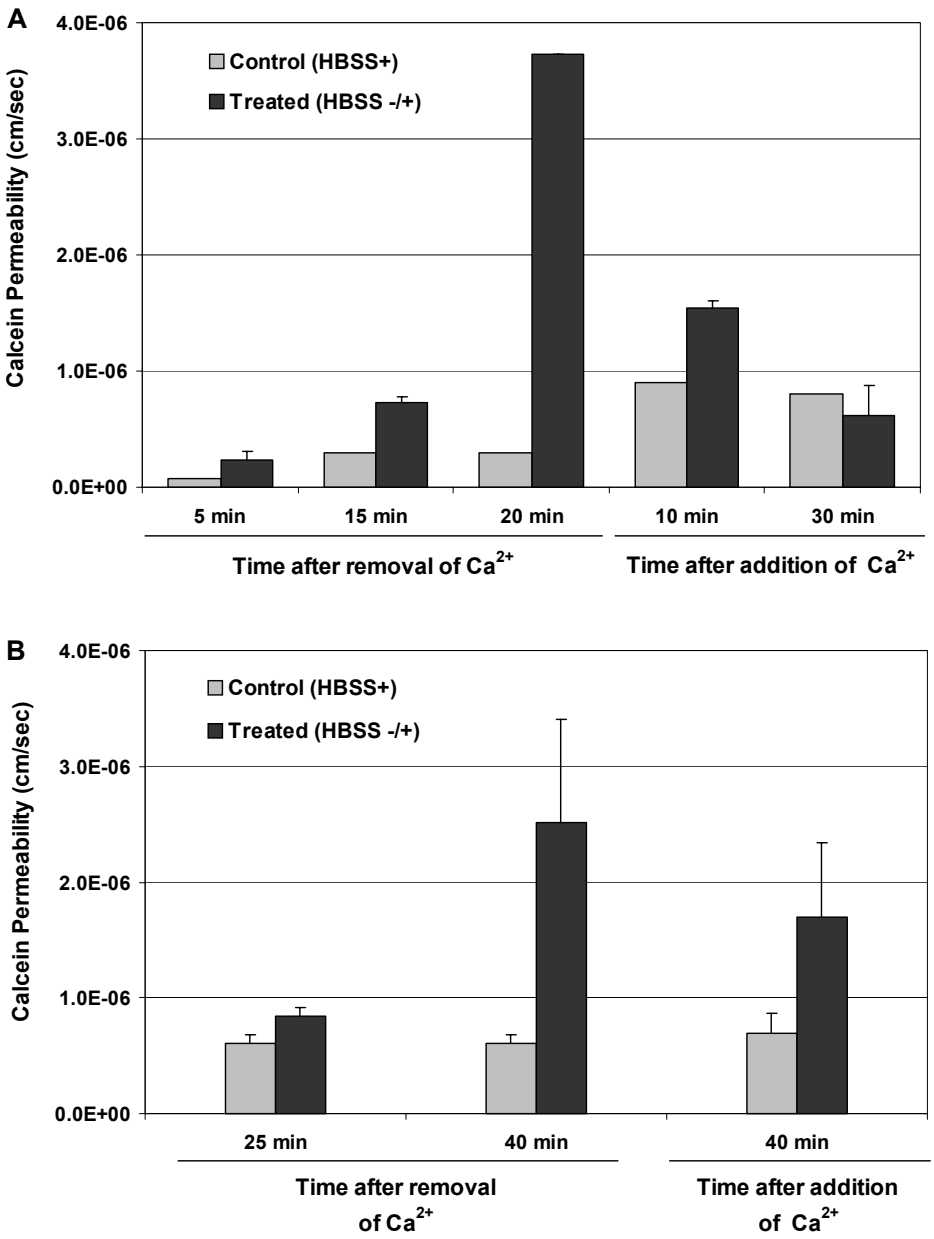

Figure 8.8 Effect of extracellular calcium depletion and addition on Caco-2 paracellular permeability of calcein. Two independent experiments were conducted to evaluate permeability. Treated Caco-2 monolayers were placed in Ca^{2+}-free HBSS (HBSS-) and monitored for up to 20 min (A) or 40 min (B). They were then switched to Ca^{2+} supplemented HBSS (HBSS+) and monitored further for calcein permeability. Control monolayers remained in HBSS+ for the duration of the experiment. [n = 1 – 4]

were initially low ($2.35 \pm 0.76 \times 10^{-7}$ cm/s) and only slightly higher than the permeability of the control monolayer. After incubation in HBSS- for 20 minutes, the permeability increased to a maximum of $3.72 \pm 0.004 \times 10^{-6}$ cm/s, which was a 12-fold increase over the permeability of the HBSS+ incubated control monolayer. At this point, the treated monolayers were switched to HBSS+ and within 30 minutes, the permeability returned to a level comparable to that of the control monolayer ($6.15 \pm 2.59 \times 10^{-7}$ cm/s vs. 8.02×10^{-7} cm/s).

In Experiment #2 (Figure 8.8B), a similar trend was observed in that permeability of the HBSS- incubated monolayers increased to a maximum of $2.52 \pm 0.89 \times 10^{-6}$ cm/s, which was about 4 times higher than that of the HBSS+ incubated control monolayers ($6.05 \pm 0.79 \times 10^{-7}$ cm/s; $p = 0.046$). The time required to reach this maximum, however, was twice as long as that observed in the first experiment (40 min vs. 20 min). When the treated monolayers were switched to HBSS+, permeability decreased, but, even after 40 minutes, was still twice as high as the controls ($1.69 \pm 0.66 \times 10^{-6}$ cm/s vs. $6.88 \pm 1.83 \times 10^{-7}$ cm/s; $p = 0.11$). Although there is some variability in the results of these experiments, averaging the two gives an estimated paracellular permeability of $3.12 \pm 0.85 \times 10^{-6}$ cm/s for calcein.

In a companion study, simultaneous measurements of the transepithelial resistance of the Caco-2 monolayers were made during the paracellular permeability experiments. Figure 8.9 shows the changes in TEER that occurred while the monolayers were incubated in HBSS- and HBSS+. In Experiment #1, the TEER for control monolayers incubated in HBSS+ remained relatively constant at about 600 Ω-cm^2. The TEER for control monolayers in Experiment #2 ranged between 500 and 600 Ω-cm^2. In

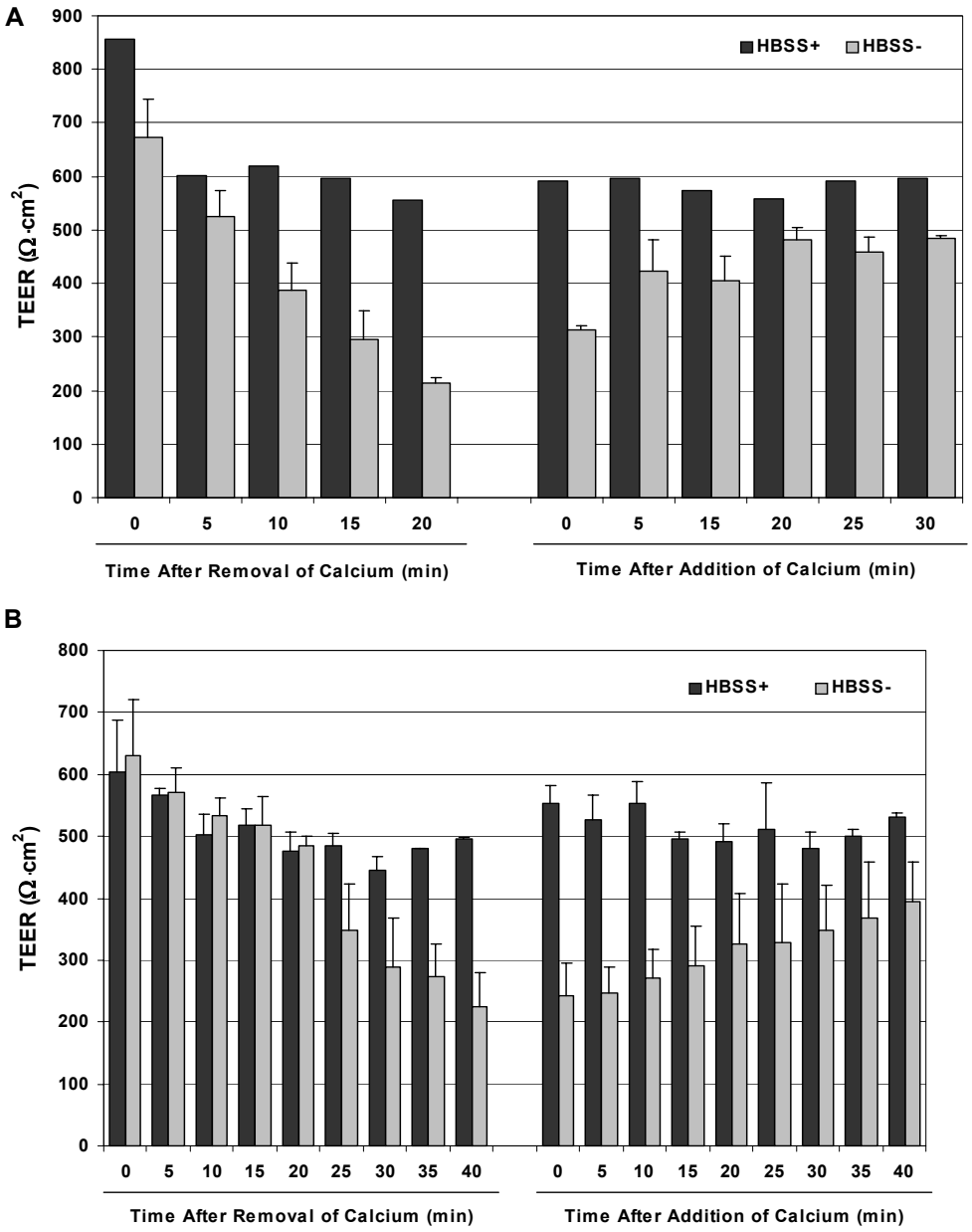

Figure 8.9 Transepithelial resistances of Caco-2 monolayers measured during extracellular calcium depletion experiments. Resistances for calcium depleted monolayers in both Experiment #1 (A) and Experiment #2 (B) dropped to less than half of the control monolayers, which remained in calcium-supplemented HBSS+. Upon switching to HBSS+, resistances of monolayers in both experiments increased to within 30% of controls. [n = 1-4]

both experiments, the TEER for monolayers incubated in HBSS- dropped to almost 200 Ω-cm2. When these monolayers were switched to HBSS+, TEER began to increase almost immediately (the rate of increase was slightly faster for Experiment #1) until they were ~70 - 80% of control resistances.

8.2.6 Discrepancies in Mole Balances for Permeability Experiments

When mole balances were performed on the monolayers to ensure that the number of moles lost from the apical solution was equal to the number of moles transported into and/or across the cells, inconsistencies in the results were found. For some experiments, the decrease in the amount of calcein in the donor solution during the course of the experiment was higher than the total amount of calcein that accumulated in the receiver solution. This was true for both unelectroporated and electroporated monolayers. Even when electroporated monolayers were analyzed for calcein uptake by flow cytometry, the total amount of calcein did not add up. In a few cases, the amount of calcein calculated to be in the donor solution at the end of the experiment was higher than the amount of calcein present at the beginning of the experiment, but this can probably be attributed to the variability associated with having to dilute the apical samples.

Another factor that could have affected the mole balances of the electroporated monolayers could be the cells themselves. Caco-2 cells are known to have efflux mechanisms which actively pump foreign material out of the cell and play a role in the low absorption of some drugs (Feller et al., 1995; Hidalgo and Li, 1996). In fact, researchers have found that Caco-2 cells pre-loaded with calcein, rapidly transported the marker from the cytoplasm (Feller et al., 1995; Fujita et al., 1997). It is also possible that

there could be some type of metabolism of the markers within the cell, especially in the case of BSA, which would be prone to degradation by proteases.

8.3 Discussion

The results presented in this chapter show that electroporation does increase the permeability of intestinal epithelial monolayers. However, the mechanism by which permeability increases is not easily determined. As Figure 8.10 illustrates, there are three potential pathways via which transport can occur after electroporation. Paracellular transport, which occurs between the cells, is the primary route of transport of molecules across intact epithelium *in vitro* and *in vivo*. Transcellular transport across the cells is not a common route of transport for hydrophilic molecules, but could potentially be enhanced by electroporation, which permeabilizes cell membranes. Finally, since electroporation can cause cell death, cells could lift off the membrane and leave gaps through which transport could occur (transmonolayer transport). Any, or all, of these pathways could play a role in the increased permeability observed after electroporation.

8.3.1 Paracellular Transport

In Section 8.2.5, when Caco-2 monolayers were incubated in calcium-free HBSS to open the tight junctions, the paracellular permeability of the monolayers, $P_{paracellular}$, to calcein increased to $3.12 \pm 0.85 \times 10^{-6}$ cm/s. In comparison, the total permeability of electroporated Caco-2 monolayers to calcein, $P_{electroporation}$, was determined to be $2.56 \pm 1.5 \times 10^{-6}$ cm/s. Although $P_{electroporation}$ is slightly less than the $P_{paracellular}$, there was no

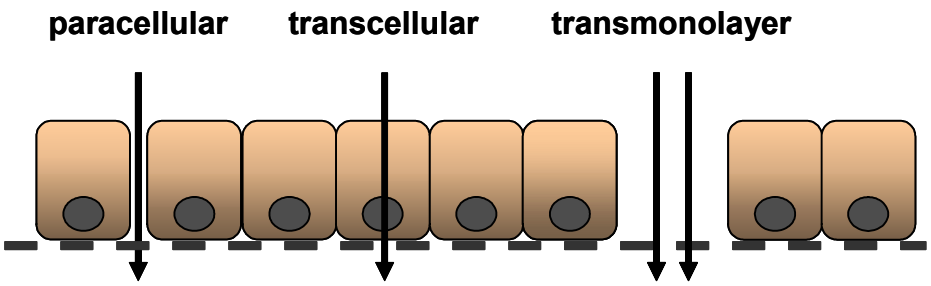

Figure 8.10 Illustration of the various pathways that could play a role in the increase in transport observed after electroporation. Paracellular (between cells), transcellular (across cells), and transmonolayer (through holes in monolayer) transport could each contribute to monolayer permeability.

statistical difference between the two values (t-test; $p = 0.60$). This means that if electroporation disrupted the tight junctions, then paracellular transport could very well contribute a great deal to the observed increase in permeability.

In two separate studies, Ma et al. examined the effects of extracellular calcium depletion (2000) and low concentrations of ethanol (1999) on the tight junction barrier of Caco-2 monolayers. They observed that the transepithelial resistance of the monolayers dropped to 20% of initial values within 10 minutes after calcium removal and to less than half of initial values within an hour after ethanol addition. When the monolayers were returned to their normal medium, barrier function was completely restored within 2 hours. In both studies, a concurrent increase in the flux of mannitol, a common paracellular tracer molecule, was observed during the period of low resistance, followed by a rapid decrease in flux as resistance returned to normal. Leonard et al.

Leonard et al. (2000a) found that iontophoresis, the application of low level currents to transport molecules by electrophoresis, resulted in increased paracellular transport of dextrans ranging in size from 4 kDa to 20 kDa and increased TEER. Within 40 minutes after the current had been turned off, both permeability and TEER returned to pre-treatment values. These, and the findings of Ma et al., are in good agreement with the permeability and resistance results obtained in our experiments with extracellular calcium depletion (Figures 8.8-8.9), where we saw an increase in Caco-2 permeability to calcein 20-40 minutes after calcium removal and a subsequent decrease in permeability back to control levels in as little as 30 minutes after calcium addition.

As will be discussed in Section 8.3.3, when calcein and BSA transport was monitored after electroporation, the rate of transport for the two markers showed no sign

of decreasing, even after three hours. In addition, resistance of the electroporated monolayers remained slightly lower than controls for the duration of the experiments (Fig. 8.7). Unless electroporation damages the cells or tight junctions in such a way that long-term opening of junctions results, which cannot be determined based on existing results, the evidence suggests that another pathway may also be involved in enhancing the permeability of the monolayers.

8.3.2 Transcellular Transport

Transcellular transport, which occurs across the cells, would likely be most evident immediately after electroporation. Because of the direction of the electric field and the orientation of the cells, electroporation causes the formation of pores at the apical and basal membranes of the cells. Ten 1-ms pulses were applied to each monolayer and, because of a limitation of the pulsing machine, the spacing between each pulse was about 15 s. This means that transport could be driven by electrophoresis during the pulses and by diffusion between the pulses. If transport occurred during electroporation through the porated apical membrane, across the cell, and then out of the basal membrane, then some amount of the marker molecule would be present in the basal chamber of the cuvette immediately after pulsing.

To determine whether this could be the case, the fluorescence intensities of samples collected from the basal compartment immediately after electroporation (within 30 sec of last pulse) were compared to basal samples of unelectroporated control monolayers at time t = 0 for both calcein and BSA (Figure 8.11). Although calcein fluorescence in the samples collected immediately after electroporation was slightly

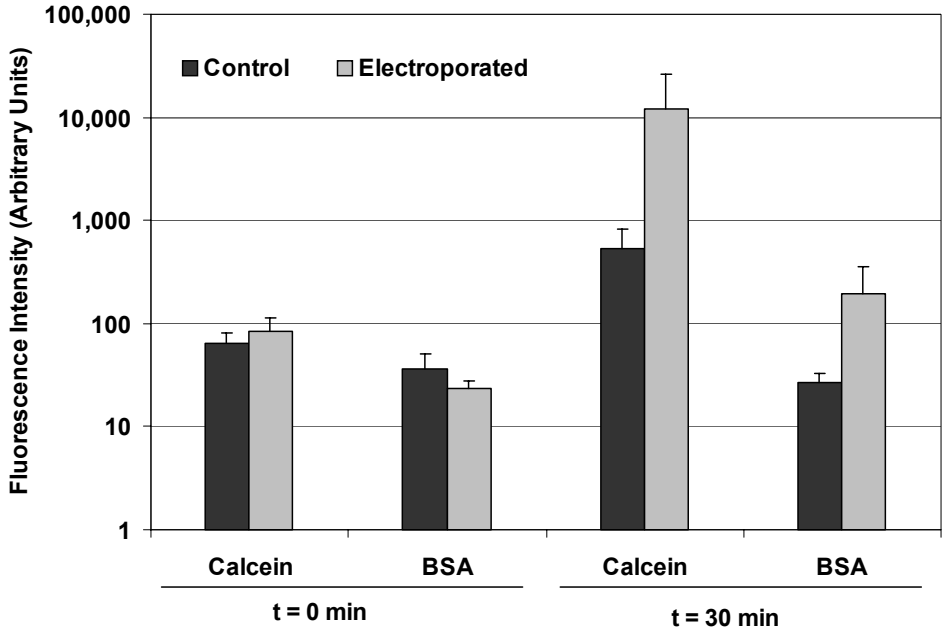

Figure 8.11 Fluorescence intensities of basal samples collected from unelectroporated and electroporated monolayers immediately after treatment (t = 0 min) and 30 minutes after treatment. Transcellular transport of calcein and BSA after electroporation was assumed to be negligible since there was no significant difference in the basal sample fluorescence of control and electroporated monolayers ($p > 0.05$; n = 6-12). Additionally, the relatively short lifetime of electropores (1 or 2 minutes) precludes their involvement in the large increase in basal sample fluorescence observed 30 minutes after treatment. [n = 6-12]

higher than the controls, it was not statistically significant ($p = 0.08$). The difference between the basal sample intensities for the control monolayers and treated monolayers was not significant for BSA as well ($p = 0.08$). In addition, the fluorescence intensities increased by two orders of magnitude for calcein and by an order of magnitude for BSA during the 30 minute period following electroporation. This increase in fluorescence cannot be explained by transport through pores formed after electroporation, since electropores do not stay open longer than a minute or so (Chang et al., 1992). Based on these results, transcellular transport of calcein and BSA after electroporation was assumed to be negligible.

8.3.3 Transmonolayer Transport

Transmonolayer transport, or transport through holes left by shedding cells, is more difficult to quantify. If dead cells lift off during the course of the permeability experiment, estimating the size and number of gaps in the monolayer is not an easy task, especially if only one or two cells lift off randomly around the monolayer. Nevertheless, some of the unelectroporated and electroporated monolayers were checked at the end of a full permeability experiment for any obvious holes or gaps. The monolayers were washed and fixed with ethanol and then treated with the nuclear stain propidium iodide to aid identification of the cells.

Figure 8.12 shows two sets of representative control monolayers (A-B) and electroporated monolayers (D-E) at the end of a permeability experiment. Each monolayer was visually scanned in its entirety and imaged at the lowest magnification so that the largest area could be seen. No large holes were evident in both unelectroporated

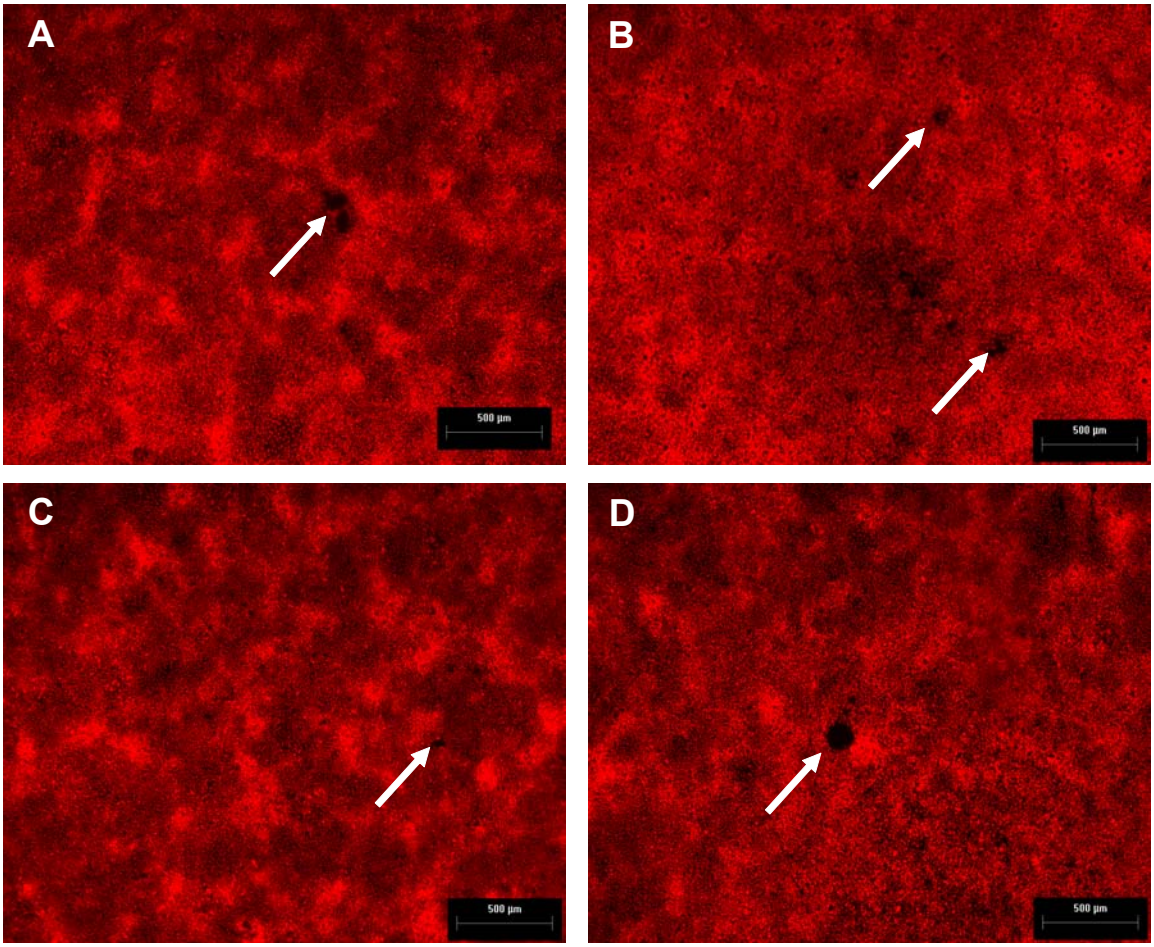

Figure 8.12 Propidium iodide staining of fixed unelectroporated (A-B) and electroporated (C-D) Caco-2 monolayers at the end of permeability studies. To determine whether there were large holes present in the monolayers that could result in transmonolayer transport of calcein, cells were fixed with ethanol and then incubated with 10 µg/ml of propidium iodide to stain all nuclei and aid identification of cells. Small holes, or gaps, (identified by white arrows) were evident in both control monolayers and electroporated monolayers.

and electroporated monolayers, which indicates that there was not a significant amount of cell death. There were small dark areas that could represent locations where cells had lifted off. However, these gaps (indicated by white arrows) were found in control and electroporated monolayers, which makes it difficult to say whether there were actual holes in the monolayer or just regions where the nuclei were more widely spaced.

There is some additional supporting evidence that cells may have detached from the monolayer. Figure 8.13 shows the results of four independent experiments in which the transport of calcein and BSA across three Caco-2 monolayers was monitored over time before and after electroporation. Before electroporation occurred at time t = 0 h, the accumulation of calcein and BSA in the basal compartment was relatively low. After electroporation, the rate of accumulation increased significantly, indicating increased permeability of the monolayers to the two markers. In two experiments, accumulation was relatively linear for both calcein (Fig. 8.13A) and BSA (Fig. 8.13B) after electroporation. In another set of experiments, however, a sudden increase in the transport was observed for both calcein and BSA (Figs. 8.13C,D). This increase could be the result of the detachment of dead cells from the monolayers.

For calcein, a large increase occurred in the first 30 minutes after electroporation in Monolayer C, corresponding to a permeability of 1.1×10^{-5} cm/s, followed by slower transport ($P = 2.4 \times 10^{-6}$ cm/s) for the rest of the experiment (Fig. 8.13C). The transport of BSA was relatively low for the first hour after electroporation and then two of the three monolayers had a large increase in transport (Fig. 8.13D). The permeability before the jump was about 1.3×10^{-7} cm/s and 1.1×10^{-7} cm/s for Monolayers A and B,

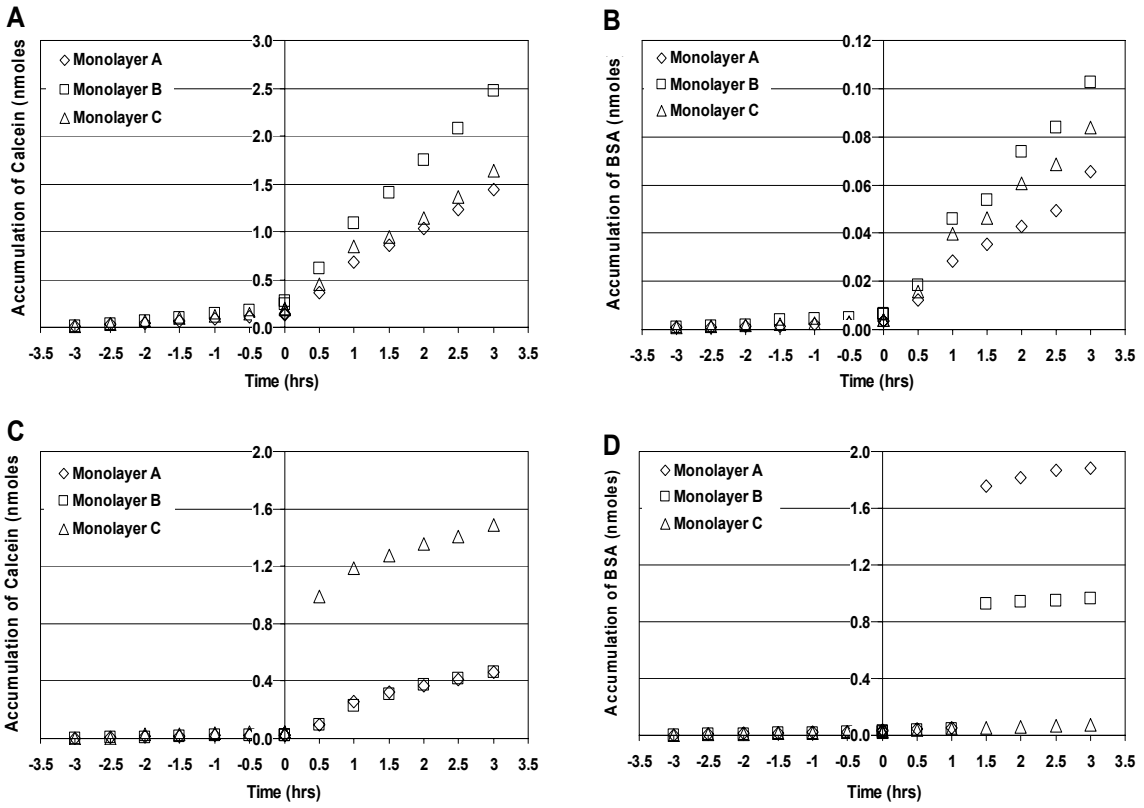

Figure 8.13 Calcein (A,C) and BSA (B,D) accumulation over time before and after electroporation from four independent experiments. Electroporation took place at time t = 0 h. Calcein and BSA transport was linear with time for most monolayers (A,B); however, in a few monolayers there were sudden increases in transport that could perhaps be explained by the detachment of cells from the monolayer (C,D).

respectively. After the jump, the permeabilities of these two monolayers increased to 5.4 x 10^{-7} cm/s and 1.5 x 10^{-7} cm/s, respectively. Monolayer C maintained a post-electroporation permeability of 1.1 x 10^{-7} cm/s for the duration of the experiment.

The fact that the accumulation of marker molecules in the basal compartment did not level off after three hours (Figure 8.13) and that the resistances of the electroporated monolayers remained consistently lower than the control monolayers (Figure 8.7) suggests that there may have been some cell loss after electroporation. If this was the case, then transmonolayer transport may have contributed to the increase in permeability seen after electroporation. Unfortunately, there is not enough information to be able to quantify and correlate the loss of a few cells to changes in the overall permeability.

8.4 Conclusions

Electroporation increased the permeability of confluent Caco-2 monolayers to calcein and bovine serum albumin. The increase in permeability was size dependent and was enhanced by the application of multiple pulses (when total exposure time was held constant). When the various barriers to transport were evaluated, the monolayer was found to be the primary barrier. The route by which permeability was increased could be a combination of paracellular and transmonolayer transport, but it is likely that transmonolayer transport was the major contributor. The results of these experiments demonstrate that electroporation could be useful for increasing the permeability of intact intestinal epithelium and, thus, enhance the absorption of poorly absorbed drugs.

CHAPTER IX

9. NUCLEIC ACID DELIVERY TO MONOLAYERS BY ELECTROPORATION

9.1 Introduction

Since the first demonstration of electroporation-mediated gene transfer and expression over twenty years ago (Neumann et al., 1982), electroporation has rapidly become a common laboratory tool for *in vitro* transfection of bacterial, plant, and mammalian cells (Neumann et al., 1989; Chang et al., 1992). Electroporation has also proven to be very useful for *in vivo* gene delivery in animal models as evidenced by published accounts of successful gene delivery to corneal epithelium (Oshima et al., 1998), murine melanoma (Rols et al., 1998), skeletal muscle (Mir et al., 1999), and other tissues (Jaroszeski et al., 1999; Jaroszeski et al., 2000; Trezise, 2002).

The majority of *in vitro* gene transfection protocols for adherent cells call for removal of cells from their substrate and/or the use of subconfluent cells for increased expression (Ravid and Freshney, 1998; Sambrook and Russell, 2001). However, many types of epithelial cells only exhibit the characteristics of *in vivo* epithelium when they are cultured to full confluence and are allowed to differentiate into mature epithelium. Unfortunately, many methods of transfection, including lipofection, work much less efficiently on differentiated cells, as described by Uduehi et al. and Matsui et al., who monitored cationic lipid-mediated transfection in two types of epithelia, Caco-2 intestinal epithelial cells (Uduehi et al., 1999) and airway (bronchial and tracheal) epithelial cells (Matsui et al., 1997). In both studies, a common theme was observed: increased

resistance to transfection with cationic lipids as the cells became more differentiated, e.g., the formation of tight junctions and apical features such as microvilli or cilia.

Many protocols for gene transfection have been published that show that the determination of optimal electroporation parameters for successful transfection of DNA is largely empirical (Nickoloff, 1995; Lynch and Davey, 1996; Cataldo et al., 1998). Some researchers have found that the application of combinations of short, high voltage pulses (which porate the cells) and long, low voltage pulses (which electrophoretically drive the DNA into the cells) yielded good results in *in vitro* (Sukharev et al., 1992) and *in vivo* transfection experiments (Bureau et al., 2000; Satkauskas et al., 2002). A variation of this approach was used in these experiments.

This study will evaluate the ability of electroporation to effectively transfect well-differentiated T84 intestinal epithelial monolayers with reporter plasmid DNA to express luciferase or green fluorescent protein. The resulting DNA uptake and protein expression were compared with uptake and expression after lipid-mediated transfections to determine whether electroporation could transfect these cells more efficiently.

9.2 Experimental Results

9.2.1 Luciferase Expression in Confluent T84 Monolayers after Lipofection

Figure 9.1 shows the expression of luciferase after transfection with a range of LipoTAXI® lipid concentrations (0 mM – 0.1 mM) and amounts of gWiz™-Luc plasmid (5 μg – 30 μg). Luciferase expression was measured 48 h after transfection using a

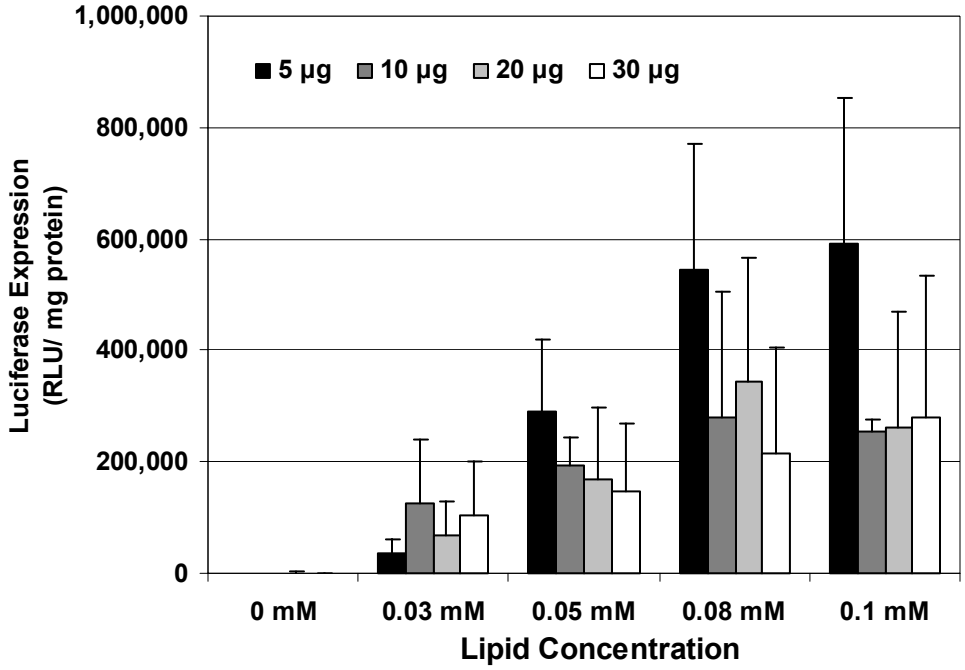

Figure 9.1 Luciferase expression over a range of lipid concentrations and DNA amounts after transfection of confluent T84 monolayers with the cationic lipid LipoTAXI. Transfection with 5 µg of DNA and either 0.08 mM or 0.1 mM of lipid yielded the highest levels of expression. Although expression appears to vary with lipid concentration and DNA amount, statistical analysis by two-way ANOVA showed no dependence of luciferase expression on the two variables ($p=0.09$ and 0.42, respectively). [n = 3]

luminometer and is reported as the number of relative light units expressed per milligram of cellular protein (RLU/mg protein).

At all but the lowest lipid concentration, transfection with 5 μg of plasmid yielded the highest amount of luciferase expression (up to 6 x 10^5 RLU/mg protein), while transfection at the other conditions resulted in expression that ranged from about 0.7 – 3.5 x 10^5 RLU/mg protein. Luciferase expression appeared to increase to a plateau as the lipid concentration increased and decrease as the DNA amount increased. Statistical analysis by two-way ANOVA, however, showed that there was no significant difference in luciferase expression when the lipid concentration was changed ($p = 0.09$) or when the DNA amount was changed ($p = 0.42$). Despite this, 0.08 mM LipoTAXI was the highest concentration used to treat monolayers because of the potential for toxicity at high lipid concentrations.

9.2.2 Combining High and Low Voltage Pulses for Transfection by Electroporation

As described in Section 4.5.4, a combination of short, high voltage pulses and long, low voltage pulses were used to introduce plasmid DNA into confluent T84 monolayers. Prior to performing the actual transfections, the high voltage (HV), 300 V – 300 μs, pulse and the low voltage (LV), 25 V – 20 ms, pulse were tested on the monolayers to check calcein uptake and cell viability. The results, which were obtained by flow cytometry, helped identify potential conditions that could be used for later transfections.

Figure 9.2A shows the uptake of calcein by confluent T84 monolayers after electroporation with high and low voltage pulses or with combinations of the two. Again,

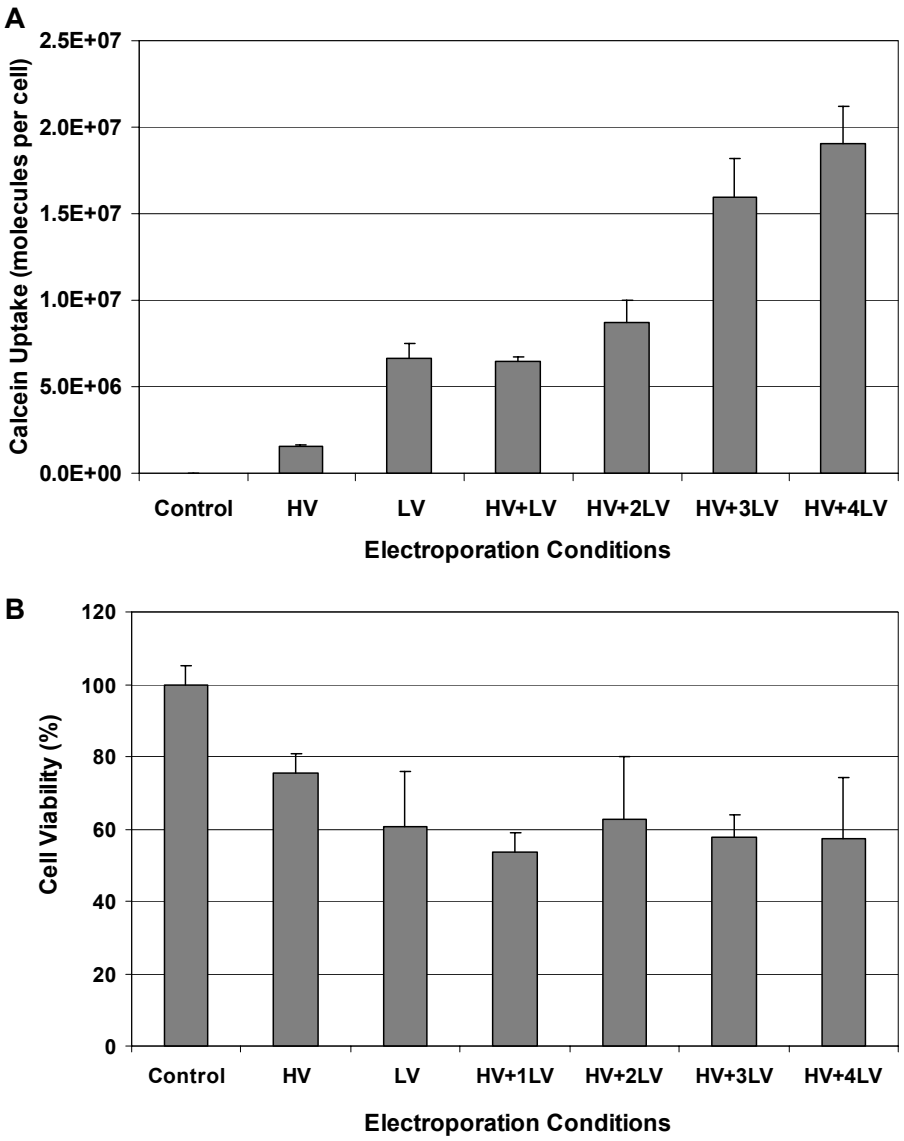

Figure 9.2 Determining an optimal electroporation condition for transfection experiments. (A) Calcein uptake by T84 monolayers after electroporation with combinations of short, high voltage pulses and long, low voltage pulses, increased with the strength of the condition applied ($p < 0.001$). (B) Cell viability dropped after electroporation, but showed a weak dependence on electroporation conditions ($p=0.06$). The HV + 3LV condition was chosen for use in future transfection experiments (see text) The extracellular concentration of calcein was 10 μM. [n = 3; HV = 300V – 300 μs; LV = 25V – 20 ms]

electroporated monolayers show a significant increase in calcein uptake over unelectroporated control monolayers. Uptake increased as the strength of the electroporation conditions increased ($p < 0.001$). The single low voltage pulse (LV) resulted in uptake that was six times that of the single high voltage pulse (HV). However, there was little difference in uptake between the LV, HV + 1LV, and HV + 2LV conditions ($p = 0.22$). Electroporation with an additional low voltage pulse (HV + 3LV) increased calcein uptake almost 2-fold above the HV + 2LV condition, while the HV + 4LV condition did not significantly increase uptake above the adjacent condition ($p = 0.43$).

The viability of the T84 monolayers decreased after electroporation (Figure 9.2B), but the dependence was not statistically significant ($p = 0.06$). Comparisons of the viabilities for all of the treated monolayers showed an even weaker dependence on the electroporation conditions ($p = 0.85$). Since the viabilities were all similar, calcein uptake became the determining factor for choosing a transfection condition, which meant that the HV + 3LV or HV + 4LV condition could be used. Although the viabilities at the HV + 3LV and HV + 4LV conditions were not significantly different, resistance recovery experiments showed that the monolayers electroporated with the former condition recovered their original resistance more rapidly (12 hrs vs. 24 hrs). Since future experiments with these monolayers will require the monolayers to be used in less than 24 h, the HV + 3LV condition was chosen for all subsequent transfection experiments.

9.2.3 Luciferase Expression in Confluent T84 Monolayers after Electroporation

After identifying a promising electroporation condition, confluent T84 monolayers were electroporated with the gWiz™-Luciferase reporter plasmid to determine the levels of luciferase expression that could be achieved. In the next set of experiments, monolayers were treated with combinations of short, high voltage pulses and long, low voltage pulses and with increasing amounts of DNA for comparison with the expression obtained after lipofection.

9.2.3.1 Dependence of Expression on Electroporation Conditions

To ensure that the HV + 3LV condition identified in the previous experiments with calcein also yielded the most expression, several combinations of the high and/or low voltage pulses were also tried. A plasmid amount of 30 μg was used to evaluate luciferase expression after treatment.

Figure 9.3 shows that, luciferase expression tended to increase as the strength of the condition or the number of pulses applied increased ($p = 0.0003$). A relatively low amount of expression ($< 2 \times 10^5$ RLU/mg protein) resulted when either a single high voltage pulse (HV) or a single low voltage pulse (LV) was applied. When the two were applied in combination (HV + LV), an additive effect on expression was observed. Applying three high voltage pulses (3HV) in succession increased expression only 2-fold over the single high voltage pulse. Statistical analysis showed no significant difference between the LV and the HV ($p = 0.10$), 3HV ($p = 0.26$), or HV + LV ($p = 0.27$) conditions.

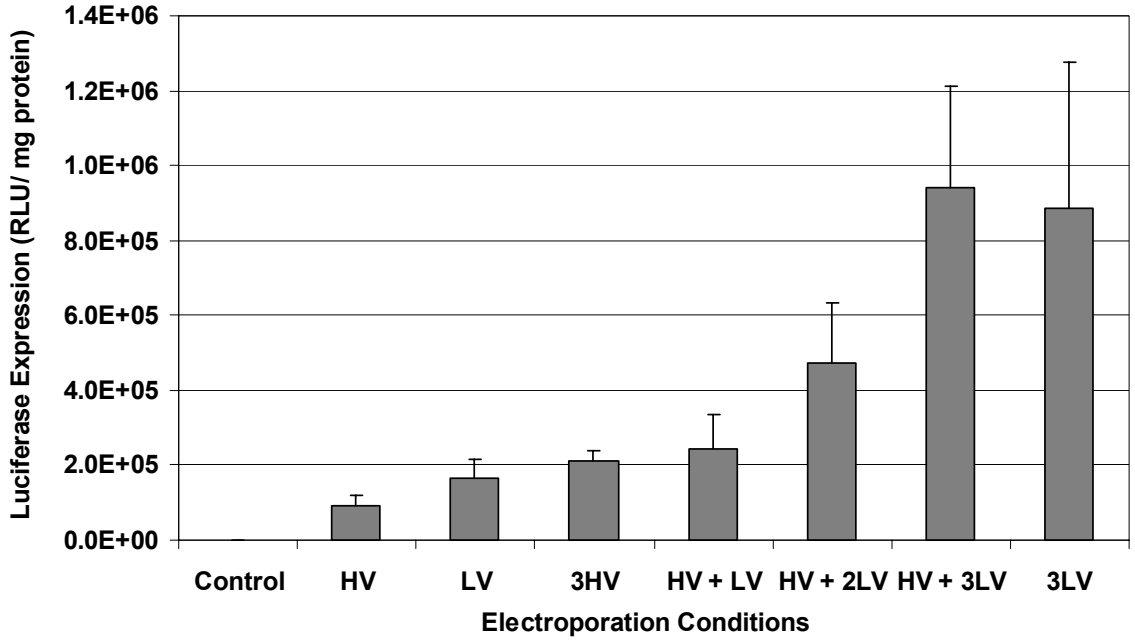

Figure 9.3 Luciferase expression tends to increase as the strength and/or number of electroporation pulses applied increase. Combinations of short, high voltage pulses and long, low voltage pulses were applied to confluent T84 monolayers. The HV+3LV and 3LV conditions yielded the most expression, indicating that the HV pulse may not be necessary. DNA amount was held constant at 30 μg of gWiz™-Luciferase expression plasmid. [n = 3; HV = 300 V – 300 μs; LV = 25 V – 20 ms]

When the single, high voltage pulse followed by one or more long, low voltage pulse protocol was applied, expression appeared to increase as each additional pulse was applied ($p = 0.10$). For the strongest condition, HV + 3LV, expression reached 9.3×10^5 RLU/mg protein. However, when expression at this condition was compared to expression at the 3LV condition (8.8×10^5 RLU/mg protein), the difference between the two was not statistically significant ($p = 0.85$). This suggests that the single short high voltage pulse may not be necessary to permeabilize the cells. This is in contrast to *in vivo* studies of electroporation-mediated gene transfer to skeletal muscle in which expression was highest when a high voltage pulse was combined with the low voltage pulse(s) (Bureau et al., 2000; Satkauskas et al., 2002). Since the additional short high voltage pulse did not appear to affect cell viability (Figure 9.2B), the HV+3LV was still used as the electroporation pulse protocol for subsequent transfections.

9.2.3.2 Dependence of Expression on Amount of DNA

Figure 9.4 shows that when confluent T84 monolayers were electroporated with the HV+3LV condition, luciferase expression depended strongly on the amount of gWiz™-Luc plasmid present, which ranged from 5 μg to 60 μg (ANOVA; $p < 0.001$). Expression increased steadily and reached a maximum level of 3×10^6 RLU/mg protein, which was five times better than the maximum expression obtained after lipofection (6×10^5 RLU/mg protein). Electroporation with DNA amounts ranging from 10μg to 20 μg resulted in statistically similar levels of luciferase expression of about 5×10^5 RLU/mg protein ($p > 0.05$). Monolayers electroporated with 5 μg of plasmid expressed about 2×10^5 RLU/mg protein, which is less than the highest level of expression achieved by

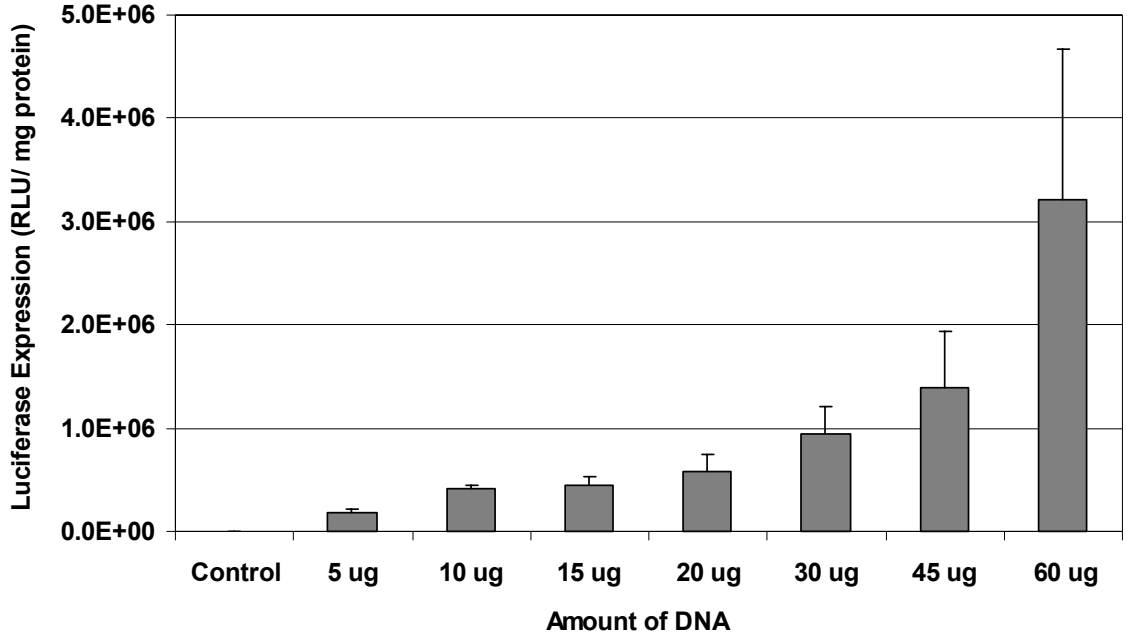

Figure 9.4 Luciferase expression after electroporation increases with DNA amount. The amount of DNA present during electroporation was increased from 5 µg to 60 µg. Confluent T84 monolayers were electroporated with the HV + 3LV condition using the specified amounts of gWiz™-Luciferase expression plasmid. [n = 3; HV = 300 V – 300 µs; LV = 25 V – 20 ms]

lipofection at this concentration (6 x 10^5 RLU/mg protein). However, for DNA amounts greater than 5 μg, electroporation consistently yielded more luciferase expression than lipofection. In addition, for the DNA amounts studied, luciferase expression after electroporation did not saturate with increasing amounts of DNA as it did after lipofection (Figure 9.1).

9.2.4 GFP Expression in Confluent T84 Monolayers after Lipofection

Using reporter plasmids that expressed green fluorescent protein (GFP), the abilities of lipofection and electroporation to efficiently transfect and express GFP in confluent intestinal epithelial monolayers were again compared. Confluent T84 monolayers were treated with either pEGFP-N1 or gWiz™-GFP and the cationic lipid LipoTAXI and then imaged 24 h later using epifluorescence microscopy.

Figures 9.5 and 9.6 show that there was very little GFP expression in confluent monolayers after lipofection. In the image fields shown, only 1 – 3 GFP positive cells were visible for monolayers treated with 10 μg of pEGFP-N1 plasmid and either 0.03 mM (Figure 9.5A) or 0.05 mM (Figure 9.5B) of LipoTAXI. When the T84 monolayers were transfected with 5 μg gWiz™-GFP expression plasmid and 0.08 mM of LipoTAXI, GFP expression was again very low (Fig. 9.6A), even though this condition yielded the most luciferase expression in previous experiments with lipofection (Fig. 9.1). Transfection with 10 μg of the gWiz plasmid at the same lipid concentration also produced very little GFP expression (Fig. 9.6B). These results illustrate the difficulty experienced when transfecting confluent intestinal epithelial monolayers with cationic lipids.

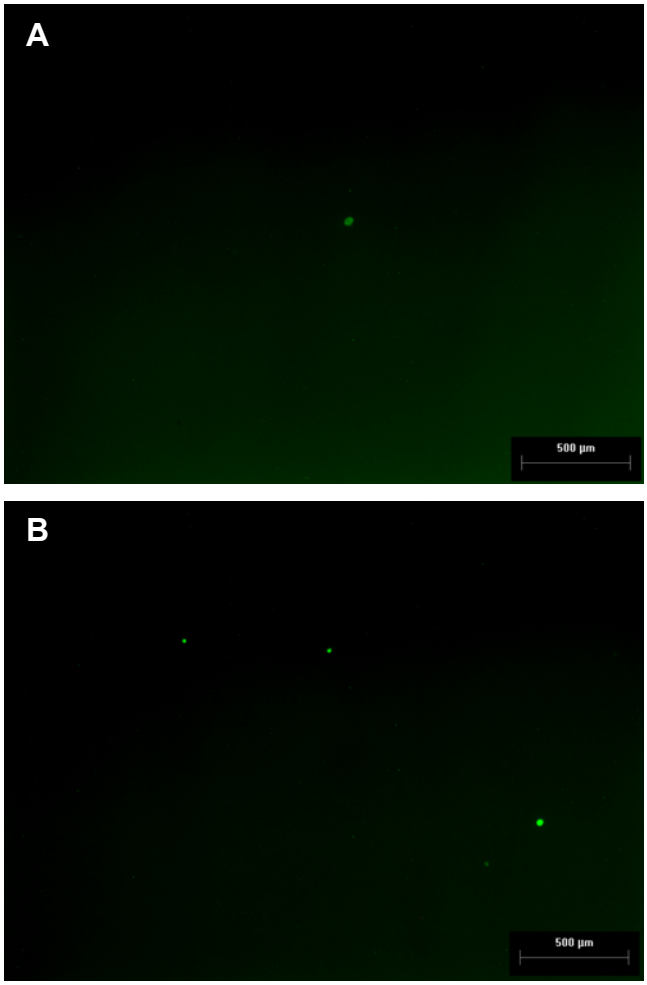

Figure 9.5 Transfection of confluent T84 monolayers with LipoTAXI resulted in very little GFP expression. Monolayers were transfected with either (A) 0.03 mM or (B) 0.05 mM of LipoTAXI and 10 µg pEGFP-N1. Monolayers were imaged by epifluorescence microscopy 24 h after transfection.

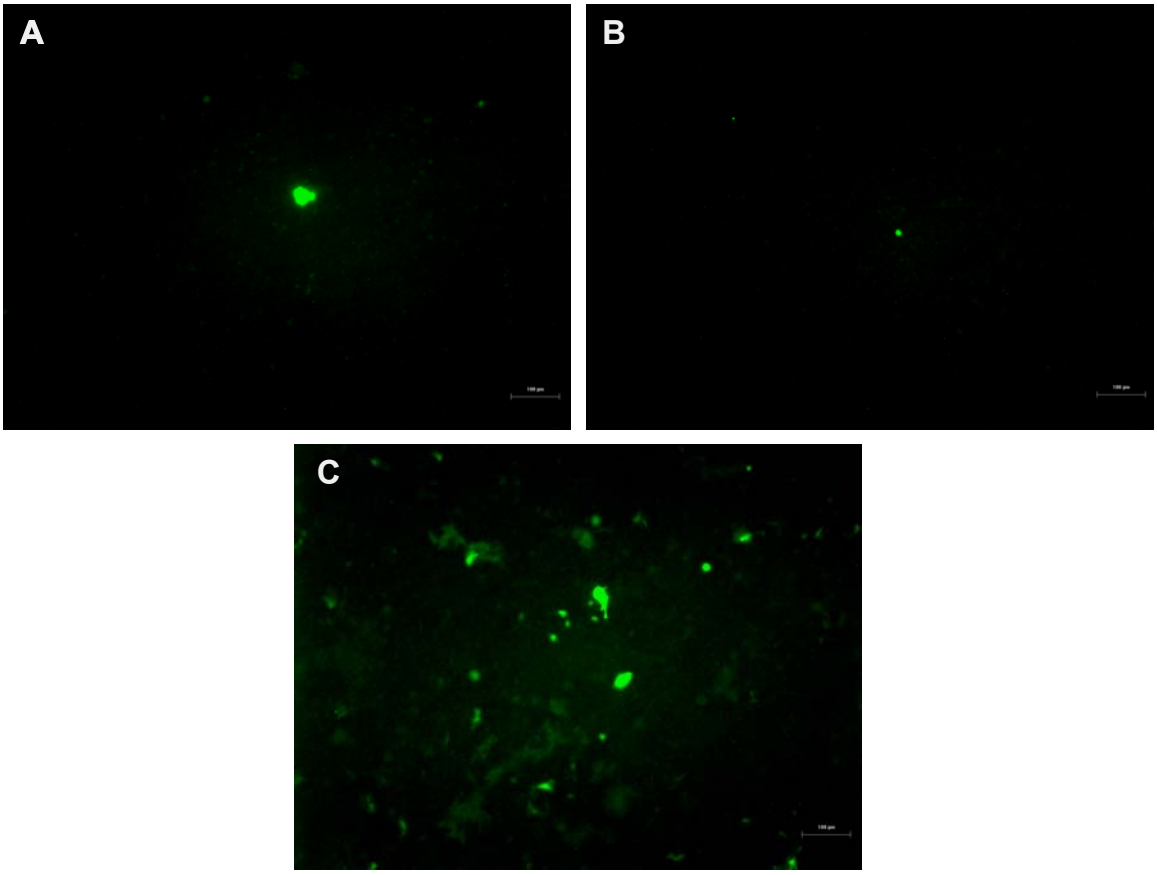

Figure 9.6 GFP expression in confluent T84 monolayers after lipofection is significantly less than after electroporation. Lipid-treated monolayers were transfected with 0.08 mM of LipoTAXI and either 5 µg (A) or 10 µg (B) of gWiz™-GFP expression plasmid. The 5 µg condition was found to be optimal for luciferase expression in previous experiments (Fig. 9.1). (C) Expression in monolayers electroporated with 10 µg of the same plasmid using the HV + 3LV condition had higher levels of GFP expression. [HV = 300 V – 300 µs; LV = 25 V – 20 ms]

9.2.5 GFP Expression in Confluent T84 Monolayers after Electroporation

Using the HV+3LV electroporation condition, confluent T84 monolayers were electroporated with either the pEGFP-N1 or gWiz™-GFP reporter plasmids and analyzed 24 h later for GFP expression by standard epifluorescence microscopy. Where stated, estimates of the density of cells expressing GFP were made by counting the number of GFP positive cells in each field of view using the image acquisition/analysis software ImagePro Plus (Media Cybernetics) as described earlier (Section 4.5.2).

In referring back to Figure 9.6, which shows a comparison of GFP expression in confluent T84 monolayers after lipofection and electroporation, expression after electroporation (Figure 9.6C) was significantly higher than expression after lipofection (Figure 9.6B), when the same amount of gWiz™-GFP plasmid was used (10 μg). Results from experiments with the second plasmid, pEGFP-N1, were very similar. Figure 9.7 shows expression in confluent T84 monolayers after electroporation with 20 μg (Figure 9.7A,B) and 30 μg (Figure 9.7C,D) of pEGFP-N1. Two additional images of the same monolayers, taken at a higher magnification were included in the figure for a closer view of expression (Figures 9.7B, D).

Estimates of the density of GFP expression in the images in Figure 9.7 were made by counting the number of GFP positive cells and dividing by the field area. The monolayers transfected with 20 μg of plasmid had densities of approximately 1300 ± 340 cells/cm^2 (n = 2), while monolayers electroporated with 30 μg of plasmid had densities of about 2900 ± 1300 cells/cm^2 (n = 2). Control monolayers, which were not electroporated, showed little to no expression of GFP (images not shown).

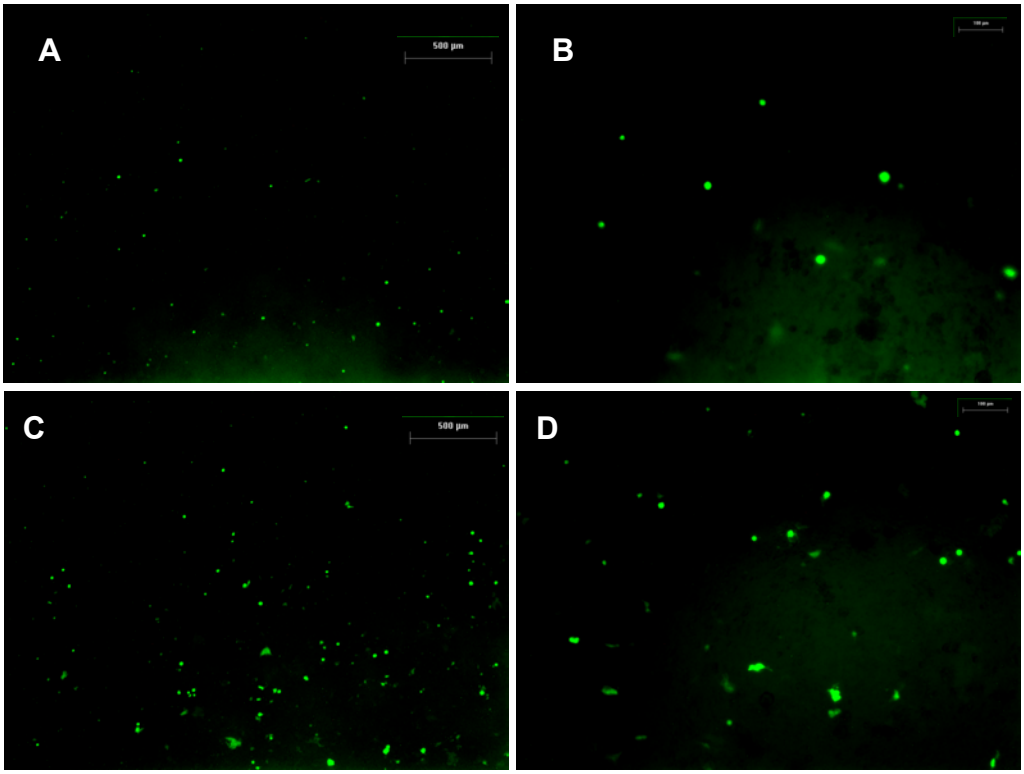

Figure 9.7 GFP expression in confluent T84 monolayers 24 h after electroporation. Monolayers were electroporated with either 20 µg (A,B) or 30 µg (C,D) of pEGFP-N1 using the HV + 3LV pulsing protocol. Unelectroporated monolayers incubated with DNA served as controls and showed little to no expression (not shown). Images B and D are higher magnifications of images A and C, respectively. [HV = 300 V – 300 µs; LV = 25 V – 20 ms]

In a replicate experiment carried out under the same conditions with 20 μg of pEGFP-N1 plasmid, electroporation yielded a density of about 8700 cell/cm^2 in confluent monolayers (Figure 9.8A), which is again higher than expression observed after lipofection. Just for comparison, monolayers were electroporated with 20 μg of pEGFP-N1 using the milder HV + 2LV condition (Figure 9.8B). Expression was lower (~3400 cells/cm^2), which supported the results obtained with calcein (Figure 9.2).

A rough approximation of the percentage of cells expressing GFP can be made by dividing the number of GFP-positive cells in the entire monolayer by the number of all cells in the monolayer. Multiplying the density of GFP positive cells calculated from the fluorescence micrographs by the growth area of the membrane (4.7 cm^2) gives an estimate of the total number of cells expressing GFP in the monolayer. The number of all cells in the monolayer was determined by dissociating the cells from the monolayer by trypsinization and performing a cell count using a Coulter Counter. The total number of T84 cells in a monolayer seeded on a 4.7 cm^2 membrane was found to be 1.26 ± 0.15 x 10^6 cells (n = 4). Based on these calculations, the highest percentage of cells in a confluent monolayer demonstrating expression of GFP after electroporation was ~ 3% (for a density of 8700 cell/cm^2). Although relatively low, this result was still better than the almost negligible GFP expression observed after lipofection.

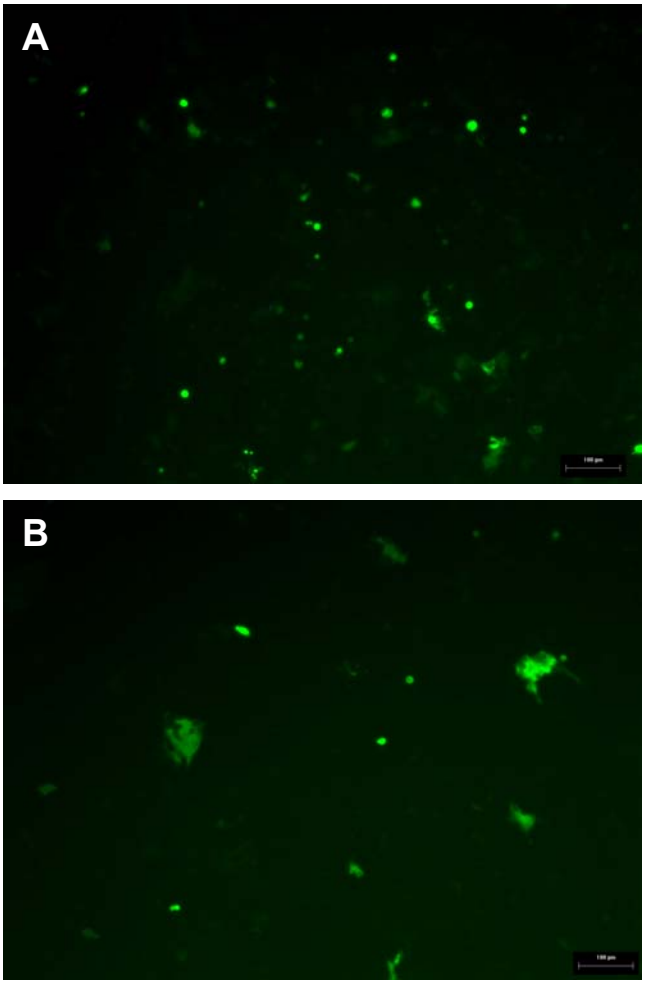

Figure 9.8 GFP expression in confluent T84 monolayers increased as the electroporation condition strength increased. Monolayers electroporated with 20 µg of pEGFP-N1 using the HV + 3LV (A) condition showed higher numbers of GFP positive cells than those electroporated with the HV + 2LV condition (B). HV = 300 V – 300 µs; LV = 25 V – 20 ms.

9.2.6 DNA Uptake after Lipofection and Electroporation

When reporter plasmid expression was evaluated, results showed that electroporation was as good, if not better, than a cationic lipid at successfully treating polarized, confluent intestinal epithelial monolayers. However, in both cases, the amount of expression was rather low. The following experiments were conducted to help determine whether the low expression levels could be due to low uptake of the plasmid DNA itself.

To study DNA uptake, the gWiz™-GFP plasmid was fluorescently labeled using the DNA intercalating dye YOYO-1 at a 100:1 DNA to dye molar ratio and transfected into confluent T84 monolayers by lipofection or electroporation. The uptake results after transfection with 0.08 mM LipoTAXI were compared to those from electroporation with the HV+3LV pulse protocol. The monolayers were incubated for 3–4 hours after treatment and then imaged by epifluorescence microscopy.

Uptake of stained DNA complexed with lipid by confluent T84 monolayers after lipofection is shown in the images presented in Figure 9.9. If the overall fluorescence of the monolayers is used as a measure of uptake of the lipid-DNA complexes, then the control monolayer had very little uptake, as indicated by the lack of green fluorescence (Figure 9.9A). A decrease in lipid-DNA uptake was observed as the amount of DNA present during lipofection increased from 5 μg to 30 μg. Uptake was highest in the monolayers transfected with 5 μg of DNA (Figure 9.9B), which correlates with the results obtained after luciferase transfections (Figure 9.1) and could indicate an optimal lipid:DNA ratio. At higher concentrations of DNA, fluorescence (and therefore uptake)

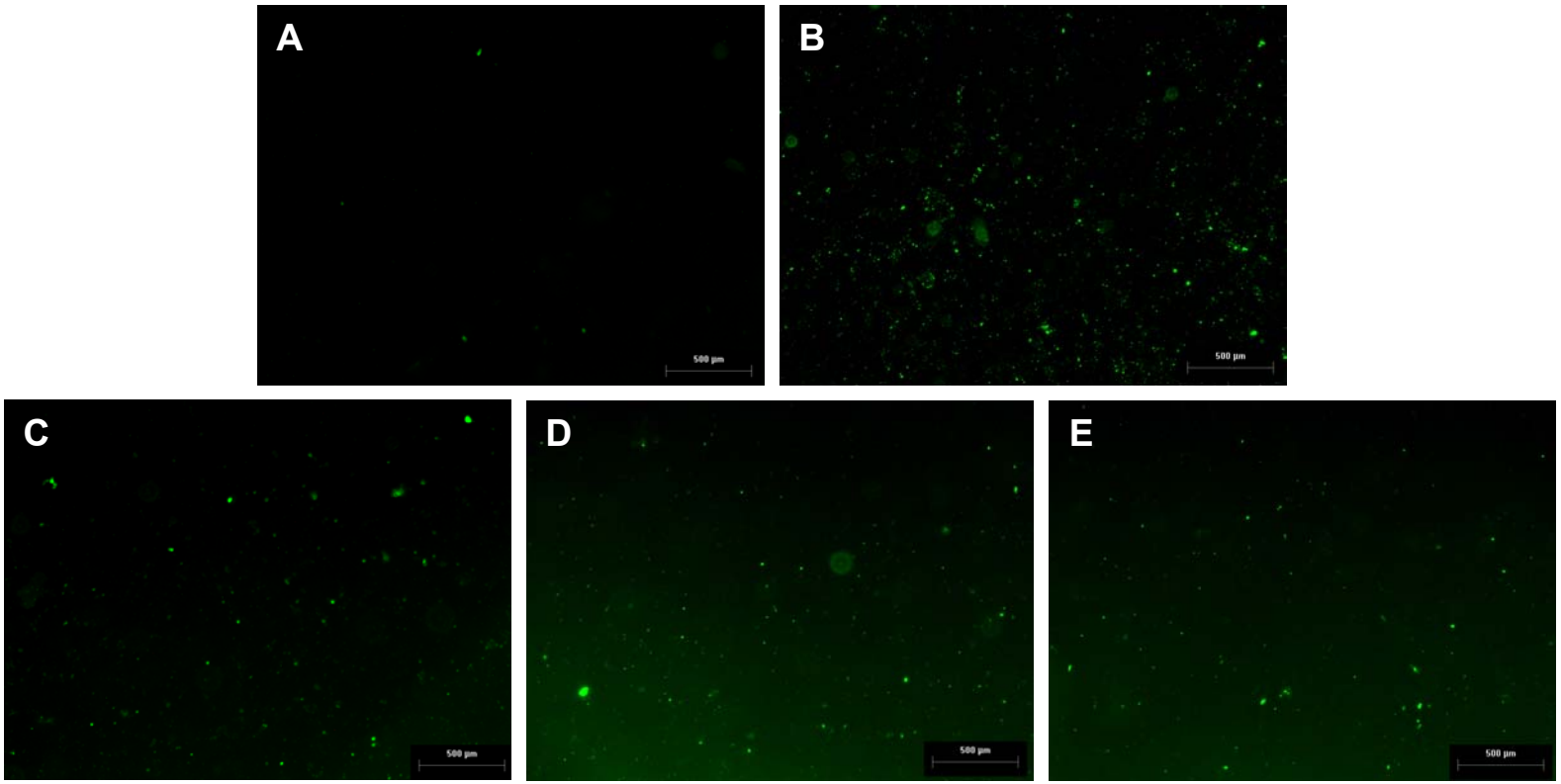

Figure 9.9 Lipid-mediated uptake of fluorescently labeled DNA by confluent T84 monolayers decreases with increasing DNA concentration. gWiz™-GFP expression plasmid was labeled with the DNA intercalating dye YOYO-1 at a molar ratio of 100:1 base pairs to dye molecules. Treated monolayers were transfected with 0.08 mM LipoTAXI and (B) 5 µg, (C) 10 µg, (D) 20 µg, and (E) 30 µg of DNA. The control monolayer incubated with just 20 µg of DNA from Figure 9.10 has been included for comparison (A). Fluorescence imaging was performed 3-4 hours after transfection. All exposure times are the same (40s).

dropped significantly (Figure 9.9C-E), which again correlates with the luciferase transfection results.

Delivery of the stained DNA by electroporation into confluent T84 monolayers resulted in high levels of uptake, when compared to the unelectroporated control monolayer (Figure 9.10A). In contrast to lipofection, uptake increased as the amount of DNA present during electroporation increased from 5 μg to 30 μg (Figure 9.10B-E). Again, this correlates with the results observed after transfection with the luciferase expression plasmid (Figure 9.4) and the GFP expression plasmid (Figure 9.7). In addition, since all of the images in Figures 9.9 and 9.10 were taken using the same exposure time, it can be inferred, based on the overall fluorescence intensity of the images, that electroporation appears to deliver more DNA into the cells than lipofection.

According to these results, the inability to introduce DNA into the confluent intestinal epithelial monolayers does not appear to be a limitation of electroporation or, for low DNA amounts, of lipofection. Electroporation, in particular, caused a significant amount of uptake of DNA. However, when the extent and distribution of DNA uptake in the monolayers are compared to the amount of GFP expression presented earlier in this chapter, it is evident that the DNA uptake was significantly higher than the GFP expression. Potential reasons for this disparity will be discussed in more detail in the discussion section of this chapter.

A final observation made while analyzing the DNA uptake images was evidence of the difference in the uptake mechanism after lipofection versus electroporation. After lipofection, uptake of the labeled DNA appeared in the image as punctate spots of fluorescence. These spots could indicate uptake of the lipid-DNA complexes by

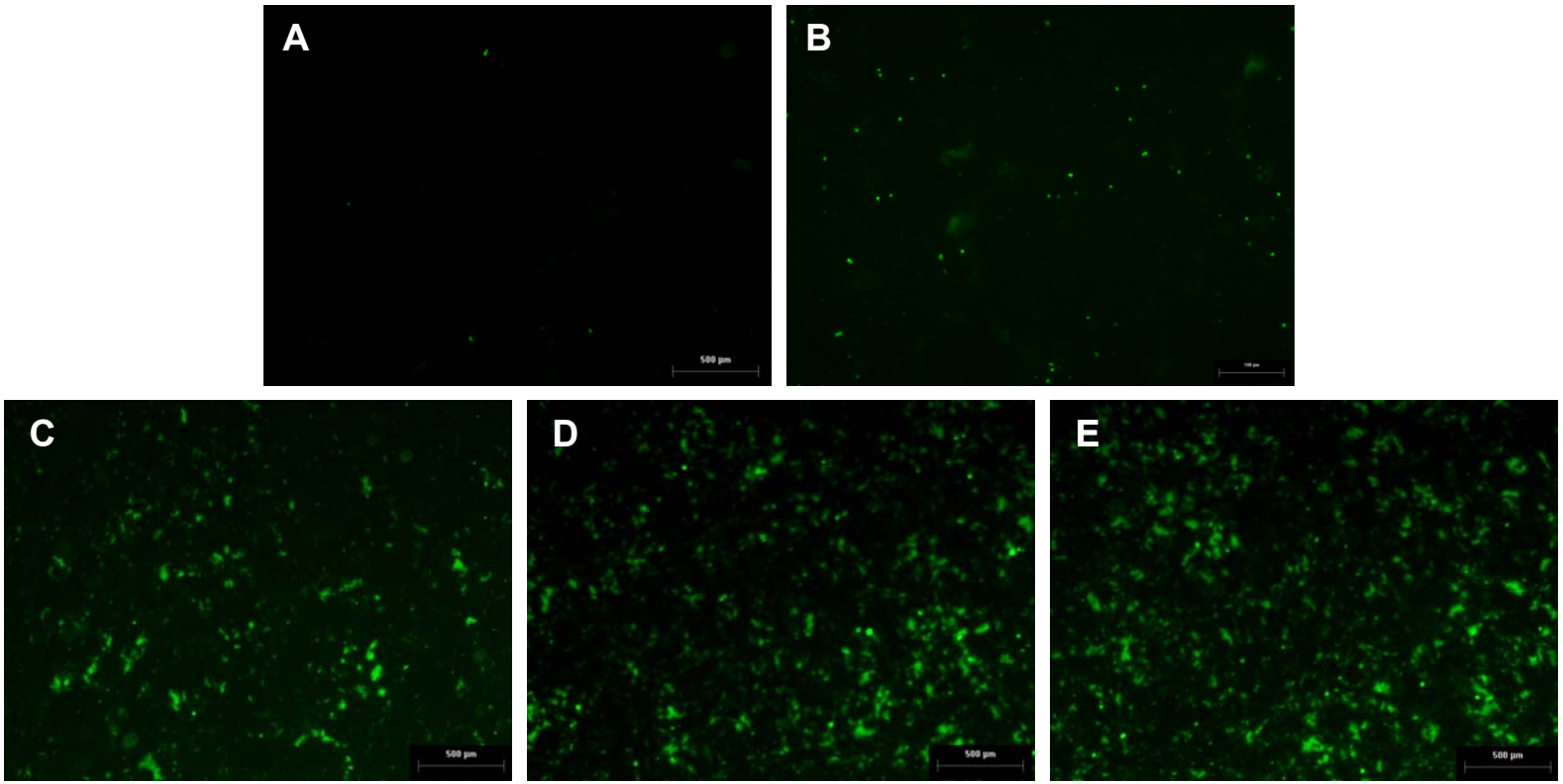

Figure 9.10 Electroporation-mediated uptake of fluorescently labeled DNA by confluent T84 monolayers increases with increasing DNA concentration. The gWiz™-GFP plasmid was labeled with the DNA intercalating dye YOYO-1 at a molar ratio of 100:1 base pairs to dye molecules. (A) The unelectroporated control monolayer was incubated with 20 µg of DNA. Treated monolayers were transfected using the HV + 3LV pulsing protocol and (B) 5 µg, (C) 10 µg, (D) 20 µg, and (E) 30 µg of DNA. Fluorescence imaging was performed 3-4 hours after transfection. HV = 300 V – 300 µs; LV = 25 V – 20 ms. All exposure times are the same (40s).

endocytosis, the hypothesized mechanism by which complexes are taken into cells (Bichko, 1998). Uptake after electroporation, on the other hand, appeared more diffuse, which would be expected if holes are being made in the cell membrane through which DNA would be transported directly into the cell interior (Xie et al., 1990; Klenchin et al., 1991; Sukharev et al., 1992).

9.3 Discussion

Polarized T84 intestinal epithelial monolayers were treated with either electroporation or with lipofection using LipoTAXI to evaluate the transfection and resulting expression of two reporter plasmids. When compared to lipofection, electroporation resulted in more luciferase and GFP expression in confluent T84 monolayers under almost all conditions tested.

The one condition at which luciferase expression was higher after lipofection was for 5 μg of plasmid and 0.08 mM – 0.1 mM LipoTAXI (Figures 9.1). This condition also resulted in the most DNA uptake for lipofection (Figure 9.9B) and could indicate an optimal lipid to DNA molar ratio (~5:1). Since GFP expression under these conditions was very low however (Figure 9.5-9.6), it is possible that only a few cells were successfully transfected and those cells expressed large amounts of luciferase.

When the images of GFP expression and DNA uptake after electroporation were compared (Figures 9.6-9.8 vs. Figure 9.10), it became obvious that high levels of uptake did not translate into high numbers of cells with expression. In electroporation experiments, only 3% of cells, at most, were positive for GFP expression. This could be

an indication of some type of inefficiency in the processing of the DNA after it enters the cell.

It is well known that it is difficult to obtain high levels of expression in polarized, confluent epithelial monolayers using conventional methods of transfection like cationic lipids. The steps involved in lipofection, i.e., endocytosis of the lipid-DNA complexes into the cells, release of the complexes from the endosome, dissociation of the DNA from the lipid, and DNA transport into the nucleus, are all barriers to expression, with nuclear import being the most rate limiting barrier (Zabner et al., 1995). As a result, it is common practice to use cells in the mid-log phase of growth to take advantage of the breakdown of the nuclear membrane during cell division (Tseng et al., 1999; Sambrook and Russell, 2001). When this approach is taken, very high levels of expression can be obtained in these cells, as we found when we transfected subconfluent Caco-2 and T84 monolayers with the pEGFP–N1 reporter using the cationic lipid Lipofectin®.

Figure 9.11 shows the expression of green fluorescence protein (GFP) over time in subconfluent Caco-2 monolayers and for different concentrations of DNA in monolayers after transfection with Lipofectin. For both cell lines, a significant amount of GFP expression, which occurred over the entire membrane growth area, was evident 1 day after transfection (Figure 9.11B, E, F) and lasted for at least 4 days, although it diminished as new cells replaced old ones (Figure 9.11D). Subconfluent T84 monolayers transfected in the same manner showed similar levels of GFP expression after treatment with either 5 μg (Figure 9.11E) or 10 μg (Figure 9.11F). Expression in the T84 cells also lasted at least 96 hours (not shown). Control monolayers, which were incubated with DNA and no lipid, showed little to no expression of GFP (Figure 9.11A).

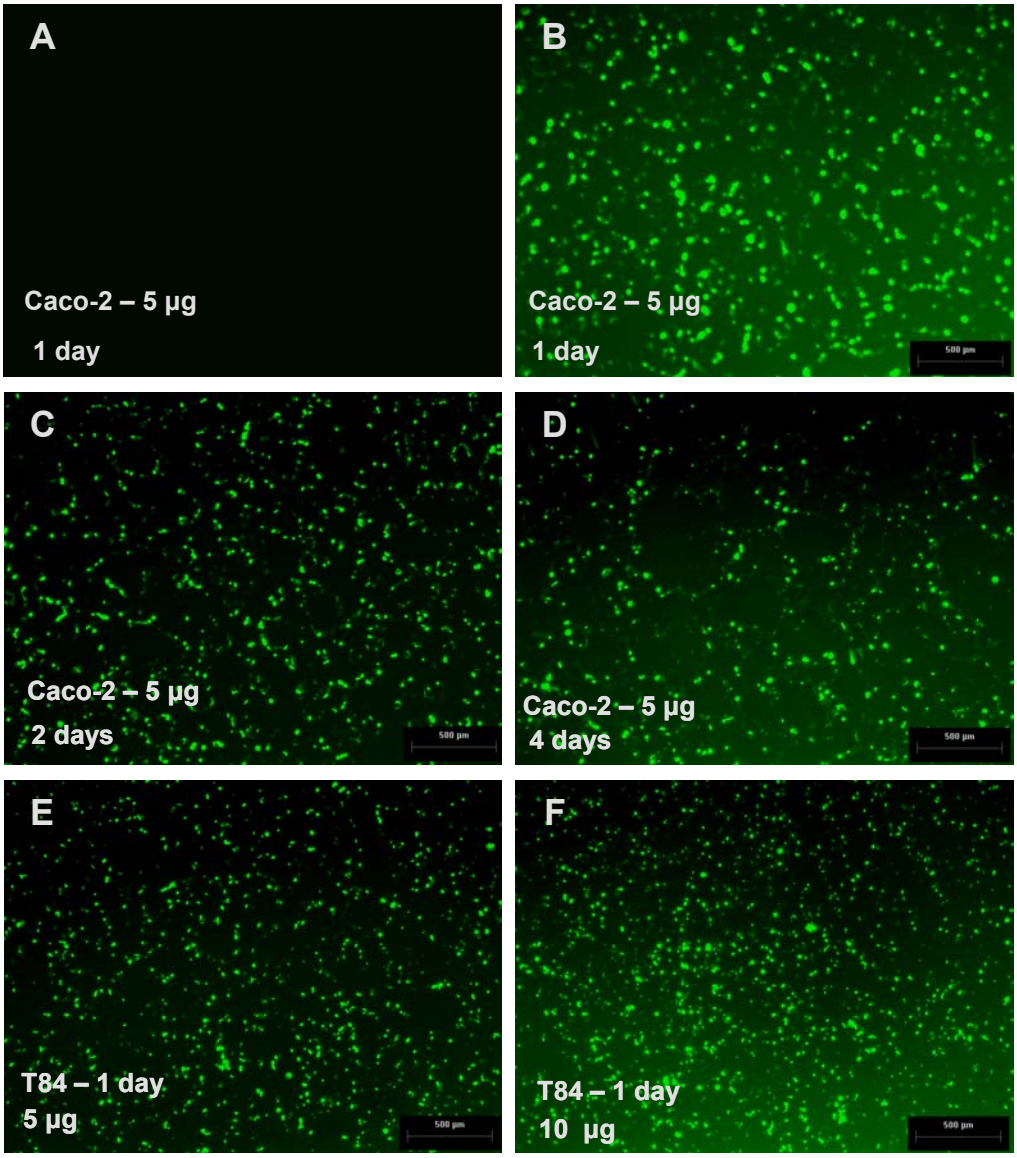

Figure 9.11 GFP expression is very high after lipid-mediated transfection of subconfluent Caco-2 (B-D) and T84 (E-F) monolayers. Expression of GFP reached very high levels within 1 day of transfection and lasted for at least 4 days. Transfected monolayers were treated with the posted amount of pEGFP-N1 and 60 µg of Lipofectin. The control monolayer (A) was treated with DNA alone. Caco-2 monolayers were used 2 days after seeding and T84 monolayers were used 1 day after seeding.

When the transfected subconfluent Caco-2 monolayers were observed at higher magnification, colonies or "islands" of cells were observed. In many epithelial cell lines, the cells on the perimeter of these islands are typically proliferating, undifferentiated cells, which do not exhibit the characteristics of mature epithelium that cells located in the center of the islands do (Matsui et al., 1997). Figure 9.12A is a fluorescence microscopy image of subconfluent Caco-2 cells with cells expressing GFP indicated by white arrows. When coupled with a bright field microscopy image of the same field (Figure 9.12B), with the white arrows placed in the same locations, the images show that GFP expression took place almost exclusively in the proliferative, undifferentiated cells located at the edges of these islands. Expression was rare in the cells located in the centers of the colonies.

The cells located in the center of the islands are most like the confluent epithelial monolayers used in the transfection experiments discussed in this chapter. While there is some proliferation in confluent monolayers, the majority of cells are at rest, which would make diffusion of DNA into the nucleus difficult. It was interesting to note that even though most of the monolayers treated with lipofection showed relatively little expression (Figures 9.5, 9.6), some confluent monolayers treated with the lipid showed large amounts of DNA uptake (Figure 9.9). This could mean that the cells are taking up the complexes, but once inside, either the steps involved in lipofection (release of complex from endosomes, dissociation of lipid and DNA) are being hindered or the DNA, once released, cannot cross the nuclear membrane of the non-dividing cells.

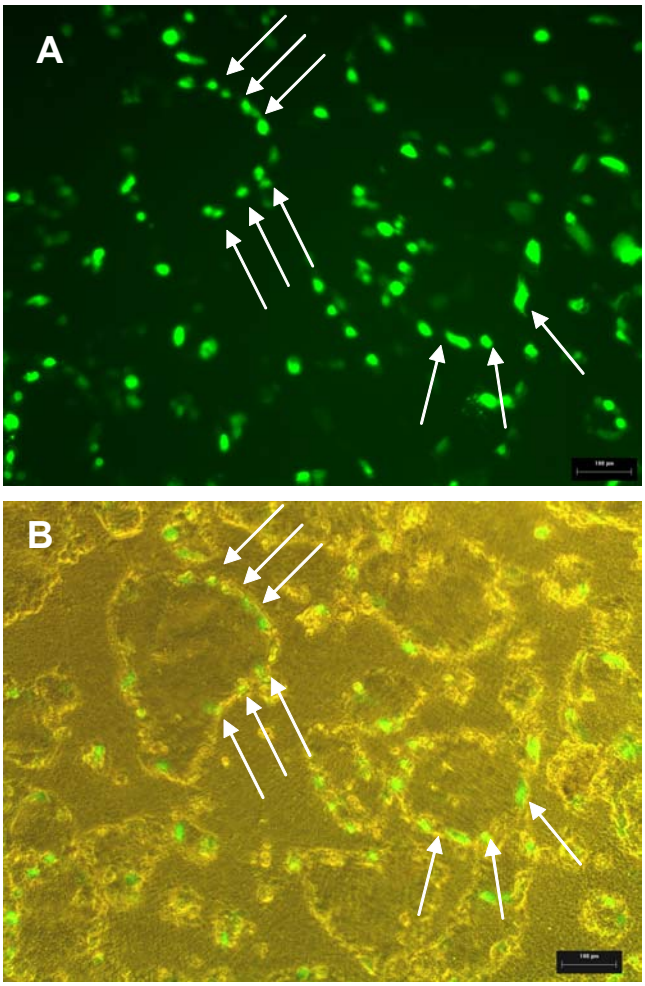

Figure 9.12 GFP expression in subconfluent Caco-2 monolayers occurred primarily in cells located at the edges of cell islands. (A) The fluorescence microscopy image shows the GFP expression 24 h after treatment with Lipofectin. (B) The bright field microscopy image (w/ fluorescence overlay) shows that the location of these GFP positive cells (indicated by white arrows) is almost exclusively at the edges of cell "islands". Typically, the edge cells are proliferative and still undifferentiated, while central cells are more differentiated.

Just as for lipofection, the nuclear membrane may also be a significant barrier against achieving high numbers of cells with expression after electroporation. Susceptibility of the naked DNA to degradation by cytoplasmic nucleases could also be a potential problem (Lechardeur et al., 1999). Despite this, electroporation was still able to achieve more expression than lipofection. Comparisons of the fluorescence intensities of the images made in the DNA uptake studies indicate that electroporation may deliver more DNA into the cells than lipofection as well (Figure 9.9 vs. Figure 9.10). It is possible that the more DNA that is loaded into the cells, the higher the probability that some DNA will bypass barriers to transfection, and the better the chances that expression will occur.

9.3 Conclusions

Polarized intestinal epithelial monolayers were transfected with two reporter plasmids using electroporation and lipofection. When compared to lipofection, luciferase and GFP expression were found to be higher after electroporation, especially at higher concentrations of DNA. DNA uptake studies showed that both electroporation and lipofection (under certain conditions) can deliver relatively large amounts of DNA into the cells, but it appears that intracellular barriers to transfection limit the amount of expression achieved. Electroporation appears to be able to bypass these barriers, to some extent, through its ability to deliver more DNA into the cell than lipofection.

CHAPTER X

10. DELIVERY OF INFLAMMATION-MEDIATING MOLECULES BY ELECTROPORATION

10.1 Introduction

The epithelial cells that line the mucosal surface of the intestine serve as a protective barrier to prevent harmful agents from gaining access to the interior and adversely affecting the body. When in the presence of "threat" stimuli such as bacteria, viruses, inflammatory cytokines, or physical stress, these cells initiate a proinflammatory signal transduction pathway regulated by the family of transcription factor proteins known as NFκB (Thanos and Maniatis, 1995). This cascade of events is known to play a role in inflammatory syndromes or diseases such as asthma (Yamamoto and Gaynor, 2001), rheumatoid arthritis (Makarov, 2000), and inflammatory bowel disease (IBD) (Schreiber et al., 1998; Schmid and Adler, 2000), and also in cancer (Schwartz et al., 1999; Yamamoto and Gaynor, 2001).

Several approaches for inhibiting the NFκB-mediated inflammatory pathway have been studied. Most involve blocking the activity of one or more of the intermediate components of the pathway to prevent activation of NFκB. As stated in Chapter 2, many of the drugs used to treat IBD have been shown to inhibit the activation of NFκB. The mechanisms of action for these drugs include inhibiting the activities of the proteins that phosphorylate, ubiquitinate, or degrade IκB and inducing the synthesis of new IκB, which binds and sequesters free NFκB in the cytoplasm (Yamamoto and Gaynor, 2001).

In addition to drug therapy, researchers have also studied the potential of gene therapy for treatment of diseases that involve this pathway. Various methods of delivery were employed to introduce nucleic acids both *in vivo* and *in vitro*. One study involved the intravenous and rectal administration of antisense oligonucleotides directed against NFκB to diminish experimental colitis in rats (Neurath et al., 1996). In another study, successful intranasal delivery of a plasmid that expressed a protein to treat experimental colitis in rats was reported (Jobin and Sartor, 2000). Finally, viral delivery of a plasmid vector that expressed a mutated form of IκB, called the IκBα super-repressor, successfully inhibited NFκB activation in mammalian cells *in vitro* (Elewaut et al., 1999). The mutated protein is modified at its sites of phosphorylation to prevent it from being targeted for degradation, which leads to continued retention of NFκB in the cytoplasm.

In this study, electroporation was evaluated for *in vitro* gene delivery into intestinal epithelial cell monolayers. A plasmid that expressed hemagglutinin (HA) –tagged IκBα was electroporated alone and in combination with other plasmids into these cells to try to inhibit TNFα-mediated activation of NFκB. Secretion of the cytokine IL-8 was used initially as a marker of inflammation. In later experiments, expression of the reporter protein, luciferase, was used to measure inhibition of NFκB.

10.2 Experimental Results

10.2.1 Delivery of IκBα Expression Plasmid

Confluent T84 monolayers were electroporated with 20 μg/ml (30 μg) of a plasmid that expressed hemagluttinin-tagged IκBα (pIκB-HA) to determine whether the expressed protein would inhibit the production of the cytokine IL-8. Figure 10.1 shows

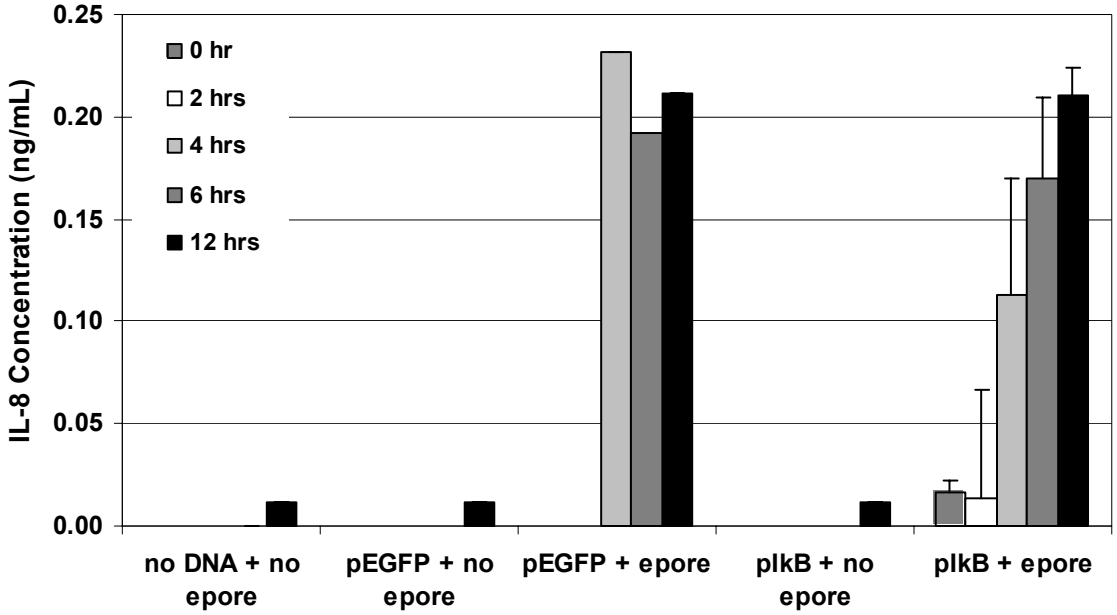

Figure 10.1 Electroporation-induced IL-8 secretion by confluent T84 monolayers may be temporarily inhibited after electroporation with an IκB-expression plasmid. Secretion by monolayers electroporated with pIκB-HA was monitored for 24 h and compared to unelectroporated monolayers with and without the plasmid, and monolayers electroporated with and without the control plasmid, pEGFP-N1. Samples of the basal medium were collected at 0 h (▨), 2 h (□), 4 h (▩), 6 h (▩), and 12 h (■). [n = 1–2]

the secretion of IL-8 during the first 12 hours of the 24-hour recovery period after electroporation. As expected, unelectroporated monolayers, with and without the IκB plasmid present, secreted very little IL-8 (final basal concentration reached ~ 0.1 ng/ml). Monolayers that were electroporated with the control plasmid, pEGFP-N1, or with our plasmid of interest, pIκB-HA, showed a significant increase in IL-8 secretion within 4 hours after electroporation. The final basal concentration was approximately 17 times that of the unelectroporated monolayers. The monolayers electroporated with pIκB-HA appeared to have lower levels of IL-8 secretion than the pEGFP electroporated monolayers in the first four hours after treatment. Statistically, however, only the difference between IL-8 secretion at 2 hours and 12 hours for the monolayers transfected with pIκB-HA proved to be significant (Student's t-test: $p = 0.02 < 0.05$).

After recovery, some of the monolayers were exposed to TNFα (10 ng/ml) for 6 to 8 hours to further stimulate IL-8 secretion. This would allow us to determine whether any IκB expressed during the recovery period would inhibit the secretion of IL-8 in response to TNF. Two fresh T84 monolayers, one stimulated and one left unstimulated, were included as controls. Figure 10.2, which illustrates the secretion of IL-8 after TNF stimulation, shows that the unelectroporated control monolayers (No DNA and pIκB) had similar amounts of IL-8 secretion that were comparable to secretion by the TNF stimulated control monolayer. The unstimulated monolayer showed no IL-8 secretion. The important finding, however, is that IL-8 secretion by monolayers electroporated with pIκB-HA was higher than its corresponding control. This indicates that either the

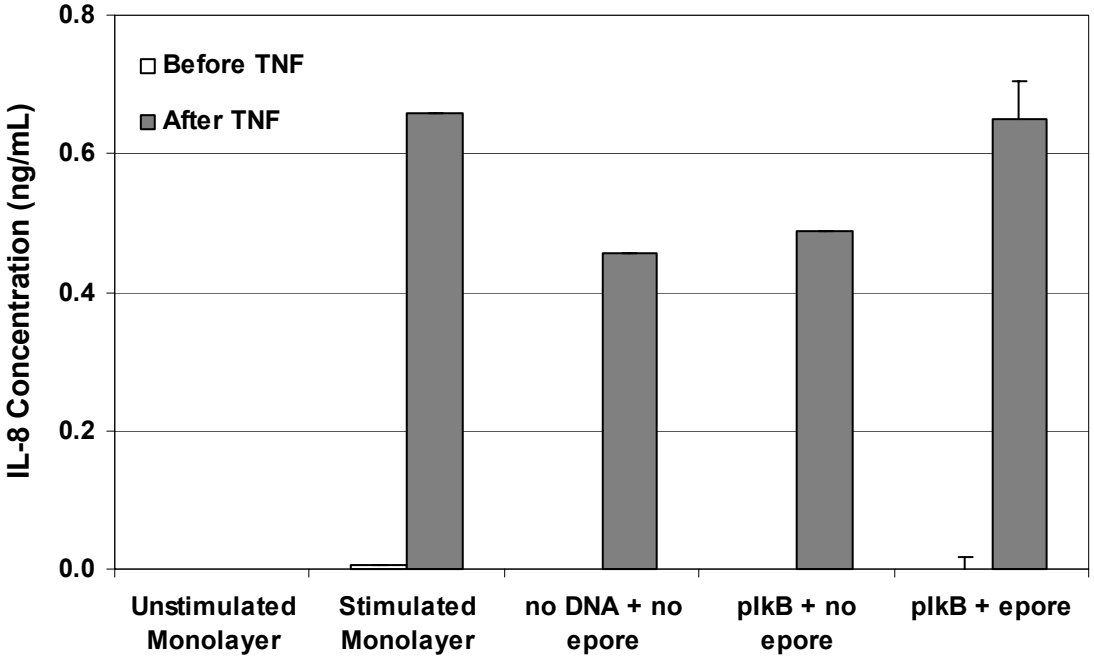

Figure 10.2 IL-8 secretion by T84 monolayers electroporated with pIκB-HA after stimulation by TNFα for 6-8 h. Monolayers electroporated with the IκB expression plasmid showed no decrease in IL-8 secretion when compared to unelectroporated controls. [n = 1-3]

expressed IκB did not inhibit IL-8 secretion or that there was not enough IκB expressed to suppress secretion by the entire monolayer.

To determine which possibility was true, new T84 monolayers were electroporated with pIκB-HA and lysed at various time points for up to 24 hours after transfection. Depending on the experiment, various controls were included for comparison. All monolayers were analyzed for IκB expression by SDS-PAGE and Western blotting. The Western blot in Figure 10.3A shows that expression of IκB-HA occurred within 4 hours after electroporation and was present for at least 24 hours. The amount of protein expressed appeared to decrease over time, which could indicate possible degradation of the protein. The control monolayers, including the monolayer transfected with LipoTAXI, show no IκB-HA expression.

Although the Western blot confirms expression of IκB-HA, when a visual comparison is made between the size and intensity of these bands and those of endogenous IκBα (Figure 10.3B), the amount of IκB-HA being expressed is very small. The average intensity of the endogenous IκBα bands, as determined by densitometry, was approximately 5 times higher than that of the darkest band of IκB-HA (the 4 h time point). The fact that the samples used for the IκBα blot were diluted 1:2 (to decrease endogenous IκBα band intensity and make it easier to see any expressed IκB-HA) further underscores the low amount of expression.

IL-8 secretion was also monitored during the recovery period to determine whether the expressed IκB-HA would inhibit electroporation-induced secretion. Figure 10.3C shows that IL-8 secretion increased with time for the electroporated monolayers as observed in previous experiments. However, the presence of IκB-HA appeared to have no

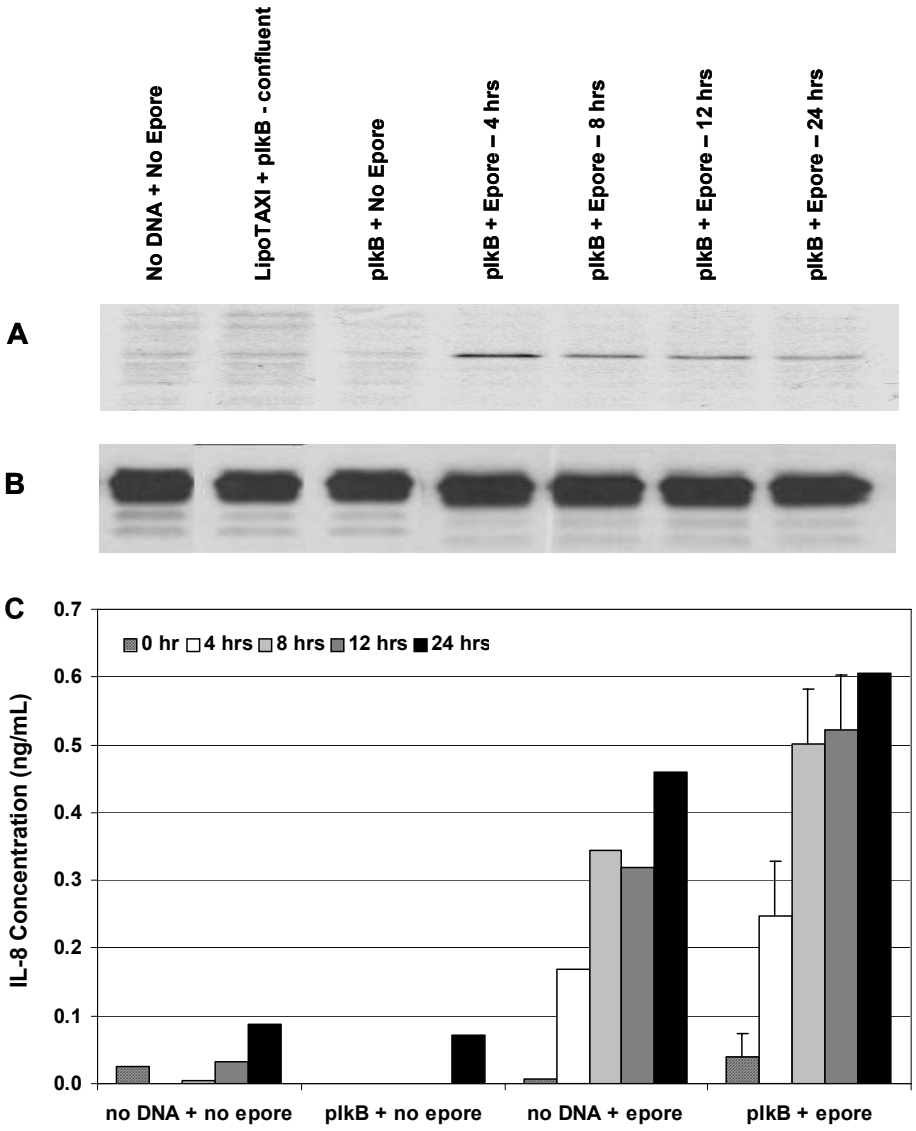

Figure 10.3 Monitoring IκB-HA expression over time in T84 monolayers after electroporation. (A) Western blot showing IκB-HA expression over time after electroporation with the HV + 3LV condition. (B) Western blot of endogenous IκBα for the same samples. IκB-HA and endogenous IκBα were detected with anti-HA and anti-IκBα antibodies, and the exposure time for their blots were 30 min and 30 s, respectively. Samples for IκBα blot were diluted 1:2. (C) IL-8 secretion by these monolayers was monitored and was found to be unaffected by the expressed IκB-HA. [n=1-4; IκB-HA molecular weight ~42 kDa; endogenous IκBα molecular weight ~37 kDa]

effect on IL-8 secretion. In fact, the monolayers electroporated with pIκB-HA showed slightly higher levels of IL-8 secretion than the monolayer electroporated with no DNA.

Since it is possible that the presence of the DNA, which can be toxic to cells, could affect IL-8 secretion, the experiment was repeated and a monolayer electroporated with gWiz™-Luc as a control plasmid was included. The results of this experiment are shown in Figure 10.4. Again, some expression of IκB-HA after electroporation with pIκB-HA (Figure 10.4A) was evident, but this time the amount of protein expressed was even less than what was observed in the first experiment. Expression appeared to peak at about 8 hours versus the 4 hours seen in the first experiment. A comparison with endogenous IκBα (samples diluted 1:10) yielded a 3-fold average difference in band intensities (Figure 10.4B). Monitoring of IL-8 again showed no decrease in secretion with IκB present (Figure 10.4C). Secretion by these monolayers was still greater than secretion by those electroporated with no DNA or with gWiz™-Luc.

10.2.2 Co-transfection of IκB Expression Plasmid with Reporter Plasmids

When it appeared that the amount of IκB expressed after transfection by electroporation was insufficient to inhibit the secretion of IL-8 by the entire monolayer, a different approach (described in Section 4.8) was tried. The monolayers were electroporated with both the plasmid that expressed IκB-HA and a plasmid that expressed a reporter protein when the cells were stimulated with TNFα. As stated in Section 4.8.1, efforts to electroporate pIκB-HA with a plasmid that expressed the reporter protein chloramphenicol acetyl transferase (CAT) when NFκB binds to its promoter proved

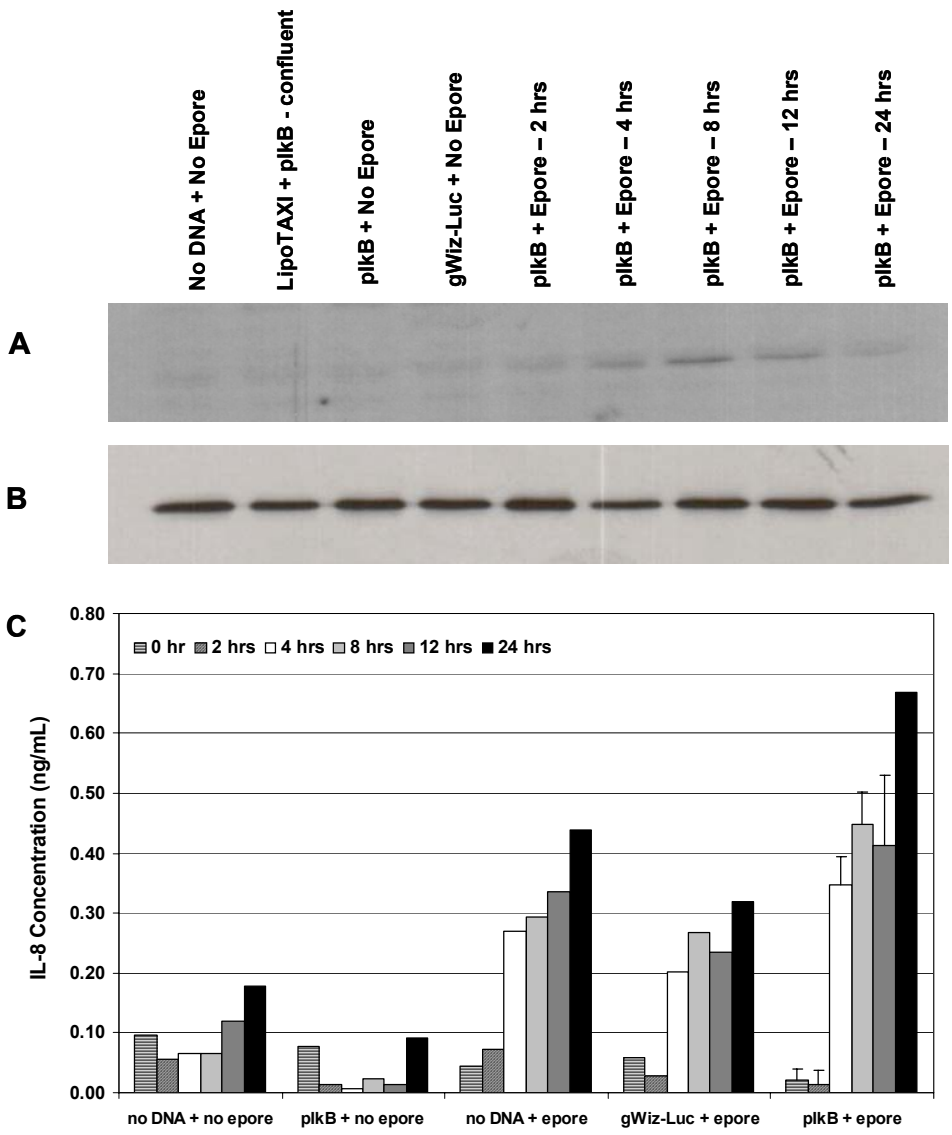

Figure 10.4 Second Western blot showing IκB-HA expression over time after electroporation with the HV + 3LV condition (A). Western blot of endogenous IκBα for the same samples (diluted 1:10) (B). IκB-HA and endogenous IκBα were detected with their respective antibodies and the blots exposed for 30 min and 30 s, respectively. IL-8 secretion by these monolayers was monitored and was again found to be unaffected by the expressed IκB-HA (C). [n=1-4; IκB-HA molecular weight ~42 kDa; endogenous IκBα molecular weight ~37 kDa]

unsuccessful because the amount of CAT expressed was below the detection limit of the assay used for detection.

Since luciferase assays can be 10,000 times more sensitive than the CAT assays, a plasmid that expressed luciferase when free NFκB binds to its promoter (pNFκB-Luc) was chosen as an alternative. The two plasmids, pIκB-HA and pNFκB-Luc, were electroporated into confluent T84 monolayers at specified ratios, while keeping the amount of pNFκB-Luc constant at 15 μg. Monolayers exposed to TNFα, which triggers the release of NFκB, were expected to have increased levels of luciferase expression. A standard luciferase plasmid with a CMV promoter (pCMV-Luc) was used as a control.

Figure 10.5 shows the expression of luciferase by TNF stimulated and unstimulated monolayers co-transfected with pIκB-HA and pNFκB-Luc and by monolayers co-transfected with pIκB-HA and the control plasmid pCMV-Luc. There was no significant difference between the expression by pCMV-Luc alone or co-transfected with increasing amounts of pIκB-HA (one-way ANOVA, $p = 0.76$). The NFκB-Luc treated monolayers that were not stimulated with TNFα had relatively low levels of luciferase expression (< 9000 RLU/mg protein). When treated monolayers were stimulated with TNFα, luciferase expression increased significantly. Depending on the individual experiment, expression by TNF-stimulated monolayers ranged from 7 to 30 times that of the unstimulated monolayers.

According to these results, which are an average of four different experiments, luciferase expression did not decrease as the amount of pIκB-HA was increased. Statistically, there was no significant difference between the expression observed for

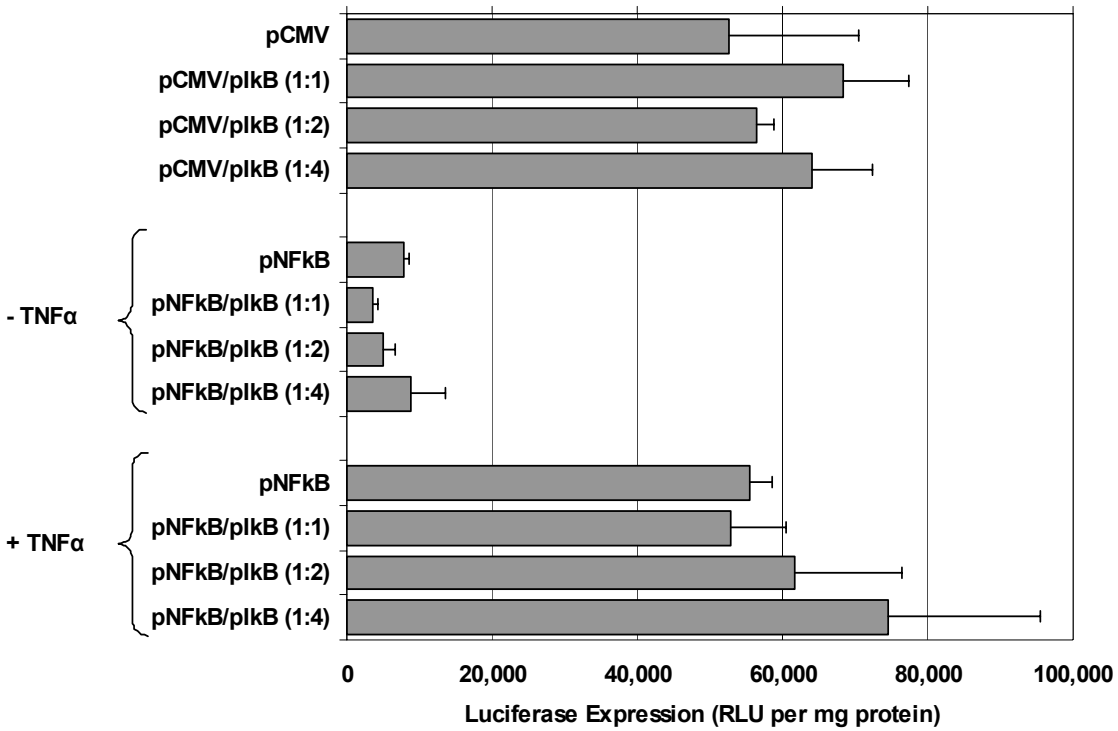

Figure 10.5 Luciferase expression results from pIκB-HA/NFκB-Luc plasmid co-transfection experiments. Using the HV + 3LV pulsing protocol, monolayers were electroporated with either pNFκB-Luc alone or at the specified ratio with pIκB-HA. TNF-stimulation triggered an average 18-fold increase in luciferase expression over unstimulated monolayers. Increasing amounts of pIκB-HA did not inhibit NFκB activation, resulting in similar levels of luciferase expression for all conditions. [n=4]

pNFκB-Luc transfected alone or with varying amounts of pIκB-HA (ANOVA, $p = 0.65 > 0.05$). However, when the results from the TNF stimulated monolayers in Figure 10.5 are replotted to show each individual experiment, the results are not as clear (Figure 10.6). In two experiments (#1 and #3), luciferase expression tended to decrease as the amount of IκB-HA present was increased, while in the other two experiments (#2 and #4), luciferase expression increased with increasing amounts of IκB-HA.

To confirm whether IκB-HA was expressed, the cell lysate used to assay luciferase expression was also analyzed by SDS-PAGE and Western blot analysis. The protein was detected with an anti-HA antibody. Figure 10.7 shows the expression of IκB-HA for each of the samples from the four experiments plotted in Figure 10.6. There was some expression of the protein, but it was so low, the radiography film had to be exposed to the blot for one hour before the bands could be seen clearly. The intensity of the bands correlates well with the amount of the plasmid pIκB-HA present during electroporation, but does not correlate with the results of each experiment. Although all of the experiments exhibit some IκB-HA expression, only experiments 1 and 3 showed decreased luciferase expression as the amount of pIκB-HA was increased.

10.3 Discussion

10.3.1 IκB Expression Plasmid Delivery

Confluent T84 monolayers were electroporated with 20 μg/ml of pIκB-HA in an effort to inhibit IL-8 secretion. In an initial experiment, the expressed IκB appeared to inhibit IL-8 secretion induced by electroporation (Figure 10.1). However, when these

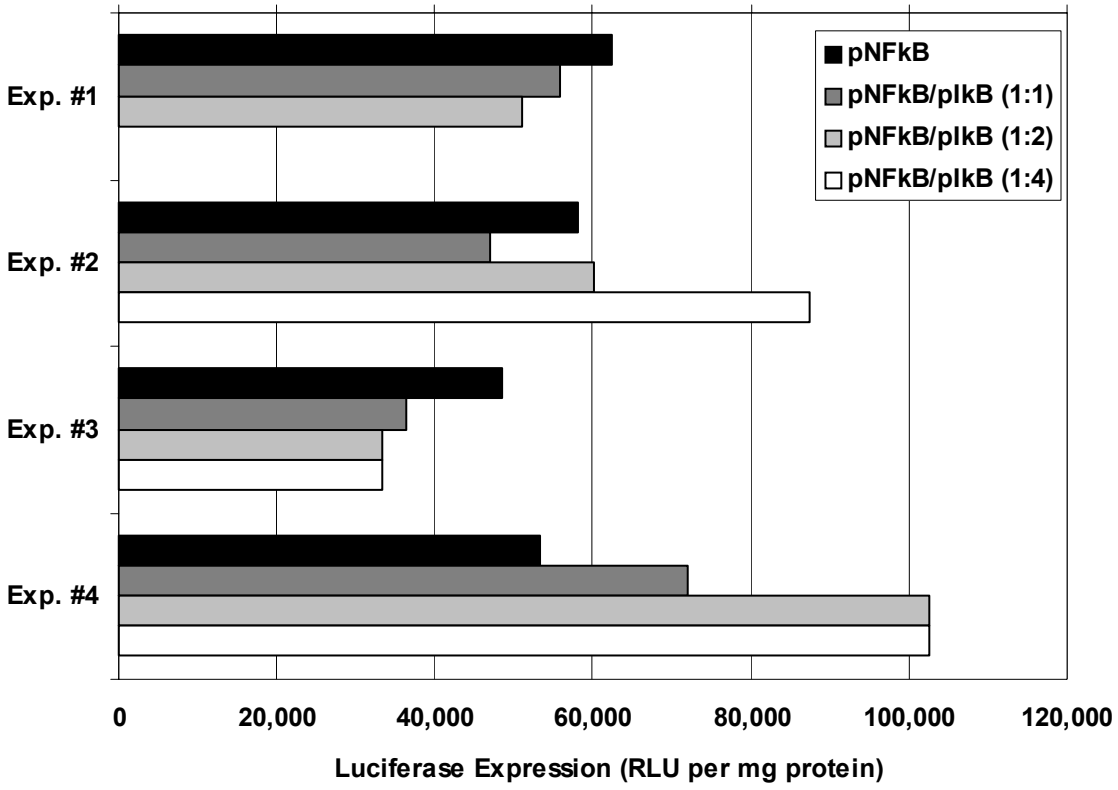

Figure 10.6 Luciferase expression by TNF-stimulated T84 monolayers from individual pIκB-HA/pNFκB-Luc co-transfection experiments. Data from Figure 10.5 were replotted to show results from each replicate. Experiments 1 and 3 demonstrated the anticipated decrease in luciferase expression as the amount of pIκB-HA was increased. Experiments 2 and 4 did not show a decrease in luciferase expression.

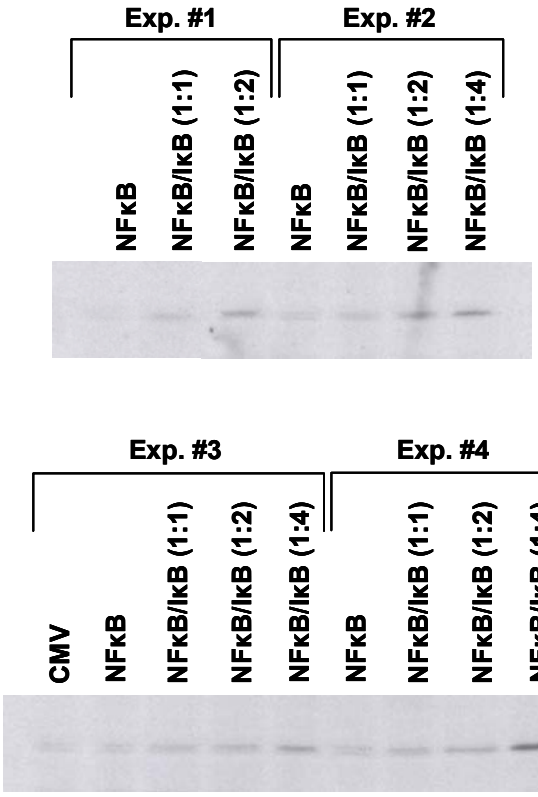

Figure 10.7 Western blot analysis showing evidence of IκB-HA expression from pIκB-HA/pNFκB-Luc co-transfection experiments. The protein, which was detected with an anti-HA antibody, was expressed in very low quantities. The blots had to be exposed for one hour in order to see the bands. [IκB-HA molecular weight ~42 kDa]

same monolayers were exposed to TNF, production of IL-8 remained undiminished (Figure 10.2). Monitoring of IκB-HA expression over time showed the appearance of the protein within 4 hours of transfection and then a decrease in the amount of protein over the next 20 hours (Figure 10.3.A). A similar result was obtained, but with a peak in expression at 8 hours, when this experiment was repeated (Figure 10.4.A).

As reported in Chapter 9, transfection efficiencies in confluent monolayers after electroporation are relatively low (~3%). This was evident in the size and intensity of the bands in both Western blots, which indicate that there was relatively little IκB-HA being expressed in the monolayers, especially when compared to the bands for endogenous IκBα (Figures 10.3.B & 10.4.B). Other indications of the low transfection efficiency were the antibody dilutions and radiography film exposure times used to detect the bands. The blots for IκB-HA expression had to be incubated in a higher antibody concentration than usual (1:250 dilution instead of 1:1000) and had to be exposed for 30 minutes and longer in order to see the bands clearly. In comparison, a 1:1000 dilution of antibody and 1 min exposure time for the endogenous IκB blots was more than sufficient to detect the bands.

Based on these results, and the fact that IL-8 secretion in these experiments was unaffected by the IκB-HA expressed (Figures 10.3.C & 10.4.C.), we surmised that there was not enough IκB being expressed to inhibit IL-8 secretion by the entire monolayer. Although it is possible that much of the IκB-HA in the cells was degraded by the end of the TNF stimulation period, it is more likely that there were too few cells expressing IκB-HA. As a result, the IL-8 secretion by the untransfected cells may have swamped out the decrease in secretion by the successfully transfected cells.

10.3.2 pIκB-HA/pNFκB-Luc Co-transfection Experiments

Experiments to co-transfect pIκB-HA with pNFκB-Luc were conducted to bypass the problem of low transfection efficiency. The principle behind this approach was that cells taking up the plasmid, pNFκB-Luc, would express luciferase when stimulated by TNFα. TNF causes the degradation of endogenous IκB and the subsequent release of NFκB. The free NFκB then binds to the promoter of pNFκB-Luc and initiates the expression of luciferase. When the cells take up both plasmids, the expressed IκB-HA was expected to bind the NFκB freed by TNF stimulation, prevent its binding to the promoter, and ultimately prevent luciferase expression.

An initial concern with using the co-transfection approach was the possibility of pIκB-HA physically interfering with the transport of pNFκB-Luc into the cells, especially at higher concentrations of the plasmid. The standard reporter plasmid, pCMV-Luc, was used as a control plasmid to evaluate this possibility. Figure 10.5 showed that there was no significant difference between luciferase expression by pCMV-Luc alone or with pIκB-HA ($p = 0.76$). This indicates that presence of the other plasmid did not impede the ability of pCMV-Luc to enter the cell and express luciferase. It also demonstrated that measurable levels of luciferase expression could be achieved, even with relatively low transfection efficiencies.

When pIκB-HA and pNFκB-Luc were transfected together into the monolayers, the difference in luciferase expression by the unstimulated monolayers versus the stimulated monolayers was as expected (Figure 10.5). The unstimulated monolayers had relatively low levels of luciferase expression. The little that was expressed is probably a result of the minor inflammatory response electroporation triggers in these cells. The

stimulated monolayers had luciferase expression levels that were, on average, over 12 times that of the unstimulated monolayers. This means that TNF successfully triggered the release of NFκB and its subsequent binding to the plasmid promoter.

The ability of the IκB-HA expressed after co-transfection to inhibit this expression of luciferase was not so easily determined. Even though Western blot analysis showed expression of IκB-HA in each of the four experiments performed (Figure 10.7), luciferase expression was inhibited in only two experiments (Figure 10.6). It is unclear why this was the case, but two possible reasons will be discussed. First, just as with the transfection of pIκB-HA alone, it is possible that there was not enough IκB-HA expressed to prevent the binding of NFκB to the promoter of pNFκB-Luc. Since NFκB is normally found bound to endogenous IκB, it is reasonable to assume that it would be found in the same large quantities observed for IκB (Figures 10.3 and 10.4). As a result, even if the expressed IκB did bind some NFκB, there may have been a significant amount of free NFκB left to initiate luciferase expression.

A change in the electroporation apparatus might yield better expression results. When T84 monolayers grown on 0.33 cm^2 inserts were electroporated with pIκB-HA using the smaller cuvette designed for the siRNA experiments, higher levels of protein expression were achieved, when using comparable amounts of DNA per unit area, than what was observed using the 4.7 cm^2 ring and the InSitu™ system (Figure 10.8). When the samples were analyzed by Western, small IκB-HA bands were clearly visible after only a 5 min exposure (vs. 1 h for bands in Figure 10.7)

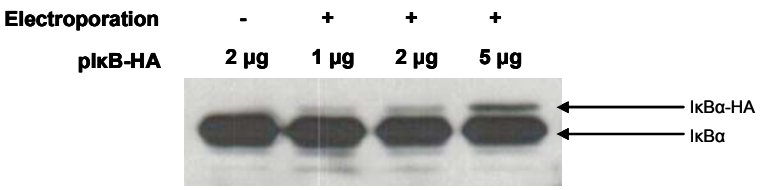

Figure 10.8 IκB-HA expression in T84 monolayers electroporated using the smaller cuvette design. Monolayers were grown on 0.33 cm^2 inserts and electroporated with the specified amount of DNA using two 50 V – 20 ms pulses. Significantly more expression was observed using this apparatus when compared to expression using the InSitu™ system shown in Figure 10.7. Blot was exposed for 5 min. [IκB-HA molecular weight ~42 kDa; endogenous IκBα molecular weight ~37 kDa]

A second potential reason the co-transfections did not always work could involve degradation of the expressed IκB-HA, especially in the case of monolayers stimulated with TNF. With the exception of the HA tag, the expressed IκB is essentially the same as endogenous IκBα, including the serine residues at which phosphorylation occurs. This means that when the cells were stimulated with TNFα, IκB-HA could have been phosphorylated and targeted for subsequent degradation. If this was the case, then degradation was obviously not complete, since some expression of the protein was still visible, but the ability of expressed IκB to inhibit activation of NFκB could have still been affected. One way to avoid degradation could involve electroporating a plasmid that expressed the IκBα super-repressor. This protein, which can also be tagged with HA, is mutated at the serine residues that play a role in phosphorylation, thus making the protein resistant to degradation and able to inhibit NFκB activation.

Although inhibition of NFκB activation by plasmid delivery did not work as well as we would have liked, other means of inhibiting this pathway may prove to be more successful. Even if efficient inhibition of NFκB activation is achieved, the issue of how to inhibit the transcription factor without affecting the other essential functions it regulates (e.g., cell growth, adhesion, apoptosis) would still be a concern. Several studies have shown that complete inhibition of NFκB in animal models can lead to serious side effects (Baldwin, 1996; Schmid and Adler, 2000). Therefore, additional research is needed to identify ways that the negative effects of NFκB can be inhibited with specificity.

10.4 Conclusions

Confluent T84 monolayers were electroporated with plasmids that were meant to inhibit NFκB activation after stimulation with TNFα. Delivery of a plasmid that expressed IκB-HA showed no effect on IL-8 secretion, probably because of low transfection efficiency. Results from co-transfection experiments with the IκB-expression plasmid and a plasmid that expressed luciferase upon binding of NFκB to its promoter were inconclusive since NFκB was inhibited in some experiments, but not in others. A common problem with both sets of experiments appeared to be low levels of IκB protein expression. Although results from one experiment indicated that a change in electroporation apparatus might provide better results, other methods of inhibition, such gene silencing by siRNA transfection (which will be discussed in the next chapter), may be more successful.

CHAPTER XI

11. GENE SILENCING BY ELECTROPORATION-MEDIATED SIRNA TRANSFECTION

11.1 Introduction

The previous two chapters demonstrated that gene expression in confluent intestinal epithelial monolayers by electroporation can be relatively inefficient, when compared to the large amounts of DNA that can be loaded into the cells. Poor trafficking of the plasmid DNA into the nucleus could one reason for this problem. If one is interested in inhibiting the function of a particular cellular process by introducing a genetic molecule, one alternative to plasmid DNA is the use of short-interfering RNAs, or siRNAs. These molecules, which are typically only 21-23 base pairs long, mediate a process called RNA interference (RNAi) and have received much attention in recent years because of the highly specific manner in which they can inhibit, or silence, a particular gene (Hannon, 2002).

RNAi is the inhibition of gene expression through the introduction of double-stranded RNAs that are homologous to the gene of interest (Zamore, 2002). In the cytoplasm, the dsRNAs are cleaved by an enzyme called Dicer into short-interfering RNAs (siRNAs), which in turn bind to a ribonuclease enzyme called RNA-induced silencing complex (RISC). The siRNA guides the RISC to its complementary target mRNA, which is then degraded by the ribonuclease, thereby preventing (silencing) expression of the gene. This phenomenon, thought to be a defense mechanism against viral infection, was originally observed in plants, fungi, and worms (Baulcombe, 2002),

but when dsRNAs longer than 30 bp were introduced into mammalian cells, they triggered a shut down of all protein synthesis in the cells (Shi, 2003). It wasn't until Elbashir et al. (Elbashir et al., 2001a) demonstrated that introduction of shorter RNAs (21 – 22 bp) into mammalian cells resulted in highly specific gene silencing, that this field of research really began to grow. Because of the specificity and efficiency with which siRNAs target a gene for silencing, they have generated a significant amount of interest in their use as a tool for studying gene function (Harborth et al., 2001; Elbashir et al., 2002) and as a potential therapeutic (Shuey et al., 2002; Check, 2003).

Since gene expression was relatively low in confluent monolayers after plasmid transfection, siRNA transfection was evaluated as a possible alternative. Of particular interest, was the fact that the site of action for these molecules is in the cytoplasm and not the nucleus. Also, because siRNAs are much smaller than plasmids, we surmised that there should be less difficulty to introduce them into intestinal epithelial monolayers. These experiments were conducted to determine whether electroporation could be used to transfect intact monolayers with siRNAs to initiate silencing of lamin A and lamin C, intermediate filament-type proteins found on the nuclear envelope.

11.2 Experimental Results

Confluent T84 monolayers were electroporated using a modified cuvette designed for use with smaller cell culture inserts with 0.33 cm^2 growth areas (see Section 4.9). siRNA directed against the nuclear envelope proteins lamin A (70 kDa) and lamin C (65 kDa) was chosen to test the ability of electroporation to knock down production of a protein of interest. For a visual image of where the lamins are located, Figure 11.1 shows

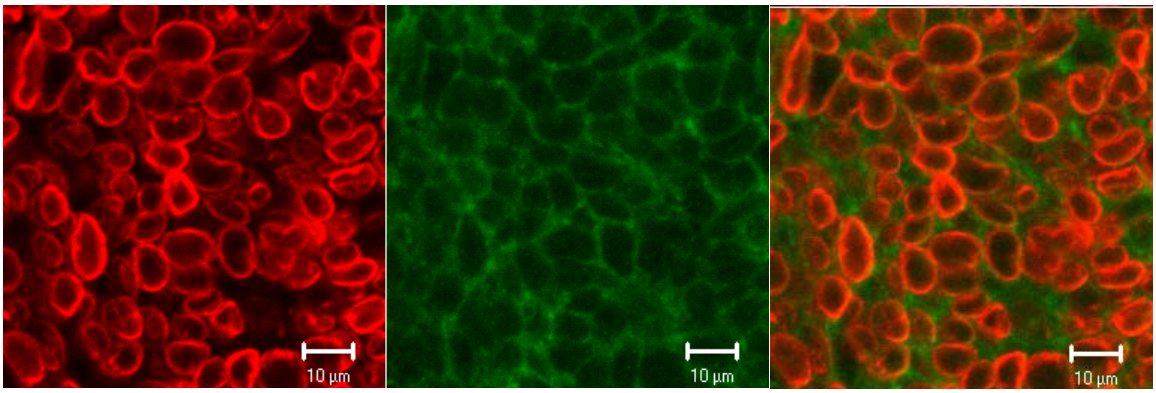

Figure 11.1 Immunofluorescence staining of lamin A/C (red; right), the tight junction protein JAM (green; middle). The lamins are intermediate filament-like proteins located on the inner side of the nuclear envelope. Lamin C is a variant of lamin A and has an almost identical gene sequence. JAM was used to help outline the cell boundaries.

a T84 monolayers that has been stained by immunofluorescence for lamin A/C and the tight junction protein JAM (to distinguish cell boundaries). Inhibition of lamin A/C has become a standard control protocol for evaluating siRNA transfection (Elbashir et al., 2001a). The amount of siRNA and the time at which the monolayers were lysed were varied to determine any dependence of inhibition on time and siRNA concentration. A single 50 V – 20 ms pulse was applied to introduce the siRNA because of its success at delivering the protein, BSA, into these cells. Transepithelial resistance returned to initial values within 24 hours after pulsing with this condition (personal observations).

The first step in this study was to conduct an experiment to determine at what point after transfection there would be the most knockdown of the lamins. Three separate monolayers were electroporated with 100 nM of lamin A/C siRNA and lysed at 24 h, 48 h, and 72 h. An unelectroporated monolayer incubated with 100 nM of the siRNA for 72 h was included as a control. The Western blot in Figure 11.2 shows that there was a significant decrease in the amount of lamin A/C present 24 hours after transfection. When a comparison was made between the intensities of the bands, siRNA knocked down lamin A and C to 50% and 58% of control levels, respectively. As time passed, lamin production recovered so that between 48 and 72 h, lamin A/C returned to 85 - 90% of the control. After detecting the lamins, the blot was stripped and re-probed with an antibody to IκBα, which served as an internal control and confirmed equal loading of protein in the gel. The similarity in size of the IκBα bands in this companion blot indicates that the reduction in lamin A/C band intensity was not due to cell loss after electroporation.

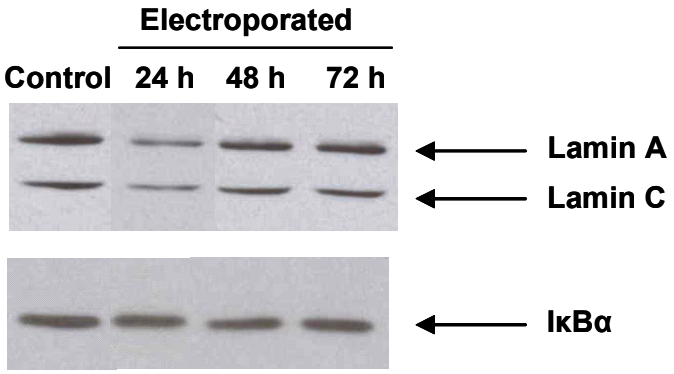

Figure 11.2 siRNA directed against lamin A/C temporarily knocks down production of the nuclear envelope proteins. Confluent T84 monolayers were electroporated with 100 nM lamin A/C siRNA using a single 50 V – 20 ms pulse. Monolayers were lysed at the specified times after transfection and analyzed by SDS-PAGE and Western blotting. After detection of the lamins with their respective antibodies, the blot was stripped and re-probed for IκBα, which served as an internal control, and confirmed equal loading of protein in the gels. Blots were exposed for 30 s. [Molecular weights: Lamin A = 70 kDa; Lamin C = 65 kDa; IκBα = 37 kDa]

After observing that most inhibition occurred 24 h after siRNA transfection, the extracellular concentration of the lamin siRNA was then varied to check for a dependence on the amount of siRNA. The monolayers were electroporated with a 50 V – 20 ms pulse using concentrations of lamin siRNA ranging from 10 nM to 1 μM. The resulting decrease in lamin production was analyzed 24 h later. Inhibition of lamin A/C tended to increase as the concentration of lamin siRNA increased, although there were a couple of concentrations at which there was no discernable change (100 nM and 200 nM) (Figure 11.3A). At the lowest concentration used, 10 nM, there was no reduction of lamin A/C, which could be an indication of a threshold for inhibition. An approximately 15 - 20% reduction in lamin A/C was observed after transfection with 20 nM and 50 nM siRNA. At 500 nM, lamin A/C was reduced by 50%. The highest extracellular siRNA concentration, 1 μM, siRNA caused a 90% reduction in lamin A/C. The IκB band for the 1 μM siRNA condition was slightly smaller than the other bands, which could indicate some loss of cellular material, but the decrease was not enough to account for the almost complete loss of lamin.

Several other controls were included to ensure that any inhibition observed was due to the lamin siRNA alone. To show that electroporation did not have an effect on lamin A/C, a confluent T84 monolayer treated with a 50 V – 20 ms pulse and no siRNA was compared to an unelectroporated monolayer. The bands for both monolayers were similar in size and intensity and showed no reduction in lamin A/C (Figure 11.3B). As an added control, non-silencing siRNA was introduced by electroporation at two concentrations, 200 nM and 2 μM. This control siRNA did not have an effect on lamin A/C, which confirms the specificity of the lamin A/C siRNA (Figure 11.3B).

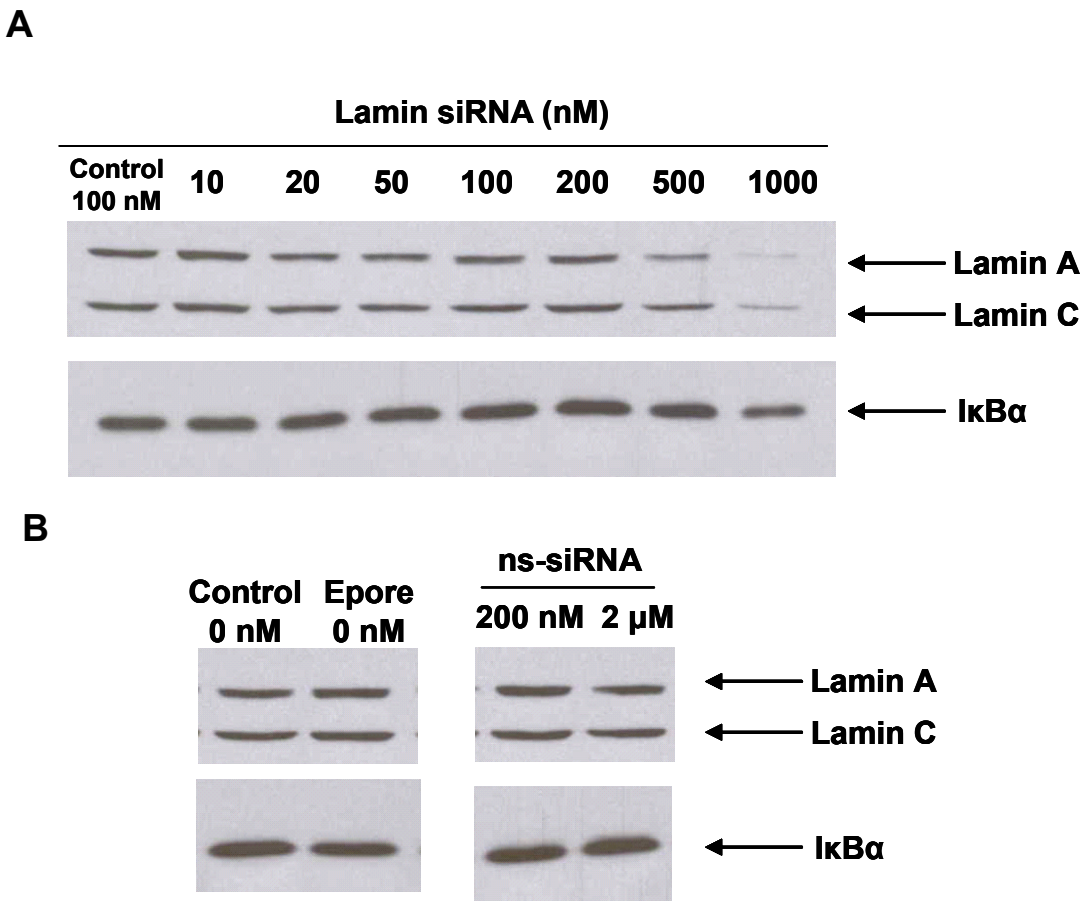

Figure 11.3 (A) Western blots showing the dependence of gene silencing on lamin A/C siRNA concentration. Confluent T84 monolayers were electroporated with a 50 V – 20 ms pulse using siRNA amounts ranging from 10 nM to 1 μM. Monolayers were harvested 24 h after transfection. (B) Included for comparison were an unelectroporated monolayer with no siRNA, a monolayer electroporated with no siRNA, and two monolayers electroporated with 200 nM or 2 μM of non-silencing siRNA (ns-siRNA). The two ns-siRNA controls demonstrate the specificity of the lamin A/C siRNA. All blots were stripped and reprobed for IκBα to confirm equal loading of protein. [Molecular weights: Lamin A = 70 kDa; Lamin C = 65 kDa; IκBα = 37 kDa]

It was not clear why no effect was observed at the 100 nM and 200 nM concentrations, especially since the 100 nM concentration was successful in Figure 11.2. It could be that the band for the "no electroporation + 100 nM siRNA" control monolayer was not as heavy as previous controls and as a result the band for the treated monolayer appeared darker than the control. It is also possible that the electroporation pulse was not delivered as efficiently. During the course of experiments, it was observed that the aluminum electrode became pitted and worn very easily, and as a result, should have been replaced more frequently.

A replicate experiment was performed to retest inhibition of lamin A/C in T84 monolayers at siRNA concentrations of 100 nM, 500 nM, and 1 μM. The dependence of inhibition on time was also re-evaluated after finding that other studies involving lamin A/C siRNA transfection by both polyfection and electroporation, saw inhibition up to 48 hours after transfection (Elbashir et al., 2001a; Jiang et al., 2003). Figure 11.4 shows the reduction of lamin A/C 24 h and 48 h after lamin siRNA transfection at three different concentrations. When compared to an unelectroporated control monolayer, levels of lamin A and lamin C 24 hours after transfection were both about 60% of the control at 100 nM, 75% and 65%, respectively, at 500 nM, and 36% at 1 μM. At 48 hours after transfection, inhibition was still evident, with lamin A and lamin C levels that had decreased to approximately 56% of the control at 100 nM, 59% and 50%, respectively, at 500 nM, and 32% and 23%, respectively, at 1 μM.

11.3 Discussion

The use of siRNAs to modify cellular function could be a useful alternative to

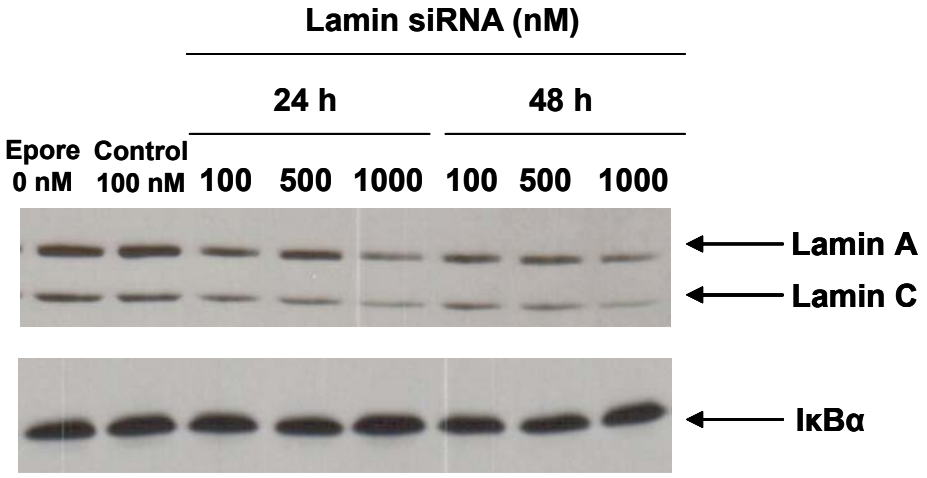

Figure 11.4 Western blot replicate showing inhibition of lamin A/C after siRNA transfection. Monolayers were electroporated with a 50 V – 20 ms pulse using siRNA concentrations of 100 nM, 500 nM, or 1 μM and then lysed at either 24 h or 48 h after transfection. Inhibition lasted for at least 48 hours in this experiment. No siRNA and unelectroporated and controls showed no inhibition of the lamins. Blot was stripped and reprobed for IκBα to show equal loading of protein. [Molecular weights: Lamin A = 70 kDa; Lamin C = 65 kDa; IκBα = 37 kDa]

plasmid DNA. The site of action of these molecules is the cytoplasm, where they bind and target messenger RNA (mRNA) for degradation (Elbashir et al., 2001b; Baulcombe, 2002; Zamore, 2002). This means that transport into the nucleus, where the transcription and translation processes necessary for protein expression after plasmid transfection, is not necessary. In addition, the size of these small molecules (~22 bp) is significantly less than the size of standard plasmids (~5000 bp), which makes them much easier to deliver.

Most studies of siRNA have used the proprietary formulation Oligofectamine™ or cationic lipids to transfect subconfluent adherent cells (Elbashir et al., 2001a; Yu et al., 2002). A few have used electroporation to transfect fibroblast, adipocytes, stem cells, and hepatocytes in suspension (Jiang et al., 2003; Oliveira and Goodell, 2003; Wilson et al., 2003). To the best of our knowledge, there have no published reports of siRNA transfection into polarized, confluent intestinal epithelial monolayers using electroporation or other methods of delivery, although transfection of subconfluent Caco-2 cells with Oligofectamine™ has been reported (Balamurugan et al., 2003).

Although expression after lipofection was quite low in our studies with confluent T84 monolayers (see Chapter 9), the DNA uptake results showed that lipid-mediated uptake of plasmid DNA by these monolayers can be relatively high under certain conditions (Figure 9.9). This suggests that siRNA transfection with lipids should be more successful than plasmid transfection, since nuclear transport is not necessary to have an effect. However, when lipid-mediated transfection of confluent T84 monolayers with siRNA was attempted by researchers in Dr. Asma Nusrat's laboratory at Emory University, they were not able to obtain satisfactory gene silencing (personal communication). After our success with electroporating epithelial monolayers, Dr.

Nusrat's group has since begun evaluating electroporation as a method of siRNA delivery into these cells.

The results of our experiments with siRNA transfection are very promising. The fact that monolayer integrity recovered in 24 hours and that silencing also occurred in that time could prove to be useful in protocols where monolayers can be treated, allowed to recover, and be ready for use the next day. The trend of increasing lamin A/C silencing as the siRNA concentration increased, is consistent with trends reported by others (Elbashir et al., 2002; Jiang et al., 2003). The minimum amount of siRNA required to see silencing in our experiments is higher than what was observed in the study by Elbashir, et al. (20 nM vs. 2 pM), but this could possibly be because of the many differences between the two experiments, e.g., cell type, cell confluence, transfection method, etc. Despite this, the results obtained provide a good foundation for future experiments with siRNA-mediated gene silencing in intestinal epithelial monolayers.

11.4 Conclusions

Successful transfection of siRNA, which bypasses the need for nuclear import and subsequent transcriptional and translational processing, was demonstrated for the first time in polarized intestinal epithelium. The extent of silencing of the nuclear envelope proteins lamin A/C occurred within 24 hours of transfection and increased with increasing siRNA concentration. These results demonstrate the potential for modification of intestinal epithelial function by electroporation-mediated siRNA transfection and open up a wide range of possibilities for the study and, perhaps, treatment of intestinal disorders.

CHAPTER XII

12. CONCLUSIONS

The ability to introduce exogenous drugs, proteins, or genes into intact, intestinal epithelium could greatly facilitate the study, and potential treatment, of various intestinal disorders. In this study, electroporation of two cell lines that model the intestinal epithelium resulted in extensive, uniform uptake of calcein, a small fluorescent tracer, and fluorescein-labeled bovine serum albumin (a protein). In both cell lines, molecular uptake, which reached on the order of 10^6 calcein molecules per cell and 10^5 BSA molecules per cell, increased with increasing pulse strength, length, and number. Cell viability decreased as the parameters were increased indicating a trade off. When total exposure time was kept constant, however, neither uptake nor viability changed significantly.

Intestinal epithelial monolayers electroporated with a range of conditions experienced a loss of resistance and tissue barrier function that recovered at different rates depending on the cell line and the strength of the condition applied. For some conditions, monolayers were able to recover physically in less than a day. In addition to causing a temporary loss of barrier function, electroporation also induced a temporary inflammatory response (increased secretion of IL-8), but monolayers were able to recover normal function within 12 hours.

The permeability of confluent Caco-2 monolayers to calcein and bovine serum albumin was significantly enhanced by electroporation and was found to be size dependent. When the various barriers to transport were evaluated, i.e., the monolayer,

the aqueous boundary layers, collagen matrix, and filter, the monolayer was found to be the primary barrier. Transmonolayer transport, i.e., through small holes in the monolayer, is the most likely route by which permeability enhanced; although paracellular (between cells) transport may also contribute. Transcellular (across cells) transport was found to be negligible.

Electroporation's ability to transfect confluent T84 monolayers, which are refractory to conventional methods of transfection, with plasmid DNA was initially evaluated using luciferase and GFP reporter plasmids. A combination of an optional single, short high voltage pulse and three long, low voltage pulses was found to yield the most luciferase expression. For the most part, electroporation was more successful at transfecting confluent intestinal epithelial monolayers than lipofection. Despite high levels of DNA uptake after both lipofection and electroporation, however, the overall transfection efficiency was essentially zero for the former and only ~3% for the latter.

When confluent T84 monolayers were electroporated with plasmids that would inhibit activation of the NFκB-mediated inflammatory pathway, results were not consistent. In a few cases, activation was inhibited, but, more often, no change in activation was observed. The most likely reason is low expression of the inhibitory protein, IκBα, as observed for the reporter plasmids.

The fact that expression after plasmid transfection was not high led to an interesting addition to the research. Electroporation of short interfering RNAs (siRNAs) into confluent T84 monolayers was found to be very efficient at silencing the nuclear envelope proteins, lamin A and lamin C in as little as 24 hours. Unlike plasmids, the site of action of these small nucleic acid fragments is the cytoplasm, not the nucleus, and, as a

result, they do not require transcriptional and translational processing. To our knowledge, this is the first time successful transfection of siRNA into polarized intestinal epithelium was demonstrated. The use of siRNAs could prove to be a useful alternative to plasmids for inhibiting or modifying intestinal cell function *in vitro* and, perhaps *in vivo*.

We have demonstrated that electroporation can be used to efficiently deliver a wide range of molecules, from small tracers to large nucleic acids, into polarized, intestinal epithelial monolayers. These results could lead to improved models of the intestinal epithelium by providing researchers a relatively simple and easy way to introduce exogenous molecules into these monolayers and modify cellular function, and could form the basis for improved treatment of diseases that affect the intestine *in vivo*.

CHAPTER XIII

13. RECOMMENDATIONS

I would recommend that the following experiments be performed. Since flow cytometry appears to underestimate the cell viability of the monolayers after electroporation (Section 7.3.2), a method of quantifying the viability in situ would be useful. Although transepithelial electrical resistance (TEER) gives a qualitative measure of cell viability, by providing information about how quickly the cells recover barrier function, quantitative numbers about the percentage of cells that survive electroporation could also be useful.

As stated in Section 4.2.4, the voltage experienced by the monolayers during electroporation is less than the voltage applied to the cuvette. Unfortunately, we were unable to determine this actual voltage with our equipment. It is possible that a more sophisticated oscilloscope, with a higher sampling rate that would allow us to view minute changes in the voltage and current traces, would have aided our efforts. Also, since changes in cuvette geometry could also affect the voltages and currents, it may be necessary to develop a new cuvette design. The adherent cell cuvettes obtained from EquiBio, Ltd. were not as rigid as the cuvettes used for suspension cells and, as a result, deformations in the plastic could, for example, affect the electrode spacing, which would, in turn, affect the voltage delivered to the cells.

Development of a new cuvette design could also aid plasmid delivery experiments, as illustrated in Figure 10.8 where IκBα-HA expression was higher after using the alternative cuvette. It is possible that the smaller design, which required a much lower

electroporation volume, also resulted in a shorter distance for the DNA to travel to the cells, which led to the increased expression. A similar cuvette could be designed for the larger culture inserts with rigid electrodes of fixed spacing that are situated in such a way that the amount of medium necessary for electroporation is minimized.

The results reported in this thesis demonstrate that electroporation will be a useful tool for manipulating cell culture models of the intestinal epithelium. Future experiments with the technique, however, could involve moving to a more complex geometry such as excised intestinal tissue. In *ex vivo* experiments, similar to skin electroporation, either the innermost layers or the full thickness of the intestinal wall could be initially electroporated with fluorescent marker molecules. Confocal microscopy could then be used to determine how deeply marker molecules can be delivered. Permeability studies could be conducted to evaluate whether electroporation can similarly increase transport across epithelial tissue as it did across epithelial monolayers. Experiments with biologically active molecules, such as proteins or nucleic acids, could also be performed.

Electroporation of both *ex vivo* and *in vivo* epithelium is not expected to be as straightforward as treatment of the *in vitro* monolayers since monolayers have a 2-dimensional geometry and epithelial tissue has a 3-dimensional structure. This more complex structure would have implications on both the electrode design and on the resulting uptake of molecules by the cells.

In *ex vivo* experiments, the tissue could be mounted so that the electrodes can be placed on the mucosal and serosal sides of the intestinal tissue, thus allowing the electric field to pass directly across the entire wall thickness. This set-up would not be possible *in vivo*, since the electrodes cannot be placed on either side of the intestinal wall. They

would have to be introduced rectally in an endoscopic-like manner and the electric field applied with both electrodes on the mucosal side of the intestine. In addition, the area to be treated would have to be cleansed (to prevent the electroporation of potentially dangerous luminal contents from entering the cells or crossing the epithelial barrier) and, perhaps, bathed in a saline solution (to facilitate electroporation).

The effect of the electric field on the cells is another issue that will have to be taken into consideration when electroporating intestinal tissue. In contrast to *in vitro* models, the epithelial lining of the intestine consists of different types of cells of various sizes and shapes. In addition, the location of these cells on structures such as the villi and microvilli means the cells will have different orientations with respect to the electrodes. All of these could result in non-uniform effects of the electric field on the cells and heterogeneous uptake of molecules.

APPENDIX A

Supplemental Results

A.1 Toxic Effect of Cationic Lipids on Intestinal Epithelial Cells

In Figure A.1, two sets of bright field microscopy pictures of Caco-2 monolayers are presented. The cells in Figure A.1A are control cells that were exposed to plasmid DNA (pEGFP-N1) only, while the cells in Figures A.1B,C were exposed to Lipofectin and transfected with pEGFP-N1. These monolayers were imaged 4 days after seeding, which was 2 days after transfection for the treated cells. At the time of imaging, control cells appeared almost 100% confluent, with very few gaps appearing only at the edges of the monolayer near the membrane edge. The transfected cells, on the other hand, still had not formed a confluent monolayer after four days. Islands of cells were still very prevalent, which could indicate that the cationic lipids had an inhibitory effect on the growth of these cells. By 6 days after seeding (4 days after transfection), the cells finally filled in to form an intact monolayer, although rings of potentially still dividing cells were evident (Figure A.1D).

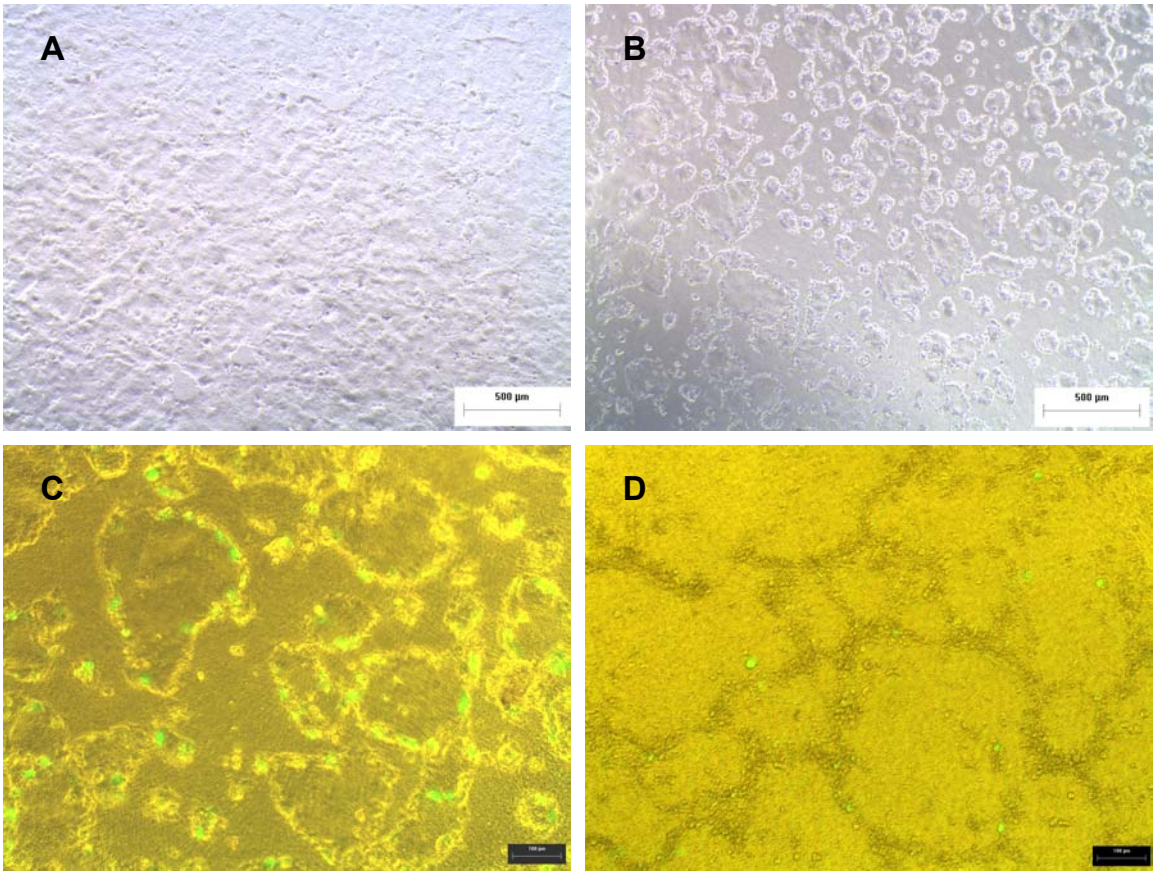

Figure A.1 Cell growth was slowed when Caco-2 cells were transfected with the cationic lipid. Four days after-seeding, or 48 h after transfection, the monolayers exposed to the lipid appeared very patchy and were not confluent (B, C). The control monolayer, which was not exposed to lipid, was almost fully confluent by this time (A). The lipid transfected monolayers did not fill in until eight days after seeding, although areas where the islands met were still visible.

A.2 Comparison of LipoTAXI and Lipofectin Cationic Lipid Formulations

Although Lipofectin worked well in initial experiments, a switch was made to the cationic lipid mixture, LipoTAXI (Stratagene), because it was readily available in our laboratory. To ensure that similar results would be achieved with this lipid, subconfluent T84 monolayers were transfected one day after seeding with 10 μg of pEGFP-N1 and either 0.05 mM LipoTAXI or 60μg/ml Lipofectin. The LipoTAXI concentration was chosen based on the manufacturer's recommended range of lipid quantity. GFP expression by subconfluent monolayers treated with LipoTAXI was comparable to that observed in monolayers treated with Lipofectin (Figure A.2). The density of GFP positive cells after exposure to LipoTAXI and Lipofectin were estimated to be 2,000 cells/cm^2, and 1500 cells/cm^2, respectively. Although expression was lower than previously observed (perhaps because the cells were more confluent than usual), based on the similarity in results, LipoTAXI was concluded to be acceptable for use as the lipofection reagent in future experiments.

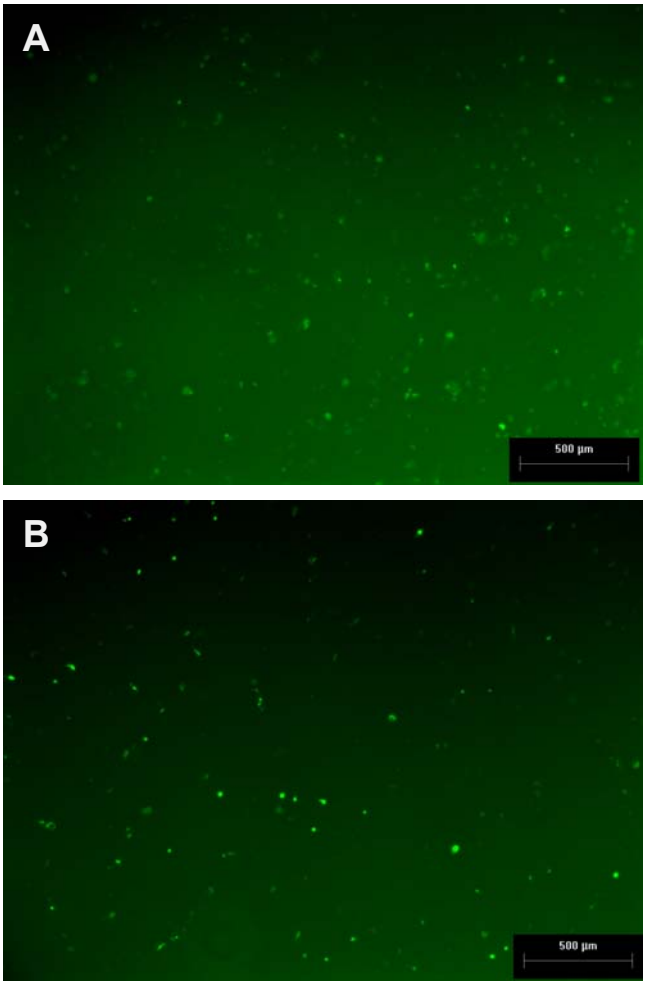

Figure A.2 The cationic lipid formulations, LipoTAXI (A) and. Lipofectin (B), yielded similar levels of GFP expression in subconfluent T84 monolayers. Monolayers were treated with either 0.05 mM LipoTAXI or 60 µg/ml of Lipofectin and 10 µg pEGFP-N1 and imaged 24 h later.

A.3 Recombinant IκB Protein Delivery Results

A few experiments were conducted to determine whether electroporation could be used to deliver a protein to inhibit NFκB activation. The protein to be delivered was recombinant IκBα, which was obtained as a gift from Dr. Neish. The protein contained a His•Tag sequence (a series of consecutive histidine residues), which made it possible to distinguish it from endogenous IκB by size. Based on the results of experiments with electroporating FITC-labeled BSA, a condition of 50V-5ms was chosen for electroporating the IκB protein into T84 monolayers. This condition resulted in the uptake of about 10^5 BSA molecules per cell and a viability of approximately 90% (see Chapter 7) and was expected to produce similar results for delivery of IκB protein molecules.

Electroporation of Recombinant IκBα

Confluent T84 monolayers were electroporated with 50 μg/ml of recombinant IκBα in HEPES-buffered DMEM added apically and then allowed to recover for one hour at 37°C. In addition to having an unelectroporated monolayer incubated with IκBα for an hour, several other controls were also included. Two monolayers (unelectroporated and electroporated) incubated with no protein and two monolayers (unelectroporated and electroporated) incubated with 50 μg/ml of FITC-labeled BSA served as controls to ensure that any change in the inflammatory response is specific to the presence of IκBα. Another set of samples consisting of replicates of the monolayer conditions just described were added for comparison.

After the one hour incubation, one set of monolayers was washed twice with warm DMEM and then exposed basally to 10 ng/ml TNFα in complete medium for 8 hours. The replicate set of monolayers was placed in just complete medium for those 8 hours. During this time, 200 μL samples of the basal medium were collected at 0, 2, 4, 6, and 8 hrs to test for the secretion of IL-8. Equal volumes of fresh medium were added after each sampling time. Following TNF stimulation, the monolayers were lysed, on ice, in 400 μL of cold SDS lysis buffer and stored at -70°C until later analysis by SDS-PAGE and Western blotting.

Analysis of IL-8 Secretion and Protein Delivery

To determine whether the introduction of IκBα protein inhibited IL-8 secretion, the samples of the basal medium collected during TNF stimulation were analyzed for the presence of IL-8 by sandwich ELISA. The same ELISA protocol used during the functional recovery experiments described in Section 4.4.2 was used to calculate the amount of IL-8 secreted in response to TNFα (See Appendix B for detailed protocol).

The cell lysates were analyzed for the presence of endogenous and recombinant IκBα by SDS-PAGE and Western blotting using the protocols described in Appendix B, Section VII. A 12.5% polyacrylamide separating gel was used to separate the protein, which was probed with the same anti-IκBα primary antibody (1:1000) and horseradish peroxidase-labeled secondary antibody (1:1000) used in the pIκBα-HA transfection experiments Section 4.6.2. Since the recombinant IκBα protein contained the His•Tag sequence, it was slightly larger than endogenous IκBα and could, therefore, be easily distinguished.

Immunofluorescence staining was used to visualize the localization of the recombinant IκB protein within the cells. One hour after electroporation, the monolayers were washed 3 times in HBSS+, fixed in 3.7% paraformaldehyde for 20 minutes at room temperature, and then stained according to Immunofluorescence Protocol #1 detailed in Appendix B, Section VIIE.

Negative Results for Recombinant IκBα Delivery Experiments

Unfortunately, the results of these experiments were not successful. First, when IL-8 secretion by T84 monolayers electroporated with recombinant IκBα was monitored after TNFα stimulation a decrease in secretion was observed (Figure A.3). TNF stimulated monolayers without IκB showed the same amount of, if not lower, IL-8 as the monolayers treated with the protein. Replicate monolayers with that were not stimulated with TNF had close to basal levels of secretion (not shown). When the lysates of the monolayers were analyzed by Western blot (Figure A.4) and immunofluorescence (Figure A.5) to check that recombinant IκB was delivered intracellularly, both the unelectroporated and electroporated monolayers showed the presence of the protein. This made it impossible to determine whether the protein was delivered to the cells. It is likely that the extracellular protein was not sufficiently washed from the monolayers (despite repeated attempts to do so), which would have contaminated the unelectroporated control samples during the lysing required for the Western and the permeabilization step required for immunofluorescence.

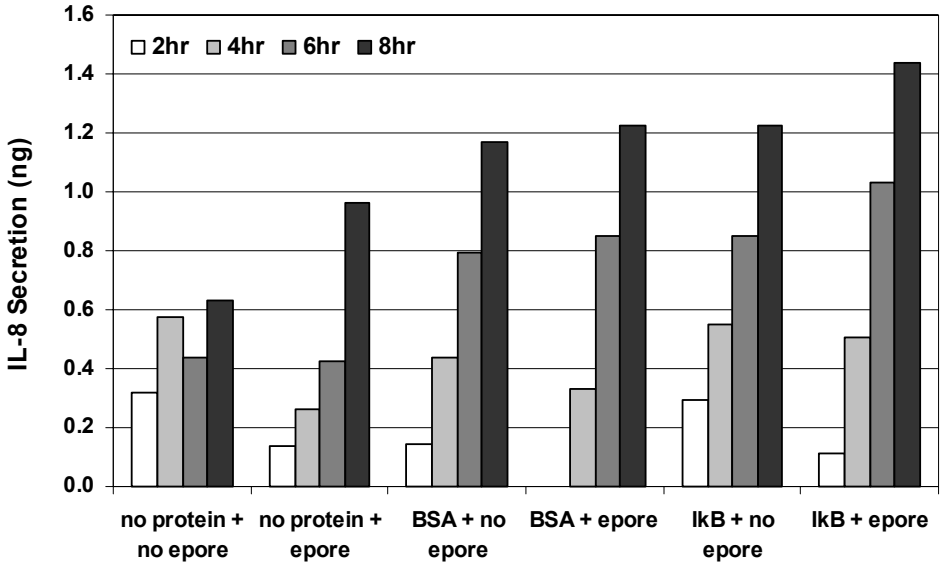

Figure A.3 IL-8 secretion by T84 monolayers after TNF stimulation was not inhibited by electroporation of recombinant IκBα into the cells.

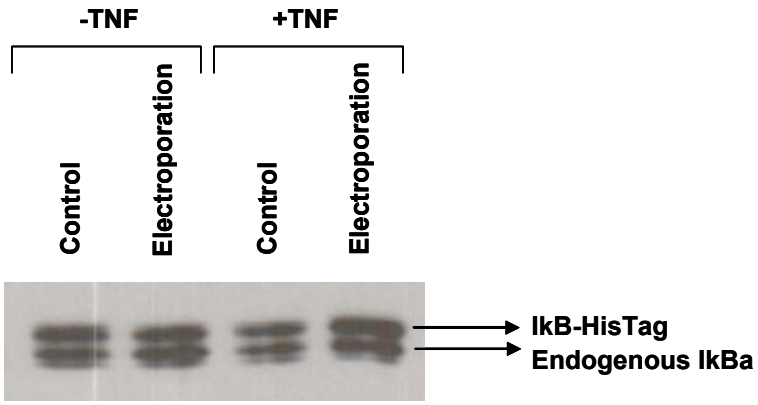

Figure A.4 Western blot analysis showed recombinant IκB present in the lysates of both unelectroporated and electroporated cells.

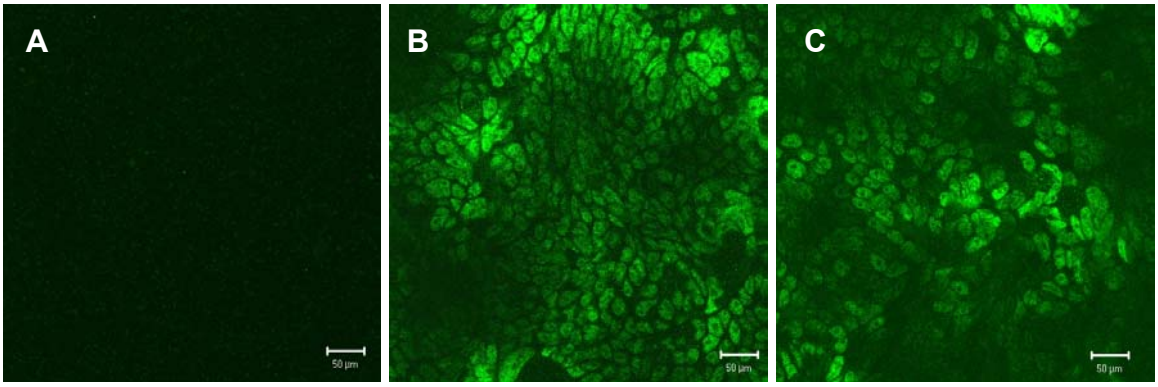

Figure A.5 Immunofluorescence staining for the His-Tag sequence also showed the presence of the protein in both (B) unelectroporated and (C) electroporated monolayers. (A) Monolayers that were not exposed to the protein and probed with an antibody to His-Tag showed no fluorescence.

APPENDIX B

Detailed Experimental Protocols

Table of Contents

VI. Analysis of Flow Cytometry Data with WinMDI Software

VII. Molecular Biology Protocols
- A. IL-8 ELISA
- B. Plasmid Amplification and Purification
  1. Bacterial Transformation
  2. Streaking Out a Single Colony of Bacteria
  3. Small Plasmid Prep to Check Transformation
  4. Restriction Digests of Plasmid
  5. Agarose Gel Electrophoresis
  6. Sacred Stock of Plasmid
  7. Purification of Large Batches of Plasmid
  8. Preparation of Glycerol Stocks of Bacteria
  9. DNA Precipitation and Resuspension
- C. Information About Plasmids and Restriction Digests
  1. pEGFP-N1
  2. pGL3-control
  3. pIκB-HA
  4. pIL8-CAT
  5. pNFκB-Luc
  6. pCMV-Luc
- D. Western Blots: From Start to Finish
  1. Sample Lysis in SDS Lysis/Loading Buffer
  2. SDS-PAGE Gels
  3. Wet Electrophoretic Transfer
  4. Protein Immunoblotting (Western)
- E. Immunofluorescence Staining
  1. Protocol #1
  2. Protocol #2

I. RECIPES FOR FLUORESCENT SOLUTIONS

A. Calcein (1 mM stock solution)

Supplies:
- Small vial of high purity calcein (Molecular Probes)
- Phosphate Buffered Saline (PBS)

Procedure:
1. To make 14 ml of 1 mM stock solution of calcein, measure out exactly 0.0087 g of calcein using a small weigh boat and spatula.
2. Carefully pour the calcein powder into a 15 ml conical centrifuge tube. (Keep the weigh boat)
3. Using the electric Pipet-Aid, add 5 ml of PBS to the calcein while also rinsing the weigh boat into the centrifuge tube.
4. Wrap the centrifuge tube with aluminum foil (to protect the calcein from light).
5. Vortex the solution for several minutes or until the calcein is dissolved.
6. Add another 9 ml of PBS to the calcein solution.
7. Vortex for another minute.
8. Label the centrifuge tube with the date, the solution concentration, and your initials.
9. Keep in refrigerator.

B. FITC-labeled BSA (100 µM stock solution)

Supplies:
- Lyophilized FITC-labeled BSA (Molecular Probes – 25 mg vials or Sigma Chemical – 50 mg vials)
- Hanks Balanced Saline Solution (HBSS) or Phosphate Buffered Saline (PBS)

Procedure:
1. To make 3 ml of 100 µM stock solution using the BSA from Molecular Probes, measure out exactly 19.8 mg of BSA using a small weigh boat and spatula.
2. Carefully pour the BSA powder into a 15 ml conical centrifuge tube. (Keep the weigh boat)
3. Using a manual pipet, add 1 ml of PBS or HBSS at a time to the BSA while also rinsing the weigh boat into the centrifuge tube.
4. Pipet the solution up and down to dissolve the BSA.
5. For the BSA from Sigma, add 7.6 ml of HBSS to the 50 mg vial of BSA.
6. Mix well and aliquot into amber microcentrifuge tubes.
7. Wrap the centrifuge tube with aluminum foil (to protect the BSA from light).
8. Label the centrifuge tube with the date, the solution concentration, and your initials.
9. Keep in refrigerator.

C. Fluorescent Microspheres Solution

Supplies:

- 100% fluorescent intensity fluorescent microspheres from the LinearFlow™ Green Flow Cytometry Intensity Calibration Kit (use the most recently received kit)
- Phosphate Buffered Saline (PBS)

Procedure:

1. Get a small test tube and place 1 ml of PBS into it.
2. Vortex the bottle of microspheres to ensure that they're well mixed
3. Using the 10 µL pipettor and tip, insert the tip into the hole, turn the bottle up-side down and draw out 10 µL of beads.
4. Add the beads to the PBS.
5. Vortex.
6. Write 'µspheres', the date, and your initials on the test tube and then wrap it in foil.
7. Keep in refrigerator.

D. MESF Bead Solution

Supplies:

- Package of 5 green-striped bottles of fluorescent calibration beads (in refrigerator door; made by Flow Cytometry Standards Corporation)
- Phosphate Buffered Saline (PBS)

Procedure:

1. Get a small test tube and place 1 ml of PBS into it.
2. Take the four bottles which have intensity values on the label and add about 5 drops from each bottle to the PBS.
3. Vortex.
4. Write 'MESF', the date, and your initials on the test tube and wrap it in foil.
5. Keep in refrigerator.

II. RECIPIES FOR SALINE SOLUTIONS AND CELL CULTURE MEDIA

A. Phosphate Buffered Saline (PBS) – 1X Solution

Supplies:
- 500 ml of filtered H2O (from the U.S. Filter tap by the sink)
- 50 ml of 10X PBS made by GibcoBRL (in the refrigerator)

Procedure:
1. Put the filtered water into one of the empty 500 ml media bottles on the shelf above the 37oC oven.
2. Add the 10x PBS to the water.
3. Using lab tape, label the bottle as follows: 1X PBS, nonsterile/sterile, date, initials.
4. Keep in refrigerator.

NOTE: Alternatively, you can just used premixed PBS ordered directly from manufacturer.

B. Hanks Buffered Saline Solutions (HBSS)

Supplies:
- 1 bottle of Hanks Balanced Salts ('+' or '-') - (located in the refrigerator)
  '+' = contains calcium and magnesium
  '-' = does not contain calcium or magnesium
- 10 ml HEPES solution (from Mediatech)
- Filtered water

Procedure:
1. Obtain a 1000 ml graduated cylinder and fill it with 900 ml of filtered water.
2. Pour the Hanks powder into the water.
3. Add 10 ml of HEPES.
4. Place stirring bar into solution and mix on stirring plate until Hanks is dissolved.
5. Take cylinder of solution to the pH meter in the next lab and place on stirring plate.
6. Check pH.
7. Adjust pH as necessary to 7.4. Use HCl to lower pH and NaOH to increase pH. (You should only need a few drops of either).
8. Top off solution with filtered water to a final volume of 1000 ml.
9. Check pH again.
10. Sterily filter the HBSS (+) into two 500 ml containers using a 500 ml Steritop filter (has top only).
11. Use lab tape to label the two containers as follows: HBSS (+/-), nonsterile/sterile, date, initials.
12. Keep in refrigerator.

C. DMEM Medium w/ antibiotics

Supplies:
- 500 ml Dulbecco's Modified Eagle's Medium (DMEM)
- 5 ml Antibiotics (penicillin/streptomycin)

Procedure:
1. Add the antibiotics to the DMEM. (Use a pipettor to retrieve all of the antibiotic solution)
2. Write 'P/S', the date, non-sterile, and your initials on the label.
3. Keep in refrigerator.

D. Electroporation Medium - DMEM w/ 25 mM HEPES

Supplies:
- 500 ml Dulbecco's Modified Eagle's Medium (DMEM)
- 12.5 ml 1M HEPES

Procedure:
1. Remove 12.5 ml of DMEM.
2. Add HEPES to the DMEM.
3. Write 'DMEM + 25mM HEPES', the date, sterile/nonsterile, and your initials on the label.
4. Keep in refrigerator.

E. Caco-2 Cell Culture Medium [STERILE!]

Supplies:
- 500 ml sterile Dulbecco's Modified Eagle's Medium (DMEM) – Denise's refrigerator
- 50 ml heat-inactivated Fetal Bovine Serum (FBS) - freezer
- 5 ml antibiotics (penicillin/streptomycin) - freezer
- 5 ml L-glutamine – freezer
- 5 ml sterile HEPES - refrigerator
- 5 ml sterile MEM nonessential amino acids – refrigerator

You will have to work in the laminar flow hood for to make this media. Don't forget to work as far back in the hood as is comfortable. Also, don't leave any containers open to air and remember to spray your gloves with ethanol before you put them in the hood.

Procedure:

1. Thaw FBS, antibiotics, and glutamine in the 37^{o}C water bath.
2. Load all of the above, a Stericup filter assembly (has top and bottom), ethanol, paper towels, and marker onto a cart and take them to the hood.
3. Lift hood door and turn on the blower.
4. Spray hood down with ethanol and wipe with paper towel.
5. Spray all bottles and filter assembly with ethanol and place them in the hood.
6. Loosen the caps of the media bottles and the centrifuge tubes.
7. Add the FBS, antibiotics, glutamine, HEPES, and MEM to the DMEM media bottle. Make sure you get all of the antibiotics and glutamine.
8. Cover the DMEM bottle.
9. Open the Stericup filter assembly package in the hood.
10. Lift the lid off the upper container and pour in the DMEM solution.
11. Put the lid back onto the upper container. Tape it down to help maintain sterility.
12. Bring the entire assembly back to the lab bench.
13. Hook up the filter assembly to the vacuum aspirator and turn on the vacuum.
14. When the media solution has finished filtering into the bottom container, take the filter assembly back to the hood. Spray it with ethanol before putting it into the hood.
15. Unscrew the upper chamber and close the bottom container using the cap provided.
16. Take the label from the original DMEM bottle (try not to tear it) and place it on the new container of DMEM complete media.
17. Write 'Caco-2 medium, STERILE, the date, and your initials on the label.
18. Throw empty centrifuge tubes and empty DMEM bottle into biohazard box in our lab.
19. Spray hood down with ethanol.
20. Turn of blower and close hood. (If hood and blower were already open and on when you started, then leave them open and on).
21. Keep media in refrigerator. Store no longer than 3 weeks.

F. T84 Cell Culture Medium [STERILE!]

Supplies:

- 500 ml sterile DMEM/F12 medium w/ 15 mM HEPES - refrigerator
- 30 ml heat-inactivated newborn calf serum (NCS) - freezer
- 5 ml antibiotics (penicillin/streptomycin) – freezer
- (All reagents from Gibco, now Invitrogen)

See instructions for making Caco-2 media. Follow the same procedure to make the T84 media. Label the bottle 'T84 medium', STERILE, the date, and your initials. Store at 4°C for no longer than 3 weeks.

III. SEEDING AND MAINTENANCE PROTOCOLS FOR CACO-2 AND T84 MONOLAYERS

Seeding protocols obtained from Dr. Susan Voss (cell culture technician)

A. T84 Cells – cells seeded onto collagen-coated inserts

1. Trypsinize cells from T-162 cm^2 tissue culture flask, when cells are approximately 90% confluent (~1 week of culture).
2. Resuspend cells in 20 ml of complete medium
3. For flask culture – split 1:2
    a. Add 10 ml of cell suspension to each of 2 new culture flasks
    b. Add an additional 15-20 ml of complete medium to flasks
4. For insert culture
    a. 0.33 cm^2 insert: add 162 µl of cell suspension to each insert
    b. 4.7 cm^2 insert: add 2 ml of cell suspension to each insert
    c. Place either 1 ml (for 0.33 inserts) or 2 ml (for 4.7 inserts) of warmed complete medium in wells.

B. Caco-2 Cells – cells seeded onto collagen-coated inserts

1. Trypsinize cells from T-75 cm^2 tissue culture flask, when cells are approximately 90% confluent (~1 week of culture).
2. Resuspend cells in 10 ml of complete medium
3. For flask culture – split 1:10
    a. Add 1 ml of cell suspension to new culture flasks
    b. Add an additional 12 ml of complete medium to flasks
    c. Feed cells once a week by completely replacing spent medium with fresh
    d. Split cells 3-4 days after feeding
4. For insert culture
    a. 0.33 cm^2 insert:
        i. Dilute the 10 ml cell suspension to 20 ml
        ii. Add 80 µl of diluted cell suspension to insert
    b. 4.7 cm^2 insert:
        i. Add 150 µl of undiluted cell suspension to each insert
        ii. Bring up apical volume to 2 ml
    c. Place either 1 ml (for 0.33 inserts) or 2 ml (for 4.7 inserts) of warmed complete medium in wells.

For monolayer feeding, wait 3-4 days after initial seeding to change medium. Change medium every 48 hrs for all subsequent feedings. Use a fresh pipet for each plate of inserts to minimize potential for contamination.

IV. MONOLAYER ELECTROPORATION PROTOCOL

A. Setting Up

1. Place two 50 ml conical centrifuge tubes of DMEM into the water bath.
2. Place bottles of HBSS (+) and the non-sterile DMEM into the water bath.
3. Rack and number microcentrifuge tubes, flow test tubes, and 15 ml conical centrifuge tubes.
4. Get a tray full of ice.
5. Take ____ 6-well plates and fill each well with 2 ml of the non-sterile DMEM.
6. Make sure each plate is labeled and numbered.
7. Cover each plate with foil and place half of them on ice and the other half in the 37^{o}C oven.

B. Monolayer Electroporation

1. Washing the Monolayers – for the removal of old media and dead cells

Supplies:

- warmed HBSS(+) solution
- warmed DMEM
- 200 ml beaker
- forceps/tweezers
- small plastic container (for waste)
- 1000 ml glass beaker (for waste)

Procedure:

1. Fill the beaker about 1/3 full with warm HBSS (+).
2. Holding the filter with the tweezers, carefully aspirate the old media from the top of the monolayer and from the bottom well.
3. Gently dip the filter/monolayer into the HBSS.
4. Slowly swirl the HBSS over the monolayer and pour it out into a waste container. (Be careful with this step. If the HBSS is swirled too hard the monolayer could breakup).
5. Repeat washing twice more. (When the HBSS becomes slightly pink, pour it into the waste container and replace it with fresh solution.)
6. Pipet 2 ml of the warm DMEM into the bottom well.
7. Place the filter back into the well. Be careful not to create any air bubbles around the filter. (If air bubbles do form, use the fine tip transfer pipet to remove them.)
8. Gently place 2 ml of the warm DMEM on top of the monolayer. (Again be careful not to breakup the monolayer).
9. Repeat steps 2 through 7 for each monolayer.
10. Put the plates back into the 37^{o}C oven.

2. TEER Measurements – to check monolayer integrity.

Voltage Clamp System – see first lab notebook

Millicell ERS – Test the Millicell apparatus using the 'Test' button and make sure the readout is 1000 and 1.00 for the 2000Ω and 2kΩ settings, respectively. Measure the resistance of a small amount of media in a 50 ml conical tube and make sure it reads around 12Ω. To measure the resistance of the monolayers, insert the chopstick electrodes into each of the three access ports located around the insert. Average the readings and subtract the resistance value for a cell-free insert. Multiply this value by the area of the insert (4.7 cm^2) to obtain the TEER for the monolayer.

3. Monolayer Preparation – for electroporation

From this point forward, the monolayers have to be kept in the same order.

Supplies:

- non-sterile DMEM
- 1 mM calcein stock solution
- HBSS (+)
- InSitu™ adherent cell electroporation chamber

Procedure:

1. Take a filter with tweezers and pour off the DMEM.
2. Aspirate any remaining DMEM off the monolayer and the bottom of the filter.
3. For Costar filters: Place 1.35 ml (1350 µl) of DMEM and 0.15 ml (150 µl) of calcein on top of the monolayer.
4. For Millipore filters: Place 2.25 ml (2250 µl) of DMEM and 0.25 ml (250 µl) of calcein on top of the monolayer.
5. Cover the plate with foil and allow the cells to incubate in calcein for about 3 minutes.
6. Meanwhile, place the bottom electrode of the cuvette into the InSitu electroporation chamber and put 3 ml of DMEM into it.
7. Take the filter with the monolayer in calcein and put it into the bottom electrode. (Don't make any air bubbles)
8. Place upper electrode of the cuvette on top of the monolayer. Make sure the upper electrode is in contact with the media.
9. Close the chamber.

4. Electroporation – to introduce calcein or BSA into the cells

Equipment:

- BTX exponential-decay electroporator
- HP 10:1 voltage probe
- HP54602B oscilloscope

Procedure:

1. Connect the BTX pulser, oscilloscope, and, if necessary, the current monitor as illustrated in the Figure on the next page.
2. Set the voltage, capacitance, and resistance electroporation conditions on the BTX machine.
3. Set up the oscilloscope for the desired voltage and pulse length.
4. Pulse the cells.
5. Record the peak voltage and pulse length values from the oscilloscope. (If you can't get a reading from the oscilloscope, take these values from the BTX machine and make a note of it.)
6. Place electroporated filter in the plate of warm media in the 37^{o}C oven. (This helps the pores to reseal.)
7. Record the time.
8. Pour the 3 ml of DMEM in the bottom electrode into the waste container. Rinse the bottom electrode with HBSS and dry it with a Kimwipe.
9. Repeat the above for each monolayer.

NOTE: When finished electroporating, put trypsin in the 37^{o}C water bath and make sure you have one or two 50 ml conical tubes of DMEM complete on hand.

5. Washing the Monolayers – to remove excess calcein

Supplies:

- cold HBSS (+) solution

Procedure:

1. Dip the filter into cold HBSS (+) to rinse off calcein and pour it into the waste container.
2. Check the monolayer after each dipping to make sure none of the cells have started to lift off. If cells begin to lift off, stop washing.
3. Repeat the washing step about 5 times for each monolayer or until cells start lifting off.
4. Remove any excess HBSS (+) using a fine tip transfer pipet.

Schematic Drawing of Electroporation Equipment Setup

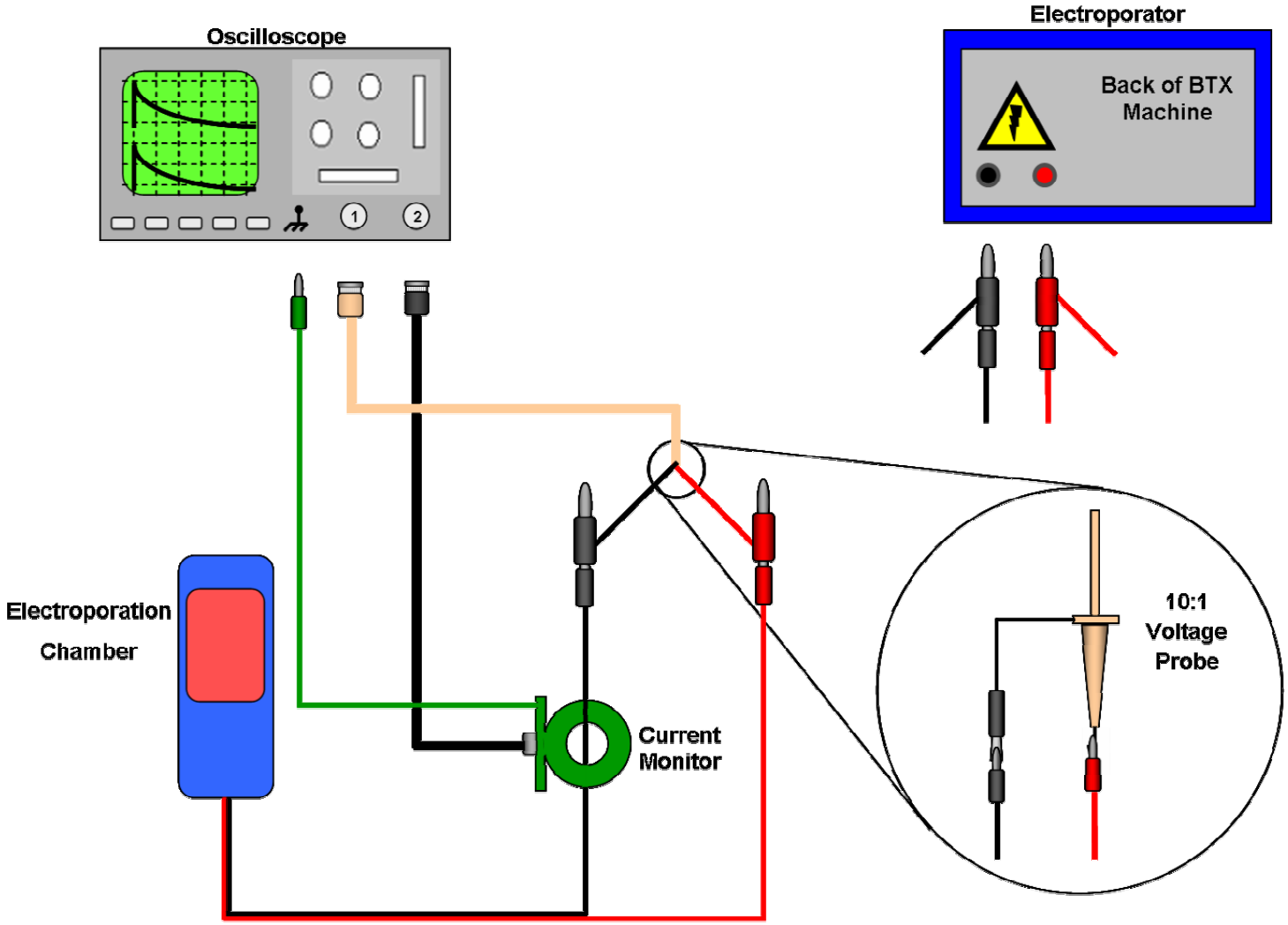

C. Dissociation of Monolayers for Flow Cytometry Analysis

1. Trypsinization – to lift the cells off the filter membranes

Supplies:

- Warm (37^{o}C) trypsin (to break up monolayer and lift off cells)
- Complete medium w/ serum (to inactivate the trypsin)

Procedure:

1. Add 1 ml of warm trypsin to each filter and put plate into the 37^{o}C oven (trypsin is most active at this temperature).
2. NOTE: if most of the cells lift off at this point, add 3 ml of DMEM complete.
3. Wait 5 minutes.
4. Take a fine tip transfer pipet and gently squirt the trypsin onto the monolayer to check if any cells are lifting off.
5. If most of the cells lift off then quickly add 3 ml of DMEM complete.
6. If most of the cells are still adherent, put the filter back into the 37oC oven for another 5 minutes.
7. Repeat as necessary.
8. For the monolayers that have been lifted off, use transfer pipets to remove the media + trypsin + cells and put them into their corresponding 15 ml centrifuge tube. Use a different pipet for each filter.
9. Keep the tubes on ice.
10. Take the centrifuge tubes to the large centrifuge and spin them down at 4^{o}C and 3200 rpm for 6 minutes.
11. While the cells are spinning, put ice in the tray holding the microcentrifuge tubes and flow test tubes.
12. When the cells are finished spinning, check for a pellet and then put the tubes back on ice.

2. Washing Cell Suspensions – to resuspend the cell suspensions in clear PBS.

Supplies:

- Cold PBS (w/o Ca^{2+} and Mg^{2+})

Procedure:

1. Pour the supernatant in the centrifuge tubes into the waste container. Remove any excess supernatant.
2. Add 1 ml of cold PBS to each tube.
3. Gently pipet up and down to break up the cell pellet and put the resuspended cells into their corresponding microcentrifuge tube. Use a different pipet tip for each sample.
4. Spin the microcentrifuge tubes down in the Eppendorf microcentrifuge for 3 minutes at 3200 rpm.

5. Check for pellet.
6. Pour off PBS supernatant.
7. Add 0.5 ml of cold PBS.
8. Pipet up and down with transfer pipet.
9. Spin the cells down again at the same settings.
10. During the spinning down steps, put 5 µL of propidium iodide and 50 µL of well-vortexed microsphere solution into each flow test tube.
11. Repeat steps 5 through 9 three more times.
12. Pour off PBS.
13. Use transfer pipet to remove all remaining PBS (be careful of the pellet).
14. Add exactly 0.5 ml of PBS and thoroughly resuspend the pellet into single cells.
15. Transfer the cells to the flow test tubes.
16. Keep the test tubes on ice.
17. The cells are now ready for flow cytometry.

V. ANALYSIS OF SAMPLES USING THE BD LSR FLOW CYTOMETER

1. Check sheath fluid tank and waste tank.
    a. Sheath fluid tank - release vacuum to open; Fill to rim if level is low.
    b. Waste tank - Empty if more than half full and add 400 ml of bleach

2. Turn on power strip behind monitors and computer.

3. Allow computer to boot and bypass the login prompt.

4. Turn on the cytometer. If first user, allow cytometer to warm-up for 30-45 minutes.

5. Make sure to do the following before running samples:
    a. Purge cytometer with bleach
    b. Set cytometer to Run and run bleach on Hi for 5 minutes.
    c. After running bleach, Run water for 5 minutes.

6. Briefly vortex each sample before running

7. Open "DigiFACS" software and stretch to fill screen.

8. Double click to open the "Esi-Caco2" experiment. This may take a little while. The last run experiment and data will open on the screen.

9. Click "Worksheet" on the menu bar and choose "New Worksheet".

10. Click inside the empty space of the new worksheet and go to the new panel on the far right. Do the following:
    a. Rename the worksheet with today's date - (mmddyy)
    b. Put today's date in the "data collected" field - (mmddyy)
    c. Set number of horizontal pages to 2
    d. Check show page breaks and page number

11. Go back to the experiment list on the far left panel, right-click "Esi-Caco2", and choose "New Specimen".

12. Click on the new specimen ("Specimen_001 ") and rename it with today's date in the "Collected" field on far right panel. - (mmddyy)

13. Delete the "Tube_001" that has been created automatically in the specimen folder.

14. Open a previous specimen folder using similar conditions to the current experiment, right-lick on "Tube_001" of that experiment, and copy the tube.

15. Re-open today's specimen folder, right-click the folder, and select "Paste" to insert the tube information. This will bring up blank plots already set up with gates as well as stat boxes. The following plots should be showing:

Plot #1 – SSC vs. FSC (w/ P1 = cells)
Plot #2 – PerCP vs. FSC (gated on P1, regions P2 = viable and P3 = dead)
Plot #3 – PE vs. FSC (gated on P1)
Plot #4 – FITC vs. FSC (region P4 = beads)
Plot #5 – Histogram of FITC (gated on P2)

16. Make sure the small arrow next to the new tube is green so that the new data will be saved here.

17. Check the Acquisition Rules under the Acquisition Tab and specify the following:
    a. # Events = 20,000
    b. Stopping: P2
    c. Storage: All Events

18. Use the following commands to perform the following actions while running samples:
    a. To run sample without saving: click Acquire
    b. To run sample and save data: click Acquire then Record
    c. To restart collection while acquiring: click Restart
    d. To stop collection: click Acquire again

19. When sample has finished collecting, click "Next" to create a new tube and set up system for the next sample.

20. After running all samples:
    a. Run bleach for 5 minutes
    b. Run water for 5 minutes
    c. Set cytometer to Standby

21. To save Data:
    a. Select today's specimen
    b. Select File, then Export
    c. Specify FACS 2.0 and click Next
    d. Specify export location (D:\export) and click details to make sure all tubes were exported

22. To Shutdown cytometer:
    a. Close DigiFACS Software
    b. Shutdown computer
    c. Turn off cytometer
    d. Turn off power supply

NOTE: These instructions were used for the original DigiFACS software. The system has since been upgraded. See Johnafel Crowe for instruction on how to use the new software.

VI. ANALYSIS OF FLOW CYTOMETRY DATA WITH WINMDI SOFTWARE

1. Double click on 'WinMDI 2.8' icon.
2. Select Density Plot and then click OK
3. Go to folder where flow data is located (I name folders by date and individual flow files either by date or Tube #)
4. Open flow file with extension *.001 (e.g., MMDDYY.001 or Tube.001)
5. Set the X-axis to 'FSC-H' and the Y-axis to 'SSC-H'. **PLOT A**
6. Change 'Smooth' to 2, uncheck 'Calculate Colors' and Click OK
7. Select 'Display' from the menu at the top, then select 'Density Plot'.
8. Select the first flow file in the group again.
9. Set X-axis to FSC-H and Y-axis to FL3 (PerCP channel) and Click OK. **PLOT B** (NOTE: can also use FL2 (PE channel)
10. Select Display-Density Plot
11. Select the first flow file in the group again.
12. Set the X-axis to FL1-H and the Y-axis to FL3. **PLOT C**
13. Activate SSC-FSC graph (click on)
14. Click left mouse button-Regions
15. Create R1
16. Click buttons to create region R1 (as shown below)
17. Click left mouse button-Regions
18. Create R2 (as shown below)

The graph should look like the plot A located below on the left.

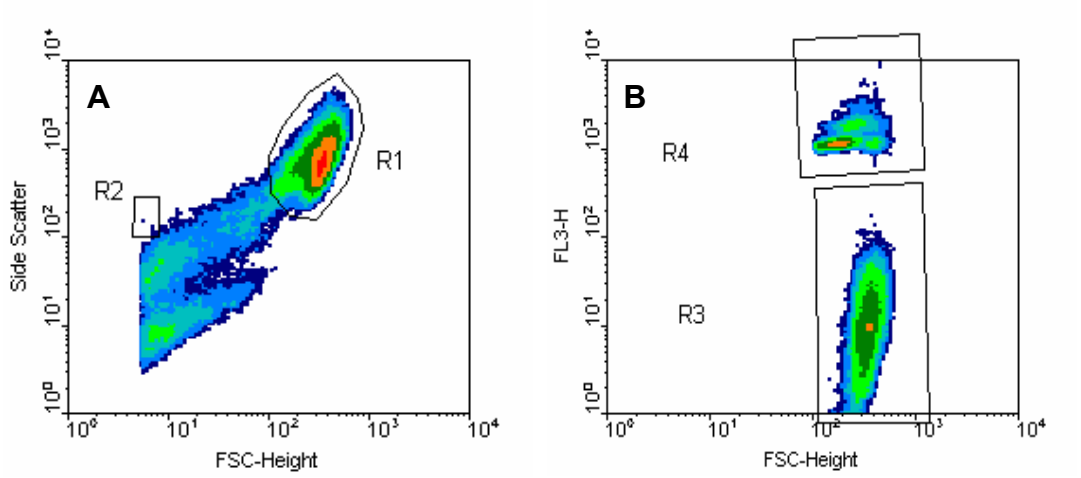

19. Click on the line in the upper right hand corner of box to minimize
20. Activate FL3-FSC graph (click on)
21. Click Left Mouse button-Gates, set R1 to OR [+]
22. Click left mouse button-Regions
23. Create R3 (as shown below)
24. Click buttons to define region R3
25. Click left mouse button-Regions
26. Create R4 (as shown below)
27. Click buttons to define region R4 (graph should look like the plot on the above right).)

28. Click left mouse button-'Stats' on PLOT #2; Format box so the following columns are showing (not necessarily the same numbers):

File: **.001
Sample ID:
Gated Events 9294
FSC-Height (1) vs FL3-H (5)

Region	X-Mean	Y-Mean	Events	
R0	404.5	246.7	9294	
R1	404.5	556.5	9294	
R2	0.0	0.0	0	
R3	412.9	15.9	8147	**[No. of viable cells]**
R4	338.9	1956.3	1080	**[No. of dead cells]**

29. Click on the line in the upper right hand corner of graph to minimize.
30. Activate Plot #3, the FL3 vs. FL1 graph (click on)
31. Click Left Mouse button-Gates, set R2 to OR [+]
32. Click left mouse button-Regions
33. Create R5 (as shown below)
34. Click buttons to define region R5

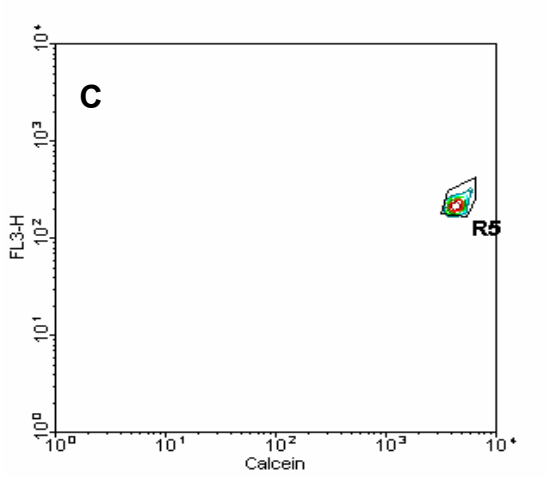

The graph should look like this one. If there appear to be no beads, ALT-PAGE DOWN to a sample that does have beads and make a gate around that. Then ALT-PAGE UP to the original sample.

35. Click left mouse button-Stats; Format box so the following is showing:

File: 072299.001
Sample ID:
Gated Events 9294
FL1-Height (1) vs FL3-H (5)

Region	X-Mean	Y-Mean	Events	
R0	404.5	246.7	9294	
R1	404.5	556.5	9294	
R2	0.0	0.0	0	
R3	412.9	15.9	0	
R4	338.9	1956.3	10	
R5	222.3	222.1	3333	**[No. of beads]**

36. Click on the line in the upper right hand corner of graph box to minimize
You should now have only two text boxes open and three graphs minimized

37. Select the 'Display' function from the menu, then select 'Histogram'.
38. Open (***.001), the first flow file of the group.
39. Change the read parameter to FL1 and Click Read
40. Click/Drag on corner of box to make bigger
41. Click left mouse button-Gates, gate on R1 and R3 by clicking AND [*] for both
42. Click OK
43. Click left mouse button-Stats (Click Format button and make sure % GATED, MARKERS, EVENTS, MEAN/CV, MEDIAN are checked.)
44. Click left mouse button-Marker
45. Set Marker 1 from 1-1023, click OK
46. Set Marker 2 from 1 to a number that makes the % gated value for M3 equal 97% of the percent gated value in M1.

You are now ready to begin collecting data; write down the values in a table

47. Record total EVENTS for R3 (Viable) and R4 (Dead) from the FL3 vs. FSC plot stats
48. Record total EVENTS for R5 (Beads) from the FL1vs. FL3 plot stats
49. Record total %GATED, MEDIAN, MEAN, CV from M3 from the FL1 histogram stats
50. For each new sample (ALT-PG DOWN), adjust M3 such that the value is 97% of that in M1

**Once finished, need to obtain data from calibration beads (usually the last sample in the group) **

51. Open new copy of the WinMDI Flow Cytometry Program.
52. Create Density Plot (Y-axis = FL1; X-axis = FSC)
53. Left mouse button-Region
54. Define Region 1 as follows below so that all four bead populations are included.

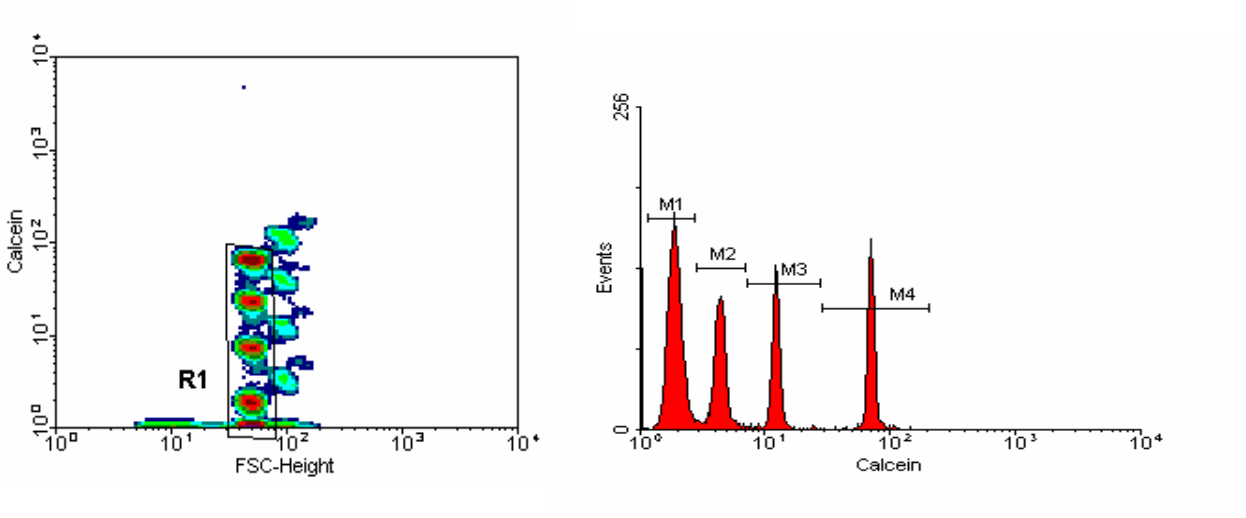

55. Display-Histogram (FL1)
50. Gate on R1 [+]
51. Create Markers around each peak
52. Record the last number in each row (***see example below***)

File: ****.015
Sample ID:
Gates: +R6
Gated Events: 14468

Param name	M	Low,High	Events	%Total	%Gated	Mean	CV	Peak,Value
Calcein	0	0,1023	14468	80.80	100.00	14.53	1507.08	2685,1
	1	19, 118	4851	27.09	33.53	1.94	3721.02	173,1.91095
	2	118, 218	2676	14.94	18.50	4.45	3626.40	107,4.41094
	3	222, 372	2014	11.25	13.92	12.56	2134.91	131,12.2983
	4	375, 594	2220	12.40	15.34	72.04	559.17	152,70.4136

Now you are ready to enter values into the spreadsheet
**Save all values, R3, R4, R5 for each sample, Marker 3 - Median, Mean, CV for each sample and MESF calibration bead values in a separate spreadsheet **

53. Don't forget to save and exit!!!!

VII. MOLECULAR BIOLOGY PROTCOLS

A. IL-8 ELISA – Protocol was obtained from Dr. Lauren Collier-Hyams in Dr. Neish's Lab. It has been modified to show more detail.

Supplies:

- Hanks Balanced Saline Solution (HBSS) – w/ calcium and magnesium
- 0.1 M $NaHCO_3$ (pH 9.6)
- 10X Wash Buffer – 25 ml aliquots stored at -70°C
  (5% Goat Serum + 1% Tween-20 in HBSS or PBS)
- 96-well plates w/ covers (Linbro®/Titertek®, ICN Pharmaceuticals, Aurora, OH)
- Antibodies:
  - Anti-human IL-8 capture antibody (R&D Systems)
  - Anti-human IL-8 antibody from rabbit (Endogen)
  - Peroxidase-labeled anti-rabbit antibody (KPL)
- TMB Microwell Peroxidase Substrate (KPL)
- Recombinant human IL-8 protein standard (R&D Systems)

Dilution Scheme for IL-8 Standards (Conc. Ranging from 0.0195 to 20 ng/ml):
Standards made by 10 serial dilutions (in the same buffer as the samples) of a 20 ng/ml solution of IL-8. 20 ng/ml solution is made by diluting 2 µL of 10 µg/ml IL-8 stock in 1 ml of buffer.

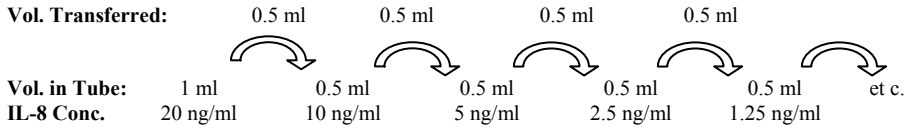

Procedure:

1. Coat 96-well plate with 100 µL R&D Systems anti-human IL-8 capture antibody. Dissolve 40 µL aliquot of antibody in 5 ml of bicarbonate buffer (need 10 ml for a whole plate) for a final concentration of 8 µg/ml. Cover plate and incubate overnight at 4°C.
2. Pour off capture antibody solution. Wash plate 4 times with wash buffer. Pat overturned plate on a stack of paper towel to remove excess liquid.
3. Add IL-8 containing samples and standards (100 µL per well) and incubate plate 1 hour at 37°C to allow IL-8 to bind capture antibody. Do two replicates of standards.
4. Pour off samples and standards. Wash plate 4 times with wash buffer.
5. Add Endogen anti-human IL-8 antibody (100 µL per well) to sandwich bound IL-8. Dissolve 40 µL aliquot in 5 ml of wash buffer (need 10 ml for whole plate). Incubate plate 1 hour at 37°C.
6. Pour off Endogen antibody. Wash plate 4 times with wash buffer.
7. Add peroxidase-conjugated anti-rabbit antibody (100 µL per well) to bind the primary antibody and allow detection of IL-8. Dilute the antibody 1:7000 in wash buffer (1.43 µL in 10 ml). Incubate plate 1 hour at 37°C.
8. Pour off detecting antibody. Wash plate 4 times with wash buffer.
9. Add KPL peroxidase substrate (100 µL per well). Gently shake plate and wait 5 - 10 min to allow color develop.
10. Read plate on absorbance spectrophotometer at wavelength of 650 nm.

B. Plasmid Amplification and Purification[5] – Protocols written up by Amelia Tomlinson of Dr. Neish's Laboratory. More detail has been added when necessary.

The following series of steps should be taken whenever any new plasmid is prepared or received. Though many little steps are involved, you will save yourself a great amount of time and effort in the long run. Detailed protocols for each of these steps follow.

1. Transform bacteria with your new plasmid.

2. Streak out a single colony of the bacteria on an agar plate with the appropriate antibiotic(s) for selection of plasmid-carrying bacteria.

3. Grow a small culture of the plasmid-carrying bacteria from a single colony, in media with the appropriate antibiotic(s). Make a small preparation (mini- or midi-prep) of the plasmid.

4. Conduct the appropriate restriction digests for your plasmid.

5. Assess the plasmid construction by agarose gel electrophoresis.

6. If plasmid is properly constructed, store the remaining sample at -20°C. Never use this aliquot for transfections, etc. It should be saved as a "sacred" stock to be used ONLY for future transformations, in the unfortunate scenario that they may be necessary.

7. Making a larger batch of plasmid for use in transfection experiments.
   a) Grow a large culture of bacteria and make a large-scale prep of the plasmid.
   b) Check this batch of plasmid by digest and electrophoresis.
   c) Quantify yield by spectrophotometry. This batch will serve as your working stock.
   d) Store at -20°C.

8. Make a glycerol stock of the transformed bacteria, and store at -80°C. Future cultures of the bacteria for plasmid preparations may be started directly from these frozen stocks.

[5] Many of the protocols in this section can be found in the popular protocol book, Molecular Cloning: A Laboratory Manual (2001), by Sambrook, Fritsch and Maniatis.

1. Bacterial Transformation

Bacterial transformations should be conducted according to the manufacturer's protocol. We've had good results with commercially available E. coli bacterial strains such as: Stratagene's *XL1-Blue Subcloning Grade Competent* (catalog# 200130) or *SoloPack™ Gold SuperCompetent* (catalog# 230350-41) *Cells* and Invitrogen's *Subcloning Efficiency* (catalog# 18265-017) or *MAX Efficiency* (catalog# 18258-012) *DH5α Competent Cells*.

1. You can transform as little as 0.5 µl of pure plasmid DNA into 50 µl of competent cells. (I usually transformed 1 to 3 ng of DNA into cells.) There is no need to use more than 50 µl cells per transformation unless the plasmid concentration is extremely low (>0.001 µg/µl). Include a tube of cells with no plasmid DNA as a control.

2. The next steps should be performed under a Bunsen burner to maintain sterility.

3. When spreading the transformed cells, dilute the cells 1:10 in 150 µl of LB (recipe below), which was placed in the center of a pre-warmed LB-agar plate containing the appropriate selective antibiotic (the manufacturer will provide information about the antibiotic concentration). The cells should be spread with a sterilized metal spreader, until the liquid is absorbed.

4. Cover the plates and incubate them agar side up (to prevent condensation on the agar) overnight at 37°C. The plate with the transformed cells should have several colonies of bacteria, while the control plate should be colony-free because of the lack of resistance to the selective antibiotic. Plates should only incubate O/N up to ~24 hrs or they will begin to overgrow and the colonies will no longer be isolated. Seal the plates with parafilm and store at 4°C until needed.

Luria-Bertani Broth Recipe
Manuf.: EM Science
Cat.#: 1.00547.0500
Composition: 10g/L peptone for casein
5 g/L yeast extract
5 g/L sodium chloride

Preparation:
a. Suspend 20 g of LB powder in 1 L (1000 ml) of purified water. Adjust the amount of powder and volume of water as necessary.
b. Autoclave (15 min @ 121°C)
c. Broth will be clear and yellowish.

2. Streaking Out a Single Colony of Bacteria

After transforming bacteria and spreading on the appropriate plates, you will hopefully yield isolated colonies of bacteria. It is important to streak a single colony of bacteria onto a fresh plate, in order to have a pure culture from which to start cultures for purification of plasmid DNA.

1. A single colony from the plate of transformed bacteria should be "picked" using a flame sterilized platinum wire loop or a sterile toothpick.
2. Streak the bacteria on a new pre-warmed LB + selective antibiotic agar plate.
3. Incubate the plate at 37°C overnight.
4. Seal plate with parafilm and store at 4°C until needed.

3. Small Plasmid Prep to Check Transformation

Pick another colony to inoculate 5 ml of liquid LB + selective antibiotics. Incubate the cells in a 37°C shaker (~250 rpm) (Innova™ 4430, New Brunswick Scientific, Edison, NJ) for 8 hours or overnight to allow the bacteria to grow. This liquid culture will be used to isolate a small amount of plasmid to check that the transformation was successful. The Qiaprep Spin Miniprep Kit (Qiagen, Valencia, CA), which has an expected yield of 20 μg of plasmid, works well for isolation and purification of the plasmid. Just follow the manufacturer's instructions.

4. Restriction Digests of Plasmids

Digests (or cutting) of the plasmids are performed to confirm the construction of your plasmid. Digests are performed using restriction enzymes, which cut at specific locations in the plasmid DNA sequence. The sites of restriction must be identified using the plasmid map, which can be obtained from the manufacturer.

1. Choose 1 or 2 enzymes that will cleave the plasmid to yield 2-3 detectable size fragments (>500 bp). If you choose 2 enzymes, set up 3 digests – 1 with each enzyme separately and 1 with both enzymes. Try to use common cheap enzymes for this purpose (EcoRI, HindIII, SalI, PstI, BglII, KpnI, etc.). Remove enzymes just before you are about to use them. Since, the enzymes are easily denatured at room temperature, keep them cold while they are out of the freezer.

2. The restriction buffer you use will depend on the enzymes you choose. Check the catalog of the company that made your enzymes, to determine which buffers to use with certain enzymes. This is especially important when performing double enzyme digests.

3. Digest reactions are usually set up in the following manner.

   Reaction: xx µl ddH2O
   x µl plasmid DNA
   x µl 10X restriction buffer
   x µl enzyme 1
   x µl enzyme 2 (if necessary)
   xx µl total volume

   Typically, only 1 or 2 µg of DNA is digested with 1 µl of each enzyme. The volume of restriction buffer should be 10-fold less than the total volume. Use the water to bring up the reaction volume. The total reaction volume can range from 25 µl – 50 µl. Add all reagents in the order listed and mix by flicking the tubes. Spin down in a centrifuge to get all liquid in the bottom of the tube.

4. Allow reactions to digest for 2-3 hrs in a water bath at the appropriate temperature (usually 37°C) in a foam/plastic floater. Make sure to check what temperature the enzyme works best at by looking in a New England Biolabs or Promega catalog. A given enzyme will always function at the same temperature and in the same buffer, no matter what company it was purchased from.

For more information about performing restriction digests, check the manufacturer's catalog or website. New England Biolabs has a particularly good website.

5. Agarose Gel Electrophoresis

Sourced from Chapter 6 of: Molecular Cloning: A Laboratory Manual, Sambrook, Fritsch and Maniatis, 1989.

Solutions:

50X TAE Stock Solution
121 g Tris Base
28.55 ml glacial acetic acid
50 ml 0.5M EDTA, pH 8.0

Dissolve tris base in just under 400 ml mqH_2O. Add glacial acetic acid and EDTA solution. Bring to a final volume of 500 ml.

0.5M EDTA, pH 8.0
Dissolve 9.3 g EDTA in nearly 500 ml mqH_2O. Adjust pH to 8.0 with NaOH pellets. Bring volume to 500 ml.

Preparation of 1% Agarose/TAE Gel

Agarose gels are used to separate DNA (and RNA) fragments, so that information about the size and construction of the molecule can be obtained.

For small gel apparatus (Easy-Cast Electrophoresis System #B1A, Owl Scientific, Portsmouth, NH)
0.5 g agarose
50 ml 1X TAE
2 µl - 5 µl ethidium bromide

1. Melt agarose in TAE in microwave for 30 s in 250 ml glass Erlenmeyer flask. Swirl flask to mix. Microwave in additional 10 sec increments until agarose is completely melted. Swirl between each heating period. **Do not** allow solution to boil over.

2. Let agarose solution cool on bench until it is warm to the touch. Add ethidium bromide, a DNA dye that fluoresces under UV light, and pour into gel caster. Immediately pull any bubble to the side of the gel using a fine pipet tip.

3. Gel takes ~45 min. to set. Place gel and caster in electrophoresis chamber (gel box) and pour TAE buffer until gel is just covered (~1 mm above gel).

Preparation of DNA Samples for Agarose Gel

1. Start with approximately 100-500 ng DNA. I usually took 10 µl of solution from the restriction digest reactions. If checking plasmid directly from a plasmid prep, take appropriate amount of plasmid and dilute to 10 µl with mgH_2O.
2. Add 2 µl 6X gel loading dye (Blue/Orange Loading Dye, Promega).
3. Mix well.

Running the Gel

1. Load 10 µl of your samples per lane.
2. Load ~10 µl of a 1 kb DNA ladder (New England BioLabs) containing DNA standard fragments of known size (1 kb ladder or Lambda/HindIII ladder should be fine for most purposes; use 100 bp ladder only when looking at very small fragments <400 bp)
3. Run gel at a constant 90 volts (PowerPac 300, Bio-Rad, Hercules, CA) using 1X TAE as the running buffer.
4. After the gel finishes running (orange dye front is ¾ of the way to the end of the gel) turn off power to the gel box.
5. Remove the gel on the tray from the apparatus and check it on a UV light box (Transilluminator, VWR Scientific, West Chester, PA) to make sure there is enough separation between the fragments.

6. I photographed the gel using the AlphaImager™ 2200 Documentation and Analysis System (Alpha Innotech Corp., San Leandro, CA).
7. If there are unused lanes, return gel on tray to buffer tank for use later (1-2 days) and secure lid so that the buffer does not evaporate

6. Sacred Stock of Plasmid

If plasmid is properly constructed, store the remaining sample at -20°C. Never use this aliquot for transfections, etc. It should be saved as a "sacred" stock to be used ONLY for future transformations, in the unfortunate scenario that they may be necessary.

7. Purification of Larger Batches of Plasmid

a. Large-Scale Plasmid Prep

Depending on the amount of plasmid needed, different commercially available plasmid purifications kits were used.

- QIAGEN or QIAfilter Endofree Giga Prep Kit (yield: 10 mg from 2.5 L bacterial culture)

- QIAGEN or QIAfilter Endofree Mega Prep Kit (yield: 2.5 mg from 500 ml bacterial culture)

- Promega Wizard ® Plus Midipreps Kit (yield: 200 µg from 100 ml bacterial culture)

Note 1: The non-endofree versions of the QIAGEN kits can also be used.
Note 2: I usually performed two Wizard Midipreps and combined the plasmid solutions after purification.

i. For each kit, inoculate a starter culture of 10 ml LB + selective antibiotic with a single bacterial colony from the most recent agar plate made.

ii. Allow the cells to grow in a 37°C shaker (~250 rpm) for ~8 hrs and then dilute the culture as indicated by the manufacturer's instructions into the appropriate volume of LB with selective antibiotics.

iii. Remember to read the instructions, warnings, and tips before beginning this part of the protocol – there are multiple steps where you have additional options to consider that may increase your DNA yield or purity.

b. Check Plasmid Prep

Repeat steps 4 and 5 with a sample of your large-scale prep. If you have any lanes left over from the gel used 1-2 days ago, you may use them here.

c. Quantify Plasmid by Spectrophotometry

The concentration of the purified plasmid can be determined by UV spectrophotometery. At a wavelength of 260 nm, 50 μg/ml of double stranded DNA has an optical density of 1.0. The concentration of the plasmid can be calculated based on this relationship. By taking the ratio of the optical density at 260 nm to that at 280 nm, an indication of the purity of the plasmid solution can be obtained. Pure DNA solutions have ratios approximately equal to 1.8 (ratios between 1.8 and 2.0 are acceptable). A ratio less than 1.8 or greater than 2.0 indicates the presence of contaminating impurities and requires the re-precipitation of the DNA (see Step 9).

i. Turn on spectrophotometer, select dsDNA program (or manually set λ=260), and allow UV light to warm up.

ii. Put 1 ml ddH2O in a quartz cuvette, place in the spec, and blank the machine against it. (If your DNA is suspended in TE buffer, then use that to blank the machine).

iii. If frozen, thaw DNA sample to be tested on ice.

iv. Dilute 1 – 5 μl DNA solution into a quartz cuvette containing 1 ml ddH2O.

v. Cover the top of the cuvette with parafilm and invert to mix.

vi. Place the cuvette into the spec, making sure to orient the cuvette such that the light beam will pass through the clear windows of the cuvette.

vii. Close the spec lid and record the readings at $\lambda = 260$ nm and at $\lambda = 280$ nm.

viii. If you have enough sample, repeat steps iv – vii twice more and average the readings.

ix. Take the average A_{260} reading and multiply it by 50 to obtain the concentration in μg/ml. Then multiply by the appropriate dilution factor (e.g., 1000 for 1 μl DNA; 200 for 5 μl DNA) to obtain the final concentration.

x. Take the ratio A_{260}/A_{280} to determine the purity of the DNA sample.

8. Preparation of Glycerol Stocks of Bacteria

Frozen stocks of bacterial culture should be maintained for use in future plasmid purifications. All steps should be carried out in media containing the appropriate antibiotics.

1. Inoculate a 10 ml volume of LB with a single colony for overnight growth in a 37°C shaker.

2. From the resulting stationary phase culture, subculture 0.5 ml into 2.0 ml LB.

3. Grow in shaker-incubator for 2 to 3 hours, until culture is at mid-log phase of growth.

4. To resulting 2.5 ml culture, add 0.5 ml 50% glycerol (filter-sterilized). Make 3 X 1 ml aliquots and freeze at -80°C. Glycerol is toxic to the bacteria, but necessary for freezing. Therefore, freeze aliquots as quickly as possible after addition of glycerol to reduce bacterial death.

Only a small amount of the glycerol stock needs to be inoculated onto a plate or into liquid media. Therefore, glycerol stocks may be conserved by scraping the frozen stock with a sterile loop or wooden stick, without allowing the stock to thaw, and inoculating LB or streaking on a plate. Alternatively, if stock does not need to preserved, thaw and spread the solution onto a plate containing appropriate antibiotics.

9. DNA Precipitation and Resuspension

If your DNA concentration is low after the large scale plasmid prep or if your solution has impurities, it is possible to re-precipitate the DNA with isopropanol and then resuspend it.

1. Add 1 ml isopropanol to <600 µL DNA (if > 600 µl, split into 2 tubes) and mix until white threads are visible. Can also add 0.7 volume of isopropanol to DNA solution.

2. Spin 10 minutes at highest speed (13,000 rpm) in benchtop centrifuge at room temperature. Carefully pour off isopropanol.

3. Wash pellet once with 0.5 ml 70% EtOH. Add EtOH to tube containing pellet and vortex – do not pipet (which will shear your plasmid DNA).

4. Spin 5 minutes as in step 2. Carefully pour off EtOH.

5. Drain excess EtOH from tube by inverting onto a paper towel.

6. Dry pellet in heat block or incubator at ~37°C for 5 minutes or less.

7. Suspend pellet in desired volume Elution buffer (if using Qiagen prep), dH2O, or TE buffer. Add to tube then vortex and heat at 40-50°C to get the DNA into solution.

C. Plasmid Information and Restriction Digests – for plasmids that I isolated and/or purified myself.

1. pEGFP-N1

Use: GFP expression vector
Source: Clontech
Map: available from manufacturer
Competent Cell Line: MAX® Efficiency DH5α Competent Cells (Invitrogen)
Antibiotic Selection: kanamycin (30 µg/ml)
Restriction Enzyme(s): XhoI and NotI (yield 2 fragments)
Example Restriction Digest (note Buffer type):

	Uncut	Cut
ddH_2O	25 µl	23 µl
pEGFP-N1 (~1.5 µg)	2 µl	2 µl
Buffer 3	3 µl	3 µl
XhoI	---	1 µl
NotI	---	1 µl
Total Volume	30 µl	30 µl

Let run for 2-3 hours at 37°C.

2. pGL3-control

Use: luciferase expression vector
Source: Promega
Map: available from manufacturer
Competent Cell Line: MAX® Efficiency DH5α Competent Cells (Invitrogen)
Antibiotic Selection: ampicillin (100 µg/ml)
Restriction Enzymes: XhoI and BamH I (yield 2 fragments)
Example Restriction Digest (note Buffer type):

	Uncut	Cut
ddH_2O	24 µl	22 µl
pGL3 (~1.5 µg)	3 µl	3 µl
Buffer 2	3 µl	3 µl
XhoI	---	1 µl
BamH I	---	1 µl
Total Volume	30 µl	30 µl

Let run for 2-3 hours at 37°C.

3. pIκB-HA

Use: HA-tagged IκBα expression vector
Source: Neish Laboratory
Map: not available
Competent Cell Line: SoloPack™ Gold Supercompetent Cells (Stratagene)
Antibiotic Selection: ampicillin (100 µg/ml)
Restriction Enzymes: SmaI and BglII (yield 2 fragments)
Example Restriction Digest: since both enzymes were not 100% active in a single buffer, the digest had to be carried out in two parts.

Digest #1:

	Uncut	Cut
ddH_2O	39 µl	37 µl
pIkB-HA (~2 µg)	6 µl	6 µl
Buffer 4	5 µl	5 µl
SmaI	---	2 µl
Total Volume	50 µl	50 µl

Let run overnight at 25°C

Digest #2:

	Cut
Cut Digest #1	25 µl
ddH_2O	10 µl
Buffer 3	4 µl
BglII	1 µl
Total Volume	50 µl

Let run for 2-3 hours at 37°C.

4. pIL8-CAT

Use: CAT expression vector with IL-8 promoter
Source: Neish Laboratory
Map: not available
Competent Cell Line: probably DH5α
Antibiotic Selection: ampicillin (100µg/ml)
Restriction Enzymes: XhoI and BamH I (yield 2 fragments)
Restriction Digest:

	Uncut	Cut
ddH_2O	21.5µl	19.5 µl
pIL8-CAT (~1.5 µg)	1 µl	1 µl
Buffer 2	2.5 µl	2.5 µl
XhoI	---	1 µl
BamH I	---	1 µl
Total Volume	25 µl	25 µl

Let run 2 hours at 37°C.

5. pNFκB-Luc

Use: luciferase expression vector with NFκB promoter
Source: Stratagene
Map: available from manufacturer
Competent Cell Line: MAX® Efficiency DH5α Competent Cells (Invitrogen)
Antibiotic Selection: ampicillin (100µg/ml)
Restriction Enzymes: (yields ?? fragments)
Restriction Digest:

	Uncut	Cut
ddH_2O	44 µl	42 µl
pNFκB-Luc (~1.5 µg)	1 µl	1 µl
Buffer 4	5 µl	5 µl
Eco0109I	---	2 µl
Total Volume	50 µl	50 µl

Let run for 2 hours at 37°C

6. pCMV-Luc

Use: luciferase expression vector
Source: Neish laboratory
Map: not available
Competent Cell Line: MAX® Efficiency DH5α Competent Cells (Invitrogen)
Antibiotic Selection: ampicillin (100µg/ml)
Restriction Enzymes: BamH I and EcoRI (yield 2 fragments). Can also cut with just EcoRI, which also yields 2 fragments.
Restriction Digest:

	Uncut	Cut
ddH_2O	42.2 µl	40.2 µl
pCMV-Luc (~1.5 µg)	2.8 µl	2.8 µl
EcoRI Buffer	5 µl	5 µl
EcoRI	---	1 µl
BamH I	---	1 µl
Total Volume	50 µl	50 µl

Let run for 2 hours at 37°C.

D. Western Blots: From Start To Finish

Protocols adapted from several sources and written up by Amelia Tomlinson of Dr. Neish's Laboratory. More detail has been added when necessary.

1. Sample Lysis in SDS Lysis/Loading Buffer

SDS-Loading Buffer Recipe for Cell Lysates

	10 ml at 1X	10 ml at 2X
1M Tris pH 6.8	625λ	1250λ
Glycerol	1000λ	2000λ
20% SDS	1000λ	2000λ
1M DTT	500λ	100λ
Type II Water	6875λ	3750λ
Bromophenol Blue	just a tiny pinch	

λ = microliters (μl)

2X SDS-Loading Buffer can be kept in aliquots at -20°C indefinitely. Thaw and dilute to 1X with dH_2O for use. Do not re-freeze.

Have ready:

1. Enough ice buckets to spread out all of your plates in a single layer
2. Chilled SDS-Lysis/Loading buffer
3. Cold 1X PBS or HBSS(+) on ice
4. A rubber policeman
5. Microtubes for samples (keep in ice)

To lyse (for 4.7 cm^2 inserts)*:

1. Take six-well plates with monolayers on inserts out of incubator and place directly on ice.
2. Wash all monolayers twice with ice-cold PBS or HBSS(+). Wash gently so that cells are not detached from inserts (i.e., don't pipet PBS/HBSS directly onto center of monolayer – pour it down the inside of the insert).
3. Add 500λ cold SDS-Lysis/Loading buffer to each monolayer. Scrape cells with a rubber policeman until you are certain that all cells have been collected. Make sure you rinse the rubber policeman in a beaker of PBS or HBSS(+) between scraping each sample, to avoid contamination.
4. Transfer lysed samples to labeled microtubes (2 aliquots per sample).
5. Keep tubes on ice until all samples are collected, then transfer to -80°C freezer.

*For the 0.33 cm^2 inserts, monolayers were lysed in 50 μl of lysis buffer

Remember:

Keep everything as cold as possible by working as quickly as possible and having all samples directly on the ice as much as possible (as opposed to, say, holding the plates in your hand).

2. SDS-PAGE Gels

Protein electrophoresis was carried out using the Lamelli discontinuous gel system (Sambrook and Russell, 2001), which is composed of a lower separating gel and an upper stacking gel. The stacking gel compresses the samples into thin bands before they enter the separating gel, thus providing better band resolution. The Mini-PROTEAN 3 Cell System from Bio-Rad was used for all SDS-PAGE.

a. Solutions

4X Stacking (Upper) Buffer
100 ml total volume:
50 ml 1M Tris-HCl pH 8.6 [0.5M]
4 ml 10% SDS [0.4%]
46 ml ddH_2O

4X Separating (Lower) Buffer
100 ml total volume:
75 ml 2M Tris-HCl pH 8.8
4 ml 10% SDS
21 ml ddH_2O

10% SDS solution
50 ml total volume
5.0 g Sodium dodecylsulfate (SDS)

Add mqH_2O to slightly less than full volume, place on stir plate until dissolved. Bring pH to approximately 7.0. Bring solution to volume with mqH20, and filter through a 0.22 micron vacuum filter.

10% APS solution
1 ml total volume
0.1 g Ammonium persulfate (APS)
1 ml mqH_2O

Gently mix APS into mqH_2O. Store 200 µl aliquots in -20°C freezer. Some protocols recommend making fresh APS for each experiment, but I have not found it to be necessary.

SDS-polyacrylamide gel running 10X buffer
1 L total volume
30 g Tris base
144 g glycine
100 ml 10% SDS

Add mqH_2O to slightly less than full volume. Adjust to pH 8.3 with concentrated HCl. Bring solution to volume with mqH20. Recheck pH.

Acrylamide Stock Solution
National Diagnostics EC-890 30% (w/v) acrylamide: 0/8% (w/v) bis-acrylamide

b. SDS-Page Gel Formulations

Recipes for separating gel are for 4 gels. Recipe for stacking gel is for 2 gels.

	Separating Gel			**Stacking Gel**
	15%	12.5%	7.5%	4.5%
Acrylamide (30:0.8)	10 ml	8.3 ml	5 ml	0.75 ml
4X Lower Buffer	5 ml	5 ml	5 ml	-----
4X Upper Buffer	-----	-----	-----	1.25 ml
ddH_2O	9.86 ml	6.6 ml	8.2 ml	3 ml
10% APS	125 µl	125 µl	125 µl	20 µl
TEMED	20 µl	10 µl	10 µl	6 µl

1. Make sure that you clean your glass plates extremely well prior to pouring gels. I usually re-wash them and then wipe them down with ethanol.

2. Combine components of gel formulation in the order indicated. Mix reagents for separating gel first. Mix well after adding water.

3. Add APS and TEMED. As soon as the APS and TEMED are added, the gel will begin to polymerize. Mix well.

4. Pour into gel apparatus to 1.8 cm from top of short glass (~4.5 ml).

5. Add a thin layer of water (1 ml) to top of separating gel (it will float on top, really) as it is polymerizing to create a strongly defined meniscus.

6. When separating gel has polymerized (30-45 min), pour off the water, and wick up any remaining water with chromatography paper without touching the gel.

7. Mix reagents for stacking gel. Fill gel apparatus to the top with stacking gel, and insert combs. Watch for bubbles. It is fine if solution overflows.

   NOTE: You may choose to save time by formulating the stacking gel without APS or TEMED at the same time that you formulate the resolving gel, adding the APS and TEMED when ready to pour the stacking gel.

8. Allow stacking gel to polymerize (20-30 min), carefully remove combs and rinse each well several times with dH_2O to remove unpolymerized solution.

c. Sample Preparation, Gel Loading, and Trimming

Supplies:

- Heat block
- Benchtop microcentrifuge
- Gel loading pipet tips
- Kaleidoscope protein standards

Gel Electrophoresis Protocol

1. Heat frozen cell lysate samples for 5 minutes at 95°C to inactivate proteases that might degrade the proteins. (Be careful when removing tubes, since lids are prone to popping off after heating.)
2. Spin down samples at 13,000 rpm (?? g) for 5 minutes on a tabletop centrifuge (Biofuge Pico, Heraeus Instruments, Hanau, Germany).
3. Set up the gel in the vertical electrophoresis system (Mini-PROTEAN 3 Cell System, Bio-Rad).
4. Load 10 – 12 µl of a standard containing several proteins of known molecular weight (Kaleidoscope Standards, Bio-Rad).
5. Load an appropriate amount of sample (depending on well size, can be as little as 5 µl. I loaded 15 - 30 µl) into individual wells in the stacking gel. Try to load samples as quickly and neatly as possible to keep the sample from becoming too diffuse.
6. Connect electrophoresis system to a DC power supply (PowerPac 300, Bio-Rad), and run at a constant 100 V until the dye front of the cell lysates runs off the bottom of the gel (~2 hrs).
7. Remove the gel from the electrophoresis chamber and carefully separate the glass plates so as not to break the gel.
8. Trim the stacking gel from the separating gel and throw it (stacking gel) away.
9. If running multiple gels, notch one or more corners of the gel to distinguish it from the others.

3. Wet Electrophoretic Transfer - Protocol adapted from Antibodies: A laboratory manual (Harlow and Lane, 1988), and from protocol provided by H. Zeng.

a. Solution

Transfer Buffer
4 L total volume
12.5 g Tris base
57.6 g glycine
800 ml methanol

Add mqH_2O to slightly less than full volume. Stir in cold room until fully dissolved. Bring up to full volume with mqH_2O. Store at 4°C.

b. Transfer Protocol

1. Equilibrate the gel in cold transfer buffer, for approximately 15 minutes.
2. Cut 1 nitrocellulose membrane and 2 pieces filter paper to size for each gel to be transferred, and soak for 15 minutes in transfer buffer. Additionally, soak fiber pads in transfer buffer.
3. Pour transfer buffer into a Pyrex dish (or other suitable container). Put black (-) panel of the transfer apparatus into this container. On this panel, layer the following in the order indicated:

   pre-wetted fiber pad → saturated filter paper → pre-equilibrated gel → pre-wetted nitrocellulose transfer sheet → saturated filter paper → pre-wetted fiber pad.

4. Push out all air bubbles before closing the apparatus. One method which works well is to gently roll a tube or scoopula over the entire sandwich from center to edge after laying down the nitrocellulose sheet, and again after the final fiber pad.
5. Close the transfer apparatus, and place in the transfer-running tank. Pay close attention to direction of current (negative to positive):

   black panel = cathode = negative
   red or clear panel = anode = positive

6. Place a stir bar in the transfer-running tank, and fill with transfer buffer.
7. Place apparatus on stir plate in cold room, and run transfer at 200 mA for 2 hours at 4°C.
8. Remove gel sandwich from apparatus, trim nitrocellulose membrane to size of gel and mark it with the same notch(es) used for the gel.
9. Throw away filter paper, nitrocellulose remnants and gel.

4. Protein Immunoblotting (Western)

a. Solutions

5X TBS
1 L total volume
12.1 g Tris base
40.0 g NaCl

Add mqH_2O to slightly less than full volume, place on stir plate until dissolved. Adjust pH to 7.6 with concentrated HCl. Bring solution to volume.

1X TBS-Tween (TBS-T)
500 ml total volume
100 ml TBS
500 µl Tween 20

Bring to volume with mqH_2O.

5% Blotto
5% (w/v) nonfat milk powder in 1X TBS-T

Mix and bring to volume. Filter solution to eliminate any clumps of milk powder (may not be necessary). Store solution at 4°C for no more than 24 hours. It shouldn't matter, but it does: we get the cleanest blots using Kroger brand dried milk.

ECL™ Western Blotting Detection Reagents - emits light in a chemiluminescent reaction with horseradish peroxidase
2-part solution available from Amersham Pharmacia Biotech (RPN 2106). Store reagents at 4°C. Do not mix until immediately prior to use, as ECL remains active for only approximately 1 hour after mixing.

b. Immunoblotting Protocol

1. Place the trimmed and marked nitrocellulose blots in 5% Blotto solution for 1 hour at room temperature on a shaker. Alternatively, the blots can be placed in blotto overnight at 4°C. Block each blot in a separate container, so that they are all equally exposed to the blotto.
2. Dilute primary antibody in blotto. Pour blotto off of blots and replace with antibody solution. Incubate at room temperature for one hour on a shaker, or overnight at 4°C on a shaker.
3. Pour off antibody solution, and rinse each blot in 1X TBS-T. Wash blots in approximately 15 ml TBS-T three times each, 5 minutes per wash.
4. During final wash, dilute secondary antibody in blotto. Pour TBS-T from blots, and replace with antibody solution. Incubate at room temperature for one hour on a shaker, or overnight at 4°C on a shaker.
5. Pour off antibody solution, and rinse each blot in 1X TBS-T. Wash blots in approximately 15 ml TBS-T three times each, 5 minutes per wash.
6. Pour off TBS-T and wash blot twice (5 min per wash) with TBS to remove Tween, which can cause high back ground.
7. Drain off excess TBS from blot on filter paper and place blots in ECL (mixed in equal parts) for one minute each.
8. Blot nitrocellulose blots on blot paper to dry, and wrap in plastic wrap. Be sure to avoid any wrinkles or bubbles in the plastic wrap, as this will affect the quality of the exposures. Side-opening sheet protectors actually work quite well for this, with much less hassle.
9. As quickly as possible, expose blots to autoradiograph film (XOMAT; Eastman Kodak, Rochester, NY) in the darkroom. Make exposures ranging from a couple of seconds to several minutes. I used the following times: 5 s, 30 s, 1 min, 2 min, 5 min, and 30 min. These exposure times can be adjusted depending on how strong or weak the signal is. Be sure to notch one corner of film before exposing to maintain orientation.
10. Develop films (M35 XOMAT Processor, Kodak) and observe the exposed protein bands on a light box.

c. Re-exposing or Re-Probing a Blot

If problems arise during the exposure of the blots, they can be rinsed with TBS-T followed by TBS as described earlier and then placed in ECL reagent again. They can then be exposed as usual.

Sometimes you may want to detect two different proteins in the same sample or redo the immunoblotting procedure. In these cases, it is necessary to strip the antibodies from the blot and probe the blots with new antibodies or with the same antibodies. The procedures for doing this are outlined below.

Solutions

- 0.2M NaOH – for stripping
- 1X TBS-T – for washing
- 1X TBS – for washing

Protocol

1. If blots have dried out since last exposure, it will be necessary to rehydrate the blots before stripping. To rehydrate, wash blot 3 times in 1X TBS-T, 20 minutes per wash. If stripping blot immediately after exposing, wash 3 times in 1X TBS-T, 5 minutes per wash.

2. Incubate blot in 0.2M NaOH for 5 - 10 minutes, at room temperature, on shaker. Do not leave in NaOH for long periods or you will strip your proteins off as well.

3. Wash blot 3 times in 1X TBS-T, 5 minutes per wash.

4. Repeat immunoblotting procedure, beginning with the blocking step. Blots will always need to be re-blocked after stripping.

5. Be aware that stripping is not always complete. You may see bleed-through on your exposures (bands for both the first antibody and the second).

E. Immunofluorescence Staining

There are many different protocols for immunofluorescence staining. Each lab seems to have its own way of doing it. I've provided two protocols that I used in my experiments. The first was used to check for recombinant IκB protein delivery and the second was used to stain for lamin A/C during the siRNA experiments. The results I obtained with first were not as good as the second, but this could have been due to the nature of the different experiments.

Reagents for all protocols

Paraformaldehyde (3.7% in PBS or HBSS)
Total volume = 50 ml
Add 1.85 g paraformaldehyde to 25ml 1X PBS. Heat while stirring, and add several drops of 1N NaOH. Do not boil! Check pH with pH paper, adjust to 7.4, and bring up to volume with 1X PBS or HBSS. Can store at 4°C for no more than three days.

P-Phenylenediamine (in glycerol) – fluorescence antifade reagent
Dissolve 50 mg p-phenylenediamine in 5ml 1X PBS. Add this to a solution of 40ml glycerol and 5 ml 10X PBS and mix. Using pH paper, adjust pH to approximately 8.0 with 0.5M carbonate/bicarbonate buffer. Immediately aliquot and freeze in a light-proof container at -70°C. Do not refreeze.

0.5M carbonate/bicarbonate buffer
Dissolve 2.65 g Na_2CO in 50ml mqH_2O. Add powdered $NaHCO_3$ until pH reaches approximately 9.0 to 9.4.

0.5% (v/v) Triton X-100
Total volume = 10 ml
Dissolve 50 µl Triton X-100 (Sigma Chemical) in 10 ml HBSS(+). Mix well.

Blocking Buffer 1 (0.2% (w/v) gelatin-0.08% (w/v) saponin)
Total volume = 25 ml
Dissolve 50 mg gelatin (Cat. No. GX00456, EM Science) and 20 mg saponin (Cat. No. 16109, Sigma Aldrich) in HBSS+. If necessary, warm the solution in 37°C water bath to help speed the dissolution process.

Blocking Buffer 2 (5% (w/v) BSA)
Total volume = 20 ml
Dissolve 1g BSA in HBSS+. Mix well. Try to avoid foam formation.

95% to Pure Ethanol
Kept at -20°C.

1. Immunofluorescence Protocol #1 – used for recombinant IκB protein delivery experiments. Reported volumes are for the large (4.7 cm^2) cell culture inserts.

1. Wash monolayers 3 times (5 min each) with 500 µl HBSS(+) after treatment (in my case, electroporation of T84's with recombinant IkBα protein)

2. Fix monolayers by adding 500 µl of 3.7% paraformaldehyde and incubating for 10-20 min at room temperature.

3. Wash 2X (5 min each wash) with HBSS(+).

4. Permeabilize monolayers with 0.5% Triton X-100 for 30 min at room temp.

5. Wash 2X (5 min each wash) with HBSS(+).

6. Block with 500 µl blocking buffer 1(0.2% gelatin-0.08% saponin) for 1 hour at room temp. (Can leave overnight in blocking buffer if necessary) Remove blocking buffer.

7. Place in 1^o antibody (diluted in blocking buffer) for 1 hour at room temperature.

8. Wash 1X (5 min) with HBSS(+)

9. Wash 1X (5 min) with blocking buffer.

10. Place in 2^o antibody (diluted in blocking buffer) for 1 hour at room temperature. Cover with foil-covered top to protect fluorescence.

11. Wash 2X in HBSS(+). (Can leave overnight if necessary)

12. Trim membrane down and cut into two or more pieces to prevent ripples during mounting.

13. Mount membrane pieces in p-phenylenediamine on a microscope slide. Might be wise to mount some cell-side up and some membrane-side up in case membrane flips over during the process.

14. Place coverslip on slide and seal edges with clear nail polish.

2. Immunofluorescence Protocol #2 – used for lamin siRNA transfection experiments. Reported volumes are for the small (0.33 cm^2) cell culture inserts.

1. Wash monolayers 3X with 100µl HBSS+ (5 min each wash).

2. Fix and permeabilize monolayers with 100 µl ice cold ethanol (at least 95% pure) for 20 minutes at -20°C.

3. Wash monolayers 3X with 100 µl HBSS+ (5 min each wash) to rehydrate the cells.

4. Block with 100 µl blocking buffer 2 (5% BSA) for 1 hour at room temp or overnight at 4°C.

5. Aspirate off blocking buffer and add 60 µl of 1° antibody (diluted in blocking buffer). Incubate for 1 hour at room temperature.

6. Wash monolayers 3X with 100 µl HBSS+ (5 min each wash).

7. Add 60 µl of 2° antibody (diluted in blocking buffer) and incubate monolayers for 1 hour at room temperature.

8. Wash monolayers 3X with 100 µl HBSS+ (5 min each wash).

9. If desired, add counterstain, e.g. Hoechst nuclear stain, at this point.

10. Wash monolayers 2X with 100 µl HBSS+ (5 min each wash).

11. Excise and mount monolayers in antifade reagent as described in Steps 12-14 of Protocol #1.

REFERENCES

Adam, S.A. (2001). The nuclear pore complex. *Genome Biol* 2:7.1-7.6.

Alberts, B. (1994). *Molecular Biology of the Cell*, Garland Pub., New York.

Anderle, P., Niederer, E., Rubas, W., Hilgendorf, C., Spahn-Langguth, H., Wunderli-Allenspach, H., Merkle, H.P. and Langguth, P. (1998). P-Glycoprotein (P-gp) mediated efflux in Caco-2 cell monolayers: the influence of culturing conditions and drug exposure on P-gp expression levels. *J Pharm Sci* 87:757-762.

Artursson, P. and Karlsson, J. (1991). Correlation between oral drug absorption in humans and apparent drug permeability coefficients in human intestinal epithelial (Caco-2) cells. *Biochem Biophys Res Commun* 175:880-885.

Artursson, P., Karlsson, J., Ocklund, G. and Schipper, N. (1996). Studying transport processes in absorptive epithelia in *Epithelial Cell Culture: A Practical Approach*. Shaw, A.J. (eds.), Oxford University Press, New York, 111-133.

Artursson, P., Palm, K. and Luthman, K. (2001). Caco-2 monolayers in experimental and theoretical predictions of drug transport. *Adv Drug Deliv Rev* 46:27-43.

Baert, F., D'Haens, G.D. and Rutgeerts, P. (2003). Postoperative prevention of recurrence of Crohn's disease in *Inflammatory Bowel Disease: From Bench to Bedside*. Targan, S.R., Shanahan, F. and Karp, L.C. (eds.), Kluwer Academic Publishers, Boston, 697-709.

Baeuerle, P.A. (1998). Pro-inflammatory signaling: last pieces in the NF-kappaB puzzle? *Curr Biol* 8:R19-22.

Bagley, S., Goldberg, M.W., Cronshaw, J.M., Rutherford, S. and Allen, T.D. (2000). The nuclear pore complex. *J Cell Sci* 113 (Pt 22):3885-3886.

Bailey, C.A., Bryla, P. and Malick, A.W. (1996). The use of the intestinal epithelial cell culture model, Caco-2, in pharmaceutical development. *Adv Drug Deliv Rev* 22:85-103.

Balamurugan, K., Ortiz, A. and Said, H.M. (2003). Biotin uptake by human intestinal and liver epithelial cells: role of the SMVT system. *Am J Physiol Gastrointest Liver Physiol* 285:G73-77.

Baldwin, A.S., Jr. (1996). The NF-kappa B and I kappa B proteins: new discoveries and insights. *Annu Rev Immunol* 14:649-683.

Banga, A.K., Bose, S. and Ghosh, T.K. (1999). Iontophoresis and electroporation: comparisons and contrasts. *Int J Pharm* 179:1-19.

Baron, S., Poast, J., Rizzo, D., McFarland, E. and Kieff, E. (2000). Electroporation of antibodies, DNA, and other macromolecules into cells: a highly efficient method [In Process Citation]. *J Immunol Methods* 242:115-126.

Bartoletti, D.C., Harrison, G.I. and Weaver, J.C. (1989). The number of molecules taken up by electroporated cells: quantitative determination. *FEBS Lett* 256:4-10.

Baulcombe, D. (2002). RNA silencing. *Curr Biol* 12:R82-84.

Beg, A.A. and Baldwin, A.S., Jr. (1993). The I kappa B proteins: multifunctional regulators of Rel/NF-kappa B transcription factors. *Genes Dev* 7:2064-2070.

Bichko, V.V. (1998). Cationic Liposomes in *DNA Transfer to Cultured Cells*. Ravid, K. and Freshney, R.I. (eds.), Wiley-Liss, Inc., 193-211.

Black, R.E. and Lanata, C.F. (2002). Epidemiology of diarrheal diseases in developing countries in *Infections of the Gastrointestinal Tract*. Blaser, M.J., Smith, P.D., Ravdin, J.I., Greenberg, H.B. and Guerrant, R.L. (eds.), Lippincott Williams & Wilkins, Philadelphia, 11-29.

Blaser, M.J., Smith, P.D., Ravdin, J.I., Greenberg, H.B. and Guerrant, R.L., Eds. (2002). *Infections of the Gastrointestinal Tract*, Lippincott Williams & Wilkins, Philadelphia.

Bright, G.R., Kuo, N.T., Chow, D., Burden, S., Dowe, C. and Przybylski, R.J. (1996). Delivery of macromolecules into adherent cells via electroporation for use in fluorescence spectroscopic imaging and metabolic studies. *Cytometry* 24:226-233.

Brody, T.M., Larner, J. and Minneman, K.P. (1998). *Human Pharmacology : Molecular to Clinical*, Mosby, St. Louis.

Bureau, M.F., Gehl, J., Deleuze, V., Mir, L.M. and Scherman, D. (2000). Importance of association between permeabilization and electrophoretic forces for intramuscular DNA electrotransfer. *Biochim Biophys Acta* 1474:353-359.

Burkitt, H.G., Young, B., Heath, J.W. and Wheater, P.R. (1993). *Wheater's Functional Histology : A Text and Colour Atlas*, Churchill Livingstone, Edinburgh ; New York.

Canatella, P.J., Karr, J.F., Petros, J.A. and Prausnitz, M.R. (2001). Quantitative study of electroporation-mediated molecular uptake and cell viability. *Biophys J* 80:755-764.

Canatella, P.J. and Prausnitz, M.R. (2001). Prediction and optimization of gene transfection and drug delivery by electroporation. *Gene Ther* 8:1464-1469.

Cataldo, L.M., Wang, Z. and Ravid, K. (1998). Electroporation of DNA into cultured cell lines in *DNA Transfer Into Cultured Cells*. Ravid, K. and Freshney, R.I. (eds.), Wiley-Liss, Inc., 55-67.

CCFA (2003a). *About Crohn's Disease*. Crohn's and Colitis Foundation of America, New York.

CCFA (2003b). *About Ulcerative Colitis*. Crohn's and Colitis Foundation of America, New York.

Chang, D.C., Chassy, B.M., Saunders, J.A. and Sowers, A.E., Eds. (1992). *Guide to Electroporation and Electrofusion*, Academic Press, New York.

Check, E. (2003). Gene regulation: RNA to the rescue? *Nature* 425:10-12.

Chernomordik, L.V. (1992). Electropores in lipid bilayers and cell membranes in *Guide to Electroporation and Electrofusion*. Chang, D.C., Chassy, B.M., Saunders, J.A. and Sowers, A.E. (eds.), Academic Press, New York, 63-76.

Chopra, S. and May, R.J. (1989). *Pathophysiology of Gastrointestinal Diseases*, Little Brown, Boston.

Chowrira, G.M., Akella, V. and Lurquin, P.F. (1995). Electroporation-mediated gene transfer into intact nodal meristems in planta. Generating transgenic plants without in vitro tissue culture. *Mol Biotechnol* 3:17-23.

Conn, K.J., Degrterev, A., Fontanilla, M.R., Rich, B.C. and Foster, J.A. (1998). Calcium phosphate transfection in *DNA Transfer to Cultured Cells*. Ravid, K. and Freshney, R.I. (eds.), Wiley-Liss, Inc., 111-124.

Dharmsathaphorn, K. and Madara, J.L. (1990). Established intestinal cell lines as model systems for electrolyte transport studies. *Methods Enzymol* 192:354-389.

Dharmsathaphorn, K., McRoberts, J.A., Mandel, K.G., Tisdale, L.D. and Masui, H. (1984). A human colonic tumor cell line that maintains vectorial electrolyte transport. *Am J Physiol* 246:G204-208.

DiDonato, J.A., Hayakawa, M., Rothwarf, D.M., Zandi, E. and Karin, M. (1997). A cytokine-responsive IkappaB kinase that activates the transcription factor NF-kappaB. *Nature* 388:548-554.

DiDonato, J.A., Mercurio, F. and Karin, M. (1995). Phosphorylation of I kappa B alpha precedes but is not sufficient for its dissociation from NF-kappa B. *Mol Cell Biol* 15:1302-1311.

Dignass, A.U. (2001). Mechanisms and modulation of intestinal epithelial repair. *Inflamm Bowel Dis* 7:68-77.

Dimitrov, D.S. and Sowers, A.E. (1990). Membrane electroporation--fast molecular exchange by electroosmosis. *Biochim Biophys Acta* 1022:381-392.

Dujardin, N., Van Der Smissen, P. and Preat, V. (2001). Topical gene transfer into rat skin using electroporation. *Pharm Res* 18:61-66.

Eckmann, L., Kagnoff, M.F. and Fierer, J. (1993). Epithelial cells secrete the chemokine interleukin-8 in response to bacterial entry. *Infect Immun* 61:4569-4574.

Egan, L.J. and Sandborn, W.J. (2003). Clinical pharmacology in inflammatory bowel disease: optimizing current medical therapy in *Inflammatory Bowel Disease: From Bench to Bedside*. Targan, S.R., Shanahan, F. and Karp, L.C. (eds.), Kluwer Academic Publishers, Boston, 495-521.

Elbashir, S.M., Harborth, J., Lendeckel, W., Yalcin, A., Weber, K. and Tuschl, T. (2001a). Duplexes of 21-nucleotide RNAs mediate RNA interference in cultured mammalian cells. *Nature* 411:494-498.

Elbashir, S.M., Harborth, J., Weber, K. and Tuschl, T. (2002). Analysis of gene function in somatic mammalian cells using small interfering RNAs. *Methods* 26:199-213.

Elbashir, S.M., Lendeckel, W. and Tuschl, T. (2001b). RNA interference is mediated by 21- and 22-nucleotide RNAs. *Genes Dev* 15:188-200.

Elewaut, D., DiDonato, J.A., Kim, J.M., Truong, F., Eckmann, L. and Kagnoff, M.F. (1999). NF-kappa B is a central regulator of the intestinal epithelial cell innate immune response induced by infection with enteroinvasive bacteria. *J Immunol* 163:1457-1466.

Feller, N., Broxterman, H.J., Wahrer, D.C. and Pinedo, H.M. (1995). ATP-dependent efflux of calcein by the multidrug resistance protein (MRP): no inhibition by intracellular glutathione depletion. *FEBS Lett* 368:385-388.

Firth, K.L., Brownell, H.L. and Raptis, L. (1997). Improved procedure for electroporation of peptides into adherent cells in situ. *Biotechniques* 23:644-646.

Fogh, J., Fogh, J.M. and Orfeo, T. (1977a). One hundred and twenty-seven cultured human tumor cell lines producing tumors in nude mice. *J Natl Cancer Inst* 59:221-226.

Fogh, J., Wright, W.C. and Loveless, J.D. (1977b). Absence of HeLa cell contamination in 169 cell lines derived from human tumors. *J Natl Cancer Inst* 58:209-214.

Foye, W.O., Lemke, T.L. and Williams, D.A. (1995). *Principles of Medicinal Chemistry*, Williams & Wilkins, Baltimore.

Fujita, T., Yamada, H., Fukuzumi, M., Nishimaki, A., Yamamoto, A. and Muranishi, S. (1997). Calcein is excreted from the intestinal mucosal cell membrane by the active transport system. *Life Sci* 60:307-313.

Gasiorowski, J.Z. and Dean, D.A. (2003). Mechanisms of nuclear transport and interventions. *Adv Drug Deliv Rev* 55:703-716.

Ghosh, P.M., Keese, C.R. and Giaever, I. (1993). Monitoring electropermeabilization in the plasma membrane of adherent mammalian cells. *Biophys J* 64:1602-1609.

Gift, E.A. and Weaver, J.C. (1995). Observation of extremely heterogeneous electroporative molecular uptake by Saccharomyces cerevisiae which changes with electric field pulse amplitude. *Biochim Biophys Acta* 1234:52-62.

Gonzalez-Mariscal, L., Contreras, R.G., Bolivar, J.J., Ponce, A., Chavez De Ramirez, B. and Cereijido, M. (1990). Role of calcium in tight junction formation between epithelial cells. *Am J Physiol* 259:978-986.

Greenberg, H.B., Matsui, S.M. and Loutit, J.S. (1999). Small intestine: Infections with common bacterial and viral pathogens in *Textbook of Gastroenterology*. Yamada, T., Alpers, D.H., Lain, L., Owyang, C. and Powell, D.W. (eds.), Lippincott, Williams, and Wilkins, Philadelphia, 1611-1640.

Greenleaf, W.J., Bolander, M.E., Sarkar, G., Goldring, M.B. and Greenleaf, J.F. (1998). Artificial cavitation nuclei significantly enhance acoustically induced cell transfection. *Ultrasound Med Biol* 24:587-595.

Gres, M.C., Julian, B., Bourrie, M., Meunier, V., Roques, C., Berger, M., Boulenc, X., Berger, Y. and Fabre, G. (1998). Correlation between oral drug absorption in humans, and apparent drug permeability in TC-7 cells, a human epithelial intestinal cell line: comparison with the parental Caco-2 cell line. *Pharm Res* 15:726-733.

Hannon, G.J. (2002). RNA interference. *Nature* 418:244-251.

Harborth, J., Elbashir, S.M., Bechert, K., Tuschl, T. and Weber, K. (2001). Identification of essential genes in cultured mammalian cells using small interfering RNAs. *J Cell Sci* 114:4557-4565.

Heller, R., Gilbert, R. and Jaroszeski, M.J. (1999). Clinical applications of electrochemotherapy. *Adv Drug Deliv Rev* 35:119-129.

Hicks, G.G., Chen, J. and Ruley, H.E. (1998). Production and use of retroviruses in *DNA Transfer Into Cultered Cells*. Ravid, K. and Freshney, R.I. (eds.), Wiley-Liss, Inc., 1-25.

Hidalgo, I.J. and Li, J. (1996). Carrier-mediated transport and efflux mechanisms in Caco-2 cells. *Adv Drug Deliv Rev* 22:53-66.

Histology Epithelial Tissues, Chapter 5 in *Histology Guide*, 80-96.

Ho, N.F.H., Raub, T.J., Burton, P.S., Barsuhn, C.L., Adson, A., Audus, K.L. and Borchardt, R.T. (2000). Quantitative approaches to delineate passive transport mechanisms in cell culture monolayers in *Transport Processes in Pharmaceutical Systems*. Amidon, G.L., Lee, P.I. and Topp, E.M. (eds.), M. Dekker, New York, 219-316.

Ho, S.Y. and Mittal, G.S. (1996). Electroporation of cell membranes: a review. *Crit Rev Biotechnol* 16:349-362.

Jaroszeski, M.J., Gilbert, R., Nicolau, C. and Heller, R. (1999). In vivo gene delivery by electroporation. *Adv Drug Deliv Rev* 35:131-137.

Jaroszeski, M.J., Heller, R. and Gilbert, R. (2000). *Electrochemotherapy, Electrogenetherapy, and Transdermal Drug Delivery : Electrically Mediated Delivery of Molecules to Cells*, Humana Press, Totowa, N.J.

Jiang, Z.Y., Zhou, Q.L., Coleman, K.A., Chouinard, M., Boese, Q. and Czech, M.P. (2003). Insulin signaling through Akt/protein kinase B analyzed by small interfering RNA-mediated gene silencing. *Proc Natl Acad Sci U S A* 100:7569-7574.

Jobin, C. and Sartor, R.B. (2000). The I kappa B/NF-kappa B system: a key determinant of mucosal inflammation and protection. *Am J Physiol Cell Physiol* 278:C451-462.

Jung, H.C., Eckmann, L., Yang, S.K., Panja, A., Fierer, J., Morzycka-Wroblewska, E. and Kagnoff, M.F. (1995). A distinct array of proinflammatory cytokines is expressed in human colon epithelial cells in response to bacterial invasion. *J Clin Invest* 95:55-65.

Karlinger, K., Gyorke, T., Mako, E., Mester, A. and Tarjan, Z. (2000). The epidemiology and the pathogenesis of inflammatory bowel disease. *Eur J Radiol* 35:154-167.

Karlsson, J., Ungell, A., Grasjo, J. and Artursson, P. (1999). Paracellular drug transport across intestinal epithelia: influence of charge and induced water flux. *Eur J Pharm Sci* 9:47-56.

Klenchin, V.A., Sukharev, S.I., Serov, S.M., Chernomordik, L.V. and Chizmadzhev Yu, A. (1991). Electrically induced DNA uptake by cells is a fast process involving DNA electrophoresis. *Biophys J* 60:804-811.

Krishna, G., Chen, K., Lin, C. and Nomeir, A.A. (2001). Permeability of lipophilic compounds in drug discovery using in-vitro human absorption model, Caco-2. *Int J Pharm* 222:77-89.

Kwee, S. and Celis, J.E. (1991). Electroporation as a tool for studying cell proliferation and DNA synthesis in human cultured cells grown in monolayers. *Bioelectrochem Bioenerg* 25:325-332.

Kwee, S., Gesser, B. and Celis, J.E. (1992). Electroporation of human cultured-cells grown in monolayers .3. Transformed cells and primary cells. *Bioelectrochem Bioenerg* 28:269-278.

Kwee, S., Nielsen, H.V. and Celis, J.E. (1990). Electropermeabilization of human cultured-cells grown in monolayers: Incorporation of monoclonal antibodies. *Bioelectrochem Bioenerg* 23:65-80.

Lacy, E.R. (1988). Epithelial restitution in the gastrointestinal tract. *J Clin Gastroenterol* 10:S72-77.

Langer, R. (1998). Drug delivery and targeting. *Nature* 392:5-10.

Lechardeur, D., Sohn, K.J., Haardt, M., Joshi, P.B., Monck, M., Graham, R.W., Beatty, B., Squire, J., O'Brodovich, H. and Lukacs, G.L. (1999). Metabolic instability of plasmid DNA in the cytosol: a potential barrier to gene transfer. *Gene Ther* 6:482-497.

Leonard, M., Creed, E., Brayden, D. and Baird, A.W. (2000a). Evaluation of the Caco-2 monolayer as a model epithelium for iontophoretic transport. *Pharm Res* 17:1181-1188.

Leonard, M., Creed, E., Brayden, D. and Baird, A.W. (2000b). Iontophoresis-enhanced absorptive flux of polar molecules across intestinal tissue in vitro. *Pharm Res* 17:476-478.

Li, C.K., Seth, R., Gray, T., Bayston, R., Mahida, Y.R. and Wakelin, D. (1998). Production of proinflammatory cytokines and inflammatory mediators in human intestinal epithelial cells after invasion by Trichinella spiralis. *Infect Immun* 66:2200-2206.

Liang, H., Purucker, W.J., Stenger, D.A., Kubiniec, R.T. and Hui, S.W. (1988). Uptake of fluorescence-labeled dextrans by 10T 1/2 fibroblasts following permeation by rectangular and exponential-decay electric field pulses. *Biotechniques* 6:550-558.

Liu, Y., Nusrat, A., Schnell, F.J., Reaves, T.A., Walsh, S., Pochet, M. and Parkos, C.A. (2000). Human junction adhesion molecule regulates tight junction resealing in epithelia. *J Cell Sci* 113:2363-2374.

Lu, S., Gough, A.W., Bobrowski, W.F. and Stewart, B.H. (1996). Transport properties are not altered across Caco-2 cells with heightened TEER despite underlying physiological and ultrastructural changes. *J Pharm Sci* 85:270-273.

Lynch, P.T. and Davey, M.R. (1996). *Electrical Manipulation of Cells*, Chapman & Hall, New York.

Ma, T.Y., Nguyen, D., Bui, V., Nguyen, H. and Hoa, N. (1999). Ethanol modulation of intestinal epithelial tight junction barrier. *Am J Physiol* 276:G965-974.

Ma, T.Y., Tran, D., Hoa, N., Nguyen, D., Merryfield, M. and Tarnawski, A. (2000). Mechanism of extracellular calcium regulation of intestinal epithelial tight junction permeability: Role of cytoskeletal involvement. *Microsc Res Tech* 51:156-168.

Madara, J.L. (1999). Epithelia: Biologic principles of organization in *Textbook of Gastroenterology*. Yamada, T., Alpers, D.H., Lain, L., Owyang, C. and Powell, D.W. (eds.), Lippincott, Williams, and Wilkins, Philadelphia, 141-156.

Madara, J.L., Colgan, S., Nusrat, A., Delp, C. and Parkos, C. (1992). A simple approach to measurement of electrical parameters of cultured epithelial monolayers: Use in assessing neutrophil-epithelial interactions. *J Tissue Cult Methods* 14:209-216.

Madara, J.L. and Dharmsathaphorn, K. (1985). Occluding junction structure-function relationships in a cultured epithelial monolayer. *J Cell Biol* 101:2124-2133.

Madara, J.L., Stafford, J., Dharmsathaphorn, K. and Carlson, S. (1987). Structural analysis of a human intestinal epithelial cell line. *Gastroenterology* 92:1133-1145.

Makarov, S.S. (2000). NF-kappaB as a therapeutic target in chronic inflammation: recent advances. *Mol Med Today* 6:441-448.

Marieb, E.N. (2000). *Essentials of Human Anatomy and Physiology*, Benjamin Cummings, San Francisco.

Matsui, H., Johnson, L.G., Randell, S.H. and Boucher, R.C. (1997). Loss of binding and entry of liposome-DNA complexes decreases transfection efficiency in differentiated airway epithelial cells. *J Biol Chem* 272:1117-1126.

Mayo (1994). Gastrointestinal Diseases. Mayo Clinic Foundation for Medical Education and Research, Rochester, Minnesota.

McCormick, B.A., Colgan, S.P., Delp-Archer, C., Miller, S.I. and Madara, J.L. (1993). Salmonella typhimurium attachment to human intestinal epithelial monolayers: transcellular signalling to subepithelial neutrophils. *J Cell Biol* 123:895-907.

McCormick, B.A., Parkos, C.A., Colgan, S.P., Carnes, D.K. and Madara, J.L. (1998). Apical secretion of a pathogen-elicited epithelial chemoattractant activity in response to surface colonization of intestinal epithelia by Salmonella typhimurium. *J Immunol* 160:455-466.

Mir, L.M., Bureau, M.F., Gehl, J., Rangara, R., Rouy, D., Caillaud, J.M., Delaere, P., Branellec, D., Schwartz, B. and Scherman, D. (1999). High-efficiency gene transfer into skeletal muscle mediated by electric pulses. *Proc Natl Acad Sci U S A* 96:4262-4267.

Moore, R., Carlson, S. and Madara, J.L. (1989). Rapid barrier restitution in an in vitro model of intestinal epithelial injury. *Lab Invest* 60:237-244.

Muller, K.J., Horbaschek, M., Lucas, K., Zimmermann, U. and Sukhorukov, V.L. (2003). Electrotransfection of anchorage-dependent mammalian cells. *Exp Cell Res* 288:344-353.

NDDIC (2003a). Crohn's Disease. National Institute of Diabetes and Digestive and Kidney Diseases (NIDDK), NIH Publication No. 03-3410.

NDDIC (2003b). Ulcerative Colitis. National Institute of Diabetes and Digestive and Kidney Diseases (NIDDK), NIH Publication No. 03-1597.

Neumann, E., Schaefer-Ridder, M., Wang, Y. and Hofschneider, P.H. (1982). Gene transfer into mouse lyoma cells by electroporation in high electric fields. *EMBO J* 1:841-845.

Neumann, E., Sowers, A.E. and Jordan, C.A. (1989). *Electroporation and Electrofusion in Cell Biology*, Plenum Press, New York.

Neumann, E., Toensing, K., Kakorin, S., Budde, P. and Frey, J. (1998). Mechanism of electroporative dye uptake by mouse B cells. *Biophys J* 74:98-108.

Neurath, M.F., Pettersson, S., Meyer zum Buschenfelde, K.H. and Strober, W. (1996). Local administration of antisense phosphorothioate oligonucleotides to the p65 subunit of NF-kappa B abrogates established experimental colitis in mice. *Nat Med* 2:998-1004.

Nickoloff, J.A. (1995). *Animal Cell Electroporation and Electrofusion Protocols*, Humana Press, Totowa, N.J.

Nusrat, A., Delp, C. and Madara, J.L. (1992). Intestinal epithelial restitution. Characterization of a cell culture model and mapping of cytoskeletal elements in migrating cells. *J Clin Invest* 89:1501-1511.

Nusrat, A., Parkos, C.A., Liang, T.W., Carnes, D.K. and Madara, J.L. (1997). Neutrophil migration across model intestinal epithelia: monolayer disruption and subsequent events in epithelial repair. *Gastroenterology* 113:1489-1500.

Oliveira, D.M. and Goodell, M.A. (2003). Transient RNA interference in hematopoietic progenitors with functional consequences. *Genesis* 36:203-208.

Oshima, Y., Sakamoto, T., Yamanaka, I., Nishi, T., Ishibashi, T. and Inomata, H. (1998). Targeted gene transfer to corneal endothelium in vivo by electric pulse. *Gene Ther* 5:1347-1354.

Palm, K., Luthman, K., Ros, J., Grasjo, J. and Artursson, P. (1999). Effect of molecular charge on intestinal epithelial drug transport: pH- dependent transport of cationic drugs. *J Pharmacol Exp Ther* 291:435-443.

Parkos, C.A. (1997). Cell adhesion and migration. I. Neutrophil adhesive interactions with intestinal epithelium. *Am J Physiol* 273:G763-768.

Pegues, D.A., Ohl, M.E. and Miller, S.I. (2002). Salmonella, including *salmonella typhi* in *Infections of the Gastrointestinal Tract*. Blaser, M.J., Smith, P.D., Ravdin, J.I., Greenberg, H.B. and Guerrant, R.L. (eds.), Lippincott, Williams, & Wilkins, Philadelphia, 669-697.

Pouton, C.W. (1998). Nuclear import of polypeptides, polynucleotides and supramolecular complexes. *Adv Drug Deliv Rev* 34:51-64.

Prausnitz, M.R. (1999). A practical assessment of transdermal drug delivery by skin electroporation. *Adv Drug Deliv Rev* 35:61-76.

Prausnitz, M.R., Corbett, J.D., Gimm, J.A., Golan, D.E., Langer, R. and Weaver, J.C. (1995). Millisecond measurement of transport during and after an electroporation pulse. *Biophys J* 68:1864-1870.

Prausnitz, M.R., Lau, B.S., Milano, C.D., Conner, S., Langer, R. and Weaver, J.C. (1993). A quantitative study of electroporation showing a plateau in net molecular transport. *Biophys J* 65:414-422.

Prausnitz, M.R., Milano, C.D., Gimm, J.A., Langer, R. and Weaver, J.C. (1994). Quantitative study of molecular transport due to electroporation: uptake of bovine serum albumin by erythrocyte ghosts. *Biophys J* 66:1522-1530.

Raptis, L.H., Firth, K.L., Brownell, H.L., Todd, A., Simon, W.C., Bennett, B.M., MacKenzie, L.W. and Zannis-Hadjopoulos, M. (1995a). Electroporation of adherent cells in situ for the introduction of nonpermeant molecules in *Animal Cell Electroporation and Electrofusion*. Nickoloff, J.A. (eds.), Humana Press, Totowa, NJ, 93-113.

Raptis, L.H., Liu, S.K., Firth, K.L., Stiles, C.D. and Alberta, J.A. (1995b). Electroporation of peptides into adherent cells in situ. *Biotechniques* 18:104-110.

Ravid, K. and Freshney, R.I. (1998). *DNA Transfer to Cultured Cells*, Wiley-Liss, New York.

Read, M.A., Whitley, M.Z., Williams, A.J. and Collins, T. (1994). NF-kappa B and I kappa B alpha: an inducible regulatory system in endothelial activation. *J Exp Med* 179:503-512.

Rols, M.P., Delteil, C., Golzio, M., Dumond, P., Cros, S. and Teissie, J. (1998). In vivo electrically mediated protein and gene transfer in murine melanoma. *Nat Biotechnol* 16:168-171.

Rols, M.P. and Teissie, J. (1990). Electropermeabilization of mammalian cells: Quantitative analysis of the phenomenon. *Biophys J* 58:1089-1098.

Rubas, W., Cromwell, M.E.M., Shahrokh, Z., Villagran, J., Nguyen, T.-N., Wellton, M., Nguyen, T.-H. and Mrsny, R.J. (1996). Flux measurements across Caco-2 monolayers may predict transport in human large intestinal tissue. *J Pharm Sci* 85:165-169.

Rubas, W., Villagran, J., Cromwell, M., Mcleod, A., Wassenberg, J. and Mrsny, R. (1995). Correlation of solute flux across Caco-2 monolayers and colonic tissue in vitro. *Stp Pharma Sci* 5:93-97.

Sambrook, J., Fritsch, E.F. and Maniatis, T. (1989). *Molecular Cloning: A Laboratory Manual*, Cold Spring Harbor Laboratory Press, Plainview, New York.

Sambrook, J. and Russell, D.W. (2001). *Molecular Cloning : A Laboratory Manual*, Cold Spring Harbor Laboratory Press, Cold Spring Harbor, N.Y.

Satkauskas, S., Bureau, M.F., Puc, M., Mahfoudi, A., Scherman, D., Miklavcic, D. and Mir, L.M. (2002). Mechanisms of in vivo DNA electrotransfer: respective contributions of cell electropermeabilization and DNA electrophoresis. *Mol Ther* 5:133-140.

Saunders, J.A. and Bates, G.W. (1992). Genetic manipulation of plant cells by means of electroporation and electrofusion in *Guide to Electroporation and Electrofusion*. Chang, D.C., Chassy, B.M., Saunders, J.A. and Sowers, A.E. (eds.), Academic Press, New York, 471-483.

Schenborn, E. and Groskreutz, D. (1999). Reporter gene vectors and assays. *Mol Biotechnol* 13:29-44.

Schmid, R.M. and Adler, G. (2000). NF-kappaB/rel/IkappaB: implications in gastrointestinal diseases. *Gastroenterology* 118:1208-1228.

Schreiber, S., Nikolaus, S. and Hampe, J. (1998). Activation of nuclear factor kappa B inflammatory bowel disease. *Gut* 42:477-484.

Schuerer-Maly, C.C., Eckmann, L., Kagnoff, M.F., Falco, M.T. and Maly, F.E. (1994). Colonic epithelial cell lines as a source of interleukin-8: stimulation by inflammatory cytokines and bacterial lipopolysaccharide. *Immunology* 81:85-91.

Schwartz, J.J. and Rosenberg, R. (1998). DEAE-Dextran Transfection in *DNA Transfer to Cultured Cells*. Ravid, K. and Freshney, R.I. (eds.), Wiley-Liss, Inc., 179-191.

Schwartz, S.A., Hernandez, A. and Mark Evers, B. (1999). The role of NF-kappaB/IkappaB proteins in cancer: Implications for novel treatment strategies. *Surg Oncol* 8:143-153.

Sears, C.L. and Acheson, D.W.K. (2002). Enteric bacterial toxins in *Infections of the Gastrointestinal Tract*. Blaser, M.J., Smith, P.D., Ravdin, J.I., Greenberg, H.B. and Guerrant, R.L. (eds.), Lippincott, Williams & Wilkins, Philadelphia, 89-107.

Shaw, A.J., Ed. (1996a). *Epithelial Cell Culture: A Practical Approach*, Oxford University Press, Oxford.

Shaw, A.J. (1996b). Modeling epithelial tissues *in vitro* in *Epithelial Cell Culture: A Practical Approach*. Shaw, A.J. (eds.), Oxford University Press, New York, 1-16.

Shi, Y. (2003). Mammalian RNAi for the masses. *Trends Genet* 19:9-12.

Shuey, D.J., McCallus, D.E. and Giordano, T. (2002). RNAi: Gene-silencing in therapeutic intervention. *Drug Discov Today* 7:1040-1046.

Smith, B.F. and Lamont, J.T. (1989). Intestinal Infections in *Pathophysiology of Gastrointestinal Diseases*. Chopra, S. and May, R.J. (eds.), Little, Brown, and Co., Boston, 171-191.

Sobel, J. and Tauxe, R.V. (2002). Epidemiology of diarrheal diseases in developed countries in *Infections of the Gastrointestinal Tract*. Blaser, M.J., Smith, P.D., Ravdin, J.I., Greenberg, H.B. and Guerrant, R.L. (eds.), Lippincott Williams & Wilkins, Philadelphia, 31-44.

Soltis, R.D. (2002). Pharmacology of agents other than antimicrobials used in gastrointestinal infections in *Infections of the Gastrointestinal Tract*. Blaser, M.J., Smith, P.D., Ravdin, J.I., Greenberg, H.B. and Guerrant, R.L. (eds.), Lippincott Williams & Wilkins, Philadelphia, 1213-1221.

Stalheim-Smith, A. and Fitch, G.K. (1993). *Understanding Human Anatomy and Physiology*, West Pub. Co., Minneapolis/St. Paul.

Sukharev, S.I., Klenchin, V.A., Serov, S.M., Chernomordik, L.V. and Chizmadzhev Yu, A. (1992). Electroporation and electrophoretic DNA transfer into cells. The effect of DNA interaction with electropores. *Biophys J* 63:1320-1327.

Tak, P.P. and Firestein, G.S. (2001). NF-kappaB: a key role in inflammatory diseases. *J Clin Invest* 107:7-11.

Taketo, A. (1988). DNA transfection of Escherichia coli by electroporation. *Biochim Biophys Acta* 949:318-324.

Talcott, B. and Moore, M.S. (1999). Getting across the nuclear pore complex. *Trends Cell Biol* 9:312-318.

Targan, S.R., Shanahan, F. and Karp, L.C., Eds. (2003). *Inflammatory Bowel Disease: From Bench to Bedside*, Kluwer Academic Publishers, Boston.

Thanos, D. and Maniatis, T. (1995). NF-kappa B: a lesson in family values. *Cell* 80:529-532.

Thomas, C.E., Ehrhardt, A. and Kay, M.A. (2003). Progress and problems with the use of viral vectors for gene therapy. *Nat Rev Genet* 4:346-358.

Trezise, A.E. (2002). In vivo DNA electrotransfer. *DNA Cell Biol* 21:869-877.

Tseng, W.C., Haselton, F.R. and Giorgio, T.D. (1997). Transfection by cationic liposomes using simultaneous single cell measurements of plasmid delivery and transgene expression. *J Biol Chem* 272:25641-25647.

Tseng, W.C., Haselton, F.R. and Giorgio, T.D. (1999). Mitosis enhances transgene expression of plasmid delivered by cationic liposomes. *Biochim Biophys Acta* 1445:53-64.

Tsien, R.Y. (1998). The green fluorescent protein. *Ann Rev Biochem* 67:509-544.

Tucker, S.P., Melsen, L.R. and Compans, R.W. (1992). Migration of polarized epithelial cells through permeable membrane substrates of defined pore size. *Eur. J. Cell Biol.* 58:280-290.

Uduehi, A.N., Moss, S.H., Nuttall, J. and Pouton, C.W. (1999). Cationic lipid-mediated transfection of differentiated Caco-2 cells: a filter culture model of gene delivery to a polarized epithelium. *Pharm Res* 16:1805-1811.

Vogel, K.G. (1978). Effects of hyaluronidase, trypsin, and EDTA on surface composition and topography during detachment of cells in culture. *Exp Cell Res* 113:345-357.

Weaver, J.C. (1993). Electroporation: a general phenomenon for manipulating cells and tissues. *J Cell Biochem* 51:426-435.

Weaver, J.C. and Chizmadzhev, Y.A. (1996). Theory of electroporation: A review. *Bioelectrochem Bioenerg* 41:135-160.

Wegener, J., Keese, C.R. and Giaever, I. (2002). Recovery of adherent cells after in situ electroporation monitored electrically. *Biotechniques* 33:348-357.

Wilson, J.A., Jayasena, S., Khvorova, A., Sabatinos, S., Rodrigue-Gervais, I.G., Arya, S., Sarangi, F., Harris-Brandts, M., Beaulieu, S. and Richardson, C.D. (2003). RNA interference blocks gene expression and RNA synthesis from hepatitis C replicons propagated in human liver cells. *Proc Natl Acad Sci USA* 100:2783-2788.

Xie, T.D., Sun, L. and Tsong, T.Y. (1990). Study of mechanisms of electric field-induced DNA transfection. I. DNA entry by surface binding and diffusion through membrane pores. *Biophys J* 58:13-19.

Yamada, T., Alpers, D.H., Lain, L., Owyang, C. and Powell, D.W., Eds. (1999). *Textbook of Gastroenterology*, Lippincott Williams & Wilkins, Philadephia.

Yamamoto, Y. and Gaynor, R.B. (2001). Therapeutic potential of inhibition of the NF-kappaB pathway in the treatment of inflammation and cancer. *J Clin Invest* 107:135-142.

Yamashita, S., Furubayashi, T., Kataoka, M., Sakane, T., Sezaki, H. and Tokuda, H. (2000). Optimized conditions for prediction of intestinal drug permeability using Caco-2 cells. *Eur J Pharm Sci* 10:195-204.

Yang, T.A., Heiser, W.C. and Sedivy, J.M. (1995). Efficient in situ electroporation of mammalian cells grown on microporous membranes. *Nucleic Acids Res* 23:2803-2810.

Yaron, A., Gonen, H., Alkalay, I., Hatzubai, A., Jung, S., Beyth, S., Mercurio, F., Manning, A.M., Ciechanover, A. and Ben-Neriah, Y. (1997). Inhibition of NF-kappa-B cellular function via specific targeting of the I-kappa-B-ubiquitin ligase. *EMBO J* 16:6486-6494.

Yee, S. (1997). In vitro permeability across Caco-2 cells (colonic) can predict in vivo (small intestinal) absorption in man--fact or myth. *Pharm Res* 14:763-766.

Yu, J.Y., DeRuiter, S.L. and Turner, D.L. (2002). RNA interference by expression of short-interfering RNAs and hairpin RNAs in mammalian cells. *Proc Natl Acad Sci U S A* 99:6047-6052.

Zabel, U. and Baeuerle, P.A. (1990). Purified human I kappa B can rapidly dissociate the complex of the NF- kappa B transcription factor with its cognate DNA. *Cell* 61:255-265.

Zabner, J., Fasbender, A.J., Moninger, T., Poellinger, K.A. and Welsh, M.J. (1995). Cellular and molecular barriers to gene transfer by a cationic lipid. *J Biol Chem* 270:18997-19007.

Zamore, P.D. (2002). Ancient pathways programmed by small RNAs. *Science* 296:1265-1269.

Zandi, E., Chen, Y. and Karin, M. (1998). Direct phosphorylation of IkappaB by IKKalpha and IKKbeta: discrimination between free and NF-kappaB-bound substrate. *Science* 281:1360-1363.

Zheng, Q.A. and Chang, D.C. (1991). High-efficiency gene transfection by in situ electroporation of cultured cells. *Biochim Biophys Acta* 1088:104-110.

CHAPTER XV
VITA

Esi Baawah Ghartey-Tagoe was born February 17, 1974 in Tuskegee, Alabama. She attended Tuskegee Institute High School and then transferred to Manhattan High School in Manhattan, KS where she graduated in 1991. She then attended Kansas State University and earned her B.S. in Chemical Engineering in December 1995. In October of the following year, she joined the Bioengineering Program at Georgia Institute of Technology to pursue a doctorate. Her dissertation was entitled "Electroporation-Mediated Delivery of Macromolecules to Intestinal Epithelial Models". She successfully defended her thesis on January 5, 2004 and was awarded her Ph.D. on May 1, 2004.